REDUCTION OF PERCEPTUAL REDUNDANCY FOR DATA COMPRESSION OF TELEVISION SIGNALS

A thesis submitted for the degree of Doctor of Philosophy in the Faculty of Engineering, University of London

by

JOHN EDWARD THOMPSON

May, 1968

Department of Electrical Engineering,
Imperial College,
University of London.

ABSTRACT

In order to transmit a signal by digital means it is necessary to quantize its amplitude range into a number of discrete levels. For television signals, 7 bits/sample are required by conventional coding in order to reduce quantizing contours in the image to an imperceptible level. A scheme is investigated in this thesis whereby the quantizer thresholds are "dithered" in a pseudo-random manner to achieve a reduction in the necessary codelength by distributing the contours over the image as a less objectionable random noise of similar power. Means are then studied for introducing correlation between samples of the dither signal to shape the spectrum of the quantizing noise in order to exploit the reduced subjective visibility of high frequency random noise. This spectrum shaping also permits substantial reduction of the noise power by pre and de-emphasis filters around the pseudo-random quantizer. Experiments are described which showed that an apparently continuous image with additive noise equivalent to 32 dB signal/white-noise ratio can be obtained from only 2 bits/sample coding. The increase in coder complexity due to dithering is far outweighed by the saving in bits/sample, and the scheme may have bearing on the economic feasibility of a PCM video telephone. Two experimental video-phone systems are described which were constructed to investigate this application of pseudo-random quantization.

CONTENTS

LIST OF SYMBOLS AND ABBREVIATIONS

$A = a_1, a_2, \ldots, a_N$	m-sequence of 0's and 1's
$B = b_1, b_2, \ldots, b_N$	m-sequence of -1's and +1's
B.D.	Binary divider
c.f.	Characteristic function
C.F.F.	Critical flicker frequency
D	Deviation
d.c.	Direct current
D(w)	Quantizing noise-feedback filter
e	Error voltage
E	Mean square error
ftL	foot-Lambert, a unit of luminance
f(x)	Shift register generator characteristic polynomial
F(w)	Signal power spectrum (general)
g	Number of S.R.G. stages spanned by multilevel decoder
h	Number of quantizing steps
H	Hadamard matrix
$H_1(w)$	Pre-emphasis filter voltage transfer characteristic
$H_2(w)$	De-emphasis filter voltage transfer characteristic
ℓ	Line pitch of television raster
m	Number of binary inputs to multilevel decoder
m-sequence	Maximal-length S.R.G. sequence
n	Number of stages in S.R.G.

$N = 2^n-1$	Length of an m-sequence from an n-stage S.R.G.
N(w)	Noise power spectrum (general)
p(v)	Probability density function (of video signal)
PCM	Pulse code modulation
p.d.f.	Probability density function
prbs	Pseudo-random binary sequence
$P(\alpha)$	Characteristic function (Fourier transform of p.d.f.)
q	Quantizer threshold separation
Q	Quantizing noise
r.m.s.	Root mean square
R_r	Autocorrelation coefficient
$R(\tau)$	Autocorrelation function
S.F.T.	Single frame trigger
S/N	Signal/noise (ratio)
S/R	Source-receiver (encoder)
S.R.G.	Shift register generator
s	A 3 MHz square wave
u	A 1.5 MHz square wave
v(t)	Video signal
V	Variance
$w_1, w_2, \ldots w_g$	Weighting coefficients in pseudo-noise decoder
W(w)	Subjective noise visibility characteristic (1 dim.)
$W(w_x, w_y)$	" " " " (2 dim.)
Y	Image luminance
ΔY	Differential luminance threshold

$\Delta Y/Y$ Fractional luminance threshold (Fechner fraction)

x , y , z Clocked binary signals; in particular :

y_1, y_2, y_3 are successive SRG outputs, clock frequency $1/\delta$

y'_1, y'_2, y'_3 " " " " " " $1/2\delta$

y''_1, y''_2, y''_3 " " " " " " $1/4\delta$

δ S.R.G. clock period (secs)

$\phi(k)$ Euler's Phi function

σ Standard deviation

$\oplus$ Addition, modulo-2

GLOSSARY

Brightness. The attribute of visual perception in accordance with which an area appears to emit more or less light. The term refers to the intensity of sensation which results from the area.

Field. One of the two or more equal parts into which a frame is divided in interlaced scanning.

Fovea. A small ellipse-shaped depression in the central region of the retina characterized by the sharpest cone vision. This is the normal centre for visual fixation and attention.

Frame. One complete scan of the picture - with the conventional 2:1 line interlace, a frame consists of 2 fields.

Kell factor. (Unless otherwise specified) The ratio of the scan line pitch to the distance along a line corresponding to one Nyquist sampling interval (LEWIS[74]).

Luminance. The luminous flux emitted, reflected or transmitted per unit solid angle per unit projected area of a surface. Luminance is a purely photometric quantity.

Nyquist rate. Numerically equal to twice the maximum signal component frequency, the Nyquist rate is the minimum

necessary sampling frequency for digital transmission of a bandlimited signal without distortion.

Picture element. The raster can be considered as a matrix of rectangular elements of sides equal to the scan line pitch and the distance along a line corresponding to one Nyquist interval. The conventional 405 line system has a square picture element.

Signal/noise ratio. The ratio of peak white-to-black video voltage (excluding blanking and synchronizing levels) to root mean square noise voltage. (For the subjective measurements, a reference noise level of 20 dB S/N was obtained using peak-peak signal 0.8 volt and 80 mV r.m.s. noise.)

Triangular noise. Noise for which the power spectral density rises as the square of frequency.

Viewing ratio. The ratio of the distance from a television monitor, at which a viewer is seated, to the picture height.

ACKNOWLEDGEMENTS

I am greatly indebted to my supervisor, Mr J.J. Sparkes, for initially drawing my attention to pseudo-random noise and gratefully acknowledge his interested guidance in the work that followed. Thanks are due to Professor E.C. Cherry for inspiration in bandwidth compression and for procuring funds for the research. The help given by Dr R. Spence in the final stages of the project is also appreciated.

Dr P.W.J. Bylanski, Mr K. Patel and Mr A.H. Robinson read the manuscript of this thesis and made many helpful comments. The technical assistance of Mr W.A. Gurnhill in constructing some of the circuit boards and of Mr A.A. White in providing spot wobble coils, together with their help in maintaining the picture generation equipment, is much appreciated. The design of the six-input modulo-2 adder was due to Mr Robinson. I am also grateful to Mr A.E. Cawkell of ASCA for keeping a computerized watchful eye on the literature. Sincere thanks are offered to my wife for subjective and objective participation in the experiments and for her continual encouragement and support.

The financial support of the Science Research Council is gratefully acknowledged, together with the interest shown by the National Research and Development Corporation in providing patent cover.

CHAPTER 1

INTRODUCTION

1.1. BACKGROUND

Communications engineers have long had Information Theory as a guide to the solution of coding problems in terms of source statistics and receiver fidelity criteria (SHANNON [111]). Present-day television systems take little account of the statistical properties of the scenes they transmit. Also, they occupy expensive channel space with information some of which is imperceptible to the human receiver. Estimates of statistical redundancy have been made from measurements of television pictures, and circuit technology has begun to allow implementation of schemes which reduce it. Comparatively little progress has been made however, in specifying a fidelity criterion on the basis of a comprehensive model of visual perception (PEARSON [92]). Solution of this coding problem has rather involved a trial and error procedure using human operator tests to evaluate promising compression schemes. Considerable improvement has been achieved over the initial system which simply satisfied the basic requirements of spatial and temporal resolution, but practicable encoders can still remove only a few of the known perceptual

redundancies.

The capacity of digital computers now permits rapid and convenient investigation of compression schemes (DAVID[22]; TRETIAK[119]; GRAHAM & KELLY[45]). However, until such time as the computer programme can incorporate a realistic model of visual perception, the final evaluation of promising schemes must remain in "real time" subjective testing.

The advantages of pulse code modulation (PCM) have been extended to the transmission of television signals (CARBREY[17]), but at the cost of large data rates. The speed and storage capabilities of digital processing are particularly favourable to compression techniques, but for television there is still considerable scepticism about the exchange between bandwidth and system complexity, which seems to characterize statistical coding schemes. As the capacity of PCM links increases (KELLEY[65]), perhaps eventually involving laser modulation, extension of visual communication to a wider range of applications (CHERRY et al[20]) must surely see incorporation of compression schemes, particularly those which reduce perceptual redundancy and equipment complexity.

1.2. TELEVISION REDUNDANCY

The function of a television system is to transmit a representation of a scene, generally a complex function of many variables, which is sufficient to create the required response in the mind of a human recipient. SHANNON[110,111] showed that a fidelity criterion is basic to the problem of transmitting information from a continuous source. It has been estimated that the capacity of the visual system, operating as an information sink, is of the order of 10^9 bits/sec. (KELLY[66]). Regarded as a channel however, measurements of recognition and reading rates suggest a capacity of only 40 bits/sec. (SZIKLAI[115]; PIERCE & KARLIN[93]). The purpose for which a television system is intended clearly has tremendous influence on its associated channel capacity. A viewphone image, supplementing the speech channel with simple cartoon-like representations of faces, might be sufficient for recognition and observation of facial expressions (PEARSON[92]) and could perhaps approach the lower bound of 40 bits/sec. A system provided for entertainment however, must present a more realistic image and demands a channel capacity nearer the upper limit. The viewer continues to assimilate information at a comparatively low rate, but with the freedom of choice which visual experience demands.

Figure 1.1 shows a block diagram of an idealized system for transmitting television signals with the minimum

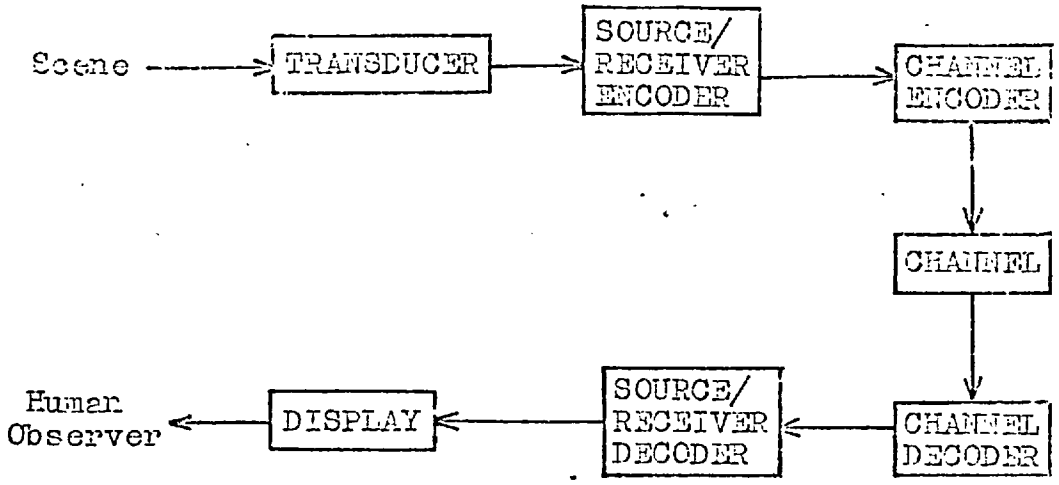

Figure 1.1. Schematic diagram of an idealized image transmission system.

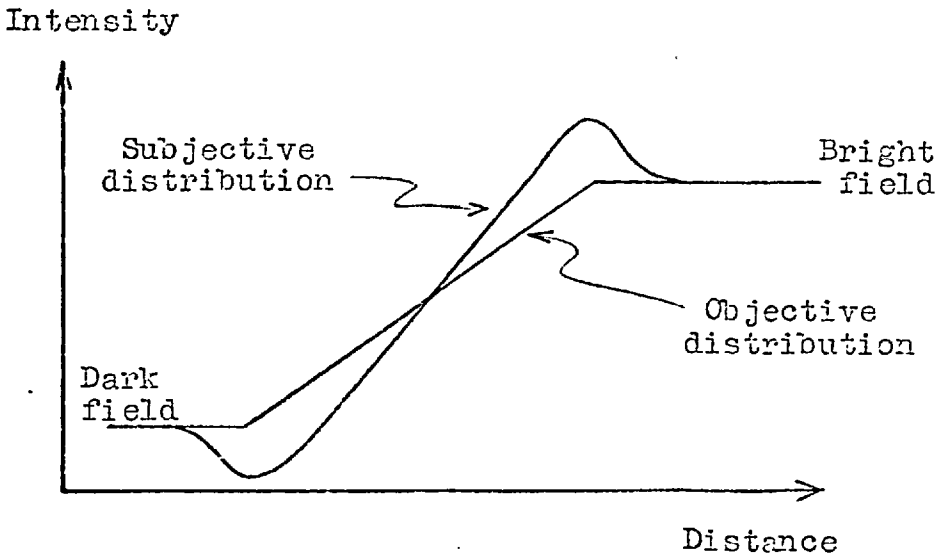

Figure 1.2. Diagrammatic representation of the Mach phenomenon (from Lowry & DePalma, ref. 76).

redundancy consistent with a specified fidelity criterion. The standards for a transducer which generates an "entertainment quality" image using non-adaptive rectilinear scanning were established in 1935 (GARRATT & MUMFORD[37]). It has long been realized however, that most scenes are highly redundant in comparison with the maximum resolution of this system. Furthermore, it is known that much of the information transmitted is imperceptible to the human viewer. Considerable effort has therefore been directed to the design of an encoder which achieves a more economical match between the source and the recipient. Ideally the source-receiver (S/R) encoder either minimizes the required channel capacity for a specified image quality, or maximizes quality for a specified capacity, by removing redundant data from the transducer output. It is usual to classify redundancy as either statistical or perceptual, although the distinction is often ill-defined. Basically, the statistical encoder exploits properties of "typical" scenes by averaging the information rate defined on a set of source probabilities, whereas psycho-physical encoders exploit properties of the viewer by eliminating data which is imperceptible. The S/R encoder is complemented at the receiver by a corresponding decoder, but whereas statistical encoding is largely a reversible process, allowing reconstruction of the coder input signal, psycho-physical coding is not.

Figure 1.1 shows a further stage of encoding, which perhaps involves reinsertion of redundancy, and which fortifies the signal against the type of transmission errors expected in the particular channel. Error-correction codes may be necessary to avoid subjectively intolerable distortions, as might arise from errors in the position data channel of a statistical S/R encoder. However, for many S/R encoders error correction is not necessary as the human receiver is quite tolerant of the type and frequency of errors which occur. Furthermore, when channel interference is below a certain threshold, almost error free transmission can be achieved using PCM (OLIVER, PIERCE & SHANNON[90]).

"Straight" PCM, in which the S/R encoder performs only the processes of sampling and quantizing, has come to be regarded as the standard against which to compare the performance of data compression schemes. Perhaps when the processes of visual perception are better understood, this will be superseded by a more realistic model on which to measure progress.

1.3. A REVIEW OF REDUNDANCY REDUCTION

In this Section, schemes for television data reduction are reviewed in respect of their exploitation of the characteristics of visual perception. Accordingly, the statistical

aspects of S/R encoding receive comparatively little attention. The reader is referred to the thesis by ROBINSON[101] for a review of compression techniques from the statistical standpoint, and to KORTMAN[71] for a detailed classification of statistical redundancy reduction methods.

It is not proposed to include a complete description of the visual system. Rather, the subjective factors relating to perceptual redundancy in television signals are discussed together with associated compression schemes. An adequate description of the visual mechanism and its properties is given by BREWER & MORRIS[32], and a comprehensive review of experimentation in visual psycho-physiology by BARTLEY[5] and GRAHAM[113]. More recent contributions to the understanding of visual perception have been reviewed by POWELL[94] (1966) and MARSH[78] (1967).

1.3.1. Brightness Discrimination

In designing an image transmission system, it is important to be able to specify a just imperceptible local change in image luminance, whether this be characteristic of the picture or due to random transmission errors. Weber found that over a wide range, the differential luminance threshold (ΔY) increases in proportion to the background luminance (Y). However, this law breaks down at low intensities where the

fractional threshold $\Delta Y/Y$ (also known as the Fechner fraction) increases. The breakdown can be largely explained (GREGORY[46]) by residual firing of retinal cells in the absence of light.

The differential threshold ΔY is also dependent upon the area and duration of the stimulus, and upon the state of adaptation of the eye. Thus the brightness of a given region increases as the luminance of its surround is reduced ; but in addition to adaptation, apparent contrast is also dependent upon the strength of any contours between the areas. Contrast enhancement seems to be connected with the general importance of borders in perception, and it is to Mach that its discovery is usually attributed (LOWRY & DePALMA[76]). A diagrammatic representation of the phenomenon is shown in Figure 1.2 (p.15) for a diffuse boundary between two areas of different brightness. Where there is a rapid decrease in luminance gradient a white line appears, and where there is rapid increase a dark line can be seen.

In consequence of these characteristics of brightness discrimination, the visibility of random luminance errors in a television image decreases :-

(i) as their size decreases,

(ii) as the local picture luminance increases, and

(iii) as picture detail increases - noise is most visible in the simply organized regions of a picture. These effects will be considered in detail in Chapter 3.

The importance which the eye attaches to boundaries has the result that the viewer is extremely critical of the false contours which occur when a video signal is quantized for transmission through a digital channel. GOODALL[40] suggested that a binary code of 6 or 7 bits per picture sample is necessary with equal step quantization to reduce contours to an imperceptible level. This includes allowance for Weber's law, which is roughly complemented by the power law of the display tube (this will be discussed further in Section 3.2.1). NEWELL & GEDDES[87] deduced a comparable result from measurements of visibility thresholds of alphanumerics in uniform surrounds. They proposed that at least 95 levels of brightness are necessary in a noise-free picture, but it was noticed that addition of noise after quantization masked contours such that at 27 dB signal/noise (S/N) ratio no more than 56 levels were perceptible. However, Goodall had reported that the addition of noise to the signal before quantization masked contours much more effectively. With 5 bits/sample quantization, contours were smeared at 60 dB input S/N ratio and completely masked at 40 dB.

Quantizing contours are known to be more objectionable than additive random noise of the same mean square value. ROBERTS[99,100] successfully applied this principle in a pseudo-random perturbation scheme which dispersed contours as a

more acceptable pseudo-random noise of similar power. It was shown by computer simulation that 3 or 4 bits/sample were sufficient to transmit an apparently unquantized image with an acceptable amount of additive noise.

BRUCE[14] demonstrated that pre-emphasis of the high frequency components of the video signal prior to digital coding, and subsequent complementary de-emphasis, could smooth quantizing contours to a useful extent. Making the assumption that fine grain quantizing noise is white and independent of the signal (BENNETT[7]), Bruce used the random interference weighting function of BARSTOW & CHRISTOPHER[3] to derive conditions which minimized r.m.s. weighted noise at the output of the de-emphasis filter. For an estimated "typical" video spectrum, these conditions predicted a maximum reduction of noise visibility of 2.8 dB. Unfortunately, Bruce misinterpreted these conditions* and constructed complementary filters which emphasized video high frequencies by only 5 dB instead of 10. Even so, it was found that just 5 dB emphasis smoothed contours sufficiently to give 5 bits/sample quality from only 4 bits/sample quantization.

Owing to the predominantly low-frequency nature of the video spectrum (FINK[32]), pre and de-emphasis can effect a

---

* Bruce derived an expression for the voltage transfer function of the pre-emphasis filter in terms of the video power spectrum and the subjective noise power weighting characteristic. The constructed filter realized this expression as its power transfer function.

much greater reduction in quantizing noise power if the latter can be first weighted in favour of high frequencies, independently of the video signal. KIMME & KUO[68] designed a noise-feedback coder which achieved this by adding to each sample before quantization a filtered combination of preceding quantizing errors. A random noise weighting function, measured specially for a low resolution television system, was used in designing a noise-feedback filter and pre and de-emphasis networks which maximized the output signal to weighted-noise ratio. BRAINARD[9] later implemented this system and conducted subjective tests which demonstrated a 12 dB improvement over a conventional 3 bits/sample coder.

R.E. GRAHAM[44] used computer simulation to evaluate means of improving the quality of noisy pictures by smoothing out the noise in simply organized regions of the image - these being the parts of the picture where additive noise is most objectionable. This is a particularly valuable technique, compatible with many compression schemes since it requires no pre-processing at the transmitter. Noise stripping was operated over a 3 x 3 matrix of picture elements subject to a detail criterion and was found to be effective for input S/N ratios down to 28 dB. Below this, smearing was extended to sharp edges in the picture.

In addition to the importance of boundaries in the processes of perception and recognition, edge rendition is

very relevant to the subjective assessment of image quality. GOLDMARK & HOLLYWOOD[39] designed an "edge crispener" which operated at the receiver to restore sharp edges lost by low-pass filtering in transmission. Triangular spikes, generated from the first time derivative of the video signal, were subtracted from the signal to speed up the edges. The crispener subjectively doubled the bandwidth of the filtered signal except for the omission of high frequency repetitive patterns and the inability to resolve closely spaced fine lines. BROWN[12] designed a simpler, but more effective, crispener which used a short delay line to obtain the second time derivative of the video signal. It was then possible to overemphasize as well as steepen fast edges. KOVASZNAY & JOSEPH[72] proposed a two dimensional image crispener, but this required a special isotropic scan which was realized by a Lissajou figure.

"Dual mode" systems

The eye cannot appreciate the magnitude and shape of short luminance transients and is therefore relatively insensitive to errors in detailed parts of the picture. This has formed the basis of a large number of compression schemes in which coarse quantization is used in transmitting picture detail. KRETZMER[73] equated picture detail to the high frequency part of the video spectrum in the band-split system of

Figure 1.3, which achieved a compression of about 2 : 1. The low frequency components of the signal were transmitted directly, but the highs were quantized to only 5 levels. High-pass filtering was effected by subtracting the lows from the unprocessed signal, as a result of which the image had spurious contours near sharp edges. These were overcome in the system proposed by SCHREIBER, KNAPP & KAY[105,106], which used an alternative method of generating the highs signal, shown schematically in Figure 1.4. Edge information was obtained by quantizing the difference between adjacent picture samples to only 8 levels (4 up and 4 down) in a tapered quantizer. Low frequency information was transmitted directly through a bandwidth of 350 kHz, and the edge data was coded into an amplitude channel and 5 bits/sample position channel. At the receiver, a specially shaped "synthetic highs" waveform was generated from the edge signal with some overemphasis to give useful crispening of the image. The elastic encoder, needed to achieve transmission of edge samples at their mean rate, was omitted but a compression ratio of 4 : 1 was estimated.

NEWELL & GEDDES[86] partially implemented both of the above dual mode schemes and found their performances to be similar. However, subjective tests showed that the Synthetic Highs system was not markedly superior to a 1 MHz low-pass filter and image crispener. Unfortunately, the characteristic of

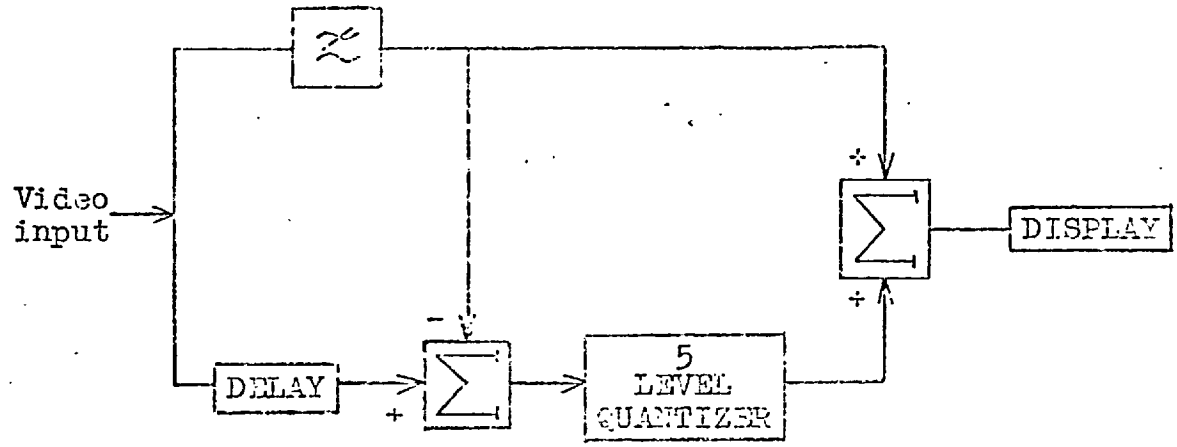

Figure 1.3. Two-band transmission scheme of KRETZMER (73).

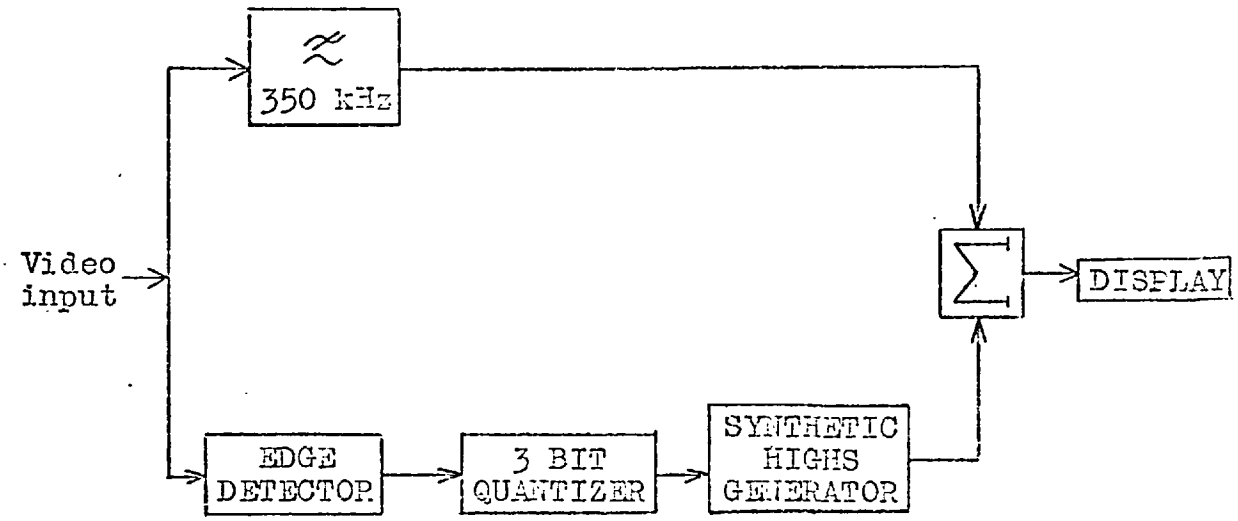

Figure 1.4. "Synthetic Highs" system of SCHREIBER, KNAPP and KAY (106).

the filter was not specified so it is difficult to draw any conclusion from this. It was pointed out that the viewer is extremely intolerant of distortions and dislocations in boundaries, and the problems associated with error-free transmission of edge information were discussed.

AKHTAR[1] proposed an intriguing two band scheme with an estimated compression of 5 : 1, in which the highs were transmitted as a hologram. Isolated fine picture detail becomes the "lows" in the hologram, which can then be transmitted through a narrow-band channel using conventional scanning methods and optical filters. The picture lows are transmitted directly through a second narrow-band channel.

JULESZ[63] proposed a further detail criterion for dual mode transmission, in which picture samples conveying detail - "edge points" - were defined as those around which the video signal changed slope significantly. Exclusion of low frequency data by this criterion was avoided by monitoring the error between the processed and original signals, and reinserting samples whenever a second threshold was exceeded. Samples were then selectively quantized such that those with both neighbours nearer than 3 elements were coded to only 4 bits, and the remainder - assumed to be edge points of low frequency regions - were coded to 7 bits. At the receiver the image was constructed by linear interpolation between the edge points. A buffer store of length between 1 and 4

lines was estimated as needed to avoid overload in the elastic encoder. A computer simulation produced satisfactory results from 2 or 3 bits/sample, with the exception of some phase errors in the location of edge points on vertical lines. It was estimated that this could be improved without a large overall increase of data by specifying the location of edge points to a fraction of a Nyquist interval.

HUANG[53] set out to halve the data rate from conventional scanning by missing out every other line and then restoring them at the receiver as the average of the two neighbouring transmitted lines. However, this was found to give a noticeable staircase effect on boundaries unless extra samples were sent at points near the contours. The final system considered transmitted only every fourth point of every fourth line together with additional points to specify the contours. Its effectiveness was limited by the total loss of fine detail lying in the omitted part of the picture.

D.N. GRAHAM[41] simulated a two dimensional extension of the Synthetic Highs system. The lows signal was derived by low-pass filtering, although optical defocussing could have been used. A method of contour coding was developed to give compression ratios for a low resolution system of between 4 and 20 to 1. It was expected that the ratios in a full resolution system would be almost twice these values, but the process was far too complicated for real-time television

(each picture required 5 minutes of computer time).

KITSOPOLOUS & KRETZNER[69] reported a development of their early system[73] in which a picture sample is assumed to convey detail if it differs from the previous sample by more than 6 % of the video range. Detail samples are then quantized to 4 bits, while the remainder - assumed to convey low frequency information - are quantized to 7 bits. A constant 4 bits/sample data rate is then obtained without buffering by omitting every other sample in low detail regions and replacing them at the receiver by interpolation. A binary signal is also required to control interpretation of the received digits. The scheme has been computer simulated, but no results were given.

Differential Quantizers

A large number of statistical compression schemes can be classified as Predictive encoders (OLIVER[89]). Such schemes transmit only "surprise" data, or the amount by which an estimate of the present picture sample based on the values of its predecessors is in error. Differential quantizers belong to this classification, but only the previous sample is used in the prediction. The transmitted signal represents the 'error' between the present sample and the one immediately preceding it.

It is usual to taper the quantization to obtain fine

steps for small difference signals, corresponding to near-uniform brightness regions, and coarse steps for the large differences produced by rapid transitions. R.E. GRAHAM[43] published photographs to show that 3 bits/sample differential quantization is markedly superior to ordinary 3 bit quantizing, although some undershoots and overshoots were visible near boundaries where the predictor was surprised. GRAHAM[42] also simulated an "alternate mode" differential quantizer, which operated a running choice between horizontal and vertical previous value prediction, according to which produced the smaller signal value. Again a tapered 3 bit quantizer was used, and photographs showed the system to be substantially better than single mode differential quantization. The largest errors now tended to occur at corners and along 45° lines. The system also included "reservoir coding", which allowed extra time to transmit detailed regions by inserting extra samples into the line blanking intervals. In view of the susceptibility of the scheme to errors occurring in transmission, it was suggested that error correction would probably be necessary in an operational system.

LIMB[75] conducted subjective tests to determine the threshold of visibility of difference errors as a function of difference amplitude. These results were used to compute the optimum threshold spacings for a 10 level differential

quantizer by a procedure due to MAX[80], which minimized weighted mean square error over the amplitude range of the difference signal. The entropy associated with the optimum thresholds for a particular picture was computed as 2 bits/sample, and the picture was judged by a number of observers to be indistinguishable from the original at a viewing distance of 8 picture heights. The number of thresholds was reduced and the optimization repeated subject to the quality criterion of being indistinguishable from the original with probability 0.5. Lower bounds of between 1 and 2 bits/sample were obtained for three pictures of various detail. However, the optimum threshold spacings depended on the probability density function of the signal so that adaptive encoding may be necessary to maintain these efficiences. In addition, the bounds must depend on the available capacity of buffer storage.

In Delta Modulation systems, the sample difference signal is quantized to only two levels, but the sampling frequency is increased to several times the Nyquist rate. O'NEAL[91] computed signal to quantizing noise ratios for various step sizes for a low resolution television system and estimated maximum values of 24 to 48 dB for sampling frequencies of 1 to 8 times the Nyquist rate. The S/N ratios were somewhat dependent on picture material and the degradation was of four types : slope overload noise on fast

edges ; grainy noise ; contouring ; and edge "business", which occurs when the sampling and line-scan frequencies are not synchronized. Since the quantizing noise is distributed over these four types, it was suggested that objectionability might be less than for the same level of Gaussian noise.

1.3.2. Visual Acuity

The retina has two types of receptors - rods and cones. The cones are responsible both for visual acuity in the fovea and for the perception of colour. The rods exist mostly in the periphery of the retina and provide low acuity awareness over a wide field of view. It has been estimated that the retina contains more than 10^8 receptors, but that the optic nerve which connects the retina to the visual cortex has only about 10^6 fibres. The discrepancy arises from bunching of receptors in the peripheral regions of the retina enabling data "preprocessing" to determine stimulus orientation, etc. The nominal resolving power of the eye, on which television standards have been based, applies only for the centre of the fovea. Resolving power decreases rapidly towards the periphery of the retina, so that with the exception of an area surrounding the fixation centre, a scene is only perceived in coarse focus.

TEER[116] pointed out that conventional television systems are highly redundant in providing nominal resolution over the entire image, and investigated the feasibility of exploiting this. A uniform scanning raster was used, but the image was defocussed towards the edges by adding components of line and field frequencies to the d.c. through the display focus coil. Slow variation of the d.c. controlled the location of the focussed fixation centre with respect to the field of view. It was concluded that a compression of 4 : 1 was possible without visible defocussing if a line of sight could be imposed on the viewer. However, this was judged to be psychologically unacceptable.

BALDWIN[2] conducted observer tests using a film projector to simulate a television image in order to establish the optimum subjective ratio of vertical to horizontal resolution. This ratio was found to peak gently at unity, but deviations of 2 : 1 from this symmetrical condition were found to be quite acceptable on high definition pictures.

The British (405 line) television scanning standards were established on the concept of a mosaic of square picture elements, permitting equal horizontal and vertical resolution. This mosaic approximately satisfies visual acuity for an observer seated at a viewing distance of 4 picture heights, i.e., at a viewing ratio of 4. It has since been realized that due to interlace and the asymmetrical structure of the

raster, the concept of a square picture element corresponding to equal resolution in the two coordinate directions is not valid. In particular, as a result of violent flicker in the Moire pattern arising from interference between scan lines and a horizontally disposed resolution wedge, definition is considerably less than one wedge line per scan line (LEWIS[74]). The ratio of resolvable wedge lines to the number of scan lines has become known as the Kell factor, for which valuos from 0.64 to 0.75 have been proposed.

JESTY[62] obtained some interesting results from measurements of television picture quality as a function of the viewing ratio. With low-pass filters to define horizontal resolution in 405 and 625 line systems, observers were asked to sit at their preferred viewing distance. Consistent results were obtained from which Jesty concluded that the 405 line system has an excess of horizontal over vertical sharpness of 50 %. Because of the interlaced line structure, the average viewer has no desire to sit nearer to the display than 8 picture heights, at which distance horizontal detail in the video band above 1.5 MHz is imperceptible. For the 625 line system, an optimum bandwidth of 2.5 MHz was suggested. Spot wobble, applied synchronously at camera and receiver, was tried in the 405 line system to reduce the visibility of the line structure without loss of vertical

resolution. As a result, the preferred viewing ratio fell to 7.

Jesty also found that apparent sharpness was not simply a function of viewing ratio, as would be expected of constant visual acuity, but was dependent on picture size such that the average observer was less critical of small pictures than large ones. This was attributed to line structure since the phenomenon had not been reported in Baldwin's optical experiments. However, it could also be connected with the perceptual process of Size Constancy (GREGORY[46]), whereby the visual system tends to compensate for changes in the retinal image with viewing distance.

LEWIS[74] has reported results in agreement with the "optimum bandwidth" estimates of Jesty. This work was concerned with a later definition of the Kell factor as the ratio of scan-line pitch to the distance along a line corresponding to twice the nominal upper video frequency. Proposed values for this range from 0.42 (Jesty) to 1.0, but Lewis showed how much of this variation is attributable to differences in specification of bandwidth.

HUANG[56] conducted a few observer tests on a rectilinear scanning system to determine the preferred direction of scan for a number of pictures. The results were inconclusive.

The receptors within the fovea are predominantly cones, which are sensitive only at high levels of illumination.

Visual acuity therefore falls off rapidly as image brightness is reduced. JESTY[61] commented that it is unnecessary to maintain nominal resolution in shadowy areas of the picture, but made no proposal as to how this redundancy might be reduced.

BEDFORD[6] has shown that at normal viewing distances an observer does not perceive colour in fine detail parts of a picture. Further studies (WILLMER & WRIGHT[125]) indicated that there is also an intermediate degree of detail at which the eye appears to have only two-colour vision, whereas three-colour vision exists in simply organized regions. These perceptual characteristics have permitted substantial compression of the bandwidth required to transmit colour television signals. In the N.T.S.C. system, in comparison with a 4 MHz luminance bandwidth, the two colour difference signals specifying colour changes in the orange-cyan and green-magenta directions are transmitted respectively through bandwidths of 1.5 MHz and 0.5 MHz. As a result of the nature of typical scenes and of rectilinear scanning, the energy of the monochrome video spectrum is concentrated near harmonics of the line scanning frequency (DERIUGIN[24]). This permits transmission of the colour signals within the luminance frequency band by spectral interleaving, although by using a subcarrier at an odd multiple of half line frequency, some high frequency dot patterning is visible.

1.3.3. Persistence of Vision and the Phi Phenomenon

The visibility of random noise was discussed earlier in connection with brightness discrimination. In fact there are also numerous temporal considerations, although their influence is not so well known (SCHREIBER[104]). The human viewer is remarkably adept at temporal integration of noise and can correlate successive scans of intensely noisy images in order to extract detail (PEARSON[92]).

The perception of rapid variations in brightness, or "flicker", is primarily dependent on excitation frequency, intensity, and the size and distance from the fovea of the retinal area illuminated. The lowest frequency at which flicker is imperceptible is termed the critical flicker frequency (C.F.F.), and within broad limits it is linearly related to the logarithm of luminance (the Ferry-Porter law). Marsh included a comprehensive discussion of the attributes of flicker perception, and HAANTJES & DeVRIJER[47] have produced curves to show how the C.F.F. for a television image varies with luminance, viewing ratio and phosphor decay time. EASTON et al[30] have recently extended subjective measurements of brightness to almost zero persistence phosphors for scanning systems incorporating lasers. FINK[32] stated that the C.F.F. is typically about 50 Hz for a luminance of 29 ftL, which is usually above the peak luminance of a television image. The British television

system works close to the flicker threshold however, such that field frequency is often below the C.F.F. for retinal areas outside the fovea.

The illusion of continuous motion is a considerably less demanding requirement of a television system than flicker fusion, and relies upon the so-called Phi phenomenon (GREGORY[46]). This may be demonstrated by connecting a lamp to each output of a bistable. If the separation of the lamps and the clock period of the bistable are small enough, a single light is seen moving across from the position of one lamp to the other. TEER[116] investigated the phenomenon for television images as a function of contrast ratio and velocity of a moving object. It was found that for a simple picture, comprising a vertical bar moving horizontally at a speed of 1 picture width per 2 seconds, 25 situations per second resulted in disturbing discontinuity at a contrast ratio of only 20. For "typical" pictures however, it was found that a critical region existed at only 8 to 10 situations per second, above which most of the pictures observed were acceptable. In these experiments, the normal field rate necessary to avoid flicker was maintained and the signal was stored and repeated for a number of fields to give the required frame frequency.

In using 2 : 1 line interlace, the conventional system halves the amount of data needed to satisfy flicker

requirements while presenting 25 complete pictures per second to preserve motion rendition. The disadvantages lie in interline flicker and increased interference with picture detail, together with line crawl and subjective line pairing which are most evident when the eye moves vertically over the picture. BROWN[13] showed that these defects significantly detract from the nominal 2 : 1 bandwidth saving when the line structure is visible. A line-interlaced picture of 225 lines was assessed by observers on a scale of several non-interlaced pictures with different numbers of lines and bandwidths. At a highlight luminance of 40 ftL, it was concluded that interlacing provides a saving of about 37 % in terms of bandwidth. At 100 ftL the saving was found to be as little as 6 %. MAURICE[62] attributed Jesty's conclusions to these deficiences of interlace, and referred to other tests which had shown that interlace increased the preferred viewing distance. Since conventional standards did not allow for these defects, there would inevitably be an excess of horizontal resolution. The experiments of Haantjes & DeVrijer showed that increased phosphor persistence allows the use of 2 : 1 interlace up to 55 ftL highlight luminance with no flicker or objectionable blurring of motion, but some difficulty was encountered in obtaining a white image.

Teer's results for "typical" pictures suggest that conventional standards are still about 2 : 1 redundant

in effecting motion rendition. Higher orders of line-interlace produce an intolerable illusion of vertical line crawl (DEUTSCH[25]), but a further 2 : 1 reduction in frame rate appears to be feasible with dot-interlace. One frame can be transmitted as 4 fields, each containing alternate picture elements in alternate lines, however some care is required in ordering the fields so as to minimize the visibility of stroboscopic effects. These disturbing effects can also occur in subcarrier systems, in which the eye is relied upon to integrate out unwanted signals over two frames. HOWSON & BELL[52] devised a method analagous to the N,T,S,C, colour system, using frequency interlace to compress the bandwidth of a monochrome video signal by 2 : 1. The upper half of the normal video band was modulated on to a subcarrier of frequency equal to an odd harmonic of half line frequency. The lower sideband then interleaved with the unmodulated signal so that the two halves of the video band could be recovered at the receiver by synchronous demodulation. However, a component of the interleaved signal remained in the display and produced an interference pattern, which though cancelling over 4 fields, gave rise to visible crawling.

DEUTSCH has demonstrated that high orders of dot-interlace can be achieved without dot crawl by pseudo-random scanning. The viewer can no longer perceive the order in

which dots appear so that no disturbing patterns or drifts occur even with 16 : 1 interlace[29]. Many systems were proposed[28] with bandwidths ranging from 1 MHz to 240 Hz, most of which had frame rates below the critical frequency for motion rendition. In these, a long persistence phosphor was used to blurr jerkiness.

There are alternatives to interlace in reducing the number of frames transmitted per second while satisfying flicker requirements, but these need large capacity storage at the receiver. One possibility is to scan selected frames at low speed for transmission, and to rescan from storage at the receiver in order to restore normal standards. BRAINARD, MOUNTS & PRASADA[11] compared two other methods using digital storage in ultrasonic delay lines for a low resolution, non-interlaced system. In "Frame Repetition", only one frame in four was transmitted and stored at the receiver. The missing frames were then restored by repeating each transmitted frame three times from storage. In the second system, a complete frame was again stored at the receiver and read for display at 60 Hz, but instead of refilling at 15 Hz, the store was selectively replenished at 60 Hz. The system resembles dot-interlace, except that all elements in the display are scanned at 60 Hz and dot crawl cannot occur due to unfortunate choice of replenishment pattern. It is interesting to note that of five

replenishment patterns tried, a pseudo-random one was markedly inferior to the other regular selections (cf. Deutsch). It was found that motion rendition was reasonably good at 15 pictures per second, although gross impairment occurred during panning and zooming. Selective Replenishment gave better continuity than Frame Repetition, but resulted in objectionable patterns and ragged edge effects on fast moving objects.

The jerkiness arising from zero order interpolation in Frame Repetition can be overcome by first order interpolation, in which one frame is merged into the next by superposing the new and old frames in continuously changing proportions. However, as in Deutsch's long persistence displays, some motion blurring results. GABOR & HILL[36] proposed a method of contour interpolation which realized the perceptual importance of contours in linearly interpolating between transmitted frames to reconstruct intermediate ones without blurring. An 8 : 1 compression scheme was simulated at very slow speed, and shown to be satisfactory except for some deterioration with rapid vertical motion.

SEYLER[108] has proposed a statistical encoder of frame differences which transmits just sufficient of the difference between successive frames to preserve the illusion of continuous motion. This is particularly efficient when only

the subject moves against a stationary background, but the buffer store which averages the rate of transmitted data becomes prohibitively large when required to cope with scene changes and camera panning or zooming. However, this can be overcome by making the system adaptive. It is known (SEYLER & BUDRIKIS[109]) that the viewer takes about 780 msec. to adapt after a scene change before the new image is perceived in detail. The new scene can be presented initially with only one tenth of the nominal resolution, becoming progressively sharper with a suitable time constant. Controlling the frame difference signal in this way, SEYLER[107] showed that a compression of 10 : 1, or more, might be achieved. It was also pointed out that conventional systems already exploit this phenomenon to some extent since most camera tubes involve charge storage over at least one frame interval, which temporarily reduces resolution in those areas where movement has occurred.

1.4. THE CONTRIBUTION OF THIS THESIS

The previous Sections have reviewed a selection of television data compression schemes in relation to some psycho-physical characteristics of visual perception. This thesis is concerned essentially with a study of quantization in which most of these characteristics are of some relevance.

In a quantized image, smooth variations of brightness are replaced by staircase waveforms which cause visible contours unless about 100 equally spaced levels are used to cover the signal range. These false contours appear between points in the scene where the luminance corresponds to a quantizer threshold voltage. Roberts therefore proposed jittering the thresholds in a noise-like way in order to distribute the contours throughout the image as an apparently additive random noise. Jittering is made possible by the provision of identical, synchronized pseudo-random noise generators at the transmitter and the receiver so that noise can be added to the video signal before quantization and the same noise can be subtracted afterwards. Roberts likened the situation to that of jiggling a grating in front of the eyes as opposed to holding it still. By moving it one can see everything, but not clearly. The process was demonstrated by computer simulation, using a long sequence of random numbers as the noise. For a practical situation, it was suggested that a 16 level pseudo-random noise might be obtained by decoding four binary outputs of a shift register generator (S.R.G.).

Pseudo-random binary sequences have received considerable attention in control systems on account of their statistical properties. It is also possible to decode various outputs of a S.R.G. to generate multilevel noise with excellent

flexibility of shaping the amplitude distribution and power spectrum. The major contribution of this thesis rests on an investigation of this flexibility with the object of extending Roberts' proposal to exploit the reduced visibility of high frequency noise.

The properties of pseudo-random noise form an integral part of this work. In particular, specification of the arrangement used to generate a multilevel sequence from a binary S.R.G. and the autocorrelation function of the basic binary sequence are used extensively in the analysis of an optimized pseudo-random quantizer. Chapter 2 therefore provides a comprehensive treatment of the S.R.G. and its properties.

In Chapter 3, the perception of random noise is discussed in detail with particular consideration of a random interference weighting function. A pseudo-random noise generator is described, together with some simple experiments which demonstrate its properties.

Chapter 4 reports real-time implementation of Roberts' scheme and some results are obtained. Subjective evaluation is described of a system (THOMPSON & SPARKES[118]) which used a 3 MHz square wave to double the precision of a 2 bit quantizer and pseudo-random noise to disperse the resultant contours. A set of equations is then derived which specify quantizing noise power spectra in areas of constant picture

intensity in terms of the input pseudo-random noise. In principle, these equations allow optimization of the quantizer by choosing a pseudo-random noise which shapes the quantizing noise spectra according to the subjective random noise weighting function. The extent to which this principle was realized is then discussed.

In Chapter 5, a 4-level pseudo-random noise is proposed which is very successful in transferring quantizing noise to high frequencies, although some contouring remains. Pre and de-emphasis of the video signal is then performed to reduce high frequency noise and to smooth the remanent contours. In this way, the quantizing noise power is reduced in addition to the subjective advantage of spectrum shaping. However, it was found that high frequency pre and de-emphasis of the video signal is not entirely compatible with digital spectral shaping in the pseudo-random quantizer. Subjective experiments were therefore carried out to determine the additional advantage of pre and de-emphasis, and to investigate the validity of the quantizer equations. Finally, the combined system is compared to the noise-feedback quantizer developed at Bell Laboratories.

Chapter 6 discusses the potentialities of pseudo-random quantization in a compression scheme for a video telephone system. Photographic results are presented of two simulated systems, one of which incorporated dot-

interlace, and which were constructed to show the picture quality obtainable with a data rate of only 1.6 Mb/sec. In particular, the performance of pseudo-random quantization in a low resolution system is demonstrated and its compatibility with dot-interlace is discussed.

CHAPTER 2

PSEUDO-RANDOM NOISE

2.1. INTRODUCTION

Pseudo-random noise is a periodic signal generated digitally according to a predetermined programme, but which exhibits over one cycle the properties associated with randomness. The first half of this Chapter is devoted to a study of the binary sequence from which the multilevel noise used in the experiments was derived.*

Periodic binary sequences can be generated in a shift register of binary elements of which selected outputs are added, modulo-2, and fed back to the register input. For certain feedback arrangements, sequences are obtained which over one period exhibit the run-length distribution expected of a random coin-tossing experiment. The only clue to the uninitiated observer that the sequence is not random lies in the property of producing the expected distribution precisely over one period. This corrective behaviour is attributable to memory, and tends to be exhibited by a human being who is asked to write down a sequence of random decisions. The property leads to a sequence autocorrelation function which

---

*References in this Chapter are to a separate bibliography on pseudo-random noise in Section 2.7.

is large at multiples of the sequence period and uniformly low elsewhere.

The randomness properties of pseudo-random binary sequences (prbs) have found widespread application in communications and control engineering. Since GOLOMB's comprehensive exposition of these properties in 1955 [12], prbs applications have appeared in radar [33], cryptographic coding [24], error correction [15], high speed counters [18], and as carriers in communications systems [22, 27, 31, 34]. INGRAM et al [19] published a particularly interesting paper on carrier generation, which discussed the wide range of power spectra available from the prbs. A symposium [11] held at the National Physical Laboratory in 1966 and two colloquia held at the I.E.E. in 1965 [20] and 1967 [21] also showed extensive use of the prbs as a noise probe for on-line measurement of system impulse response by input-output cross correlation.

The generation of multilevel sequences has received relatively little attention in the literature [2, 10]. A generalized theory does exist for the generation of p-level sequences in shift registers of p-stable elements with feedback through modulo-p adders, but binary generators have received almost exclusive application in view of their relative ease of implementation. Tristable devices have been realized [16], but p-stable devices with no transitional constraints do not exist for $p > 3$. DARNELL [3] has synthesized a p-stable generator

by (p-1) binary shift registers. However, weighted summation of a number of outputs of one or more binary shift register generators is considered to afford the most flexible and economical method of generating multilevel sequences. This will be examined in detail in the latter part of the Chapter.

2.2. THE SHIFT REGISTER GENERATOR

A shift register, comprising n bistable elements connected sequentially so that a pattern of states progresses along its length by one digit at each clock pulse, is commonly used to store an n digit binary number. It can be used to store certain sequences of lengths greater than n when some form of feedback from various bistables to the register input is provided.

Figure 2.1.

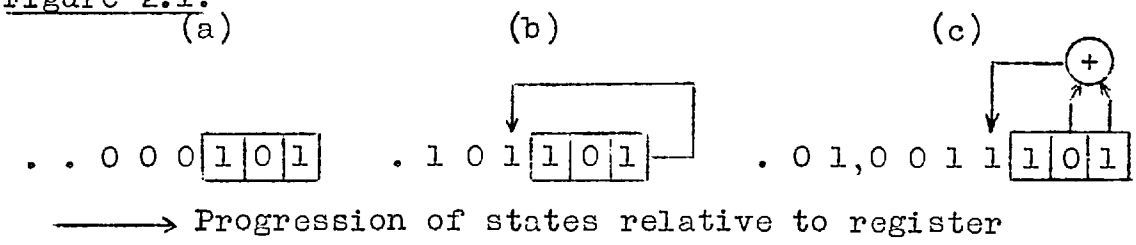

Figure 2.1(a) represents a 3 stage register in the state 101. On clocking the register, the final stage executes the sequence 1010000.., all subsequent digits being zero. The sequence can be made periodic by a direct

output-input feedback connection, as in Figure 2.1(b). A more complex feedback arrangement which combines the outputs of stages 2 and 3 in a modulo-2 adder (for which the rules appear in Table 2.2, Section 2.3.4) results in a sequence of length 7, as in Figure 2.1(c). For any finite register with feedback, there is a limit to the period of the generated sequence since if any previously generated state of the register reappears the feedback arrangement causes the whole sequence to be repeated. Thus periodicity is established, and since there are only 2^n distinct states of an n stage register and a new state appears at each clock pulse, the maximum period is 2^n. In a "linear" generator, where feedback is obtained through modulo-2 addition, the all-zeros state must be excluded since this is self perpetuating. Maximum length is therefore 2^n-1.* A sequence of period 2^n-1 digits is known as a maximal length sequence (m-sequence) and suitable feedback connections can always be found for a register of any length.

An m-sequence is defined uniquely by the feedback arrangement since it contains all possible register states, and initial loading of the register only affects the "phase" of the sequence. There are 2^{n-1} possible feedback arrangements for an n stage register however, and most of these

*A class of non-linear generators exists which use non-linear logic in the feedback path and can realize the maximum period of 2^n digits. These sequences do not have the Shift and Add property however (Sec. 2.3.3), and are of little interest here.

generate non-maximal length sequences. In such cases, the sequence depends on the initial state of the register as well as the feedback connections. The problems of how many and which connections generate m-sequences will be discussed later, but first the randomness properties of these sequences will be established.

2.3. BINARY M-SEQUENCES

2.3.1. Statistical Properties

The maximum sequence length obtainable from an n stage shift register with linear feedback is 2^n-1 digits, and this includes all combinations of n 1's and 0's except the all-zeros state. From this statement, the randomness properties of the m-sequence which liken one period to the outcome of 2^n-1 tosses of an unbiased coin can be deduced.

A run of r zeros within the sequence is defined by a 1 followed by r 0's and a 1 ; and so there are 2^{n-r-2} combinations of n digits (the all-zeros state not being one of them) which contain one run, or more, of r zeros. An m-sequence thus contains 2^{n-r-2} runs of r 0's, and by a similar argument, 2^{n-r-2} runs of r 1's

.....for $0 < r < n-1$.

In addition, for $r = n$ there is one run of r 1's, but no

run of r 0's ;

for r = n-1 the two combinations of (n-1) 1's and a 0 must lie adjacent to the all 1's state, and so there are no true runs of (n-1) 1's. There is however one run of (n-1) 0's and this accounts for both combinations of (n-1) 0's and a 1.

The total number of runs in the sequence is therefore

$$2 + 2\sum_{r=1}^{n-2} 2^{n-r-2} = 2^{n-1}$$

and of these, 2^{n-2} are runs of single digits (1's or 0's)

2^{n-3} are doublets

etc.....

Thus the sequence contains just one more 1 than 0, and of all the runs, half are of single digits, one quarter are doublets, one eighth are triplets, etc.

2.3.2. Generation of M-sequences

The determination of which feedback arrangements yield m-sequences for a register of given length is well treated in the literature and only a summary will be given here.

The Feedback Equation

An n stage feedback shift register can be characterized by an n^{th} order polynomial, for which the coefficient of x^i

is 1 if a feedback tap is attached to the ith stage and zero otherwise. Thus a register with taps on stages n,p,q,r,.. has the characteristic polynomial :-

$$f(x) = x^n \oplus x^p \oplus x^q \oplus \ldots \oplus x^r \oplus \ldots \oplus 1$$

where $\oplus$ denotes modulo-2 addition.

Any stages outside the feedback loop have only transient effect on the sequence, or provide a delayed version of this, and cannot influence the generation of the sequence. The polynomial, f(x), is therefore of the order of the final stage to provide feedback. It is assumed that all feedback paths are returned to a single input of the register. BIRDSALL & RISTENBATT[1] considered a multiple return generator, in which adder outputs were connected to two or more stage inputs (including feedforward), but it was shown that every multiple return generator has an equivalent single input configuration.

Successive application of the feedback equation, $f(x) = 0$, to a given initial content of the register can be performed to derive the entire sequence. Substitution of the present state of the ith stage for x^i in the equation

$$x^n \oplus x^p \oplus x^q \oplus \ldots \oplus x^i \oplus \ldots \oplus x^0 = 0$$

gives a value for stage '0', which represents the next state of stage 1. Figure 2.2 illustrates the procedure for a five stage generator.

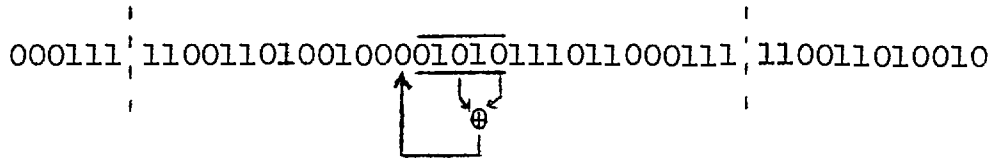

Figure 2.2. 5 stage m-sequence generator with characteristic polynomial $f(x) = x^5 \oplus x^3 \oplus 1$. The next state of stage 1 is given by $x^5 \oplus x^3 \oplus x^0 = 0$, i.e., $x^0 = x^5 \oplus x^3$.

In consequence of the rules of modulo-2 addition, it is evident that an m-sequence generator must have an even number of feedback taps. For an odd number of taps, the all 1's state is self-perpetuating and must be excluded from the sequence.

ZIERLER[37] and ELSPAS[9] have shown that there are exactly $\frac{\phi(2^n-1)}{n}$ feedback arrangements for an n stage register which will produce an m-sequence. $\phi(k)$ is Euler's phi function, and is equal to the number of positive integers less than k and relatively prime to k, including 1. Where k itself is prime, $\phi(k) = k-1$. Thus for the 5 stage generator of Fig. 2.2 only 6 of the possible 16 feedback arrangements produce m-sequences.

GOLOMB[12] derived the following conditions which must be satisfied for maximal length :

(i) f(x) must be irreducible (i.e., cannot be factored modulo-2)

(ii) f(x) must be primitive - i.e., it must not divide into $x^i + 1$ for any $i < 2^n-1$.

Where 2^n-1 is a prime number, condition (i) alone is a sufficient condition.

The principal methods of determining which polynomials generate m-sequences were discussed by Golomb, but all are cumbersome for large n. The Sieve Method consists of writing down all 2^{n-2} nth degree polynomials with an odd number of terms and progressively eliminating those which do not satisfy conditions (i) and (ii). An alternative synthetic approach can be used to generate an m-sequence by a superposition of cyclotomic cosets, from which it is then comparatively simple to derive the polynomial. This approach can also be used as a supplement to the Sieve Method, since it offers a means of ascertaining which irreducible polynomials are not also primitive. Several methods were also given of deriving other maximal length polynomials from one given one of the required order.

PETERSON[26] took the hard work out of generating m-sequences for large n by publishing a list of irreducible polynomials with identification of those which are also primitive. The list is exhaustive up to degree 16 and a selection is then given up to degree 34. For many degrees, polynomials of only 3 terms are given, but the remainder require more complex feedback configurations. Table 2.1[1,26] indicates the number of m-sequences up to degree 20 and gives one example of the simplest feedback arrangement for each degree.

Table 2.1. M-sequence length, number of distinct m-sequences, and examples of characteristic polynomials for a feedback shift register of length 2 - 20 stages.

n	2^n-1	$\frac{1}{n}\phi(2^n-1)$	f(x)
2	3	1	$x^2 \oplus x \oplus 1$
3	7	2	$x^3 \oplus x^2 \oplus 1$
4	15	2	$x^4 \oplus x^3 \oplus 1$
5	31	6	$x^5 \oplus x^3 \oplus 1$
6	63	6	$x^6 \oplus x^5 \oplus 1$
7	127	18	$x^7 \oplus x^3 \oplus 1$
8	255	16	$x^8 \oplus x^4 \oplus x^3 \oplus x^2 \oplus 1$
9	511	48	$x^9 \oplus x^4 \oplus 1$
10	1,023	60	$x^{10} \oplus x^3 \oplus 1$
11	2,047	176	$x^{11} \oplus x^2 \oplus 1$
12	4,095	144	$x^{12} \oplus x^9 \oplus x^3 \oplus x^2 \oplus 1$
13	8,191	630	$x^{13} \oplus x^5 \oplus x^4 \oplus x^2 \oplus 1$
14	16,383	756	$x^{14} \oplus x^{13} \oplus x^4 \oplus x^2 \oplus 1$
15	32,767	1,800	$x^{15} \oplus x^4 \oplus 1$
16	65,535	2,048	$x^{16} \oplus x^5 \oplus x^4 \oplus x^3 \oplus 1$
17	131,071	7,710	$x^{17} \oplus x^3 \oplus 1$
18	262,143	8,064	$x^{18} \oplus x^7 \oplus 1$
19	524,287	27,594	$x^{19} \oplus x^5 \oplus x^2 \oplus x \oplus 1$
20	1,048,575	24,000	$x^{20} \oplus x^3 \oplus 1$

Since the reciprocal of an irreducible, primitive polynomial is likewise primitive and irreducible, the reciprocals of the polynomials in Table 2.1 also yield m-sequences.

For example, for n = 12 :-

$$f(x) = x^{12} \oplus x^{9} \oplus x^{3} \oplus x^{2} \oplus 1$$

$$\overline{f(x)} = 1 \oplus x^{3} \oplus x^{9} \oplus x^{10} \oplus x^{12}$$

It is interesting to note that a generator programmed according to $\overline{f(x)}$ produces the time inverse of the sequence from f(x). This is apparent from the configurations of connections to the register defined by the respective feedback equations. The configurations are identical apart from lateral inversion.

2.3.3. The Shift and Add Property

The autocorrelation function of the m-sequence can be derived from its characteristic "Shift and Add" property, by which addition, modulo-2, of a sequence to itself shifted by an integral number of digits yields a further shifted version of the same sequence. The property follows from the fact that an m-sequence is completely defined by its feedback equation.

Consider an m-sequence, A_0, of length $N = 2^n-1$:

$a_1\ a_2\ a_3\ .\ .\ .\ a_N$ where a_i is either 0 or 1.

The generator feedback equation can be written as a

recurrence relation, so that if there are feedback taps on stages n,p,q,...r :

$$a_0 \ (= a_N) = a_n \oplus a_p \oplus a_q \oplus . \ . \ . \oplus a_r$$

With a shift of k digits, k ≠ 0, N, 2N,.. , A_k is given by :

$$a_k \ (= a_{N+k}) = a_{n+k} \oplus a_{p+k} \oplus a_{q+k} \oplus . \ . \ . \oplus a_{r+k}$$

The sequence, A', obtained by term-by-term addition of A_0 to A_k, therefore satisfies the relation :

$$a_0 \oplus a_k = (a_n \oplus a_p \oplus . \ . \oplus a_r) \oplus (a_{n+k} \oplus a_{p+k} \oplus . \ . \oplus a_{r+k})$$

$$= (a_n \oplus a_{n+k}) \oplus (a_p \oplus a_{p+k}) \oplus . \ . \oplus (a_r \oplus a_{r+k})$$

$$\text{i.e.,} \quad a'_0 = a'_n \oplus a'_p \oplus a'_q \oplus . \ . \ . \oplus a'_r$$

i.e., A' must be generated by the same feedback arrangement as A and is therefore simply a shifted version of A for any k, which is not a multiple of N.

2.3.4. Autocorrelation

In the previous Sections, the m-sequence has been considered in terms of binary numbers 0 and 1. These are the conventional states of Boolean Algebra, but to determine the autocorrelation function it is desirable to remove the d.c. component. Consider therefore the binary sequence, B, which is derived from the m-sequence A by exchanging 0 for -1, and 1 for +1. In this transformation, modulo-2 addition is

equivalent to multiplication together with a sign change, as shown in Table 2.2.

$\oplus$	0	1
0	0	1
1	1	0

Modulo-2 addition

$\overline{\oplus}$	0	1
0	1	0
1	0	1

Inverse modulo-2 addition

X	-1	+1
-1	+1	-1
+1	-1	+1

X Multiplication

Table 2.2. Rules of multiplication and modulo-2 addition.

The autocorrelation coefficients of B will be defined :

$$R_r = \sum_{i=1}^{i=N} b_i \text{ X } b_{i+r}$$

where $b_i \text{ X } b_{i+r} \equiv a_i \overline{\oplus} a_{i+r}$.

But from the Shift and Add property : $a_i \overline{\oplus} a_{i+r} = \overline{a}_{i+d}$, provided that $r \neq 0, \pm N, \pm 2N$, etc., and where the shift d depends only on r for the particular S.R.G.

Hence, $$R_r = \sum_{i=1}^{i=N} \overline{b}_{i+d} \qquad r \neq 0, \pm N, \pm 2N, \ldots$$

and since B contains one more -1 than +1,

$$R_r = -1 \qquad r \neq 0, \pm N, \pm 2N, \ldots$$

When r = 0, or a multiple of N,

$$R_0 = \sum_{i=1}^{N} (b_i)^2 = N$$

The normalized autocorrelation coefficients are therefore :

$$R_r = 1 \qquad |r| = 0,\ N,\ 2N,\ \ldots$$
$$= -1/N \quad \text{elsewhere.}$$

To obtain the autocorrelation function $R(\tau)$, it is necessary to introduce time as a continuous variable. The m-sequence becomes $B(t)$, and autocorrelation is defined :

$$R(\tau) = \int_{t=0}^{t=N\delta} B(t).B(t+\tau)\, dt.$$

where δ is the S.R.G. clock period.

Clearly, $R(\tau) = R_r$ at $\tau = r\delta$

and if $B(t)$ changes instantaneously and only at integral multiples of the clock period, then $R(\tau)$ is piecewise linear and values between $r\delta$ can be found by interpolation. Figure 2.3 shows the normalized autocorrelation function of the binary m-sequence.

2.3.5. Power Spectrum

The Wiener-Khintchine Theorem relates the power spectrum of a signal to the Fourier cosine integral of its autocorrelation function [14]. The m-sequence has a similar autocorrelation function to that of a narrow, rectangular periodic pulse and its power is confined to harmonics of the repetition frequency $1/N\delta$. The envelope of the "one sided"

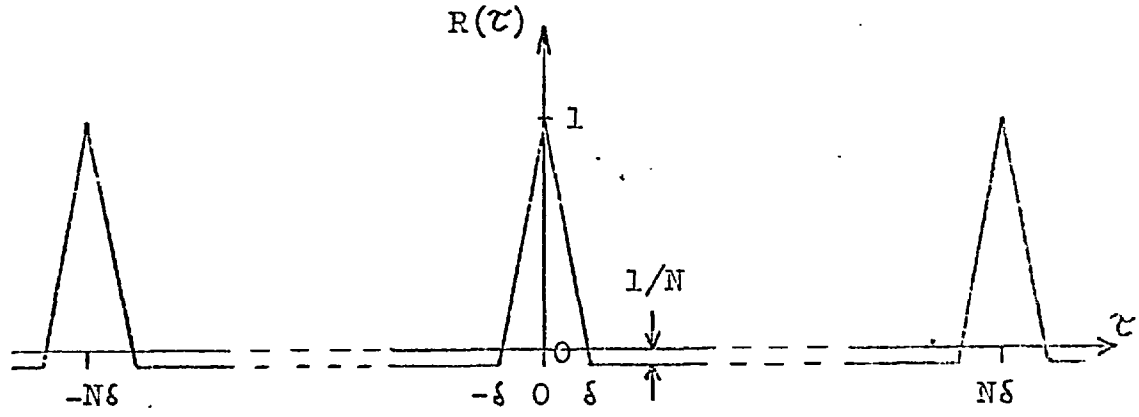

Figure 2.3. Normalized autocorrelation function of the binary m-sequence.

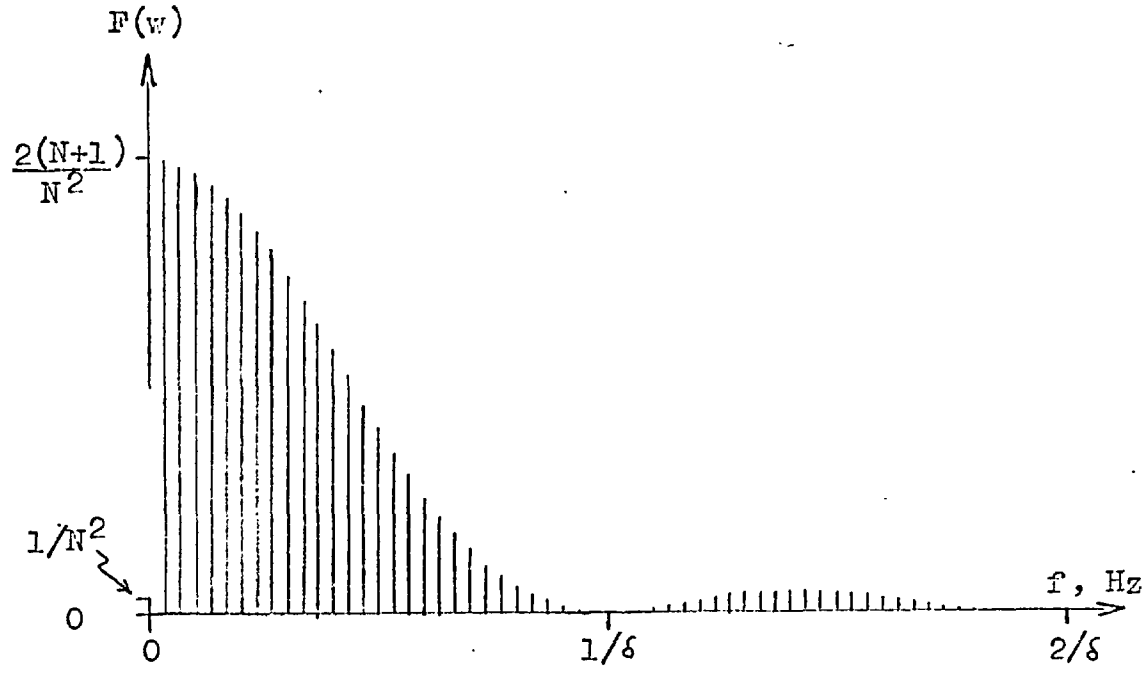

Figure 2.4. M-sequence power spectrum. Line spacing = 1/Nδ, where δ is the register clock period.

power spectrum, in which all power is contained in the positive frequency range, is defined by

$$F(w) = \frac{4}{N\delta}\int_0^{N\delta/2} R(\tau).\cos w\tau d\tau.$$

In Figure 2.3, $R(\tau)$ has a remanent d.c. component of $-1/N$ and this corresponds to the d.c. power $1/N^2$ shown in Figure 2.4. Referred to this out-of-phase correlation, $R(0)$ becomes $(\frac{N+1}{N})$ and the envelope of the line spectrum is given by :

$$F(w) = \frac{4(N+1)}{N^2\delta}\int_0^{\delta}(1 - \frac{\tau}{\delta}).\cos w\tau d\tau$$

$$= \frac{2(N+1)}{N^2}\left(\frac{\sin\delta w/2}{\delta w/2}\right)^2$$

The form of $F(w)$ is shown in Figure 2.4. Since the power of the m-sequence is determined only by its amplitude, the power density spectrum has a scaling factor inversely proportional to the sequence length. If the period of the sequence is doubled, the lines in the spectrum become twice as dense and the power of each is halved.

2.3.6. Cross-correlation Between M-sequences

The cross-correlation between two m-sequences of similar lengths but different feedback polynomials is not as uniform as their out-of-phase autocorrelation. JUDGE[22] has shown that the cross-correlation of two m-sequences of length 2^n-1 is similar to the autocorrelation of a non-maximal length sequence generated by a 2n stage register. Maximum correlation increases with the number of factors contained in 2^n-1, and correlation peaks occur at shifts which contain these factors. In particular, GOLOMB[13] proposed that the maximum normalized cross-correlation between sequences of prime length is of the order of $1/\sqrt{N}$. Correlation between sequences which are time inverses was also considered and found to exhibit much more irregularity than unconnected sequences.

2.4. NON-MAXIMAL LENGTH BINARY SEQUENCES

The autocorrelation function of the m-sequence is well behaved when computed over an integral number of periods. The out-of-phase correlation has none of the random fluctuation expected of random noise, and it is this property which makes the prbs so useful in control systems. However, in situations where the integration time is only a fraction of the sequence period, knowledge of the short-

term randomness properties is more relevant. The remaining Chapters of this thesis are concerned with such a situation, in which pseudo-random noise is to be displayed as a video signal. At any location in the television image, the eye may integrate over only a small part of the sequence period.

Local, or short term, randomness of the m-sequence is a similar consideration to the autocorrelation of non-maximal length sequences, all of which are simply parts of m-sequences. It has already been stated that of the 2^{n-1} possible feedback configurations for an n stage register, most generate non-maximal length sequences. However, no comprehensive theory exists, as for the m-sequence, capable of specifying a feedback polynomial for a particular sequence length. The procedure is rather to set an initial state in an m-sequence generator and to use a set of AND gates to recognize the final state of the required sequence (length less than 2^n-1), and then to reset the register to the initial state before the next clock pulse occurs [18].

Non-maximal length sequences exhibit a partial shift and add property in that only certain shifts give the original sequence. This emerges from the discussion of Sec.2.3.3 in view of the fact that the feedback equation is not sufficient to determine a non-maximal length sequence, unless a specified state of the register is included.

For the m-sequence, autocorrelation over only L terms,

where $L < N$, is given by :

$$R'_r = \sum_{i=1}^{L} (b_{i+d})^2 = L \qquad |r| = 0,\ N,\ 2N,\ .$$

$$= \sum_{i=1}^{L} \overline{b}_{i+d} \qquad \cdot \text{elsewhere.}$$

GOLOMB[13] considered that the only non-randomness exhibited by the m-sequence lies in its tendency to compensate such that the expected statistics are obtained precisely over one period, and that in the short term the prbs is"truly random!" It was shown that the likely value of R'_r tends to be about the same as for a truly random process, although the absolute maximum value is smaller for the prbs.

HEATH[17] was concerned with local non-randomness due to the constraint of the feedback arrangement. This is particularly evident for generators which only have adjacent

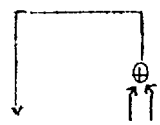

100010 111100 101000 110000 100000 111111 .....

Figure 2.5. Part of the m-sequence generated according to $x^6 \oplus x^5 \oplus 1 = 0$, showing local unbalance of 0's & 1's.

feedback taps at the end of the register. Figure 2.5 shows part of the sequence generated according to the polynomial

$x^6 \oplus x^5 \oplus 1 = 0$, which has a characteristic local unbalance of 0's and 1's. Six successive sextuples terminate in runs of 1,2,3,4,5 and 0 zeros, respectively.

In the latter part of this Chapter, the well behaved m-sequence autocorrelation function is used to analyse operations on one or more prbs to generate multilevel sequences. It is confirmed experimentally in Chapter 3 that local non-randomness is not subjectively detectable in a displayed sequence, and that this analysis is valid.

2.5. SOME BINARY OPERATIONS ON M-SEQUENCES

2.5.1. Generation of Orthogonal Sequences

If an m-sequence A (of period N) is added modulo-2 to a sequence G, which has period M such that M and N are coprime, then the resulting sequence AG has period MN. It can be shown (BRIGGS & WILLIAMS[21]) that the cross-correlation between two such sequences, AG_1 and AG_2, is of the form $R_{12} \cdot R_{AA}$, where R_{12} refers to the cross-correlation coefficients of G_1 and G_2, and R_{AA} to the autocorrelation coefficients of A. It is comparatively simple to devise very short sequences, G, which are mutually orthogonal - i.e., have zero cross-correlation at all shifts such that $R_{12} = 0$. The long sequences AG are then also orthogonal.

The autocorrelation of one of the sequences, AG_1, is given by $R_{11} \cdot R_{AA}$, and this has peaks within the period MN at multiples of N.

Orthogonal sequences can be obtained as the rows or columns of Hadamard matrices, which exist for orders 2, 4 and most multiples of 4. Those matrices of order 2^{ε}, where ε is an integer, are particularly simple to construct using the recurrence relation

$$H_{2i} = \begin{bmatrix} H_i & H_i \\ H_i & -H_i \end{bmatrix} \qquad \text{where } i = 2^{\varepsilon}, \text{ and } H_1 = 1.$$

Thus :

$$H_2 = \begin{bmatrix} 1 & 1 \\ 1 & -1 \end{bmatrix} \; ; \quad H_4 = \left[\begin{array}{cc:cc} 1 & 1 & 1 & 1 \\ 1 & -1 & 1 & -1 \\ \hdashline 1 & 1 & -1 & -1 \\ 1 & -1 & -1 & 1 \end{array}\right]$$

One matrix of order 2i may not necessarily generate 2i uncorrelated sequences as some rows are merely cyclicly shifted versions of others - for example, rows 3 and 4 of H_4 - and are therefore not orthogonal for every shift.

2.5.2.

As an example of the generation of uncorrelated sequences, consider two sequences G_1 and G_2 given by the rows of H_2. G_1 is simply a constant +1, so that the product $AG_1 = A$.

G_2 is a square wave of half the clock frequency and is clearly orthogonal to G_1. G_2 has autocorrelation :

$$R_{22} = +1 \quad \text{for even } r$$
$$= -1 \quad \text{for odd } r$$

The normalized autocorrelation coefficients of AG_2, which has period $2N$, are therefore :

$$R_{22} \cdot R_{AA} = +1 \quad \text{at } r = 0 \text{ and even multiples of } N$$
$$= -1 \quad \text{at } r \text{ equal to odd multiples of } N$$
$$= +1/N \quad \text{at other odd } r$$
$$= -1/N \quad \text{at other even } r$$

The normalized autocorrelation function of AG_2 is therefore as shown in Figure 2.6.

The power spectrum of AG_2 is obtained by Fourier integration of the autocorrelation function shown in Fig.2.6 by which it can be shown that :

$$F(w) = \left(\frac{N+1}{N^2}\,\frac{\sin\delta w/2}{(\delta w/2)}\right)^2 (1 - \cos Nw\delta) + \frac{2}{N}\left\{\frac{\sin\delta w}{\delta w} - \left(\frac{\sin\delta w/2}{\delta w/2}\right)^2\right\}$$

envelope of lines at harmonics of $1/2N\delta$. — envelope of lines at harmonics of $1/2\delta$.

The latter term arises from the low amplitude triangular fluctuation of period 2δ in the autocorrelation function and causes reduction of lines at harmonics of $1/2\delta$ in the power spectrum. The spectrum is shown in Figure 2.7 and is similar to that of the original m-sequence (see Fig.2.4)

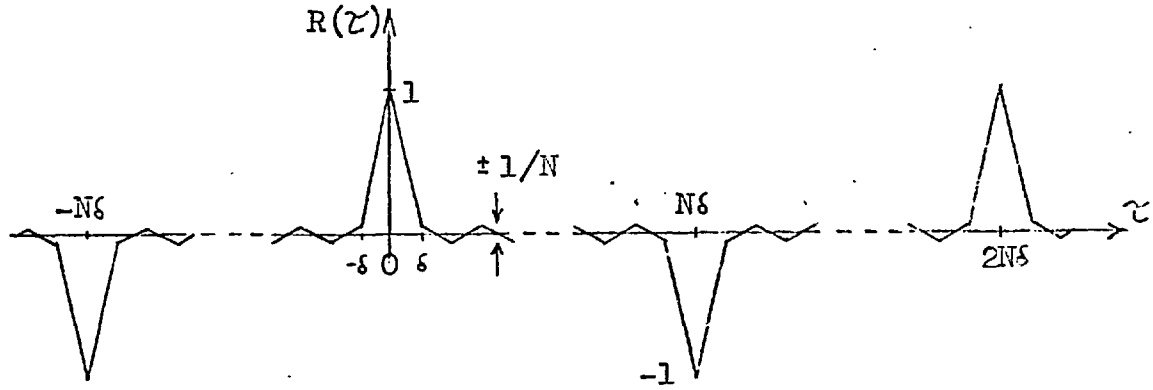

Figure 2.6. Normalized autocorrelation function of an m-sequence with alternate digits inverted.

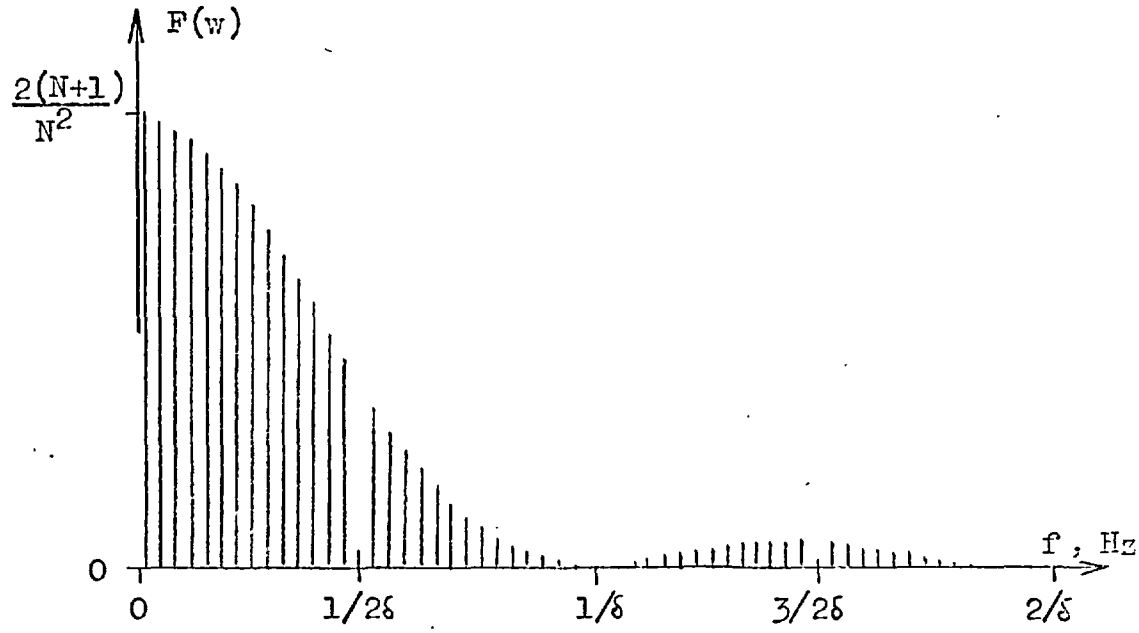

Figure 2.7. Power spectrum of an m-sequence with alternate digits inverted. Lines are at odd multiples of $1/2N\delta$.

except that the lines exist at odd multiples of $1/2N\delta$ and therefore interleave with those of the original m-sequence. This is evidence of the independence of the sequences AG_1 and AG_2.

2.5.3.

A particularly useful sequence can be obtained by clocking the generator at half the previous frequency, so that transitions now only occur at multiples of 2δ, and again adding the output (modulo-2) to a square wave of period 2δ. As in the previous Section, the autocorrelation coefficients are given by the products of the respective coefficients of the prbs and square wave :

$$
\begin{aligned}
R_r &= (+1).(+1) = +1 && \text{at } |r| = 0 \text{ and multiples of } 2N \\
&= (+\tfrac{1}{2}).(-1) = -\tfrac{1}{2} && \text{at } |r| = 1,\ 2N \pm 1,\ \ldots \\
&= (-\tfrac{1}{N}).(+1) = -\tfrac{1}{N} && \text{at other even } r \\
&= (-\tfrac{1}{N}).(-1) = +\tfrac{1}{N} && \text{at other odd } r
\end{aligned}
$$

The corresponding autocorrelation function for this sequence is shown in Figure 2.8.

Again the power spectrum is obtained by Fourier integration of the autocorrelation function. From Fig.2.8, assuming $N \gg 1$:

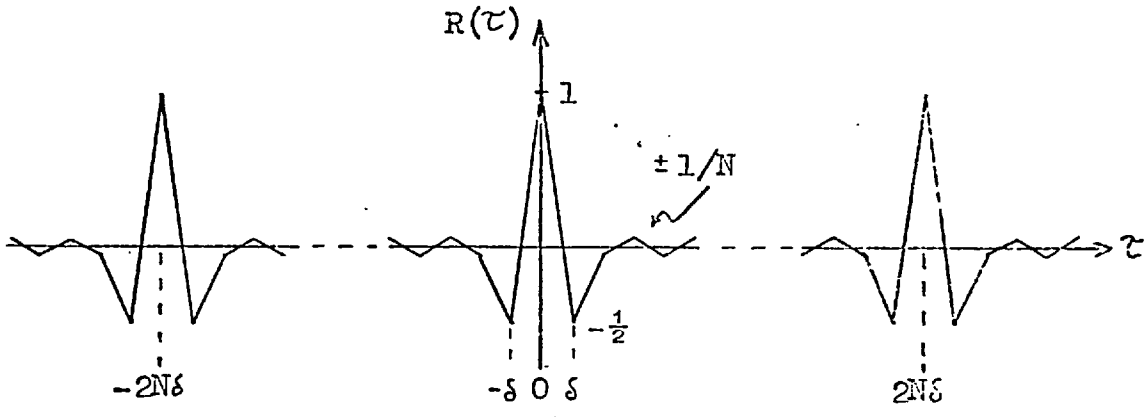

Figure 2.8. Normalized autocorrelation function of a half-rate m-sequence modulated by a square wave of frequency $\frac{1}{2\delta}$ Hz.

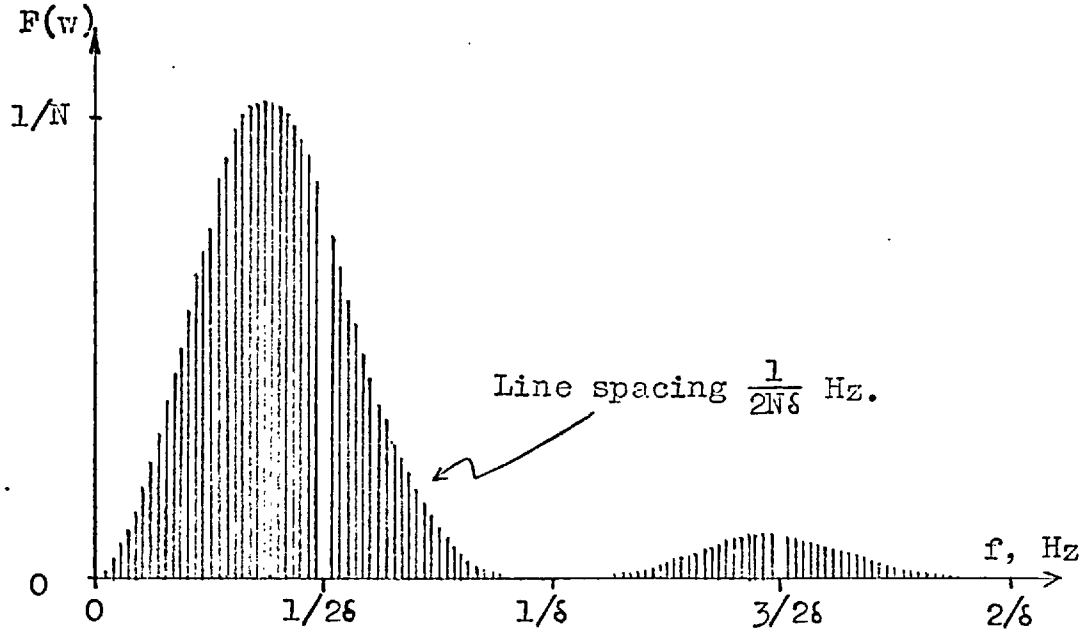

Figure 2.9. Power spectrum of a half-rate m-sequence modulated by a square wave of frequency $\frac{1}{2\delta}$ Hz.

$$F(w) = \frac{4}{2N\delta}\int_0^{\delta}(1-\frac{3\tau}{2\delta})\cos w\tau d\tau - \frac{4}{2N\delta}\int_{\delta}^{2\delta}(1-\frac{\tau}{2\delta})\cos w\tau d\tau$$

(envelope of lines @ harmonics of $1/2N\delta$)

$$- \frac{4}{2N\delta}\int_0^{\delta}(1-\frac{2\tau}{\delta})\cos w\tau d\tau$$

(envelope of lines @ harmonics of $1/2\delta$)

On evaluation, this reduces to :

$$F(w) = \underbrace{\frac{2}{N}\left\{\frac{\sin^2 \delta w/2}{\delta w/2}\right\}^2}_{\text{envelope of lines at harmonics of } 1/2N\delta} + \underbrace{\frac{2}{N}\left\{\frac{\sin\delta w}{\delta w} - \left(\frac{\sin\delta w/2}{\delta w/2}\right)^2\right\}}_{\text{envelope of lines at harmonics of } 1/2\delta}$$

The spectrum envelope is given by the first term, which is plotted in Figure 2.9 , and the latter term cancels the lines at harmonics of $1/2\delta$ Hz. Since the period of the prbs has been doubled, the line density is twice that of Figure 2.7 , but the amplitude scale of the envelope has been halved. The total power within the two envelopes is thus the same, as would be expected. Figure 2.9 illustrates the approximate frequency translation of the half-bandwidth m-sequence spectrum to a centre frequency $1/2\delta$ Hz, which is intuitively expected of this modulation process.

2.6. MULTILEVEL SEQUENCES FROM A SINGLE M-SEQUENCE

The remainder of this Chapter is devoted to the generation of multilevel pseudo-random noise from a binary m-sequence. Multilevel noise has been obtained from low-pass filters excited by a prbs input [25, 27, 29], but the S.R.G. must be clocked several times faster than the highest noise frequency component required. Furthermore, the output must be resampled if the noise is required in digital form. This Section considers an alternative digital filtering process on a single m-sequence which retains the noise in sampled form.

Weighted summation of the contents of a number of S.R.G. stages produces a multilevel pseudo-noise waveform of identical period to the prbs and offers a wide range of amplitude distributions and power spectra. DAVIES [5] has recently applied the z-transform methods of RADER & GOLD [28] to digital filtering of binary sequences, but the following analysis uses autocorrelation techniques to determine power spectra corresponding to particular weighting functions. One advantage of this method will become evident in Chapter 3 in considering two-dimensional spectra of television noise.

2.6.1.

Consider 'm' S.R.G. outputs combined in a weighting network which will be referred to as the "decoder". The m bistables are not necessarily adjacent in the register, but may span 'g' digits of the binary sequence as indicated in Figure 2.10. Clearly if $g > n$, additional bistables must be provided as delay elements to give access to the required length of sequence.

In establishing amplitude distributions of the decoder output it is convenient to first consider the input as a "complete" binary sequence of length 2^n containing all combinations of n binary digits. Allowance can then be made for the exclusion of the all-zeros state in the prbs, which differs from the complete sequence by one zero in the longest run of zeros. The decoded prbs therefore differs from the decoded complete sequence by the exclusion of one number and changes to (g-1) others in a manner dependent upon the register feedback configuration and the arrangement of the m readout locations over the g bistables. In cases where $g \leq n$, the sole modification to the complete distribution is the exclusion of one number.

The number and distribution of levels in the decoded sequence are determined by the weighting coefficients which are assigned to the respective readout locations by the decoder. These will be designated w_1 , w_2 , w_3 , . . w_g ,

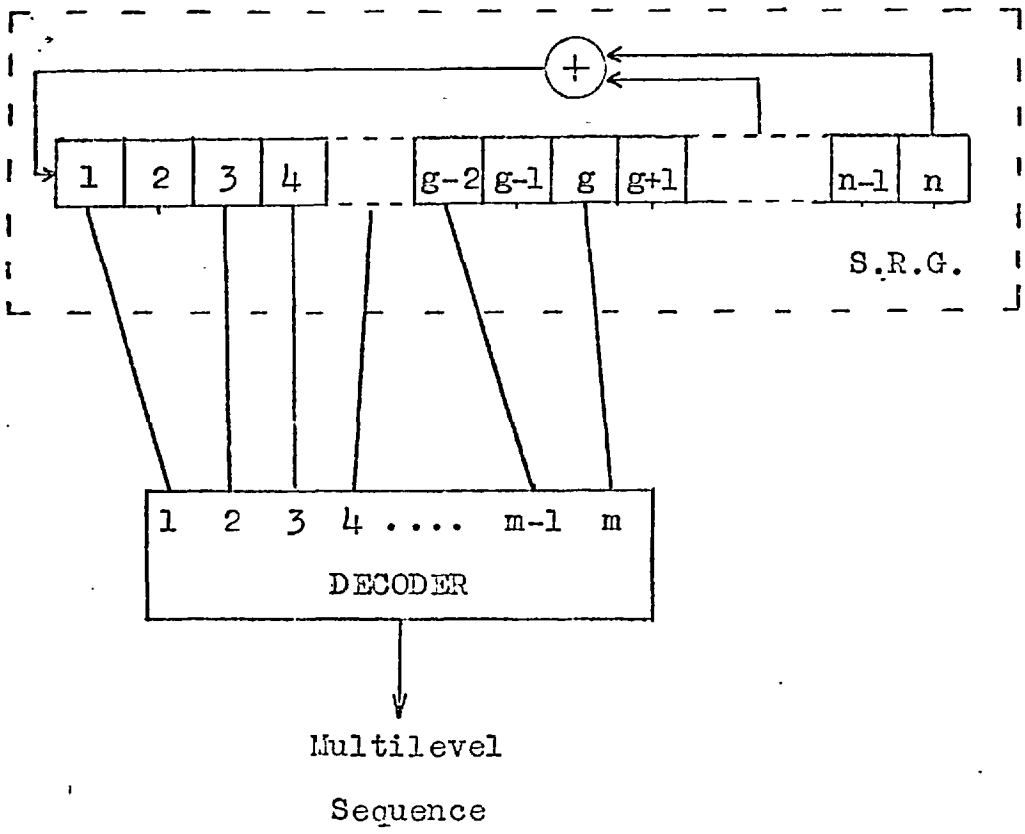

Figure 2.10. Generation of a multilevel sequence using a single binary S.R.G.

where $w = 0$ for locations within the span of g bistables which are not connected to the decoder input. The multi-level sequence can be written $(w_1B_1 + w_2B_2 + \ldots + w_gB_g)$. The autocorrelation function is broader (within one period) than for the prbs due to transitional constraints imposed by the decoder. The autocorrelation coefficients are given by

$$R_r = \sum_{\text{period}} (w_1B_1 + w_2B_2 + \ldots + w_gB_g).(w_1B_{r+1} + \ldots + w_gB_{r+g})$$

By substituting $\sum_{\text{period}} B_iB_{r+i} = N$ for $|r| = 0, N, 2N, \ldots$

$= -1$ elsewhere

it follows that within one period :

$$R_r = (N+1)\sum_{i=1}^{g-r} w_i.w_{i+r} - \left(\sum_{i=1}^{g} w_i\right)^2$$

for $|r| = 0, 1, \ldots (g-1)$.

$$= -\left(\sum_{i=1}^{g} w_i\right)^2 \qquad \text{elsewhere.}$$

For the decoded complete sequence, which has zero out-of-phase autocorrelation, the coefficients are more simply :

$$R_r = (N+1)\sum_{i=1}^{g-r} w_i.w_{i+r} \qquad |r| = 0, 1, 2, \ldots (g-1).$$

$$= 0 \qquad \text{elsewhere}$$

The non-zero coefficients can alternatively be quickly

determined from the symmetric g x g matrix of cross products

$$\begin{bmatrix} w_1^2 & w_1w_2 & \cdots & w_1w_g \\ w_2w_1 & w_2^2 & & \\ \vdots & & \ddots & \\ w_gw_1 & & & w_g^2 \end{bmatrix}$$

"Readout Matrix"

Each coefficient is obtained by summing along the corresponding diagonal parallel to the leading diagonal. Where N is large, these may also be taken as the coefficients for the decoded prbs.

The above operations are illustrated in the following Sections for two particular decoders of interest, which generate uniform and binomial amplitude distributions respectively.

2.6.2. Uniform Amplitude Distribution

The m binary inputs to the decoder can be regarded as the binary specification of a selection from 2^m decimal numbers. Each of the 2^m distinct patterns of digits appears exactly 2^{n-m} times within one period of the complete sequence, so that a uniform distribution over 2^m levels is obtained at the decoder output. The decoder is realized by a ladder network which assigns increasing powers of $\frac{1}{2}$ to the

weights w. The network shown in Figure 2.11(a) attaches greatest significance to input 1, and for low impedance sources has output impedance R.*

If the m readout locations are contained within the length of the register ($g \leq n$), exclusion of the all-zeros state from the complete sequence results only in the loss of one of the 2^{n-m} most negative numbers per period.

Of particular interest is the case where the readout locations are compact and $g = m$. The weighting coefficients are then

$$w_i = \left(\tfrac{1}{2}\right)^i$$

and the approximate autocorrelation coefficients from the readout matrix become (within one period) :

$$R = \sum_{i=1}^{m} w_i^2 = \frac{1}{4}\sum_{i=0}^{m-1}\left(\tfrac{1}{4}\right)^i = \frac{1}{3}\left(1 - \left(\tfrac{1}{4}\right)^m\right) \qquad r = 0$$

$$= \sum_{i=1}^{m-1} w_i \cdot w_{i+1} = \frac{1}{8}\sum_{i=0}^{m-2}\left(\tfrac{1}{4}\right)^i = \frac{1}{6}\left(1 - \left(\tfrac{1}{4}\right)^{m-1}\right) \qquad r = \pm 1$$

$$= \sum_{i=1}^{m-2} w_i \cdot w_{i+2} = \frac{1}{16}\sum_{i=0}^{m-3}\left(\tfrac{1}{4}\right)^i = \frac{1}{12}\left(1 - \left(\tfrac{1}{4}\right)^{m-2}\right) \qquad r = \pm 2$$

$$= \quad " \qquad\qquad " \qquad\qquad " \qquad\qquad "$$

$$= w_1 \cdot w_m = \left(\tfrac{1}{2}\right)^{m+1} \qquad r = \pm(m-1)$$

$$= 0 \qquad \text{elsewhere.}$$

---

* If the binary source impedances are not small relative to R, an additional 2R resistor must be shunted across the ladder output in order to equalize the ladder input impedance for every binary source.

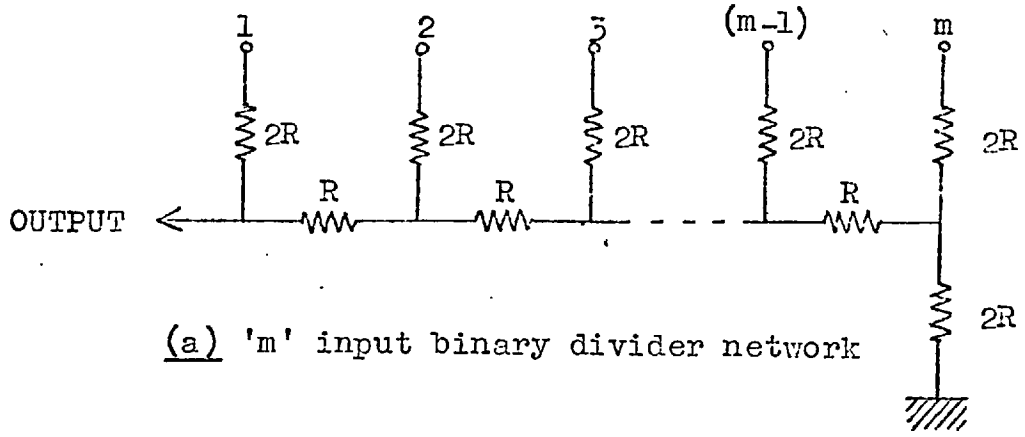

(a) 'm' input binary divider network

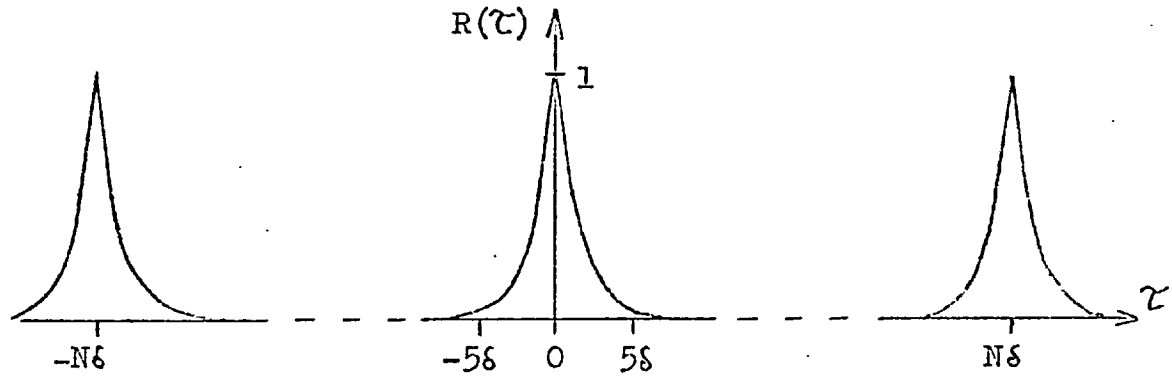

(b) Normalized autocorrelation function (for large m)

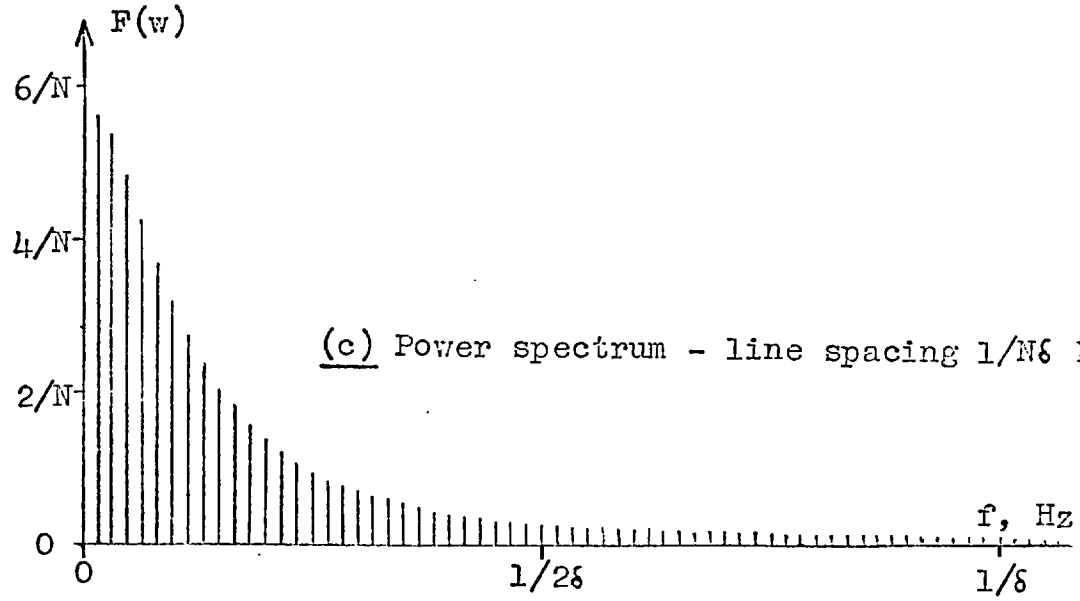

(c) Power spectrum - line spacing 1/Nδ Hz.

Figure 2.11. Multilevel pseudo-random noise with uniform amplitude distribution.

For large m, the normalized autocorrelation function can be approximated by

$$R(\tau) = (\tfrac{1}{2})^{\tau/\delta}$$

as shown in Figure 2.11(b).

The envelope of the power spectrum becomes :

$$F(w) = \frac{4}{N\delta}\int_0^{N\delta/2} (\tfrac{1}{2})^{\tau/\delta}.\cos w\tau \, d\tau$$

and the line spacing, $1/N\delta$ Hz.

If N is large, the envelope can be evaluated to give

$$F(w) \qquad \frac{4\log_e(2)}{N(\log_e^2(2) + w^2\delta^2)}$$

The form of this spectral distribution is illustrated in Figure 2.11(c).

2.6.3. Binomial Amplitude Distribution

Consider a decoder which adds with equal weight its m selections from a complete binary sequence. DAVIES[4] has devised a recurrence relation to determine the resulting amplitude distribution for a generalized modulo-p generator, but the binary case can easily be shown to produce a binomial distribution. Each of the 2^m distinct patterns of digits occurs 2^{n-m} times within one period of the sequence, and ${}^mC_i$ of these patterns contain exactly i +1's and

(m-i) -1's. Patterns containing i +1's are decoded into the number (2i-m) and this number occurs $2^{n-m} . {}^{m}C_{i}$ times within one period. A range of numbers

$$-m, -(m-2), \ldots (2m-i), \ldots (m-2), m$$

is therefore obtained with a binomial distribution. As the number of readouts (m) increases, the distribution tends to Gaussian. If $g \leq n$, exclusion of the all-zeros state from the complete sequence results only in the loss of one number '-m' per period.

If the readout locations are compact such that $g = m$, then $w_1 = w_2 = w_3 = \ldots = w_m = 1/m$, and the auto-correlation coefficients (for large N) become :

$$R_r = \sum_{i=1}^{m-r} (1/m)^2 \qquad \text{at } |r| = 0, 1, 2, \ldots (m-1)$$

$$= 0 \qquad \text{elsewhere.}$$

The corresponding normalized autocorrelation function is shown in Figure 2.12(a). It follows that the envelope of the power spectrum is given by

$$F(w) = \frac{4}{N\delta} \int_{0}^{m\delta} (1 - \tau/m\delta) . \cos w\tau \, d\tau$$

$$= \frac{2m}{N} \left(\frac{\sin(mw\delta/2)}{mw\delta/2} \right)^2$$

and the line spacing, $1/N\delta$ Hz.

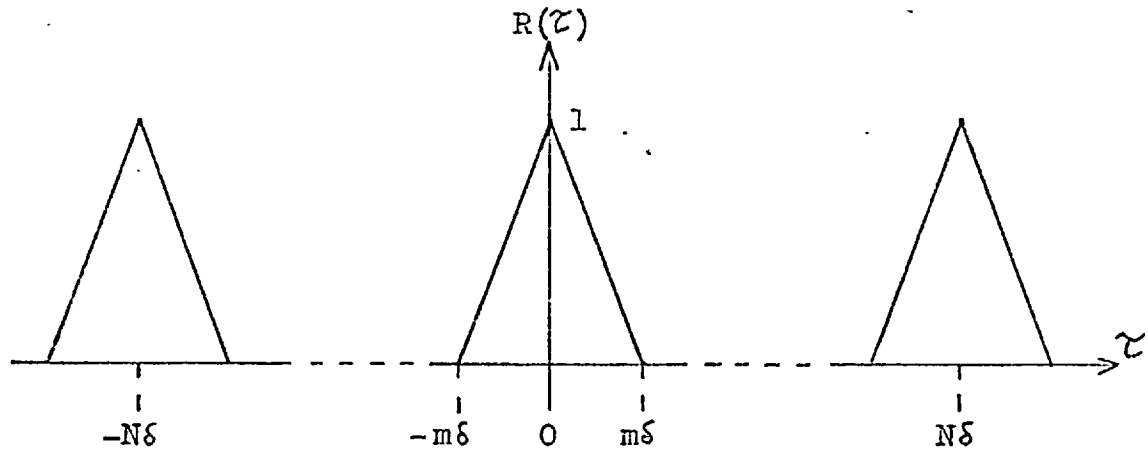

(a) Normalized autocorrelation function

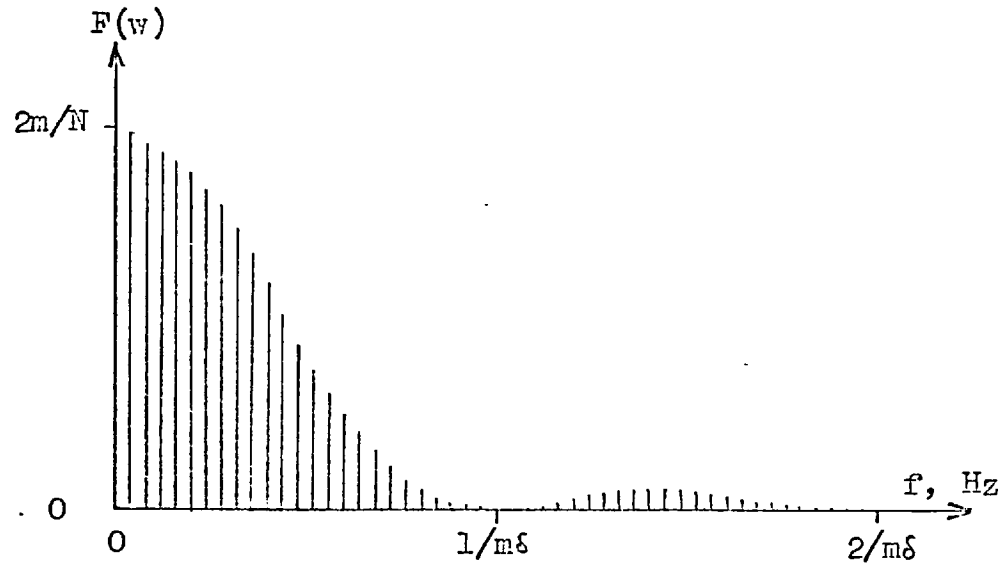

(b) Power spectrum - line spacing 1/Nδ Hz

Figure 2.12. Multilevel pseudo-random noise with binomial amplitude distribution.

The power spectrum for this (m+1) level sequence is shown in Figure 2.12(b), and it can be seen that this is similar to that of a prbs from a register clocked at one m^{th} of the previous rate. Summation of adjacent register outputs with equal weight thus effects digital low-pass filtering of the prbs.

2.6.4. Spread Correlation

The two multilevel sequences considered above show that decoding neighbouring register outputs causes bandlimiting of the basic prbs power spectrum. However, the Shift and Add property allows access to the entire sequence so that the decoder inputs can be spread over the sequence period.

In particular, consider two readout locations, assigned equal weight of $\frac{1}{2}$ and spaced by 'p' digit periods, where $0 < p < N$. The resulting three level sequence has auto-correlation coefficients :

$$\begin{aligned} R_r &= \tfrac{1}{2} && |r| = 0,\ N,\ 2N,\ \ldots \\ &= \tfrac{1}{4} && |r| = p,\ N \pm p,\ 2N \pm p,\ \ldots \\ &= 0 && \text{elsewhere} \end{aligned}$$

The power spectrum becomes :

$$F(w) = \frac{2}{N}\left(\frac{\sin \delta w/2}{\delta w/2}\right)^2 \left(\tfrac{1}{2} + \tfrac{1}{4}\cos p\delta w + \tfrac{1}{4}\cos(-p\delta w)\right)$$

$$= \frac{1}{N}\left(\frac{\sin \delta w/2}{\delta w/2}\right)^2 (1 + \cos p\delta w)$$

and the line spacing is $1/N\delta$ Hz.

The spectrum envelope is that of the basic prbs modulated by a sinusoid of which the period is inversely proportional to p. For small p, as in Section 2.6.3, the sinusoid produces bandlimiting of the prbs spectrum. For large p, the sinusoid period is too short to affect the overall shape of the spectrum envelope, but behaves like a comb filter in attenuating or enhancing selected lines. A multilevel sequence can thus be obtained with a similar wideband power spectrum to the basic prbs, provided that the readout locations are sufficiently well spaced over the prbs period. It must be remembered however, that when the pseudo-noise is to be displayed as a television signal, then a two dimensional spatial spectrum should be considered and values of p which are not harmonically related to line or field scanning periods must be chosen to avoid band-limiting or drift effects.

2.6.5. Digital High-pass Filtering

In the decoders considered so far, the weights w have been positive and operations of low-pass or comb filtering have been performed on the prbs spectrum. A high-pass filter can also be realized by including negative weights, i.e., by inverting certain register outputs. As a simple example, consider the decoder of Figure 2.13(a), which

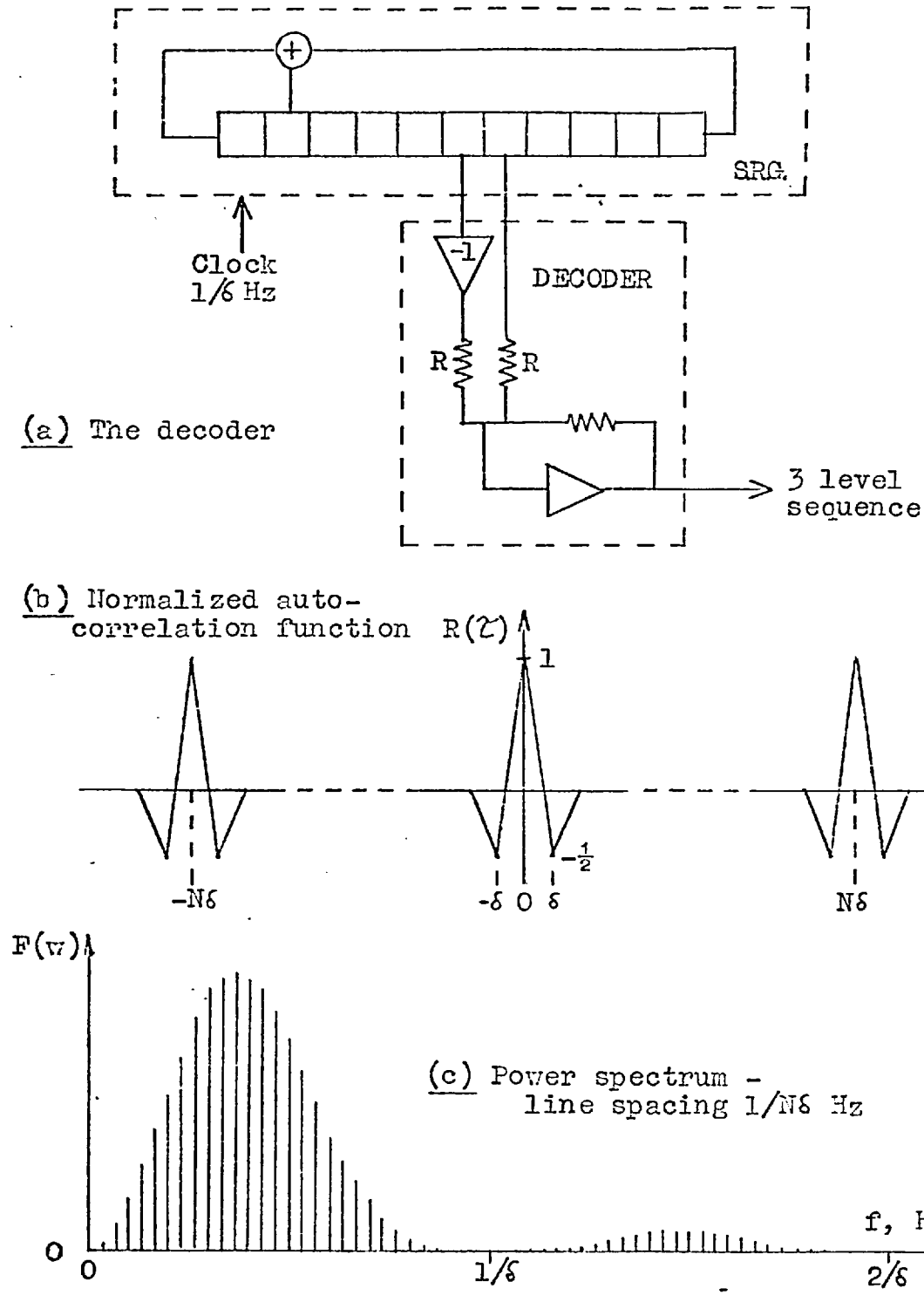

Figure 2.13. Three level sequence from two equally weighted adjacent SRG readouts, one of which is inverted.

assigns respective weights $\frac{1}{2}$ and $-\frac{1}{2}$ to two adjacent register outputs. The Readout Matrix becomes :

$$\begin{bmatrix} \frac{1}{4} & -\frac{1}{4} \\ -\frac{1}{4} & \frac{1}{4} \end{bmatrix}$$

and the corresponding approximate autocorrelation coefficients for the three level sequence are

$$\begin{aligned} R_r \text{ (normalized)} &= 1 \qquad |r| = 0,\ N,\ 2N,\ \ldots \\ &= -\tfrac{1}{2} \qquad |r| = 1,\ N \pm 1,\ 2N \pm 1,\ \ldots \\ &= 0 \qquad \text{at other } r. \end{aligned}$$

The normalized autocorrelation function is shown in Figure 2.13(b).

The envelope of the power spectrum is given by :

$$F(w) = \frac{4}{N\delta}\int_0^{\delta}\left(1 - \frac{3\tau}{2\delta}\right).\cos w\tau\, d\tau + \frac{4}{N\delta}\int_{\delta}^{2\delta}\left(\frac{\tau}{2\delta} - 1\right).\cos w\tau\, d\tau$$

$$= \frac{4}{N}\left(\frac{\sin^2 \delta w/2}{\delta w/2}\right)^2$$

with line spacing $1/N\delta$ Hz.

This spectrum is shown in Figure 2.13(c) and is similar to that of the binary product of a half-rate prbs and a $1/2\delta$ Hz square wave (see Fig.2.9).

2.6.6. Conclusion

Generation of multilevel sequences by digital filtering of the basic prbs has been illustrated in the previous Sections by specific examples rather than by a generalized analysis. However, it is evident that a suitable choice of weighting function and readout pattern on the prbs can realize almost any required amplitude distribution or power spectrum, though these characteristics are clearly interdependent. In this respect, flexibility can be increased by the use of "independent" binary components, such as might be derived from the basic prbs by modulo-2 addition of rows of a Hadamard matrix. A particularly useful binary component which contributes only high frequency power is the half-rate prbs modulated by a 1/2δ Hz square wave. Progressively narrower bands of high frequency noise can also be obtained by clocking the S.R.G. at smaller fractions of the square wave frequency.

It is not the intention of this Chapter to provide a rigorous and complete theory of pseudo-noise generation. The object is rather to impart a working knowledge of the properties of a particular class of sequences which seem relevant to this application. Many of the results obtained here will be used in later Chapters to specify objectionability of television quantizing noise, but first it is necessary to discuss the subjective factors relating to the visibility of random and pseudo-random noise.

2.7. BIBLIOGRAPHY ON PSEUDO-RANDOM NOISE

1 BIRDSALL, T.G. & RISTENBATT, M.P. - "Introduction to Linear Shift-Register Generated Sequences", Univ. of Michigan Res. Inst. Technical Report 90, October 1958.

2 CHANG, J.A. - "Generation of 5 Level Maximal Length Sequences", Electronics Letters, 2, 7, p 258, July 1966.

3 DARNELL, M. - "Synthesis of Pseudo-Random Signals derived from p-level M-sequences", Electronics Letters, 2, 11, pp 428 - 430, November 1966.

4 DAVIES, A.C. - "Probability Distributions of Pseudo-Random Waveforms Obtained from M-sequences", Electronics Letters, 3, 3, pp 115 - 117, March 1967.

5 DAVIES, A.C. - "Digital Filtering of Binary Sequences", Electronics Letters, 3, 7, pp 318 - 319, July 1967.

6 DAVIO, M. - "Random and Pseudo-Random Number Generators" Electronic Engineering, 39, 475, pp 558 - 559, September 1967.

7 EVERETT, D. - "Periodic Digital Sequences with Pseudo-noise Properties", G.E.C. Telecommunications, 33, 3, pp 115 - 126, September 1966.

8 EVERETT, D. & BRYANT, P.R. - "Transformation of Shift Register Sequences by Sampling", Digital Techniques & Network Theory Memo., G.E.C. Co.Ltd., June 1964.

9 ELSPAS, B. - "The Theory of Autonomous Linear Sequential Networks", Transactions I.R.E., CT-6, pp 45 - 60, March 1959.

10 GODFREY, K.R. - "Three Level M-Sequences", Electronics Letters, 2, 7, p 241, July 1966.

11 GODFREY, K.R. - "Theory and Application of Pseudo-Random Sequences", Control, 10, 96, pp 305 - 308, June 1966.

12 GOLOMB, S.W. - "Sequences with Randomness Properties", Contract SC-54-36611 (Req. No 639498) Glen L. Martin Co., Baltimore, June 14th 1955.

13 GOLOMB, S.W. - "Pseudo-Noise Correlation and its Applications", Contract 55-33624 (Req. 34460), Glen L. Martin Co., Baltimore, September 15th 1955.

14 GOLOMB, S.W., BAUMERT, L.D., EASTERLING, M.F., STIFFLER, J.J., & VITERBI, A.J. - "Digital Communications", (W.L. EVERITT Ed.) Prentice Hall Inc. 1964.

15 GREEN, J.H.Jr & SAN SOUCIE, R.L. - "An Error-Correcting Encoder and Decoder of High Efficiency", Proc. I.R.E. 46, 10, pp 1741 - 1744, October 1958.

16 HALLWORTH, R.P. & HEATH, F.G. - "Semiconductor Circuits for Ternary Logic", - Proc. I.E.E. 109 C, pp 219 - 225 (Mono. 482E) 1962.

17 HEATH, F.G. - "Digital Codes and Converters", Ph.D. Thesis, Manchester Univ. 1961.

18 HEATH, F.G. & GRIBBLE, M.W. - "Chain Codes and their Electronic Applications", Proc. I.E.E. 108C, (Mono. 392M) pp 50 - 57, March 1961.

19 INGRAM, D.G.W., WELLS, P., BRYANT, P.R. & EVERETT, D. - "Digital Techniques in Carrier Frequency Generation", Proc. I.E.E., 113, 2, pp 243 - 254, February 1966.

20 I.E.E. Colloquium on Random Signal Testing, 18th May 1965.

21 I.E.E. Colloquium on Pseudo-Random Sequences Applied to Control Systems, 27th January 1967.

22 JUDGE, W.J. - "Multiplexing Using Quasiorthogonal Binary Functions", Trans. A.I.E.E. Part 1, 81, pp 81 - 83, May 1962.

23 KRAMER, C. - "A Low Frequency Pseudo-Random Noise Generator", Electronic Engineering 37, p465, July 1965.

24 MAROLF, R.A. - "Pseudo-Random Sequence Generators for Very Wideband Secure Communications System", Proc. Nat. Electronics Conf. 19, p 183, Chicago 1963.

25 McFADDEN, J.A. - "The Probability Density of the Output of an RC Filter When the Input is a Binary Random Process", Trans. I.R.E. IT-5, 4, pp 174 - 178, December 1959.

26 PETERSON, W.W. - "Error Correcting Codes", M.I.T. Technology Press 1961.

27 PRICE, R. & GREEN, P.E.Jr - "A Communication Technique for Multipath Channels", Proc. I.R.E. 46, 3, pp 555 - 570, March 1958.

28 RADER, C.M. & GOLD, B. - "Digital Filter Design Techniques in the Frequency Domain", Proc. I.E.E.E. 55, 2, pp 149 - 171, 1967.

29 ROBERTS, P.D. & DAVIS, R.H. - "Statistical Properties of Smoothed Maximal Length Linear Binary Sequences" Proc. I.E.E. 113, 1, pp 190 - 196, January 1966.

30 ROBERTS, T.A. - "Analysis and Synthesis of Linear and Non-Linear Shift Register Generators", Proc. Int. Telemetering Conf. 1, pp 390 - 399, London, 1963.

31 SAGE, G.F. - "Serial Synchronization of Pseudonoise Systems", Trans. I.E.E.E. COM-12, pp 123 - 127, December 1964.

32 SCHOLEFIELD, P.H.K. - "Shift Registers Generating Maximum Length Sequences", Electronic Technology, (G.B.), 37, 10, p 389, October 1960.

33 SIEBERT, W.M. - "A Radar Detection Philosophy", I.R.E. Trans. IT-2, 3, September 1956.

34 SPRINGETT, J.C. - "Pseudo-Random Coding for Bit and Word Synchronization of PSK Data Transmission Systems", Proc. Int. Telemetering Conf. pp 410 - 422, London, September 1963.

35 TITSWORTH, R.C. - "Correlation Properties of Cyclic Sequences", Tech. Report No 32-388, Jet Prop. Lab. California Inst. Tech., Pasadena, July 1963.

36 TSAO, S.H. - "Generation of Delayed Replicas of Maximal Length Linear Binary Sequences", Proc. I.E.E. 111, p 1803, 1964, also 112, 4, pp 702 - 704, 1965.

37 ZIERLER, N. - "Several Binary Sequence Generators", Tech. Report 95, M.I.T. Lincoln Labs, September 12, 1955.

CHAPTER 3

THE PERCEPTION OF TELEVISION NOISE

3.1. INTRODUCTION

The perception of random noise was discussed briefly in Chapter 1 (Sec. 1.3.1) in reviewing previous work on television data compression. It is now necessary to establish a more quantitative model of visual perception suitable for analysing a particular compression scheme of which the characteristic degradation is additive random noise. Such a model has received a great deal of attention, principally through psychometric methods, and this work is reviewed in the following Section. The latter part of the Chapter describes a pseudo-random noise generator and some experiments which demonstrate its flexibility as a video waveform generator.

3.2. THE VISIBILITY OF RANDOM NOISE

The performance of a television system, subjected to random interference at various stages between scene and image, is generally specified by the S/N ratio at the input to the display device and a statistical description of the noise. Since the perception of noise is only weakly related

to the 1st order probability density function (HUANG & HARTMANN[57] and even less to the 3rd and higher orders (JULESZ[64]), it is usually sufficient to specify the 2nd order distribution, or in particular the noise power density spectrum. To completely specify the objectionability of a given noise it is also necessary to state a particular picture and the viewing conditions under which the observations are to be made.

The influence of these factors is discussed in detail in the following sub-sections.

3.2.1. Picture Content

The perception of random noise is often assumed to be independent of picture content, implying that the combined transfer of the display tube and the visual pathway is linear and that noise may be considered as additive. The validity of this assumption raises two considerations : the visiblity of noise as a function of mean picture luminance and the influence of picture detail.

MAURICE[79] argued that the visibility of noise which is additive at the input to the display tube should appear uniformly distributed over the grey scale. According to the Weber-Fechner law, the sensitivity/luminance characteristic of the eye is of logarithmic form and, over the

range of luminance typical of television displays, this is very nearly a cube root law. It so happens that the normal picture tube has a screen-luminance/grid-voltage transfer which approximates to a 5/2 power law and, as this almost complements the characteristic of the eye, Maurice concluded that the transfer between subjective sensation and picture tube input voltage is nearly linear.

HACKING[49] considered these relationships a little more carefully. It was pointed out that the tube gamma does not exactly complement Weber's logarithmic law with the result that the visibility of noise distributed over a grey scale decreases towards white. Also, it is known that Weber's law does not hold at low luminances where the fractional sensitivity threshold $\Delta Y/Y$ rises and causes the visibility of noise to decrease towards black. In addition, reduced contrast at low luminances due to ambient illumination causes noise visibility to fall faster towards black. In consequence of these three factors, the noise visibility function has a peak in the lower greys, which moves towards black as the maximum contrast permitted by the viewing conditions increases. Using the optical measurements of $\Delta Y/Y$ made by MOON & SPENCER[83] and assuming a tube gamma of 2.5, Hacking estimated a variation in noise visibility of 5.5 dB over the grey scale for peak highlight luminance of 10 ftL and a contrast ratio of 100:1.

NEWELL & GEDDES[87] criticized Hacking's use of optical measurements under television conditions, but obtained a similar form of noise visibility function, shown in Figure 3.1. These curves were obtained by subjective tests on a 405 line system at a viewing ratio of 5, with highlight luminance 20 ftL and contrast ratio 80:1. The continuous curve refers to noise which was white over the video band and the dashed curve to a triangular noise spectrum. The curves show that the S/N ratio for constant visibility varies by only 4 dB over most of the grey scale, which is reasonably consistent with Maurice's conclusion. This variation is less than that estimated by Hacking, but further subjective tests on the visibility of stationary patterns confirmed Hacking's results. It was proposed that for migrating noise, the greater retentivity of the eye at low luminance levels causes partial cancellation of luminance fluctuations between frames.

The above discussion refers only to noise which is effectively introduced at the display tube grid. If the television system contains some other non-linearity, the visibility of noise added before this may depend on image luminance much more significantly. This applies in particular to phosphor and photomultiplier noise in systems with flying spot scanners. Since the scanner has unity gamma, it must be followed by a gamma correction circuit with a

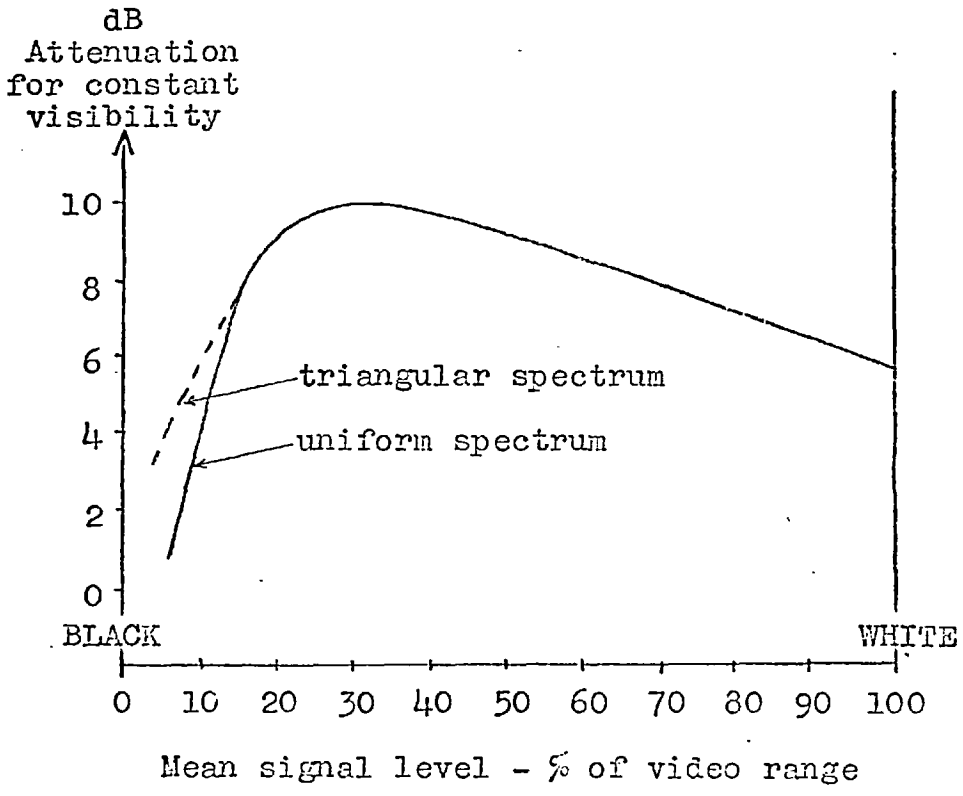

Figure 3.1. Relative visibility of noise over the grey scale (NEWELL & GEDDES, ref. 87).

2/5 root law in order to establish an overall linear transfer between scene and image luminance. Maurice considered a number of television systems and their inherent noise in some detail.

The influence of picture detail on noise visibility has already been discussed at length, since it is on this property that a large number of compression schemes rely. In this respect, any assumption of additivity in the perception of random noise is completely invalid. However, since the viewer is most annoyed by the noise in simply organized regions of the image, the presence of detail can only improve the subjective assessment of a noisy display. A model of perception which assumes additivity is thus a conservative one which relates to a worst picture.

3.2.2. Random Noise Weighting Function

In considering the appearance of random noise displayed as a television signal, it is convenient to define a two dimensional spatial spectrum, which is related to the noise power spectrum by the method of scanning. For horizontal rectilinear scanning, the horizontal spatial spectrum is identical, with change of variable, to the noise power spectrum. In the vertical direction however, the spatial spectrum is obtained by sampling the power spectrum at line

and (for the interlaced raster) field frequencies. Thus, vertically adjacent samples can be independent if the power spectrum bandwidth is greater than only 50 Hz, and alternate elements can be independent if the bandwidth exceeds 10 kHz. In consequence, the vertical spatial spectrum can be assumed white almost irrespective of the power spectrum.

Most measurements of noise visibility as a function of frequency have been confined to the one dimensional power spectrum. These measurements have assumed additivity of noise effect and relate to the power in a narrow band of random noise which creates a particular level of objectionability as the centre frequency of the band is swept over the television bandwidth. The measurements are used to construct a continuous curve, W(w), which represents the relative sensitivity of the eye to the various frequency components. Under specified viewing conditions, the objectionability of random noise with a power density spectrum N(w) is then given by

$$\int_0^\infty W(w).N(w).dw$$

Five of the estimates known to the author of W(w) for monochrome video frequencies above line frequency are summarized in Table 3.1. All are monotonically decreasing functions of noise visibility, with the exception of those

Table 3.1.

A summary of some random interference weighting functions obtained by narrow-band noise measurements above line frequency.

	Conditions	Method of measurement	Viewing ratio	Variation in visibility (dB)
GILBERT, M. (1955) (Fig. 3.2)	405 lines, 25 fr/s 2:1 interlace	4 comment rating scale	4 8	17 19
BARSTOW, J.M. & CHRISTOPHER, H.N. (1953)	525 lines, 30 fr/s 2:1 interlace. 6" x 8" raster, viewed in total darkness.	Comparison with wide-band noise	4	25
BARSTOW, J.M. & CHRISTOPHER H.N. (1962)	525 lines, 30 fr/s 2:1 interlace. 21" picture tube, Noise levels 0 - 20 dB over threshold. Highlights 10-30 ftL Amb.Ill. by reflectn	7 comment rating scale and comparison with wide-band noise	4	14
BRAINARD, R.C. KAMMERER, F.W. & KIMME, E.G. (1962)	225 lines, 30 fr/s 2:1 interlace. 5" x 5" raster. Amb.Ill. - "Low"	Comparison with wide-band noise	8	15 for stills 8 for moving
BRAINARD, R.C. (1967) (Fig.3.4(c))	160 lines, 60 fr/s no interlace 4.5" x 4.5" raster Amb.Ill. 400 lux Highlights 170 cd/m^2	Comparison with wide-band noise	8	10

found by GILBERT[38] (Fig.3.2), which reach a minimum at 2.5 MHz. However, FATCHAND[31] has shown that this minimum probably resulted from intermodulation products of the display tube non-linearity, exaggerated by the narrow-band method of measurement, and is not a characteristic of the eye. The reduced visibility of high frequency noise as compared to low frequencies is given for each of the functions in the final column of Table 3.1. Viewing conditions are also given where known.

The Table shows considerable diversity in the estimates of the overall variation of W(w), but not enough is known of the conditions under which they were obtained to allow close comparisons. BARSTOW & CHRISTOPHER[3] explained the difference between their 1953 and 1962 results by developments in display tube technology. Modern tubes allow smaller spot size, have better uniformity of focus and have reduced light scattering. The 1962 results also included the corresponding weighting function for a colour television system.

Gilbert used a four comment rating scale on which to define thresholds of "visibility" and "annoyance". The estimates of W(w) corresponding to these thresholds at viewing ratios of 4 and 8 are shown in Figure 3.2. Gilbert also quoted some results of the British Post Office which were not inconsistent with the range of these curves.

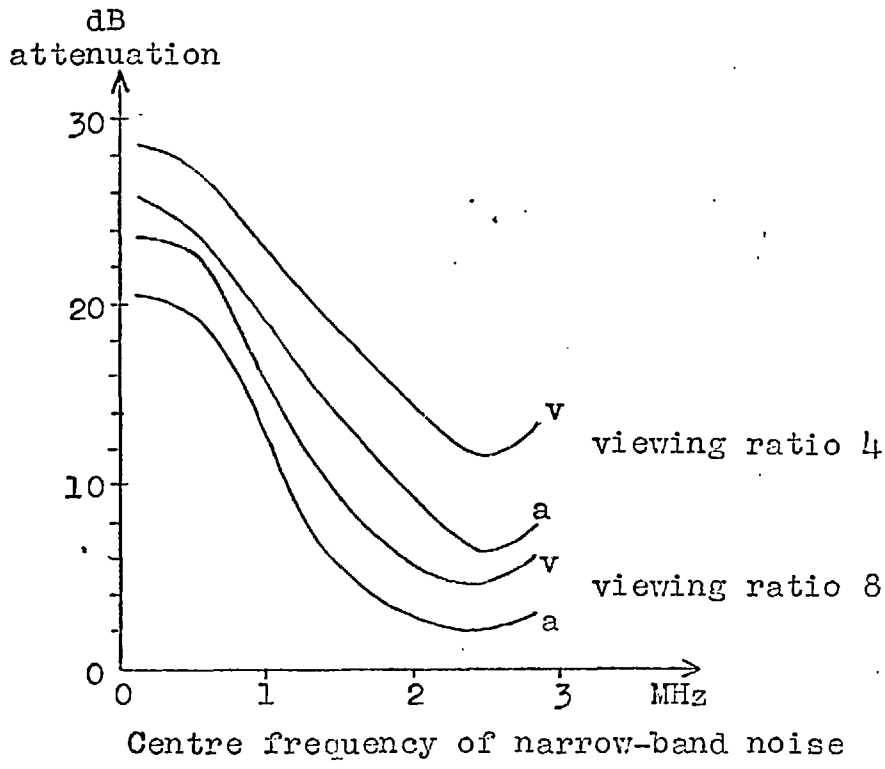

Figure 3.2. Thresholds of visibility (v) and annoyance (a) of narrow-band noise as a function of its centre frequency (from GILBERT, ref. 38).

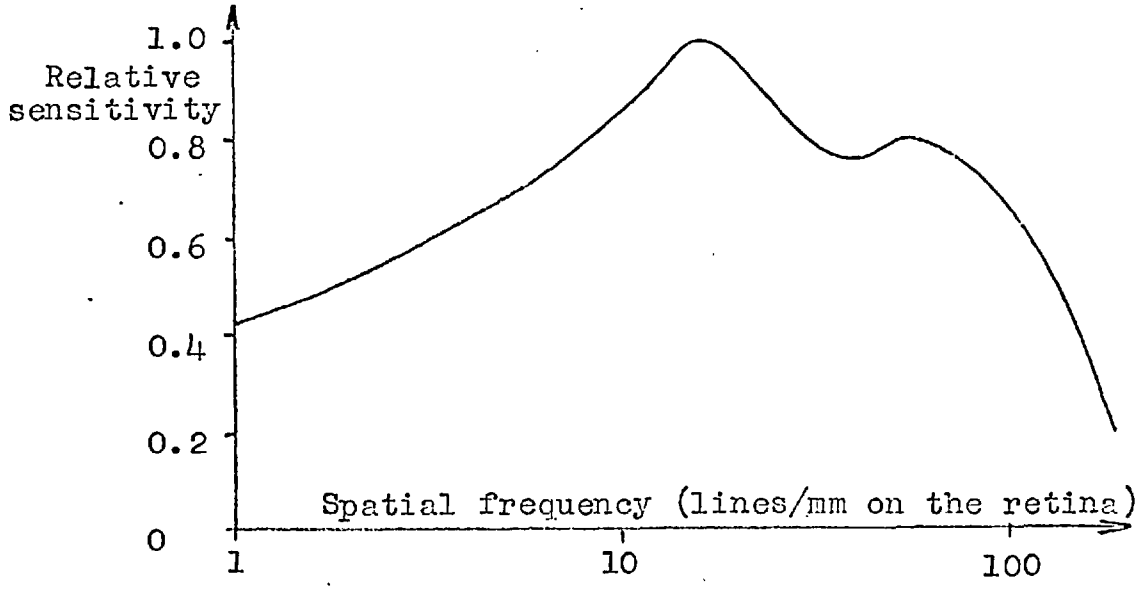

Figure 3.3. Sine-wave response of the complete visual system (from LOWRY and DePALMA, ref. 76).

The reported estimates of W(w) are consistent in that the functions fall monotonically with frequency. However, this low-pass characteristic of the visual system seems contrary to the findings of LOWRY & DePALMA[76] that the frequency response obtained by sine-wave measurements has a well-defined maximum. The visual effect of this peak is apparent as overshoot at luminous edges and is known as the Mach phenomenon (Fig.1.2, Sec.1.3.1). The sine-wave response is shown in Figure 3.3 and, in terms of the British 405 line standards, the location of the peak is near 700 kHz for a viewing ratio of 4.

HUANG[55] has suggested that the inconsistency between the results of sine-wave and narrow-band noise measurements exists because the latter are only one dimensional, whereas the eye is equally sensitive to the vertical spatial spectrum of the noise. Even for the lowest horizontal "frequency" considered, no appreciable bandlimiting is extended to the vertical direction which therefore maintains objectionability at low frequencies. Huang performed a computer simulation to produce photographic images degraded by Gaussian noises of controlled vertical and horizontal bandwidths. From subjective experiments, in which observers were asked to rank order photographs in order of preference, isopreference curves were obtained relating horizontal and vertical bandwidths and noise power. Assuming additivity of noise effect, Huang

was able to estimate the approximate shape of a two dimensional noise visibility function from these isopreference curves and it was found that, for noises of similar horizontal and vertical bandwidths, this function did indeed show a maximum as expected from sine-wave measurements. The location of the maximum depended markedly on the type of picture used and it was concluded that noises which contain frequencies similar to those of the picture are generally less objectionable. It was also noted that noises with vertical streaks (vertical bandwidth less than horizontal bandwidth) are more objectionable than noises with horizontal streaks.

BRAINARD[8] confirmed Huang's estimate of a peaked noise visibility function for stationary interference, but showed that the peak moved to very much lower spatial frequencies for moving interference. Subjective experiments were carried out using a low resolution television system (without interlace) to measure thresholds of visibility of sine-wave interference at various average luminances with no other picture signal present. Using sine-waves of 2,4,10 and 20 times the line scan frequency, horizontal bars were generated of which the visibility at a low luminance was found to peak at 15 cycles/picture height for a viewing ratio of 8. Moving bars were then generated for the same spatial frequencies by allowing the sine-wave frequencies to differ

slightly from integral multiples of frame frequency. As the difference increased, so the motion increased and it was observed that the peak in visibility moved to lower spatial frequencies. From this it was concluded that integrating over all motion difference frequencies, as would be done for random noise, the visibility peak (if it still exists) would be shifted to much lower frequencies than is evident from stationary measurements. By integrating these and other sine-wave measurements (which were well supported by the results of other workers), Brainard was able to deduce a noise visibility function which agreed qualitatively with one obtained by narrow-band noise measurements.

Brainard's narrow-band noise measurements differed from those of other workers in that bands much narrower than line frequency were used, though they were still wide enough to appear as noise, and the bands were centred either on, or midway between, multiples of line frequency. For bands centred on any harmonic of line frequency, the vertical spatial spectrum consists only of low frequency components, and Brainard obtained the noise visibility function shown in Figure 3.4(a). For bands between line harmonics, the vertical spatial spectrum consists only of high frequency components, and the visibility function was obtained as the curve shown in Figure 3.4(b). Finally, Brainard repeated

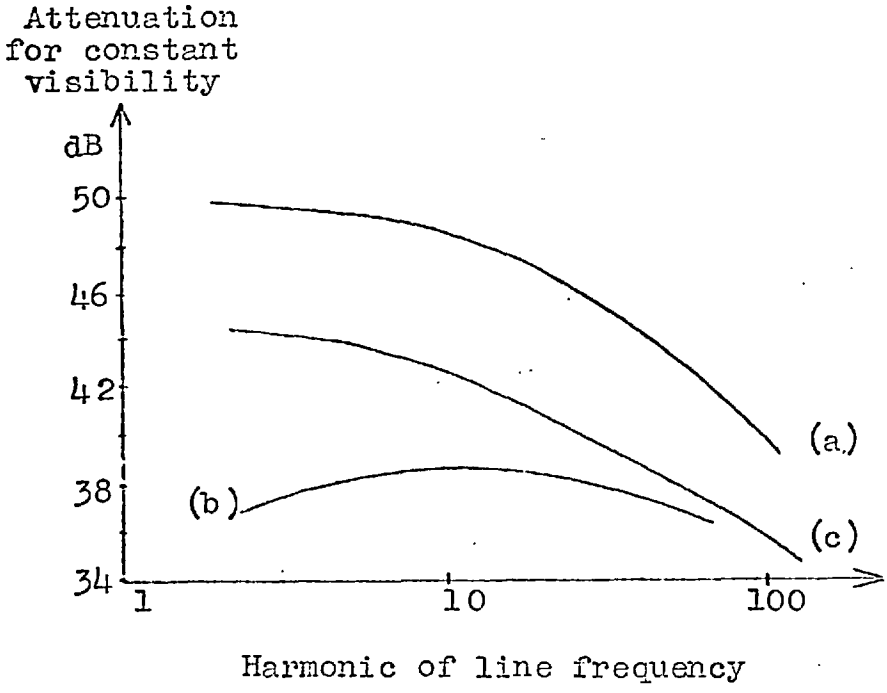

Figure 3.4. Visibility of very narrow bands of noise as a function of horizontal frequency for various vertical spatial spectra :

(a) low frequencies only

(b) high frequencies only

(c) white

(from BRAINARD, ref. 8).

the measurements with the noise bandwidth equal to line frequency, for which the vertical spatial spectrum is white at any centre frequency. The corresponding visibility function is shown in Figure 3.4(c). An important feature of Figure 3.4 is that the difference between curves (a) and (b) at low horizontal frequencies is similar to the overall variation across the band for curve (c). This supports the statement that the visual system has a similar weighting function in the two coordinate directions. Curve (c) has a lesser variation across the band than a corresponding function obtained by BRAINARD et al[10] in 1962 (see Table 3.1), although it was realized at that time that movement of picture content had a significant effect on W(w).

3.2.3. Viewing Conditions

The influence of mean picture luminance and ambient illumination on noise visibility was discussed in Sec. 3.2.1, but the dependence upon viewing ratio remains for consideration.

MERTZ[81] used the analogy of random noise in television to grain in photography to derive a formula for the "just perceptible" (one dimensional) noise power spectral distribution. Thresholds of visibility were established for white and triangular noises which were said to confirm some

unpublished measurements by M.W. BALDWIN. It was estimated that at a viewing ratio of 8, triangular noise is 6 dB less visible than white noise, but that this difference falls to only 2.5 dB and 1.0 dB as the viewing ratio is reduced to 4 and 2.5 respectively. It was also deduced that the effective noise power for a particular spectral distribution varies inversely as the square of the viewing distance. By doubling the viewing ratio, the noise power can be increased by 6 dB for constant visibility. This is supported by Gilbert's measurements of W(w) at viewing ratios of 4 and 8 (see Fig. 3.2). The two sets of curves are similar in shape, but are vertically separated by 6 dB.

3.2.4. Signal/Noise Ratio

To complete this discussion of the perception of noise, it only remains to attach some values to the S/N ratio. KILVINGTON et al[67] have established the threshold of visibility of white noise at a viewing ratio of 4 as 48 dB. However, it is also necessary to know something of observer reaction at noise levels above threshold.

The threshold functions of visibility and annoyance shown in Fig. 3.2 are of similar shape, but are separated by 3 to 4 dB. From this, Gilbert concluded that annoyance is aroused when noise attains a specific level of visibility

above threshold, and that this level is more or less independent of power spectral distribution. Other measurements of W(w), in which annoyance was determined by comparisons with white noise, have also shown the shape of W(w) to be essentially independent of the absolute S/N ratio over a wide range.

PROSSER & ALLNATT[96] obtained the distribution of observer opinion shown in Figure 3.5 for white and triangular noises over a range of about 25 dB above the thresholds of visibility. The measurements were made according to a previously proposed[97] 5 comment rating scale on 3 still pictures, in a 625 line system at a viewing ratio of 6. Highlight luminance was adjusted to 16 ftL and the ambient illumination allowed a maximum contrast ratio of 100:1. The vertical markers in Figure 3.5 indicate the scatter of the results over the three pictures. The results show that 50 % of observer opinion was favourable for white noise at 29 dB S/N ratio, and that 95 % was favourable at 39 dB. The curves also show that the subjective difference between white and triangular noise varies from 5 to 8 dB over the range 29 - 37 dB signal/white-noise ratio.

WEAVER[122] conducted an earlier set of experiments over a similar range of S/N ratio, but at a viewing ratio of 4 and using a 6 comment rating scale on both 405 and 625 line systems. Under similar conditions of illumination, the

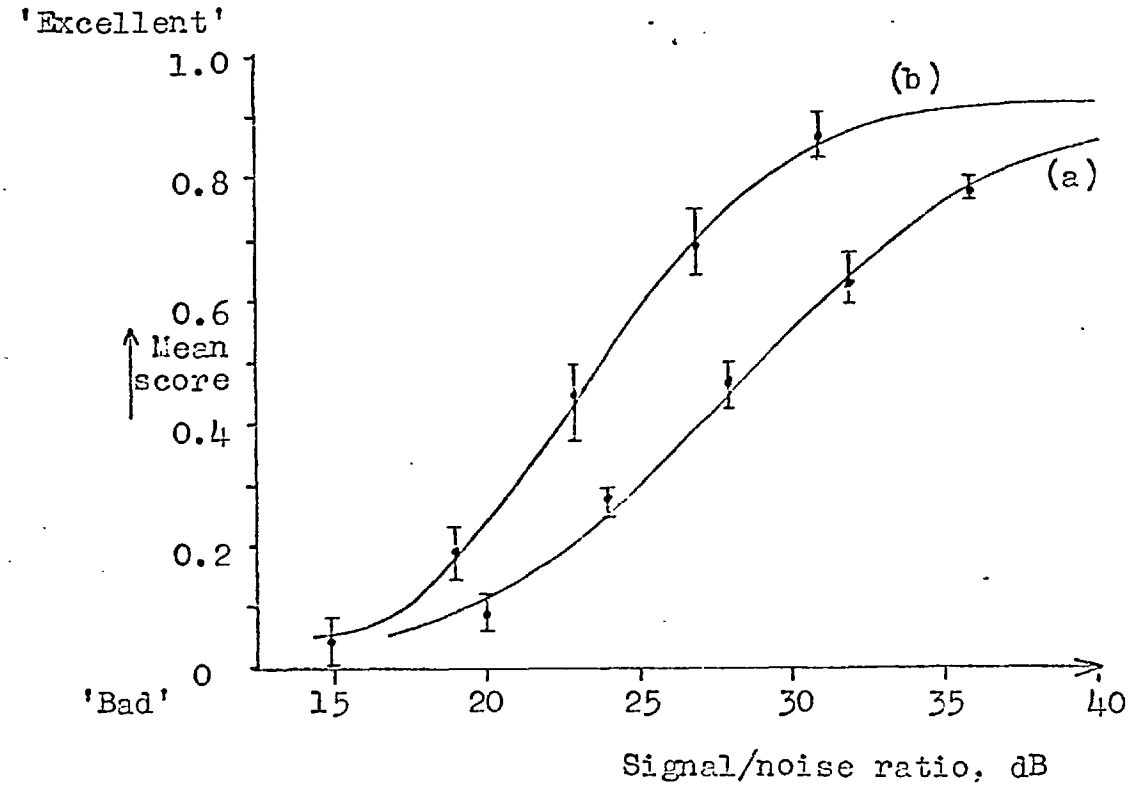

Figure 3.5. Variation of observer opinion as a function of signal/noise ratio for (a) white noise (b) triangular noise (from PROSSER & ALLNATT, ref. 96).

subjective difference between white and triangular noise was determined as 6 dB for the 405 line system and 8 dB for 625 lines, but these figures remained constant over the range of S/N ratio.

3.2.5. General Summary

The visibility of noise is greatest in the simply organized regions of a picture and gently peaks for areas in the lower greys. Under specified viewing conditions, the visual system can be represented by a frequency dependent weighting function, W(w). The shape of this function is essentially independent of absolute S/N ratio, but is somewhat influenced by picture content and movement. In consequence of W(w), white noise is about 6 dB more visible in a 405 line system than a similar power of triangular noise, though this difference diminishes at close viewing distances. W(w) is generally considered as single-dimensional, but applies equally in the vertical image direction. For migrating noise, W(w) decreases monotonically over the video band, but for "frozen" noise the two dimensional function exhibits a peak as a result of the reduced visibility of very low frequency noise. Frozen noise is generally less visible when of similar character to the picture. The threshold of noise visibility

varies inversely as the square of viewing distance, being about 48 dB for migrating white noise at a viewing ratio of 4. However, 95 % of a large observer population would be expected to accept a S/N ratio of 39 dB as favourable (in a 625 line system).

3.3. A PSEUDO-RANDOM NOISE GENERATOR

The remainder of this Chapter is concerned with the generation of pseudo-random noise and some experimental observations of the randomness properties described in Chapter 2. These experiments also serve to illustrate some of the perceptual characteristics discussed in the previous Section.

This Section briefly describes the picture generation equipment and the pseudo-random noise generator, of which some circuit diagrams and photographs are given in Appendix 8.3.

3.3.1. Standard Laboratory Equipment

The television signal was obtained from 35 mm positive transparencies in a flying spot scanner. Unity system gamma was secured by a 2/5 root law gamma corrector and all signal processing and noise addition was performed between this and

the display, so that noise appeared nearly uniformly distributed over the grey scale. The S/N ratio at the scanner output was approximately 45 dB, but this was probably less than 40 dB in the lower greys after gamma correction.

Synchronizing signals corresponding to the British 405 line system were derived from a crystal controlled oscillator at 6 MHz by the process of division shown in Figure 3.6. A mixed synchronizing signal was fed to separate "synch. input" sockets on each monitor and was not affected by any video processing. Blanking during the line and field retrace intervals was added to every processed signal immediately before display.

3.3.2. The Shift Register Generator

The S.R.G. was constructed using silicon planar transistors in saturating logic circuitry. Bistable outputs were 0 or +6 volts with switching times of about 15 nS. The "positive" output of each bistable was connected to a patch panel, together with the inputs to the modulo-2 adder, allowing access to all outputs and convenient programming of any two-tap feedback arrangement.

With a 6 MHz clock rate to provide one pseudo-random number per picture element, an 18 stage register was

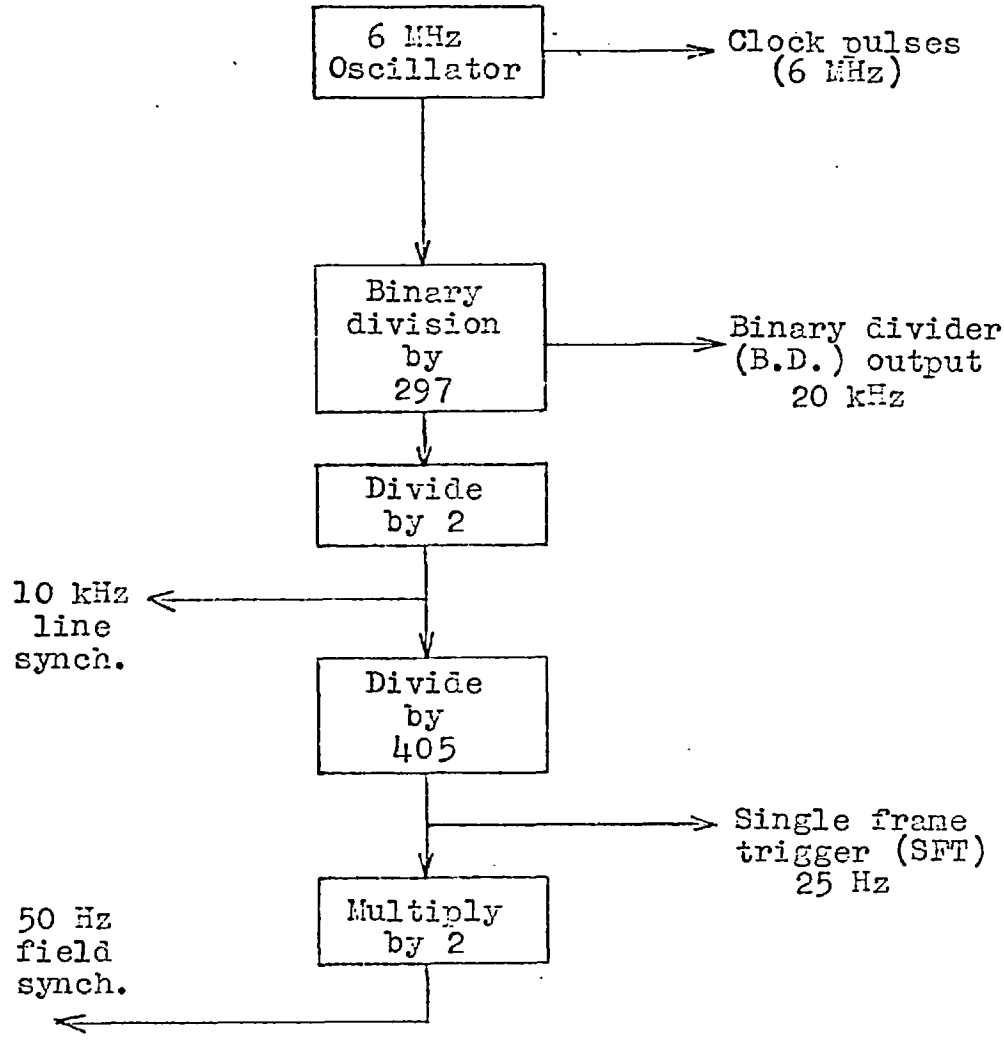

Figure 3.6. Schematic diagram of the laboratory synchronizing waveform generator.

specified to give a maximal sequence length of 262,143 digits. This corresponds to one less than the next power of 2 greater than the number of elements per frame (from Fig. 3.6 : 297 x 2 x 405 = 240,570), and overlaps the frame period sufficiently to create the impression of migrating random noise. The generator was programmed according to the polynomial $x^{18} \oplus x^{7} \oplus 1$.

A stationary noise pattern was generated when required by using the "single frame trigger" (S.F.T.) signal to reset the register. This effectively blanked out the latter 21,573 digits of the sequence and created a non-maximal length sequence of exactly frame period. However, this could not be done directly since the S.F.T. signal had a pulse length of about 5 μS, embracing 30 clock pulses. Perfect stability was achieved using a sequential system of gates and monostables, so that each S.F.T. pulse selected the next 20 kHz B.D. (binary divider) pulse, which in turn selected the next clock pulse (see Fig. 8.11, Appendix 8.3). These 25 Hz gated clock pulses were applied to the RESET input of the S.R.G. and set a pattern other than the all-zeros state, while the otherwise complete train of clock pulses was applied to the CLOCK input.

It was also required to provide the facility of frame-synchronized noise on moving pictures, which were received from the normal broadcast services. The S.R.G. was again

clocked from the 6 MHz oscillator, but this was not harmonically related to the frame rate of the broadcast signal. In spite of this, satisfactory synchronization was obtained by a similar gating process. Line and field synchronizing signals were extracted from the flywheel synchronization circuit of a specially adapted monitor, and the field signal was used to trigger a high-stability pulse generator, which in turn operated a gate to select the next laboratory clock pulse. Again, this pulse was gated from the CLOCK input to the S.R.G. and applied to the RESET input.

3.3.3. A Six-input Modulo-2 Adder

It is a property of the m-sequence that a delay of any specified number of digits within the period can be realized by the modulo-2 sum of the outputs of certain register stages, which are found by iteration of the feedback equation. Of particular interest are the delays corresponding to vertical distances in the raster of ℓ, 2ℓ, 3ℓ, etc., where ℓ is the line pitch.

For example, in the interlaced raster (see Fig. 3.7) the delay corresponding to the distance 2ℓ is equal to one line period, or 594 digits. From the feedback equation,

$$x^{18} \oplus x^{7} \oplus x^{0} = 0 ,$$

a delay of 18 digits is given by stages 0 and 7.

A delay of 19 digits is given by stages 1 and 8
so that 29 is given by 11 and 18.
But 18 is given by 0 and 7,
so that 29 is given by 11 and 0 and 7
etc. . . . . .
until 594 is given by 1,3,4,8,11,12,14 and 15.

An eight-input modulo-2 adder is therefore required to give the element which is delayed by 594 elements on stage '0' of the register. However, if the iteration is taken 4 digits further, it is found that :

598 is given by 0,1,5,12,15 and 16.

Hence, a modulo-2 adder with only six inputs can give the required delay of 594 elements, but referenced to stage '4' of the register.

It was found that a six-input modulo-2 adder was large enough to give all delays of interest on some stage of the register. This was constructed as a chain of two-input adders, as shown in Figure 3.8. Since the entire addition took a substantial part of one clock period, a bistable D_1 was included as a shaping circuit. The adder output was therefore one further element delayed on the figure given by the input selection. Two additional bistables D_2 and D_3 were also included to give access to neighbouring elements.

The delay corresponding to the distance ℓ is not so easily realized. For frame-synchronized noise, the sequence

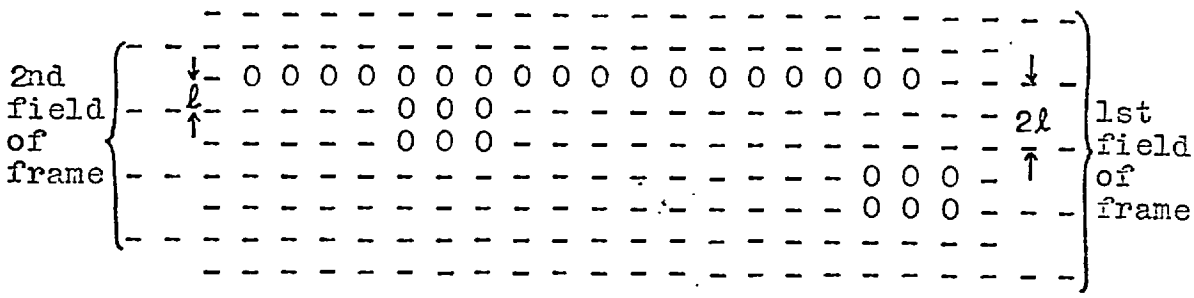

Figure 3.7. Elements of the displayed prbs simultaneously accessible as S.R.G. outputs or by modulo-2 addition (see table 3.2).

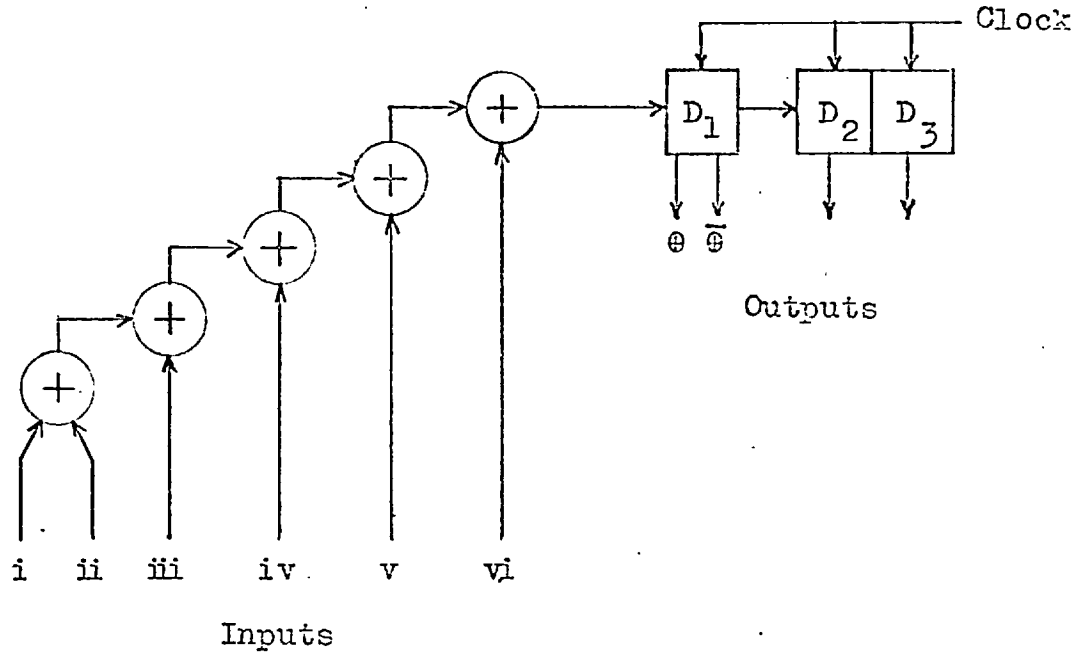

Figure 3.8. Six-input modulo-2 adder with shaping circuit D_1 and two further delay elements D_2 and D_3.

is no longer maximal length and the Shift and Add property only holds for certain shifts - in fact, shifts within the same frame. For elements within the same frame, ℓ (as indicated in Fig. 3.7) corresponds to

(field period) + $\frac{1}{2}$(line period) $\equiv$ 120,582 elements.

However, for elements of adjacent frames the effective delay corresponding to ℓ is increased by the number of elements blanked out by the reset pulse (S.F.T.),

i.e., $\ell \equiv 120,582 + 21,573 = 142,155$ elements.

The problem does not arise for the frame-asynchronous sequence, which is maximal length, and the distance ℓ is equivalent to 120,582 elements for both odd and even fields.

The register outputs which must be added modulo-2 to give the delays corresponding to ℓ, 2ℓ, 3ℓ, and 4ℓ are given in Table 3.2 together with the corresponding stages to which each delay is referenced. Using the additional delay toggles D_2 and D_3, access was simultaneously available to the 18 register stages together with any row of the other 12 locations indicated in Figure 3.7.

In addition to generating long delays, it was also possible to use the six-input adder in the S.R.G. feedback path to generate m-sequences which involved more than two feedback taps on the register.

Table 3.2. Modulo-2 adder inputs for vertical shifts in the displayed sequence $x^{18} \oplus x^{7} \oplus 1$

Shift ℓ = line pitch	Delay in elements	Register stages to be added modulo-2	Reference stage (output at D_1)
ℓ	120,582 *	4,9,13,15,18	5
2ℓ	594	0,1,5,12,15,16	5
3ℓ	121,176 *	0,3,8,11,13,15	17
4ℓ	1,188	1,2,3,7,13,15	17

* For synchronized noise, this figure applies only between elements of the same frame.

3.4. SOME EXPERIMENTS WITH PSEUDO-RANDOM NOISE

3.4.1. Sequence Length

Displayed as a television signal, the binary output of the 18 stage S.R.G. had no apparent non-randomness. Figure 3.11(a) shows the "frozen" noise of the frame-synchronized generator which exhibited a small amount of flicker as a result of interlacing two uncorrelated fields of noise. The fields are presented alternately at only 25 Hz - a frequency which is well below the minimum for flicker fusion.

M-sequences of lesser length were displayed to determine the minimum number of register stages for which the noise

is free of visible patterns. The feedback polynomials used were those given in Table 2.1 (p.56). With no other picture signal present and with noise amplitude 1 volt, noises of degrees 17, 16 and 15 were indistinguishable from degree 18 both with and without synchronization, except for a slow diagonal drift which was just detectable for asynchronized degree 17 at reduced brightness. For degrees lower than 15, regular patterns in the synchronized noise became progressively finer (see Figure 3.11(b) for degree 11) and very pronounced drifts were superimposed on the asynchronized noises.

The above observations were repeated for binary pseudo-random noise added at controlled S/N ratios to a picture signal from the flying spot scanner. Pictures of differing amounts of detail were used from the selection shown in Figure 4.9. Noises of degrees 15 and 16 were again indistinguishable from degree 18 for S/N ratios down to 10 dB, but the visibility of patterns embedded in other degree noises was found to be very dependent upon picture detail, viewing ratio and lighting conditions. The threshold of pattern visibility on high detail pictures was several dB lower than on low detail pictures. However, for asynchronized noises the high detail threshold rose towards that for low detail pictures as the viewing distance was increased.

This complex function of pattern visibility is related

to the sine-wave response of the visual system and it would be interesting to compare precise measurements for various degree noises with the results of Brainard and others. However, such measurements would be of limited relevance here and only the following approximate observations were made for reference in later Chapters. It should be pointed out that these observations only apply for the 405 line system and that the sequence lengths would interact rather differently with other line and field standards.

The diagonal drift of the degree 17 noise was not apparent at S/N ratios in excess of 20 dB for any of the pictures in Figure 4.9 and under any viewing conditions. Synchronized noises of degrees 14, 13 and 12 had no apparent patterning on these pictures at S/N ratios above 20 dB, although drifts in the asynchronized noises became visible on low detail pictures at approximately 36, 24 and 30 dB S/N ratio respectively. For degree 11, the pattern visibility threshold for synchronized noise on a low detail picture was approximately 28 dB S/N ratio under the most critical viewing conditions. Finally, for degree 11 without synchronization, and for most degrees less than 11, patterning and drift remained visible almost to the threshold of visibility of the noise itself.

3.4.2. Power Spectra

It was shown in Section 2.3.5 that the binary m-sequence has a power spectrum envelope

$$\frac{2}{N}\left(\frac{\sin\delta w/2}{\delta w/2}\right)^2$$

of lines at harmonics of $1/N\delta$ Hz, where $1/\delta$ Hz is the S.R.G. clock frequency. For an 18 stage register clocked at 6 MHz, the line spacing is only 23 Hz and the power spectrum may be considered as continuous. The spectrum has its first zero at 6 MHz and, as shown in Figure 3.9, is 0.4 and 3.9 dB down on the low frequency value at 1 and 3 MHz respectively. Over the video bandwidth therefore, the binary noise shown in Figure 3.11(a) is approximately white.

A three level signal with a rising power spectrum over the video band was generated by summing with equal weight the outputs of two adjacent register stages, one of which was inverted (see Sec. 2.6.5). The power spectral density is shown in Figure 3.10 and is approximately triangular over much of the video band. The appearance of the noise is illustrated by the photograph of Figure 3.11(c). A white three level noise of similar power was also generated by adding with equal weight two "independent" binary signals, comprising one S.R.G. output and the modulo-2 sum of this and a 3 MHz square wave. The relative visibility of the h.f. and white 3 level signals was estimated by weighting each spectrum by the noise visibility function W(w) due to

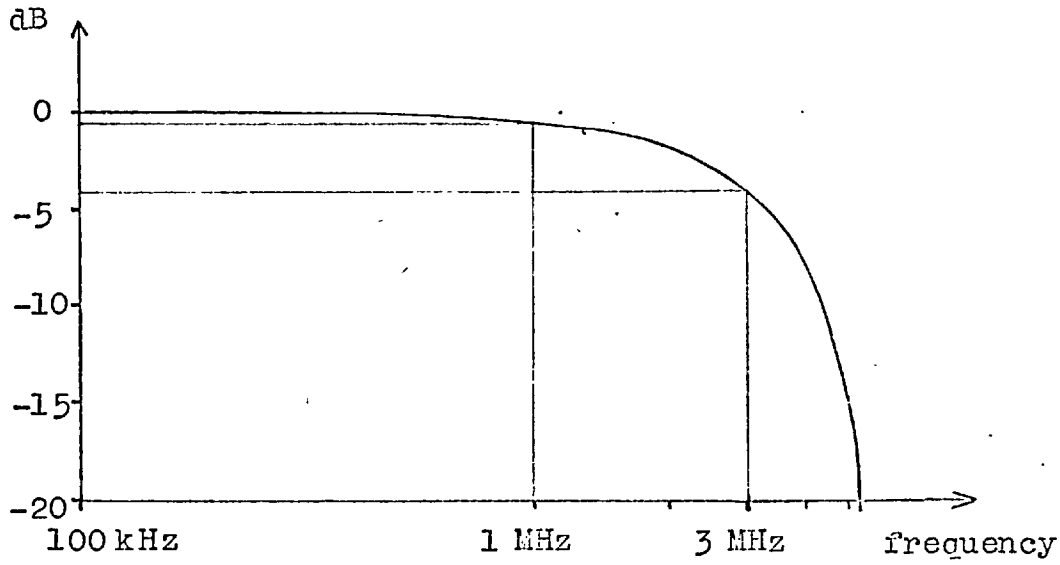

Figure 3.9. Power spectral density of a single prbs with clock frequency 6 MHz.

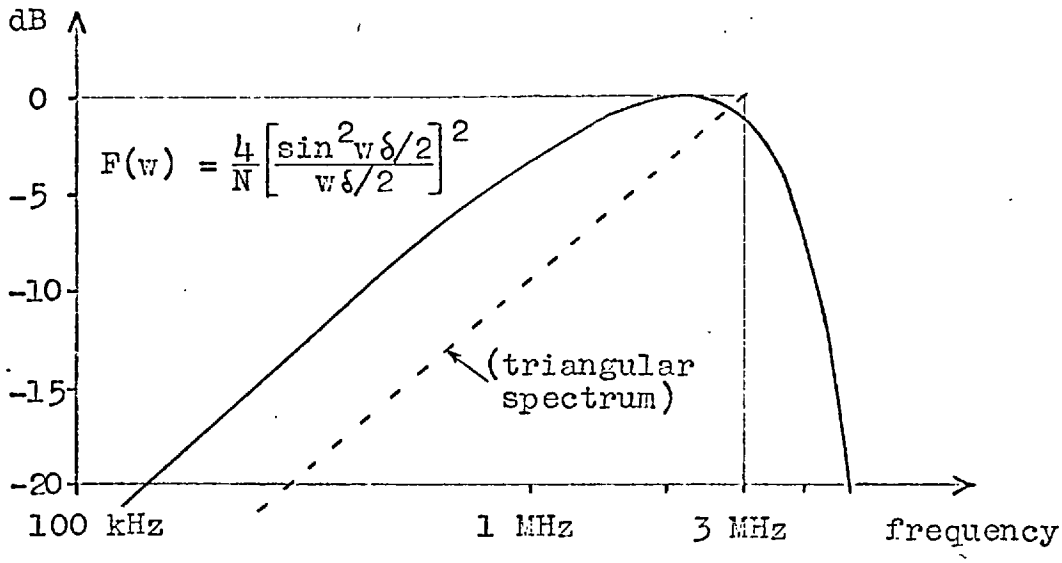

Figure 3.10. Power spectral density of the 3 level sequence from two adjacent S.R.G. outputs, one inverted.

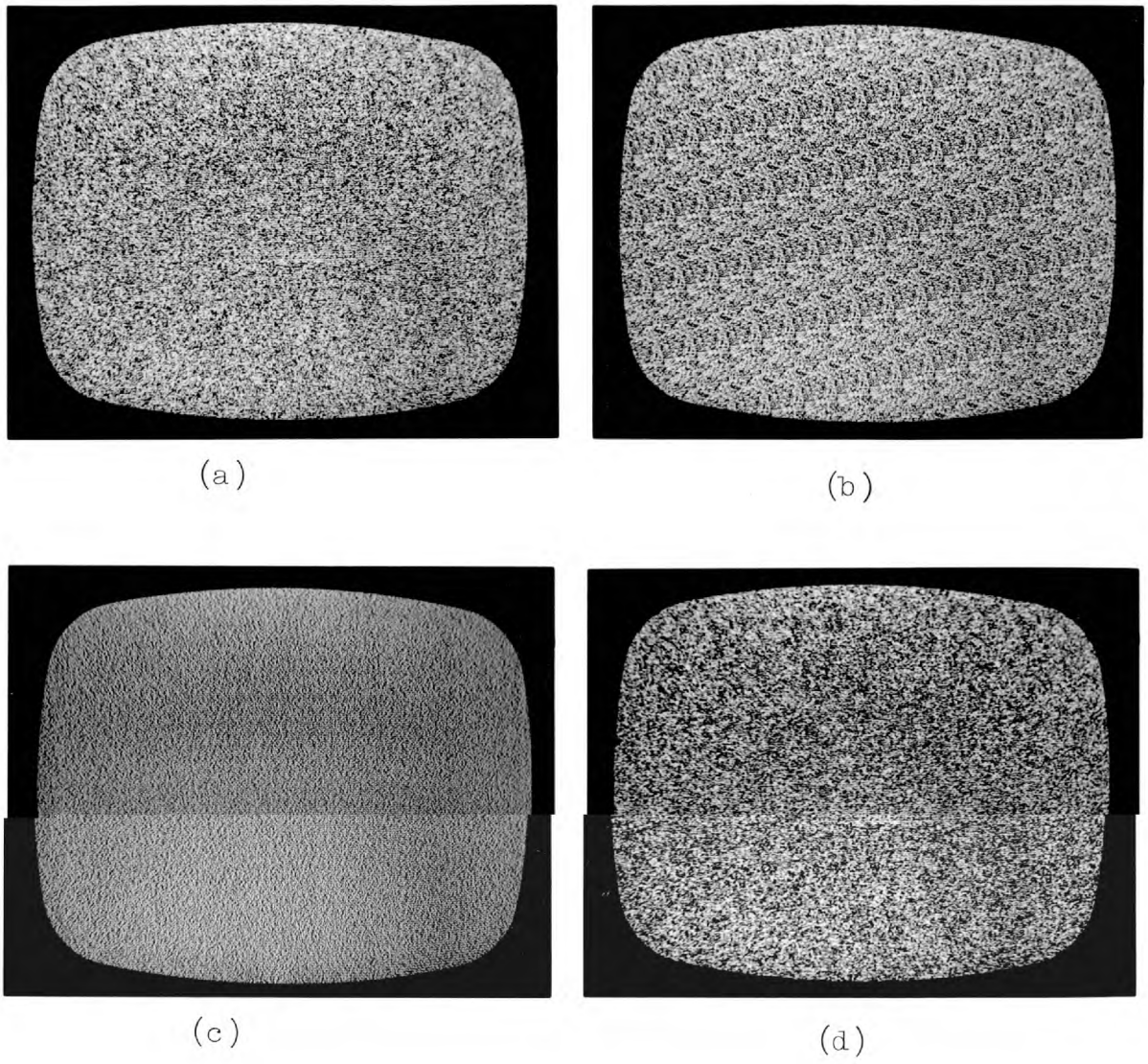

Figure 3.11. Pseudo-Random Noise

(a) Binary output of 18 stage S.R.G.

(b) Binary output of 11 stage S.R.G.

(c) 3 level sum of two adjacent S.R.G. outputs - one inverted

(d) 3 level sum of two adjacent S.R.G. outputs

Gilbert, and integrating these over the video frequency range. The ratio of the integrals gave a figure of 6 dB. This was confirmed by viewer tests, in which the noises were added to a picture signal at about 26 dB S/N ratio and compared with additive white Gaussian noise.

Figure 3.11 also shows a predominantly low frequency 3 level noise in photograph (d). This was obtained by adding two adjacent register outputs with equal weight, and has the power spectrum

$$\frac{4}{N}\left(\frac{\sin\delta w}{\delta w}\right)^2$$

which has its first zero at 3 MHz.

3.4.3. Vertical Correlation

A three level sequence was also used to investigate the effects of vertical correlation in a field of noise, facilitated by the Shift and Add property. The output of the six-input adder, with inputs specified by Table 3.2, was added with equal weight to the reference output of the register for vertical separations of ℓ, 2ℓ, 3ℓ, and 4ℓ.

The partial correlation over ℓ for synchronized noise was found to have little effect, except perhaps for a small reduction in flicker. Without synchronization, the noise grain was noticeably more coarse and a slow vertical drift was just apparent. Selection of the negative output of the

six-input adder was expected to give a rising vertical spatial spectrum of similar appearance to Figure 3.11(c). In fact the noise grain did appear finer, but severe flicker and a slight upward drift made this as objectionable as uncorrelated noise. A two-field photograph did however have a similar appearance to Figure 3.11(c). It therefore appears that due to their temporal separation of 20 mS, vertically adjacent elements in the interlaced raster cannot be used for shaping the spatial spectrum. This also applies for the separation 3ℓ, for which the drifts were found to be much more pronounced. In both cases, the orientation of the drift could be altered by stepping the S.R.G. output along the register to vary the horizontal separation of the readouts.

Vertical separations within a field were much more effective for spectrum shaping and caused no disturbing drifts. However, the maximum reduction in visibility compared to vertically white noise is less than 6 dB since the minimum readout separation is 2ℓ. The 3 level noise using the inverted output of the six-input adder has the vertical autocorrelation function shown in Figure 3.12(a), and the corresponding spatial spectrum envelope shown in Figure 3.12(b). Weighting this spectrum by W(w) and integrating over the video frequency range, the reduction in visibility over vertically white noise is estimated as 2.5 dB. Figure 3.13(a) illustrates the appearance of the noise added

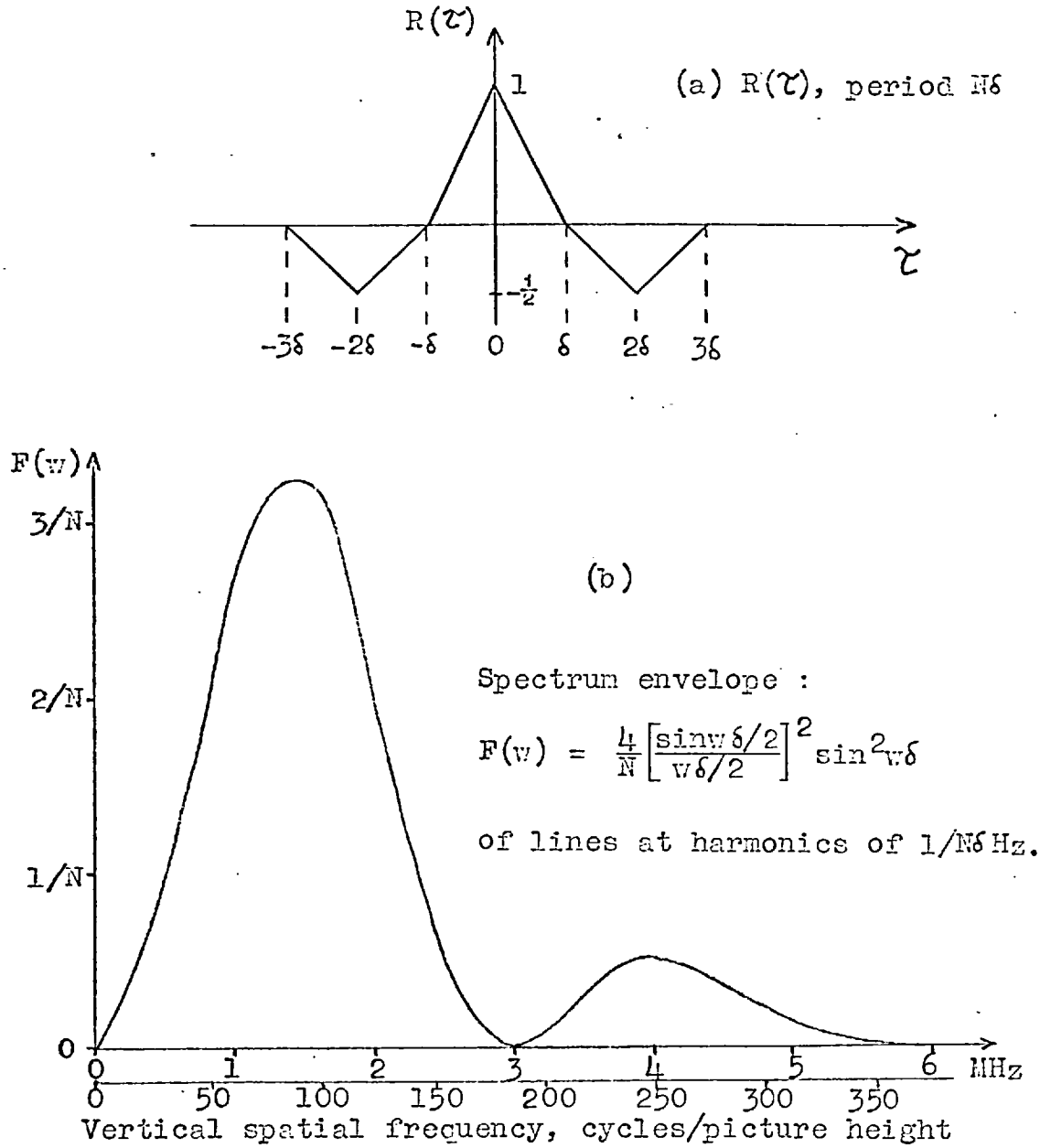

Figure 3.12. Autocorrelation function (a) and power density spectrum (b) of a 3 level sequence from 2 alternate SRG outputs, one inverted. Clock frequency 6 MHz.

(a) Horizontal spectrum white; vertical h.f.

(b) Horizontal spectrum h.f.; vertical white

Figure 3.13. 3 level pseudo-random noise added at 22 dB Signal/Noise ratio.

to a picture signal at 22 dB S/N ratio. It is interesting to compare this with Figure 3.13(b), in which the spatial spectra of the noise have been interchanged. The S/N ratio is again 22 dB, but there is no vertical correlation in the noise and its power spectrum is given by Fig. 3.12(b). Contrary to Huang's comment that noises with vertical streaks are more objectionable than noises with horizontal streaks, there was no conclusive preference for either type of asynchronized noise amongst a small number of observers.

Finally, a two dimensional high frequency noise was generated by adding with equal weight, but alternate signs, four elements of the binary noise field located as depicted by Figure 3.14. This 5 level noise combined the vertical and horizontal rising spectra of previous noises to give the expected reduction in visibility over white noise of 8.5 dB. This reduction is illustrated by the corresponding photographs of Figure 3.15.

3.4.4. Conclusion

This Section has illustrated by specific examples the flexibility of the S.R.G. for generating random television noise with a wide range of two dimensional spectra. In addition, the minimum sequence length for apparent randomness has been approximately established as a function of S/N ratio.

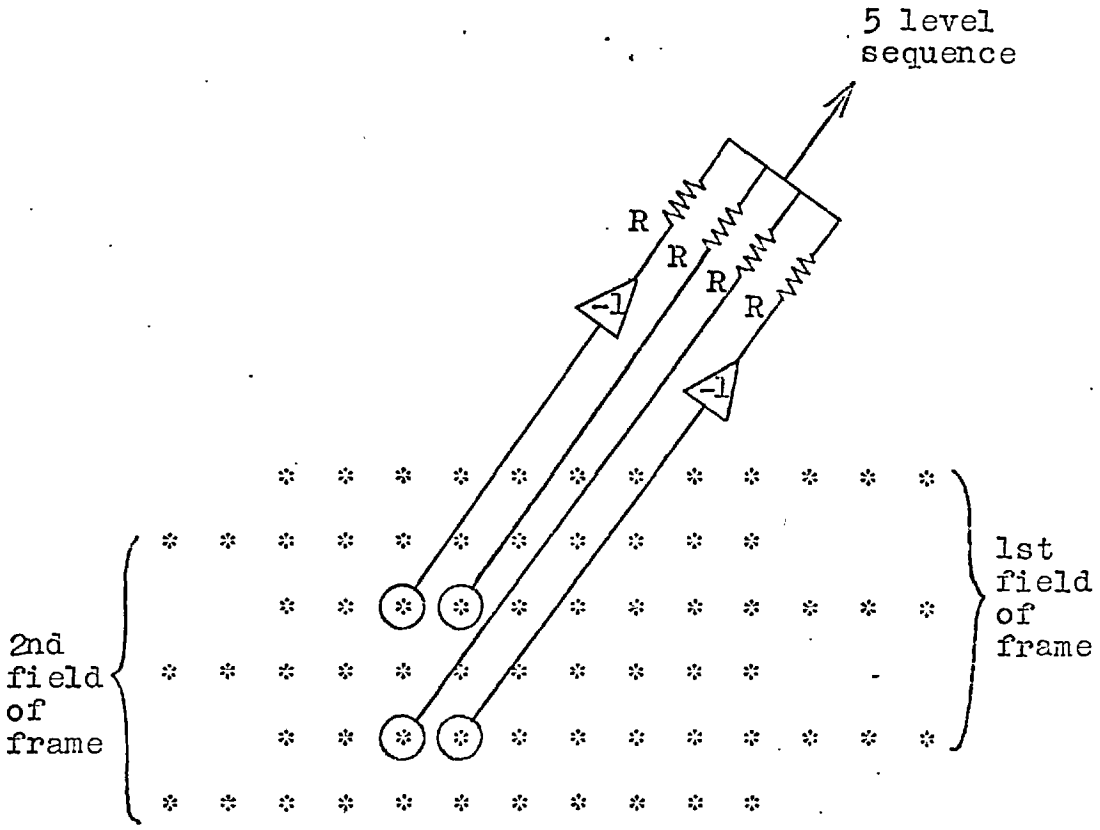

Figure 3.14. "Rectangular" decoder of 4 elements of the binary noise field generating a 5 level sequence with a 2 dimensional h,f. spectrum.

(a) White power spectrum.

(b) "Rectangular" spectrum rising to 3 MHz horizontally and '1.5 MHz' vertically.

Figure 3.15. 5 level pseudo-random noise added at 22 dB Signal/Noise ratio.

In a non-interlaced system, the flexibility of the S.R.G. for generating particular spatial spectra would be equal in the two coordinate directions and would facilitate further psychometric testing of perception of noise. In view of Brainard's conclusions from sine-wave measurements on the relevance of motion in noise visibility experiments, it would be particularly interesting to investigate Huang's isopreference curves[55] in real time for both frozen and migrating noise.

The nature of conventional scanning normally prevents vertical weighting of random noise in the received image. Huang was concerned with pseudo-random scanning systems, in which the scan may be chosen to transform any given one dimensional channel noise into an image noise which conforms to a two dimensional function of visibility. The remainder of this thesis treats a rather different situation in which quantizing contours are transformed into a more acceptable pseudo-random noise. Some of the techniques discussed in this Chapter can be applied to reduce the objectionability of a given power of noise, although flexibility is severely restricted by the non-linearity of the quantizing process.

The following Chapter is given to a study of quantization and describes some experiments with Roberts' pseudo-random quantizer.

CHAPTER 4

QUANTIZATION

4.1. INTRODUCTION

In order to transmit signals by digital means, it is necessary to reduce the analogue waveform to a sequence of narrow pulses of which the amplitudes may take only certain discrete values. Time sampling is usually periodic and of sufficient frequency to preserve rapid changes in the waveform. The amplitudes of the samples are rounded off to the nearest level of a predetermined set which is large enough to achieve a specified minimum error. The process of rounding off is termed quantization since all signal amplitudes within a defined quantum are transmitted as a single representative level, usually taken to be the mean value of the quantum. The number of levels to which the signal need be quantized is determined by the nature of the signal, being particularly large in audio and video systems. Less than 10 levels are normally sufficient to convey the statistical properties of a signal (see Sec.4.2), but about 100 are required for a television signal because the human viewer is extremely critical of the false contours which are produced in the image.

In the work to be described, the operations of analogue

to digital conversion, error free transmission through a channel and subsequent digital to analogue conversion were combined in a quantizer, which comprised the appropriate number of threshold detectors and a summing amplifier. The operation of sampling was omitted to reduce equipment complexity on a justification which will be discussed later in the Chapter. In anticipation of binary coding, quantizing fineness will be referred to in terms of bits/sample. An 'h' level quantizer is understood to comprise (h-1) threshold detectors and to require a code length of $\log_2 h$ bits/sample. The thresholds are spaced equally over the signal amplitude range hq , where q represents the threshold spacing, and give rise to the equal step characteristic shown (for 2 bit quantization) in Figure 4.1.

It is shown in Appendix 8.1 that the mean square quantizing error incurred by a signal which is confined to the range 0 to hq volts is $q^2/12$, provided that h is large or that the signal has a uniform probability density function (p.d.f.). For a signal of non-uniform p.d.f., companding can be used around the quantizer to effect the optimum threshold spacing which minimizes the mean square error (MAX[80]), but NISHIKAWA et al[88] have found that the p.d.f. of the typical television signal is approximately uniform, and this is not seriously altered by gamma correction. Furthermore, the variation of noise visibility

over the grey scale, which was discussed in the previous Chapter, is not sufficient to necessitate companding in order to maximize the signal/weighted-noise ratio.

For the 2 bit quantizer of Figure 4.1, the signal amplitude which maximizes the signal/quantizing-noise ratio is 4q, and the corresponding peak-peak-signal/r.m.s. error ratio is $20\log_{10}(4q/\frac{q}{\sqrt{12}}) = 22.8$ dB.

4.1.1. Quantizing and the Sampling Theorem

Quantizing can be considered as a sampling process on signal amplitude. The Sampling Theorem states that a signal which is bandlimited to f Hz can be reconstructed over an interval T secs from only 2fT precise measurements of signal amplitude within the interval. In sampling, values are measured at predetermined instants, but 2fT signal points could equally well be obtained by measuring the instants at which the signal passes through predetermined values. A signal could be reconstructed from a quantized version of itself provided that the thresholds were chosen to yield at least 2fT intersections within the interval. In practice however, the reconstruction filter becomes unrealizable as the appropriate interpolation function is uniquely determined by the instants at which the threshold crossings occur. A different filter would be required for each signal

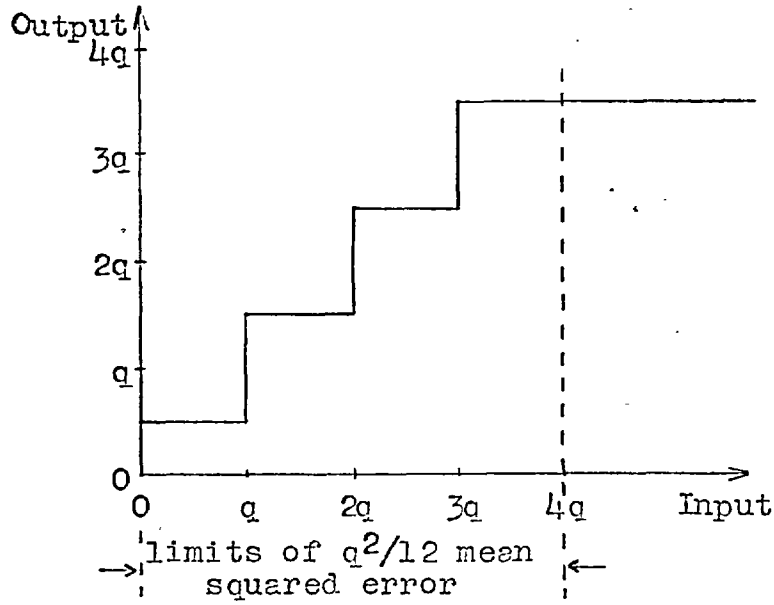

Figure 4.1. Staircase characteristic of a 2 bit equal step quantizer. The input signal amplitude which maximizes signal-to-quantizing-error ratio is 4q.

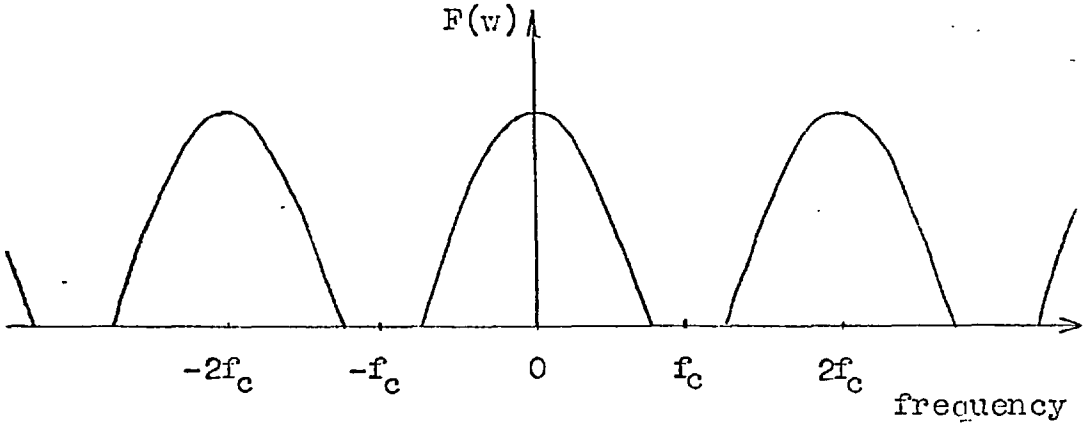

Figure 4.2. Power spectrum of a bandlimited signal sampled at $2f_c$ Hz.

(of T secs) and for each threshold spacing.

The statistical properties of most signals are preserved even after relatively coarse quantization, but the waveform is not recoverable. The statistical theory of quantization is of limited relevance to television systems, but a brief summary (ROSS[102], WATTS[120,121], WIDROW[123,124] is given in the following Section in order to introduce the concept of quantizer linearization by dithers.

4.2. STATISTICAL QUANTIZING THEORY

The Quantizing Theorem

Just as sampling is basically a time domain operation, quantizing is basically a probability domain operation. A quantizer performs a sampling process on the p.d.f. of the input signal, except that whereas time sampling yields the signal amplitude at particular instants, quantizing produces samples which represent the area of the p.d.f. over the corresponding quantal steps.

The effects of sampling are most clearly seen in the frequency domain, where straightforward multiplication is equivalent to the time domain convolution integral. Fourier analysis shows that any well-behaved function may be considered as a linear combination of sinusoids of appropriate

amplitudes, frequencies and phases. If the function v(t) is non-periodic :

$$F(w) = \int_{-\infty}^{+\infty} v(t).e^{-jwt}dt \qquad v(t) = \frac{1}{2\pi}\int_{-\infty}^{+\infty} F(w).e^{jwt}dw$$

Sampling, which is equivalent to impulse modulation, produces an infinite number of signal spectra centred on successive harmonics of the sampling frequency. The Sampling Theorem can be deduced by inspection of a typical sampled spectrum as shown in Figure 4.2. Only if the signal is bandlimited to less than half the sampling frequency can it be recovered without distortion by passing the output of the sampler through a sharp low-pass filter. Sampling at less than twice the maximum signal frequency causes the upper signal frequencies to be inseparably folded back, or "aliased".

Likewise, the effects of quantizing are most clearly seen on the characteristic function (c.f.) of the signal, which is the Fourier transform of the p.d.f. For first order statistics the c.f., denoted by $P(\alpha)$, and the p.d.f., denoted by $p(v)$, are related reciprocally :

$$P(\alpha) = \int_{-\infty}^{+\infty} p(v).e^{-j\alpha v}dv \qquad p(v) = \int_{-\infty}^{+\infty} P(\alpha).e^{j\alpha v}d\alpha$$

The c.f. of the output of an equal increment quantizer, $P^{*}(\alpha)$, emerges as a series of functions $P(\alpha)$ centred on harmonics

of the quantizing fineness 1/q and multiplied by a $\frac{\sin\alpha}{\alpha}$ term which arises from area sampling. If the quantizing grain q is sufficiently small so that no overlapping occurs, then $P(\alpha)$, and hence $p(v)$, is recoverable from the quantizer output. More formally, the Quantizing Theorem states that if the input c.f. is bandlimited such that $P(\alpha) = 0$ for $|\alpha| > \frac{1}{2}q$, then the input statistics can be recovered from the quantizer output. Furthermore, the p.d.f. of the quantizing error is independent of the p.d.f. of the input signal. Quantization is equivalent to the addition of noise 'v_N' for which :

$$\begin{aligned} p(v_N) &= 1/q \quad \text{for} \quad -\tfrac{1}{2}q < v_N < \tfrac{1}{2}q \\ &= 0 \quad \text{elsewhere} \end{aligned}$$

The moments of the input signal are recoverable from the moments of the quantizer output by subtraction of Sheppard's corrections. There is no correction for the first moment, i.e., the mean of the quantizer output is exactly the mean of the input. The correction for the second moment is $q^2/12$.

The Quantizing Theorem must also be satisfied for the higher order (joint) statistics in terms of the corresponding multi-dimensional characteristic functions. The Theorem is not as easily applied as the Sampling Theorem since the α-frequency domain does not correspond to any physically measurable quantity. Ross has proposed a "rule of thumb" as an adequate substitute for the Quantizing Theorem :

If the input signal p.d.f. has no favourite values (i.e., the signal is smoothly distributed) then 8 quantizing levels are sufficient to allow the first few moments of the quantized signal to be taken as the moments of v(t), provided Sheppard's corrections are used.

Widrow observed that once an input excites a quantizer so that the Quantizing Theorem is satisfied, then no other statistically independent input component can undo this condition, since when signals are added their c.f.'s multiply. The use of an external "dither" signal having a bandlimited c.f. was suggested as a means of "linearizing" a quantizer for any other input. If the multi-dimensional c.f. of the dither is bandlimited, then multiplication by the multi-dimensional c.f. of the signal yields a c.f. which is still bandlimited, and perhaps even narrower.

Any dither which is uniformly distributed over one quantum satisfies the Quantizing Theorem sufficiently to allow recovery of the input signal mean. This is illustrated by Figure 4.3, in which the dither is shown added to a signal value v. The quantizer output, averaged over the dither distribution, is also v.

In the remainder of this Chapter, the concept of linearization is investigated in relation to quantization of television signals.

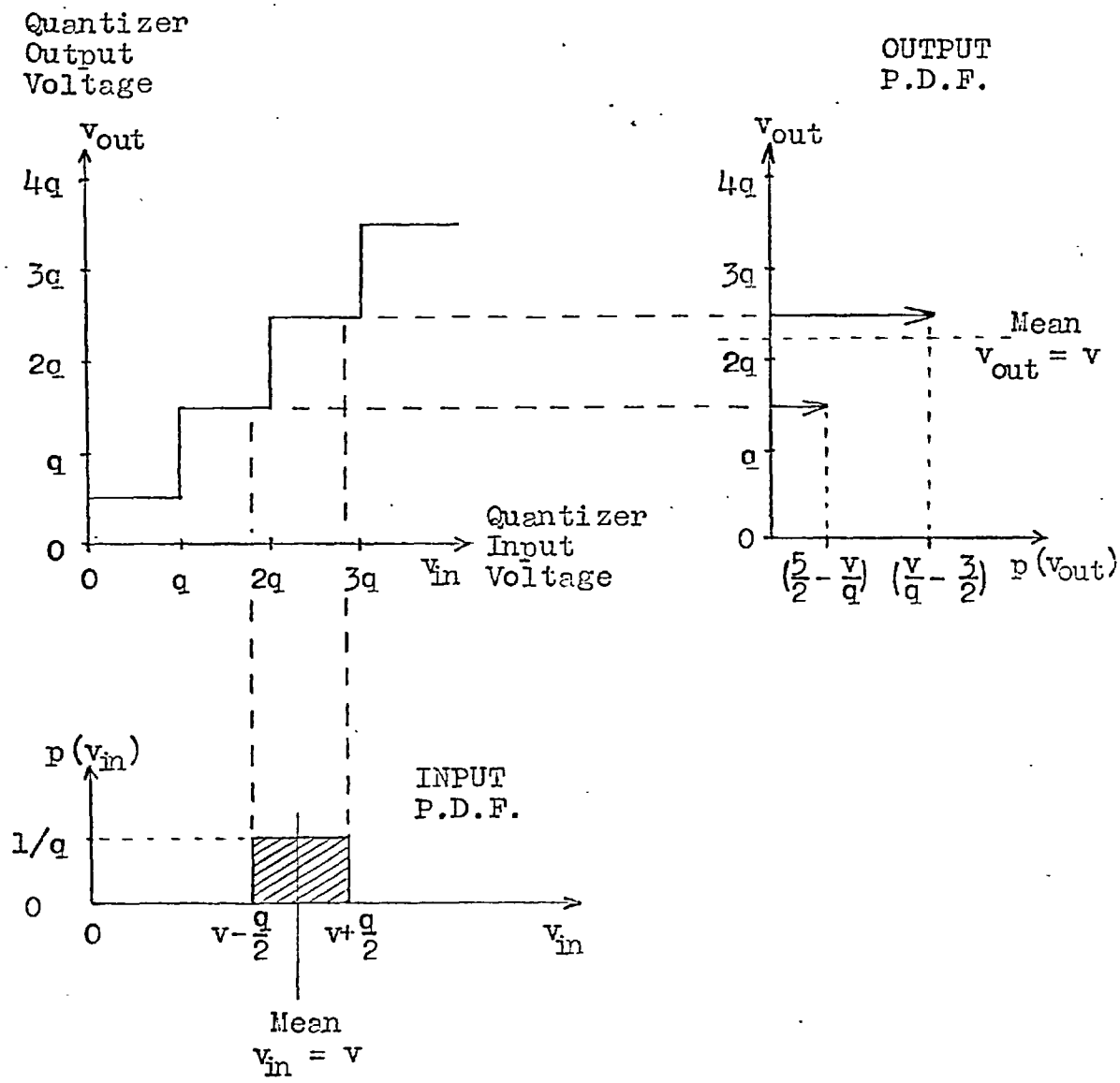

Figure 4.3. Quantizer linearization by a dither of uniform p.d.f. and peak-peak voltage q. Signal input = mean quantizer output = v.

4.3. LINEARIZATION

In terms of the signal mean and other statistics, the injection of a suitable dither can linearize a quantizer so that it behaves like a unity gain amplifier which adds one quantum of uniformly distributed random noise to the signal. For more than 8 level quantization, a dither is unnecessary and the first few moments of the input signal are recoverable at the quantizer output.

However, satisfaction of the Quantizing Theorem is not directly a useful condition for television signals. The quantizing noise waveform is causally related to the input signal - any given input uniquely determines the quantizer output and error. This causality is characterized in the television image by false contours, of which the viewer is particularly critical. The value of a noise-like dither, which is independent of the video signal, is therefore evident in breaking this causal connection and transforming contours into apparently additive noise.

Before pursuing noise-like dithering further however, it is worth digressing to consider an alternative class of periodic dithers.

4.3.1. High Frequency Dithers (FURMAN[34,35], JAFFE[60], ISHIKAWA[59])

In a time-continuous (un-sampled) system where the quantizer is followed by a low-pass or band-pass filter, a high frequency periodic dither may be used to drive the quantizing noise outside the signal band. A triangular wave of amplitude one quantum has a uniform p.d.f. and linearizes the quantizer for any signal input which does not cause saturation. The output mean, computed over one period of the dither yields precisely the input signal value. If the dither frequency is high compared to the upper limit of the signal band, the dither and the quantizing noise can be removed by filtering and the quantizer behaves as a unity gain amplifier. A sinusoidal dither is simpler to generate and inject, but retains some non-linearity which Furman has investigated as a function of dither amplitude.

Periodic dithering has been used extensively in control systems, but its spread spectrum is difficult to transmit through a sampled communications system. Experiments conducted by STUCKI[114] have shown that an acceptable television image can be transmitted through a 2 level channel which is dithered sinusoidally at 15 - 20 MHz. Since the brightness information is now contained in the instants at which the quantizer output switches, a sampling rate considerably higher than 20 MHz is required to transmit the signal in digital form. Much experimental work is needed to

determine the subjective reactions to quantization of the intervals between threshold crossings.

4.3.2. Random Dithers

In the sampled communications system, both the dither and the signal must be bandlimited to half the sampling frequency and there is little opportunity for removing the quantizing error by filtering. Here, the random dither is useful in linearizing the quantizer and in breaking the causal connection between signal and quantizing error, but at the expense of increasing the total mean square error. KORDONSKII[70] reported that the addition of low frequency noise before quantizing speech served to reduce non-linearity and to improve the transmission of weak signals which were otherwise lost between quantizer thresholds. Goodall also noticed that the false intensity contours of a 32 level television image were dispersed as a more tolerable random noise by adding noise to the signal before quantization.

Roberts investigated the use of dithers to disperse the contours in a coarsely quantized television image. The total mean square error of a dithered quantizer was expressed as the sum of two orthogonal measures of picture quality. The "variance", V, defined as the mean square difference between the output and the mean output, was used as a measure of the

amount of noise apparent. The "deviation", D, defined as the mean square difference between the input and the mean output, measured the tonal quality of the image. Accordingly, the total mean square error, E, was given by $E = V + D$. Normalized to remove the factor $q^2/12$, the process of un-dithered, or "straight" PCM is thus characterized by

$$D = 1 ; \quad V = 0 ; \quad E = 1 .$$

Addition of one quantum of random noise with a uniform p.d.f. before quantization was shown to reduce D to zero, but at the expense of increasing V, and hence E, to 2. The process was simulated on a computer and pictures were generated for 2, 3 and 4 bits/sample quantization. The dither was shown to be effective in removing contours, but the image had a "pin cushion" appearance of quantized noise.

Roberts observed that D was reduced to zero without increasing E if the dither was simultaneously subtracted from the quantizer output. For a random dither, addition at the transmitter and subtraction of an identical waveform at the receiver poses considerable storage and synchronization problems. These are overcome however, by using pseudo-random noise generated in identical feedback shift registers of sufficient length that the sequence period extends over several frames. Roberts verified that the quantizing error now appeared as one quantum of additive pseudo-random noise.

Roberts' technique can be intuitively justified by considering the addition of pseudo-noise before quantization and subtraction at the receiver as an operation on the quantizer thresholds. The threshold spacing remains constant (q), so that the total mean square error is only $q^2/12$, but the locations of the thresholds as seen by the signal appear indeterminate over a distance q. The locations change pseudo-randomly sample by sample, distributing the quantizing error uniformly over one quantum.

For a practical situation, Roberts proposed a 16 level dither obtained by decoding 4 binary outputs of a S.R.G. This has a uniform p.d.f., and is adjusted to have peak-peak amplitude $\frac{15}{16}$ q volts. The process is illustrated in Figure 4.4 for an input signal level v. With dither value '10', the voltage applied to the quantizer is (v + 10q/16). This is above threshold and the signal is transmitted as level B. At the receiver, subtraction of the dither gives the output level '10' which is 10q/16 volts below level B. With dither value '2', the voltage applied to the quantizer is (v + 2q/16). This is below threshold and the signal is transmitted as level A. Subtraction of the dither gives the output level '2', which is 2q/16 volts below level A. Similarly for the other values to give the output distribution shown. It can now be seen that if the peak-peak dither amplitude is less than q, the output distribution is divided;

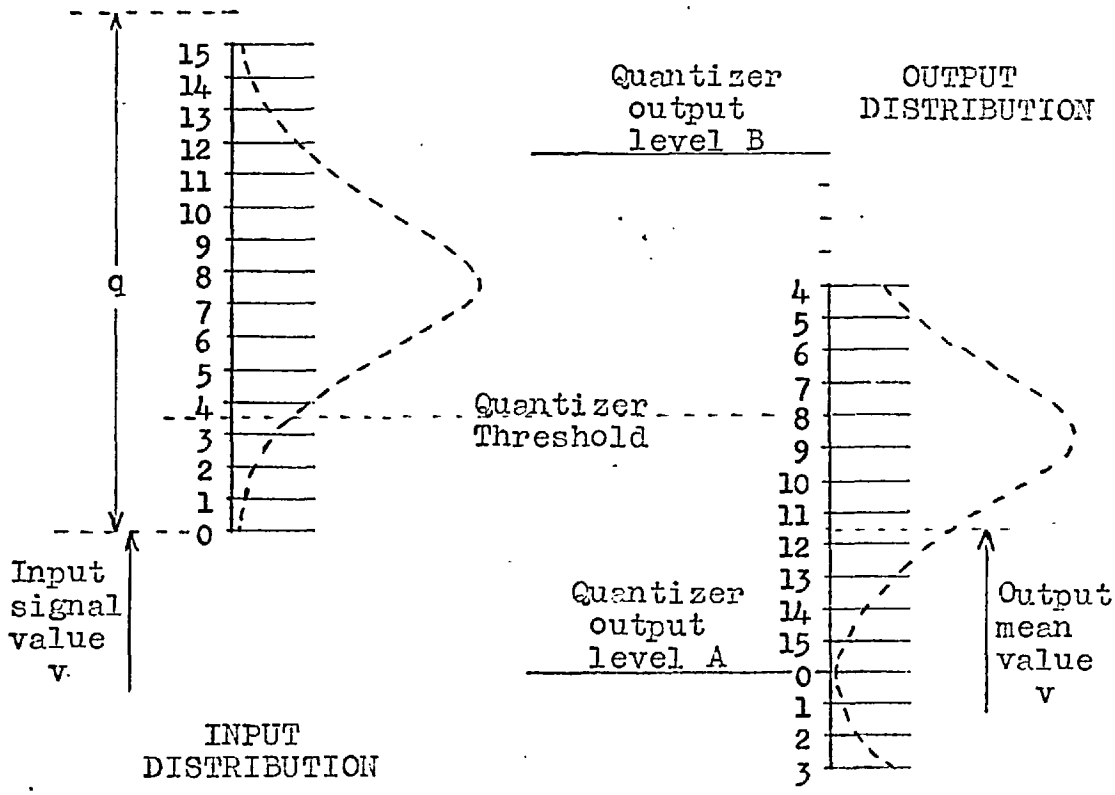

Figure 4.4. Input and output distributions for dithered quantization in which the dither is also subtracted from the quantizer output. A 16 level dither with uniform p.d.f. is shown added to signal value v. The dashed curves show a Gaussian dither distribution.

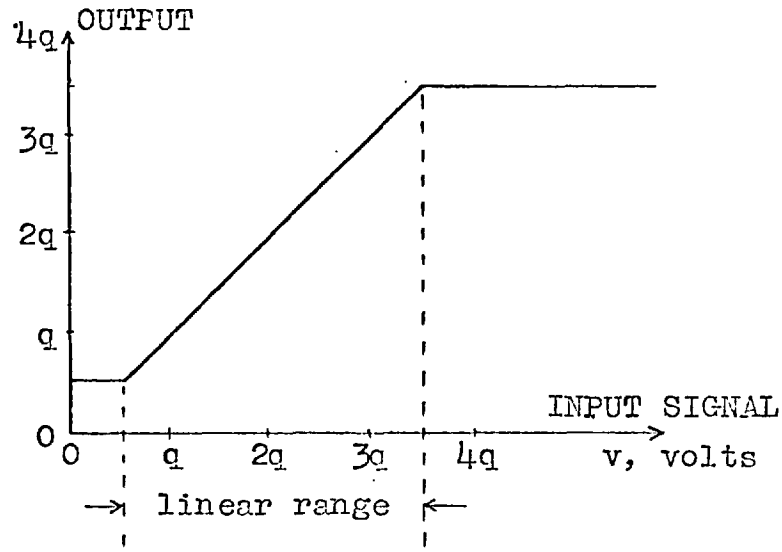

Figure 4.5. Linear range of a 2 bit dithered quantizer.

whereas if the peak-peak amplitude is greater than q, overlapping occurs. Also it is only for a uniform dither p.d.f. that the output p.d.f. is also uniform and the output mean equal to the input signal value. For the Gaussian dither, represented by the dashed curve in Figure 4.4, the output p.d.f. clearly depends upon the input signal level. By a similar consideration of higher order statistics it is also found that the dither samples must be independent if the quantizing noise distributions are to be independent of signal input level.

Figure 4.5 shows the range over which a 2 bit quantizer may be linearized by a dither of uniform p.d.f. Compared with straight quantization, the dither reduces the input signal range, over which the minimum mean square error $q^2/12$ is achieved, by one quantum. The maximum signal amplitude which does not saturate the quantizer is thus 3q, and the corresponding output S/N ratio is $20\log_{10}(3q/\frac{q}{\sqrt{12}}) = 20.3$ dB. Roberts accepted "edge effects" as a source of tonal error and retained the full signal input range (4q) of the straight quantizer. For very coarse quantization however, clipping is much more objectionable than additive noise and the reduced signal range must be accepted.

Much of the remainder of this thesis is concerned with an investigation of Roberts' technique for dithered quantization. Roberts included only one subjective factor in the

proposal - that random noise is more acceptable than false contours. It will be shown that it is also possible to include a noise weighting function which very significantly reduces the visibility of the pseudo-random quantizing noise.

The following Section describes "real time" implementation of Roberts' computer simulation. In particular, this allowed investigation of the question of whether the dither should be synchronized to the television frame frequency. Roberts felt that the dither should be free running to allow the eye to integrate the noise over time as well as space. However, reference was also made to some unpublished work by James and Mounts on a 4 bits/sample dithered system, in which synchronization was found to be preferable.

4.4. EXPERIMENTS WITH A 2 BIT PSEUDO-RANDOM QUANTIZER

4.4.1. An Investigation of Roberts' System

Roberts' scheme was implemented as shown by the schematic diagram of Figure 4.6. The picture generation equipment and the shift register generator are described in Section 3.3.

Before quantization, the television signal was band-limited to 3 MHz. According to sampling theory, 6 M samples per second would be sufficient to transmit the signal, although in practice a sampling rate 20 % higher than this

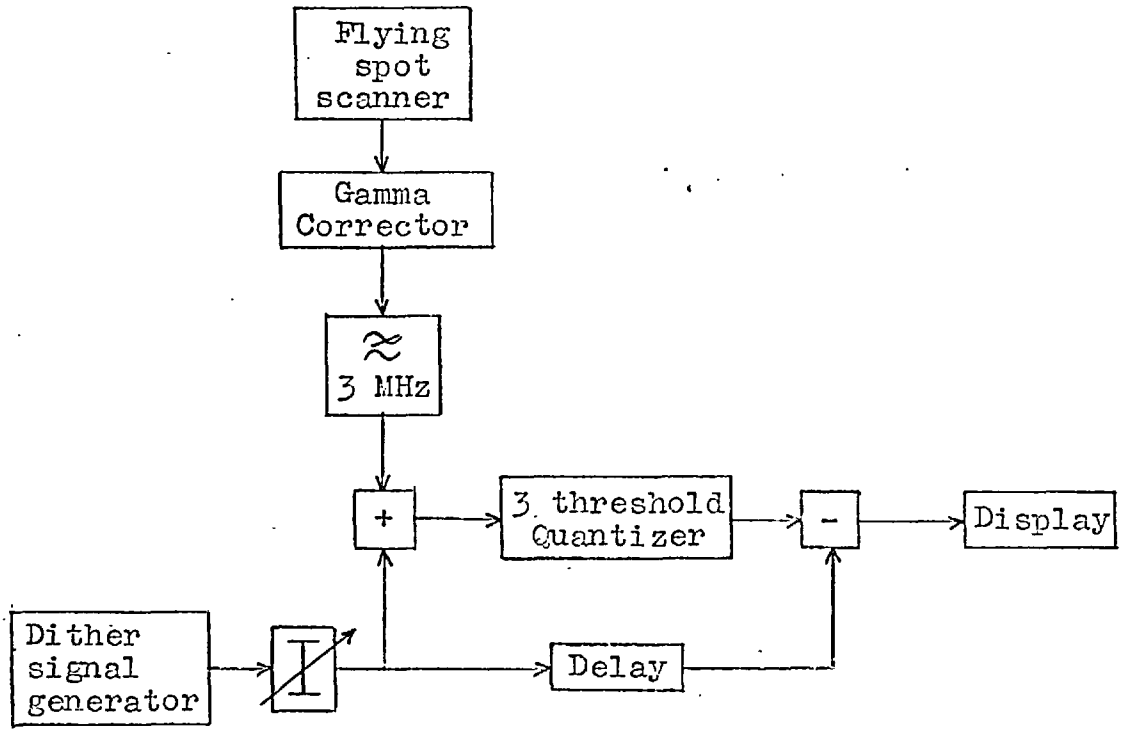

Figure 4.6. Unity-gamma system used to investigate 2 bit pseudo-random quantization.

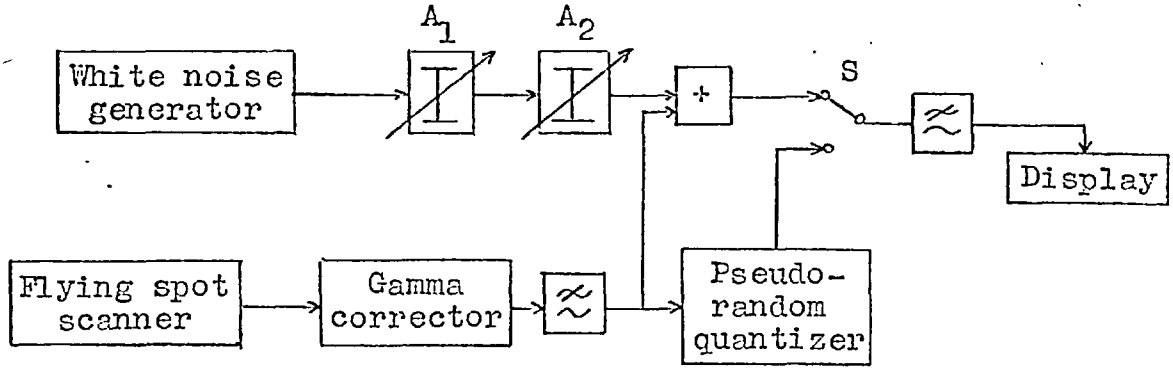

Figure 4.7. Arrangement used for subjective evaluation of the pseudo-random quantized image.

would be used to allow for the finite roll-off of the interpolation filter. The quantizing process has been reduced effectively to the simple addition of random noise uniformly distributed over one quantum and, since this noise is already in sampled form, synchronous sampling subsequent to quantizing cannot cause any aliasing into the signal band. Furthermore, in the unsampled system of Figure 4.6, no signal information is transmitted in excess of that which would be sent through a sampled system. The sampling operation was omitted on this justification in order to keep equipment complexity at a minimum. The justification is restricted since the dither is itself quantized, being the weighted sum of a number of binary S.R.G. outputs. For a 16 level dither, the image remains quantized to 6 bits after 2 bit quantization and this error would be aliased into the signal band by sampling. However, even for the coarsest dither (6 levels) used in the experiments, this error would be negligible in comparison with the apparent noise levels obtained.

The quantizer was designed to accommodate up to eight threshold detectors, each on a separate plug-in card. Detector outputs defined equal currents which were summed to produce the quantizer output, and the current amplifier had two preset gains corresponding to 2 and 3 bit quantization. The input signal (0 to 1 volt at 75 ohms) was first amplified by six (0 to -6 volts) to improve the sensitivity

and stability performance of the threshold detectors. For 2 bit quantization, three thresholds were used at -1,-3 and -5 volts. Each detector comprised a long-tailed-pair amplifier driving a single saturating transistor, with positive feedback to cause regeneration for fast switching. Some hysterisis was also included to prevent high frequency limit cycling at signal voltages near threshold. Wideband amplifiers and fast switching were essential to minimize time warping of the threshold detector outputs since the subsequent subtraction of the suitably delayed dither produced high frequency transients which tended to reduce the mean square value of the quantizing noise. This proved to be the main disadvantage of omitting the sampling operation, but careful circuit design and delay equalization reduced this effect to the order of 0.5 dB.

The 18 stage S.R.G. was clocked at 6 MHz to provide one number per picture sample. (Clock rates to generate one number per line or field were found to give intolerable streaking and flicker respectively.) A 16 level dither was obtained by decoding 4 binary components in a resistive network. The most significant component was the modulo-2 sum of a S.R.G. output and a 3 MHz square wave, and the three lesser significant components were S.R.G. outputs spaced over the sequence period by means of modulo-2 adders in order to avoid bandlimiting. The dither amplitude was

adjusted in the adder and subtractor to $\frac{15}{16}$ the spacing between thresholds, and a tapped delay line was used to equalize the delays incurred in the adder and quantizer.

The arrangement shown in Figure 4.7 was employed in some observer tests to verify the expected image quality for two bit quantization by comparison with the output of a further adder which combined unprocessed video with a variable level of white Gaussian noise. Both signals were bandlimited to 3 MHz before display so that, allowing for the part of the $(\frac{\sin \delta w/2}{\delta w/2})^2$ dither spectrum outside the video band, the expected S/N ratio was 21.3 dB. The Gaussian noise was taken from a General Radio Random Noise Generator type 1390 B, which uses a gas discharge tube as the noise source, and which had the cumulative power spectrum plotted in Figure 4.8. The noise adder had an active range such that only noise peaks higher than 4σ at peak white were clipped at a S/N ratio of 20 dB.

Six observers were tested individually on each of the six pictures shown in Figure 4.9. Each observer was asked to operate switch S (Fig. 4.7) and to adjust the attenuator A_2 until he (or she) considered the two displays to be equally acceptable. The opinion of each observer on each picture was taken as the mean of the outcomes $(A_1 + A_2)$ of two tests. A predetermined sequence of 12 randomly chosen settings of A_1 was followed for each observer to prevent

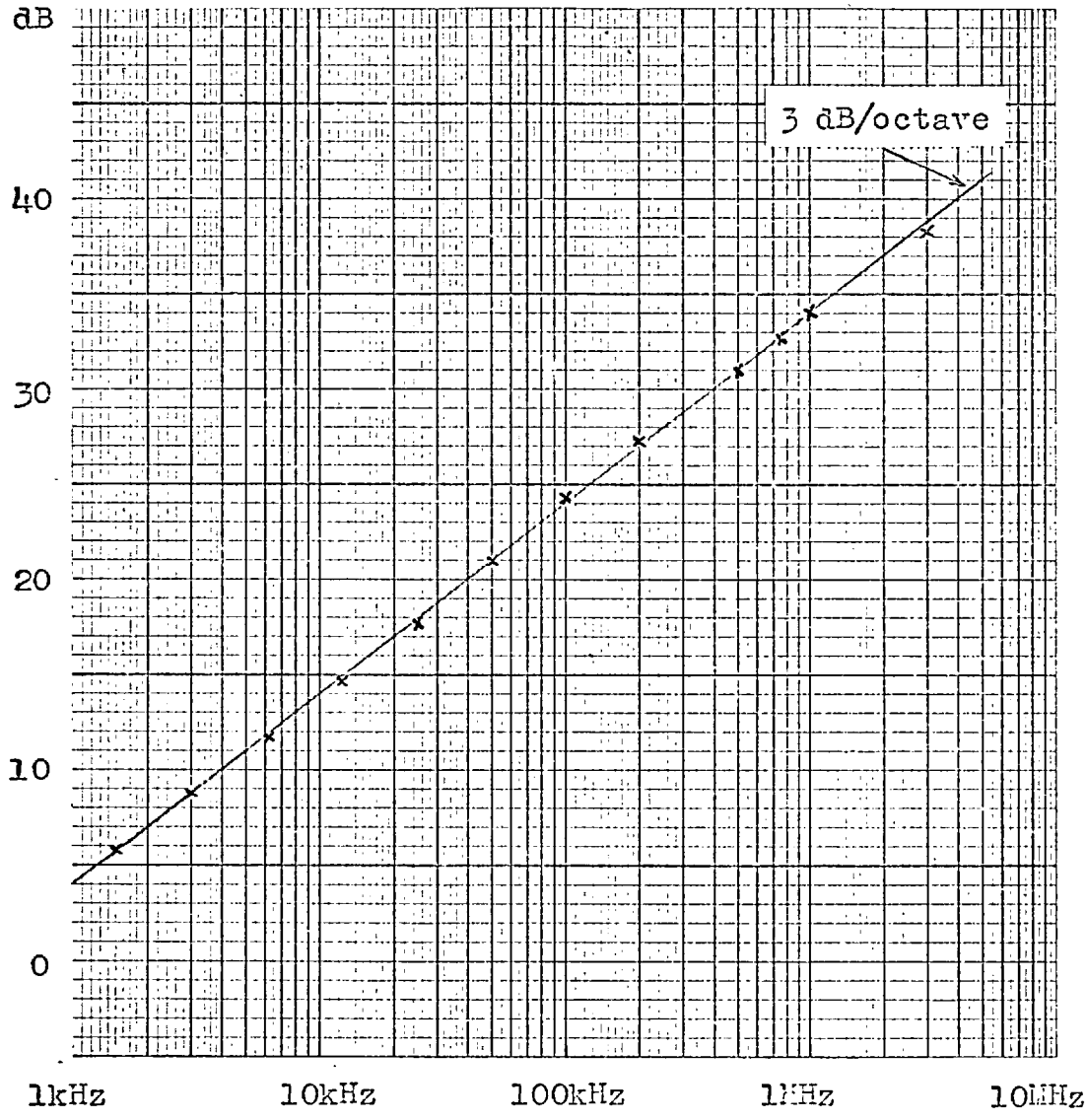

Figure 4.8. Cumulative power spectrum of the Gaussian white noise generator (General Radio 1390B) used in subjective measurements.

(a) Flick

(b) Fruit seller

(c) Helicopter

(d) Felicity

(e) Beeches

(f) Church

Figure 4.9. Pictures used in the experiments.

learning. Only two tests per picture were conducted since earlier experiments had shown remarkable consistency of observer opinion over a range of 8 settings of A_1. These tests had employed the same six observers, but only one picture - that of Figure 4.9(a). A viewing distance of 8 picture heights was adopted for a high quality 17" monitor and the tests were carried out in a special viewing room under the lighting conditions recommended by PROSSER et al[97]. Ambient illumination was adjusted to 3 lux and picture highlight luminance was maintained at 16 ftL. Readings of the attenuator A_2 were communicated verbally by means of an intercom system.

The overall mean of the 36 opinions was 22.2 dB with a variance of 0.59 dB^2. Analysis of variance[84] showed no significant difference between the variance estimates based on between-observer and between-picture degrees of freedom, but both of these were very significantly higher than that based on residual degrees of freedom.

Figure 4.10(b) illustrates the frozen noise of the 2 bit pseudo-random quantized image with the S.R.G. synchronized to frame trigger (or alternatively, a single frame photograph of the asynchronous noise evaluated in the experiments). It is interesting to compare this image quality with that of straight 2 bit quantization shown in Figure 4.10(a). The effectiveness of the dither in breaking the causal connection

(a)

(b)

Figure 4.10. 2 bit Quantization : (a) Straight

(b) Pseudo-random.

between signal and quantizing error is further illustrated by Figure 4.11. The latter images were obtained by subtracting the quantizer output from the original video and show the actual quantizing error, though at four times contrast. Figure 4.11(a) shows the error made in straight quantization of the picture of Fig. 4.9(a) into four equally spaced levels. Figure 4.11(b) shows the same mean square error, but with pseudo-random dither (the slight signal dependence arose from non-linearity of the adder). It was noticed that decoding four adjacent S.R.G. outputs, as proposed by Roberts, introduced no detectable signal dependence into the quantizing noise when displayed as in Figure 4.11(b), in spite of the broader dither autocorrelation function.

Viewer preference for free-running or frame-synchronized noise was investigated for moving pictures received from the normal broadcast services. Twelve observers were tested individually, ten being engineers but with no particular experience of television. For the 2 bit display, corresponding to 22 dB S/N ratio, each was allowed to watch either situation at will for some time and then asked which he or she found the more acceptable. 11 of the 12 chose synchronized noise with the following reasons and reservations.

Synchronization of the noise gives the impression of viewing through a dirty window - as if a thin fabric has

(a)

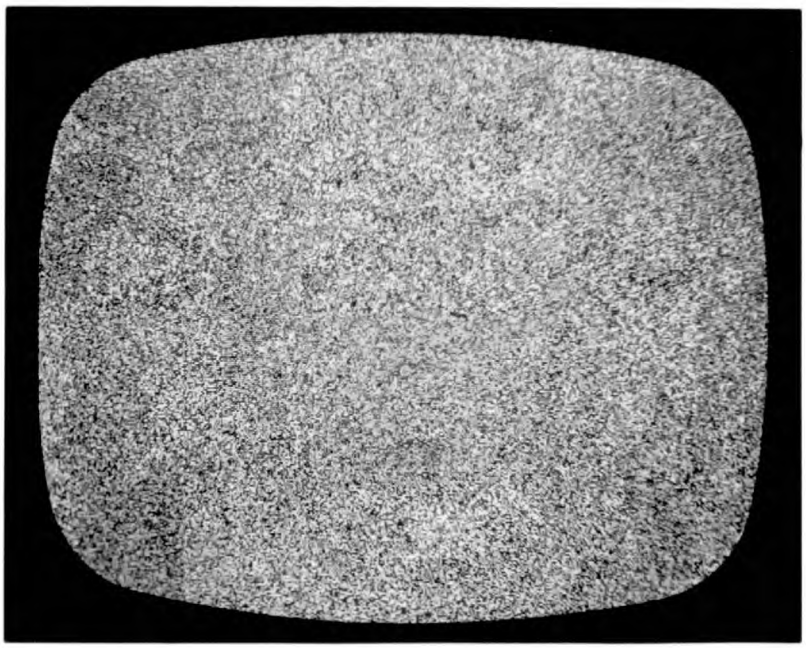

(b)

Figure 4.11. 2 bit Quantization Error : (a) Straight (b) Pseudo-random.

been inserted between the tube face and the implosion guard glass. At 22 dB S/N ratio, this tends to obscure fine detail in the picture and can be annoying unless the subject moves. The detail in faces, etc., is much more important subjectively than that in trees and backgrounds generally where the viewer may not even be aware that stationary noise has been added. Some viewers found synchronized noise particularly objectionable on fast moving pictures where there is rapid subject movement, panning and zooming. Here migrating noise becomes less noticeable. On still or slowly moving subjects however, migrating noise is very objectionable, particularly in scenes containing large background areas of uniform brightness when it becomes difficult to concentrate on the subject.

For 3 bit quantization, corresponding to 28 dB S/N ratio, each observer adhered to the preference given with the 2 bit display. However, most of the observers were familiar with signal/migrating-noise ratios of this order and better, and they were considerably more tolerant of the asynchronous dither. The synchronized dither was not of sufficient intensity to cause appreciable masking of detail and for many pictures the noise was barely even perceptible.

For entertainment purposes, synchronization of the dither was therefore judged preferable - a fortunate preference since this eliminates the need for more

synchronizing information than the readily available frame trigger to keep the transmitter and receiver noise generators in step. However, in a 2 bit system transmitting still pictures for identification purposes, the synchronized dither masks detail which migrating noise, although subjectively more annoying, allows the viewer to extract by correlating successive frames.

This concludes the investigation of Roberts' system. The remainder of this Section describes an early development of the system (THOMPSON & SPARKES[118]) which has led to a generalized proposal for optimizing the pseudo-random quantizer.

4.4.2. Development of the 2 bit Quantizer

In the initial stages of this work, it was thought that it might be possible to order successive frames of pseudo-random numbers in order to optimize the estimate of the original picture obtained by averaging the system output over two frames. It has since been shown in fact that it is not possible to improve on the mean square average error over two frames produced by Roberts' migrating dither. However, a dither was conceived which generated a less objectionable power spectral distribution of the quantizing noise.

It was realized that it is possible to obtain 3 bit precision from a 2 bit quantizer by averaging two frames, dithered by a binary signal of amplitude equal to half the quantizing interval (q) and which inverts from frame to frame. If in one frame a particular picture element incurs an error $\pm e$, the error in the next frame becomes $\pm(e - q/2)$. The average error is therefore $\pm(e - q/4)$, which lies within bounds $\pm q/4$.

The simplest dither signal - a square wave of period two frames - yields very severe flicker in low detail pictures, and even a synchronized prbs produces areas of constant intensity of sufficient size to generate annoying flicker when inverted in this way. By using a 3 MHz square wave from a bistable clocked at 6 MHz and reset such that the phase reverses frame by frame, the flicker can be reduced to the smallest area definable by the system and therefore to the least annoying level.

In the laboratory system, the 6 MHz master oscillator operated at even harmonics of line and frame frequencies so that the pattern generated by a bistable was aligned vertically, as indicated in Figure 4.12(a), and did not invert frame by frame. The output of a second bistable clocked at line frequency was therefore added modulo-2 to give the pattern of Figure 4.12(b). Since line frequency is an odd harmonic of frame frequency, this pattern now

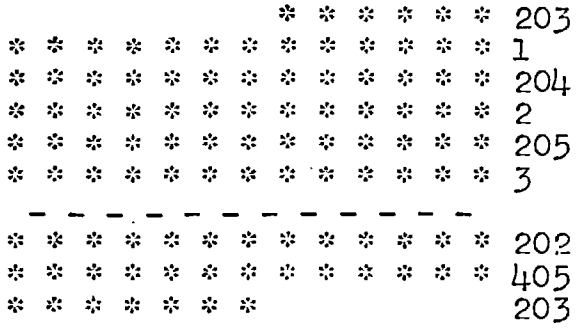

Figure 4.12.

(a) Dot pattern from a bistable clocked at 6 MHz.

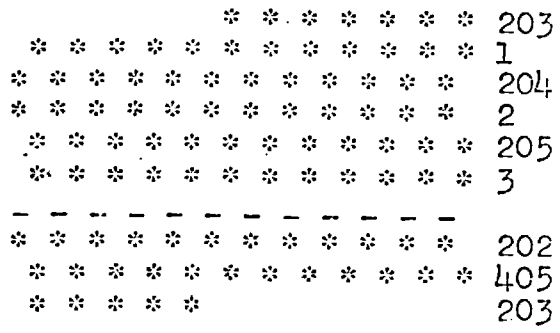

(b) Dot pattern obtained by adding modulo-2 the pattern of (a) to the output of a bistable clocked at line frequency. The pattern inverts frame by frame.

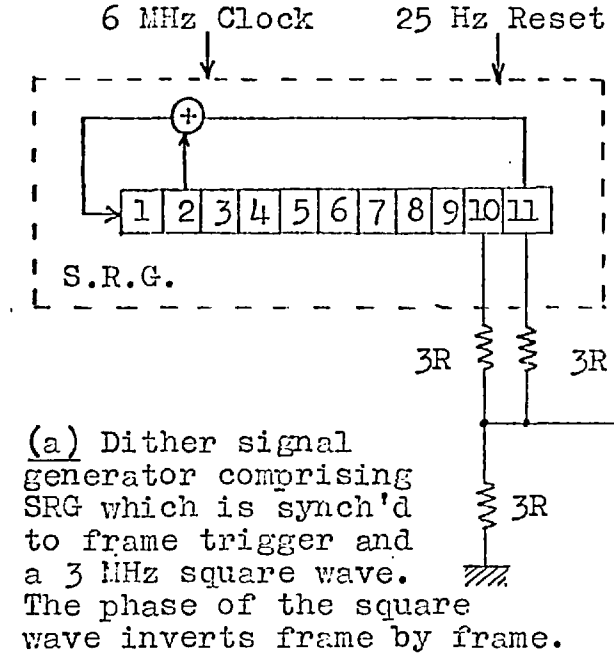

(a) Dither signal generator comprising SRG which is synch'd to frame trigger and a 3 MHz square wave. The phase of the square wave inverts frame by frame.

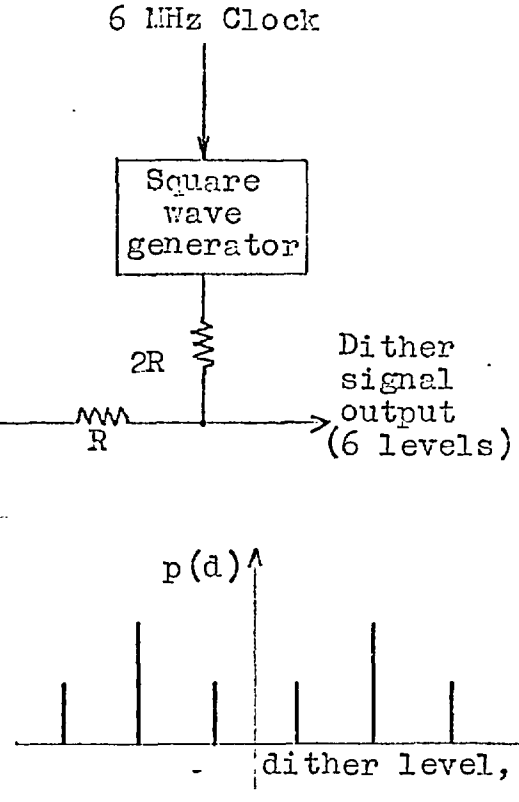

Figure 4.13.

(b) Six level dither p.d.f.

inverts frame by frame. The pattern is superior to that of Figure 4.12(a) in its almost total reduction of Moiré interference with picture detail. Lines are still paired however, and a further improvement in this respect would be effected by alternately advancing and retarding the dither by 90° at the initiation of each field (HAANTJES & TEER [48]), but this was not easily realizable in the laboratory.

Using the dither corresponding to Fig. 4.12(b), an 8 level image was obtained with an amount of fine flicker. A frame-synchronized pseudo-random noise component of amplitude $\frac{1}{2}q$ was then added to the dither to disperse the flickering contours. These disappeared for as few as two S.R.G. outputs, which were chosen and combined so as to minimize the level of flicker. It was found that two adjacent outputs combined with equal weight had the greatest smoothing effect on quantizing noise while other separations, particularly of an even number of stages, gave a considerable increase in flicker. Separation of 594 elements (one line period) produced flicker suppression only marginally worse than for adjacent readouts. Generating the dither as shown in Figure 4.13 , the image had no visible contours for most pictures even though only 24 levels were present, but had an amount of fine flicker of similar appearance to migrating white noise. Image detail was therefore not obscured, even though the dither was synchronized. Also, since the viewer

is less aware of periodicity in the pseudo-random noise when the generator is synchronized, it was possible to reduce the length of the S.R.G. to 11 stages (a period of only 3.4 lines) without patterning becoming apparent. With the 11 stage S.R.G. running asynchronously however, a diagonal drift was just detectable in large areas of constant intensity. For this condition, at least 15 stages are necessary to avoid patterning for all videp inputs.

As for Roberts' system, six observers were employed to assess picture quality in terms of additive white Gaussian noise for the six pictures of Fig. 4.9. The same verbal instruction was given, and each opinion was again taken as the mean of two tests. The grand mean of the 36 opinions gave the equivalent S/N ratio as 27.6 dB, with a variance of 0.83 dB^2. Analysis of variance showed this to be mainly attributable to between-observer degrees of freedom. With the 3 MHz pattern inverting frame by frame, none of the observers could detect any difference between the fine flicker concommittant with synchronization of the S.R.G. and the migrating noise of the asynchronous arrangement.

Figure 4.14(a) and (b) show respectively single and double frame exposures of an image obtained using the dither generator of Fig. 4.13 and signal amplitude range 3q. Saturation of the quantizer was characterized by the appearance of stationary pseudo-random noise at peak black or

(a) Single frame exposure

(b) Double frame exposure

Figure 4.14. "Flick" - 2 bits/sample pseudo-random quantization with the dither of Fig. 4.13.

white, since for video inputs greater than 3q the dither cannot cause any threshold crossings and the displayed signal in these regions is simply the inverted dither. The eye then separates the stationary pseudo-random noise from the alternating 3 MHz pattern.

Finally, the system was tested for a wide range of still pictures and also for moving pictures from the broadcast services to check that the dither did not cause interference with picture detail or movement. This was found to be the case with the exception of a small amount of Moiré interference on the high frequency bars of the B.B.C. Test Card C. No interference occurred with typescript of size compatible with the limit of system resolution, and this was no less legible than in the unprocessed image.

It was mentioned that none of the observers could tell whether the S.R.G. was synchronized or not. It is interesting to note therefore that when required, the impression of migrating noise can be created even though the S.R.G. is synchronized so that in no circumstance is it necessary to transmit more synchronizing information than frame trigger.

It was stated at the beginning of the Section that the dither generator of Fig. 4.13 was initially conceived by consideration of means of ordering pseudo-random numbers so that averaging over only two frames yields the best

estimate of the original picture. In fact this system gives identical mean square averaged error over two frames to Roberts' scheme with migrating dither. Also, the validity of the mean square averaged error criterion is dubious as the flicker frequency is only one quarter of the C.F.F. The improvement over Roberts' system arises mainly from the concentration of quantizing error into a 3 MHz component which is less visible than pseudo-random noise of similar power. Attempts were made to improve image quality for 2 bit quantization by applying the techniques discussed in Chapters 2 and 3 to shape the dither spectrum, but it was difficult to correlate their effects on quantizing noise visibility. Analytic means were therefore sought to specify the quantizer non-linearity and to relate quantizing noise and dither in order to explain why adjacent S.R.G. outputs were necessary in the generator of Fig.4.13 and to predict how further improvements in image quality might be achieved.

4.5. PSEUDO-RANDOM QUANTIZER EQUATIONS

It was shown in Section 4.3.2 that the optimum dither for linearization has independent samples and a uniform p.d.f. over one quantum. However, the viewer is relatively insensitive to the amplitude distribution of noise, and it appears that neighbouring dither samples can be highly correlated without losing the impression that the quantizing error is additive and random. There is therefore considerable scope for reducing the visibility of this error by ~~matching~~ shaping its spectrum according to the subjective weighting function W(w) through a suitable choice of dither. In order to find the optimum dither, it is necessary to be able to express the quantizing noise spectrum in terms of the quantizer inputs. In this, the only relevant work known to the author is that of BENNETT[7], in which the spectra of 4 to 8 bit quantization errors were computed for a Gaussian input. The method used the second order p.d.f. of the input signal and could possibly be applied with certain assumptions to the present case. However, this appears excessively complicated and might not directly show the effects of variations in dither parameters.

The remainder of this Chapter is given to the development of an analysis which takes account of the structure of the dither in terms of its binary components, and the causal connection between quantizer input and output, to

relate the quantizing noise spectrum to the readout configuration on the basic S.R.G. The analysis rests on the gross, but workable, assumption that the video signal remains constant over large areas of a picture, these being precisely the regions where the viewer is most critical of noise.

4.5.1. Equations for a 6 level Dither

Consider the particular six level dither generator of Figure 4.13, but with three arbitrary binary (+1,-1) inputs x, y and z , of which x is the most significant. The dither may be written :

$$\frac{q}{2}\left(\frac{x}{2} + \frac{y}{6} + \frac{z}{6}\right)$$

The dither amplitude is adjusted to 5q/6 volts, rather than q volts, to avoid overlapping of levels.

Suppose that the video signal has a constant value, which for convenience will be measured with reference to the mid point, v_m, between two threshold voltages, as shown in Figure 4.15. At this value, the dither lies between the thresholds and the detector output remains constant at the lower threshold voltage, $-\frac{1}{2}q$. For other constant video inputs, there are only five alternative binary outputs which correspond to slicing the dither signal within its six levels (3 of these are shown for a particular dither

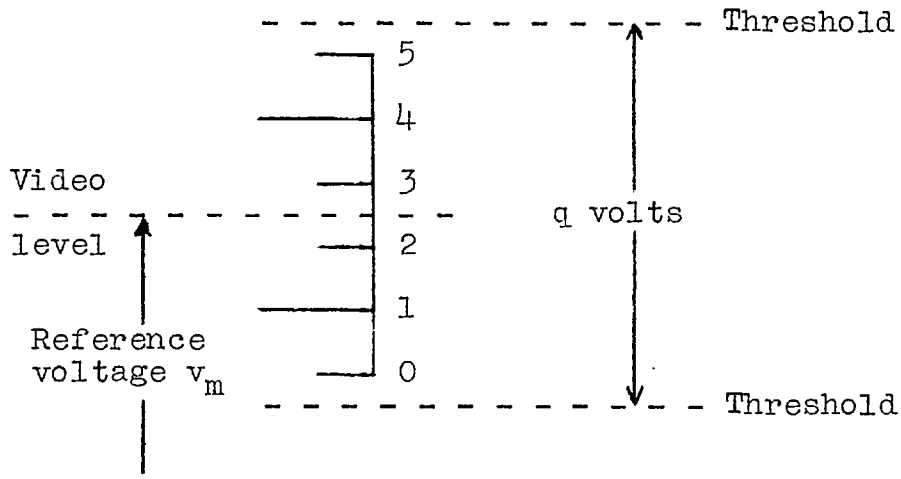

Figure 4.15. 6 level dither added to video voltage v_m.

Dither level	Binary dither components x	y	z	Slicing region	Video level (referred to v_m) corresponding to centre of slicing region	Logical expression for threshold detector output.
5	+1	+1	+1	4-5	q/6	x . y . z
4	+1	+1	-1			
	+1	-1	+1	3-4	2q/6	x . (y ∨ z)
3	+1	-1	-1			
				2-3	3q/6	x
2	-1	+1	+1			
				1-2	4q/6	x ∨ y . z
1	-1	+1	-1			
	-1	-1	+1	0-1	5q/6	x ∨ y ∨ z
0	-1	-1	-1			

Table 4.1. Binary functions generated by slicing the dither at various video levels.

in Figure 4.17(a)), and these may be expressed as logical functions of the three variables x , y and z as shown in Table 4.1.

The logical functions of Table 4.1 can be expressed as equivalent algebraic functions according to the rules :-

$$x \cdot y \equiv \tfrac{1}{2}(x + y + xy - 1)$$

$$x \vee y \equiv \tfrac{1}{2}(x + y - xy + 1)$$

Expressions for the sliced dither become :-

4-5 : $\tfrac{1}{4}(x + y + z + xy + xz + yz + xyz - 3)$

3-4 : $\tfrac{1}{4}(3x + y + z + xy + xz - yz - xyz - 1)$

2-3 : x

1-2 : $\tfrac{1}{4}(3x + y + z - xy - xz + yz - xyz + 1)$

0-1 : $\tfrac{1}{4}(x + y + z - xy - xz - yz + xyz + 3)$

The multilevel quantizer output is then obtained by multiplying the above expressions by a scaling factor $\tfrac{1}{2}q$, and subtracting the dither $\frac{q}{4}(x + \frac{y}{3} + \frac{z}{3})$:-

4-5 : $q/8.(-x + y/3 + z/3 + xy + xz + yz + xyz - 3)$

3-4 : $q/8.(x + y/3 + z/3 + xy + xz - yz - xyz - 1)$

2-3 : $q/4.(x - y/3 - z/3)$

1-2 : $q/8.(x + y/3 + z/3 - xy - xz + yz - xyz + 1)$

0-1 : $q/8.(-x + y/3 + z/3 - xy - xz - yz + xyz + 3)$

and for the reference video voltage v_m :

5-0 : $q/4.(-x - y/3 - z/3 - 2)$

Finally, the quantizing noise is obtained by subtracting the constant video input corresponding to (the centre of) each slicing region :

4-5 : $q/8.(-x + y/3 + z/3 + xy + xz + yz + xyz) - 13q/24$

3-4 : $q/8.(x + y/3 + z/3 + xy + xz - yz - xyz) - 11q/24$

2-3 : $q/4.(x - y/3 - z/3) - 12q/24$

1-2 : $q/8.(x + y/3 + z/3 - xy - xz + yz - xyz) - 13q/24$

0-1 : $q/8.(-x + y/3 + z/3 - xy - xz - yz + xyz) - 11q/24$

5-0 : $q/4.(-x - y/3 - z/3) - 12q/24$

Each of these expressions contains a function of x , y and z and a constant, or d.c. component. The latter comprises the shift of $-\frac{1}{2}q$, which is characteristic of practical quantization (this does not occur in the theoretical rounding off process), together with a signal dependent error between the mean quantizer output and the video input, which results from the non-uniform dither distribution (see Fig.4.13(b), p.162). These d.c. terms will be excluded from the quantizer (Q) equations, which will be used to determine quantizing noise spectra in terms of the binary components x , y and z. The quantizing noises are defined accordingly :-

$$Q_{45} = q/8.(-x + y/3 + z/3 + xy + xz + yz + xyz)$$

$$Q_{34} = q/8.(x + y/3 + z/3 + xy + xz - yz - xyz)$$

$$Q_{23} = q/4.(x - y/3 - z/3)$$

$$Q_{12} = q/8.(x + y/3 + z/3 - xy - xz + yz - xyz)$$
$$Q_{01} = q/8.(-x + y/3 + z/3 - xy - xz - yz + xyz)$$
$$Q_{50} = q/4.(-x - y/3 - z/3)$$

If x , y and z are outputs of the same S.R.G., products of these are also outputs of the S.R.G. with delays which can be determined from the Feedback Equation (Sec. 2.3.2). The Q-equations then express quantizing noise for a given video input as the sum of a number of weighted S.R.G. outputs and the autocorrelation techniques of Section 2.6 can be applied to determine the six quantizing noise spectra.

4.5.2. Analysis of the Experimental System

In Section 4.4.2, it was described how a subjective improvement of 5.4 dB was obtained over Roberts' system by choosing x as a 3 MHz square wave, inverting at frame frequency, and y and z as adjacent outputs of a S.R.G. which was clocked at 6 MHz. Analysis of this system will serve to illustrate the use of the Q-equations.

Designate s as the 3 MHz square wave, and y_1 , y_2 as the adjacent S.R.G. outputs. The Q-equations are obtained by substitution into the above set, of which the first becomes :

$$Q_{45} = \frac{q}{8}\left\{\frac{1}{3}(y_1 + y_2) + s(y_1 + y_2) + y_1y_2 + sy_1y_2 - s\right\}$$

It is found by iteration of the feedback equation for this S.R.G. ($x^{11} \oplus x^2 \oplus 1 = 0$) that addition modulo-2 of two adjacent outputs generates the same sequence delayed by 1029 clock intervals on the output of stage 1.

$$\text{Thus,} \quad y_1 y_2 = y_{1030}$$

It was shown in Section 2.6.4 that for the purpose of determining the envelopes of power spectra, widely spaced S.R.G. outputs may be considered independently. The contributions of the five terms in Q_{45} can therefore be considered separately in computing the power spectrum corresponding to this particular Q-equation.

(i) $\frac{1}{3}(y_1 + y_2)$ has power spectrum envelope $\frac{1}{9}\left\{\frac{8}{N}\left[\frac{\sin \delta w}{\delta w}\right]^2\right\}$ of lines at even harmonics of $1/2N\delta$.

(ii) $s(y_1 + y_2)$ has the envelope $\frac{8}{N}\left[\frac{\sin^2 \delta w/2}{\delta w/2}\right]^2$ of lines at odd harmonics of $1/2N\delta$.

(iii) $y_1 y_2 = y_{1030}$ has the envelope $\frac{2}{N}\left[\frac{\sin \delta w/2}{\delta w/2}\right]^2$ of lines at even harmonics of $1/2N\delta$.

(iv) $sy_1 y_2 = sy_{1030}$ has the envelope $\frac{2}{N}\left[\frac{\sin \delta w/2}{\delta w/2}\right]^2$ of lines at odd harmonics of $1/2N\delta$.

(v) s , a 3 MHz square wave of identical amplitude and power to a S.R.G. output, has a spectrum of lines at odd harmonics of 3 MHz.*

* see bottom p.175

Putting $\delta = (6\ \text{MHz})^{-1}$, the envelopes (i) - (v) can be summed to give the spectrum plotted in Figure 4.16(a). Inspection of the Q-equations shows that this spectrum is also obtained for Q_{01}, Q_{12} and Q_{34}. Likewise, Q_{23} and Q_{50} have identical spectra, but composed only of items (i) and (v). These are given by curve (b) in Figure 4.16. Also plotted, as curve (c), is the correspomding quantizing noise spectrum for all slicing levels using Roberts' 16 level dither generated from four independent S.R.G. outputs. The mean square value of this uncorrelated dither is very nearly $q^2/12$, and the power spectrum is given by :

$\frac{q^2}{12}\left\{\frac{2}{N}\left[\frac{\sin\delta w/2}{\delta w/2}\right]^2\right\}$ envelope of lines spaced by $1/N\delta$ Hz.

The Q-equations plotted in Figure 4.16 suggest that quantizing noise should appear in patches of either a low frequency noise together with a strong 3 MHz component, or a noise of broader spectrum together with a lesser 3 MHz component. Weighting the curves with Gilbert's estimate of W(w) and integrating over the video frequency range, the predicted difference in visibility between (b) and (c) agrees well with the figure of 5.4 dB found by subjective measurements. Curve (a) however, seems to overestimate noise objectionability by about 2 dB for

---

*By equating the energy within $N\delta$ seconds of the component at 3 MHz to the total energy in the first $2^{11}-1$ lines of the spectrum of y_1, it can be shown that this component stands 30 dB above the power per line of y_1 at low frequencies. However, this figure is of little use in estimating the relative visibility of the two binary signals.

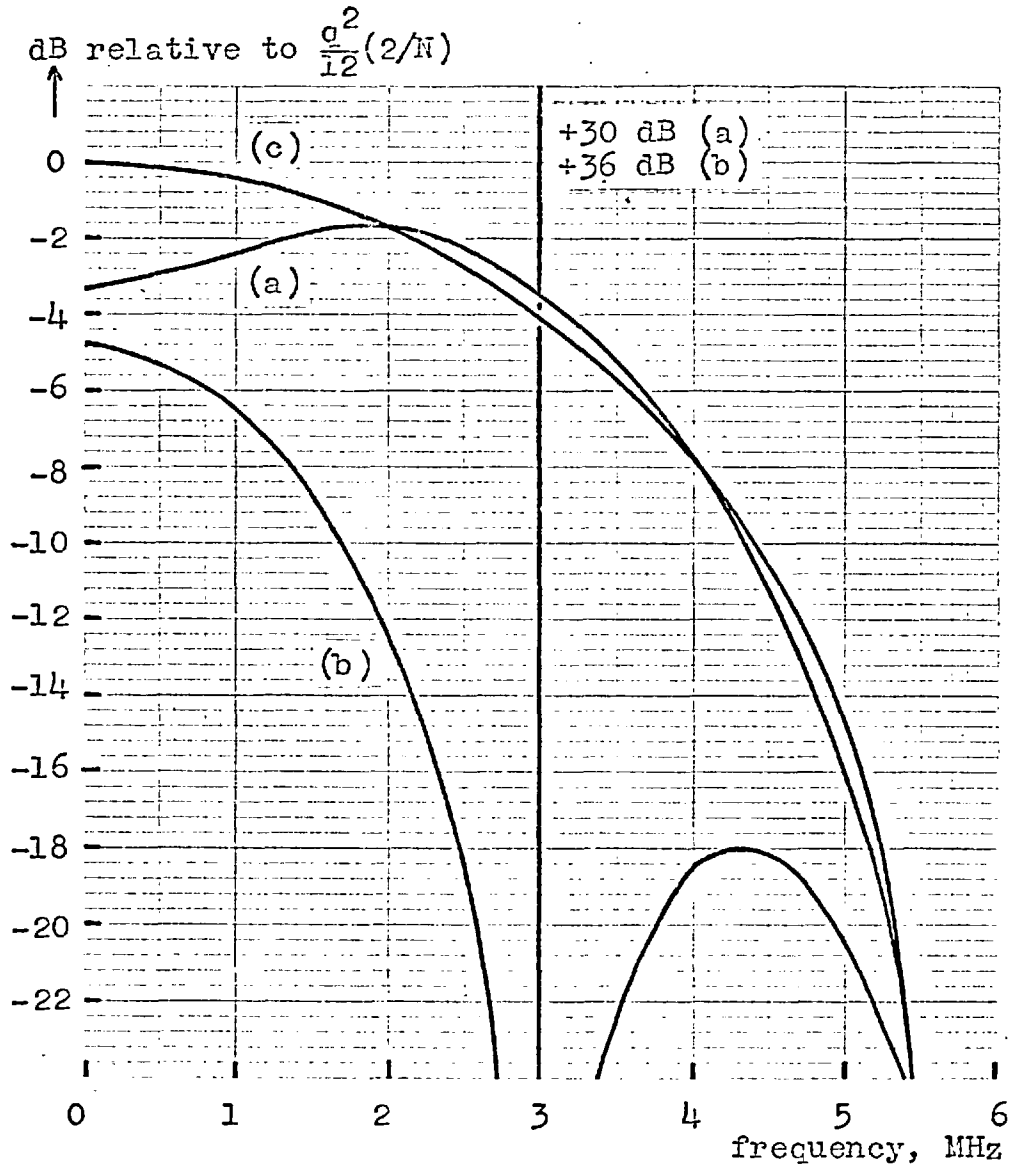

Figure 4.16. Envelopes of line spectra of quantizing noises : (a) $Q_{45}, Q_{34}, Q_{12}, Q_{01}$

(b) Q_{23}, Q_{50}

(c) all levels for an uncorrelated dither.

the corresponding levels. Much of this discrepancy can perhaps be accounted for by the different appearances of the noises. The (b)-noises are identical to the dither (Fig.3.11(d) illustrates their appearance without the 3 MHz component) and have a symmetrical distribution, whereas the (a)-noises have asymmetric distributions. Inspection of the sliced dither waveforms shown in Figure 4.17 shows that the noise Q_{01} is derived from the inverted dither (Fig.4.17(b)) by transferring the highest of the six levels to a new lowest level, the other five remaining unchanged. Its appearance is therefore characterized by black speckles, and likewise that of Q_{45} by white speckles. Q_{12} and Q_{34} again have different appearances, but have similar distributions to Q_{45} and Q_{01} respectively. Patchiness of the noise was apparent on a processed grey scale, but not on any of the processed pictures although the speckles were quite visible (see Fig. 4.14).

The upper curve (a) of Fig. 4.16 and its corresponding Q-equations serve to explain the necessity for the two S.R.G. outputs to be adjacent in the dither generator of Fig. 4.13. The four equations contain similar terms :-

$$Q_{45} = \frac{q}{8}\left[\frac{1}{3}(y+z) + s(y+z) + yz + syz - s\right]$$

For two adjacent register outputs, the term (y+z) has a low frequency spectrum with its first zero at 3 MHz. Multiplic-

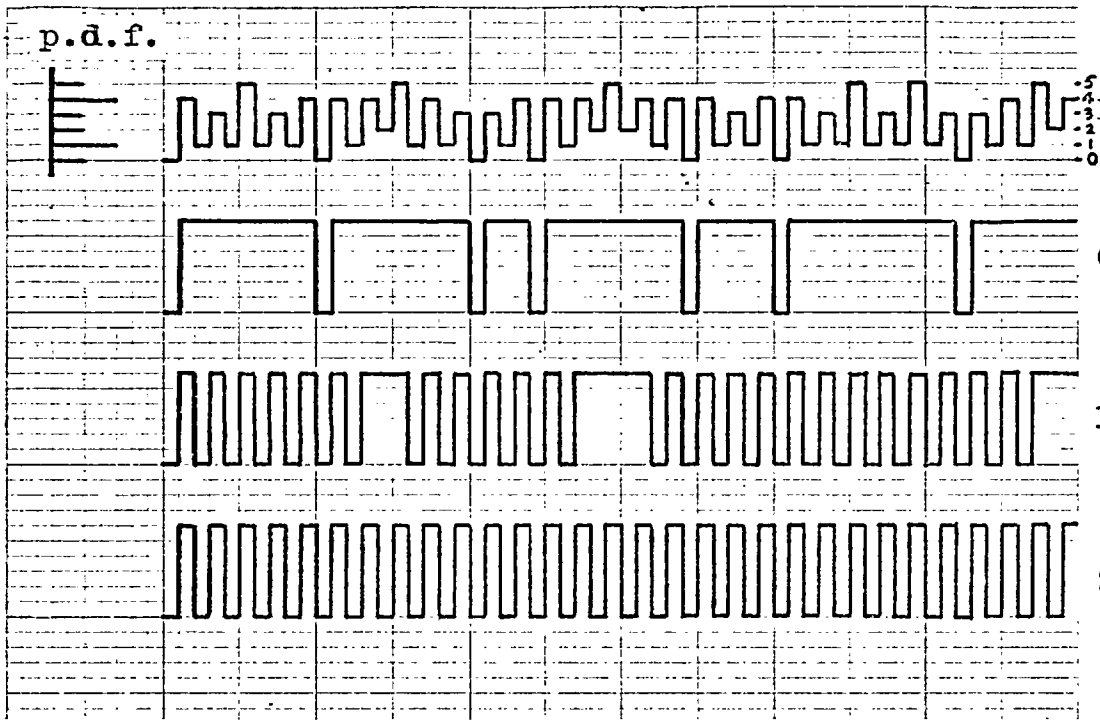

(a) Six-level dither and 3 of the 5 sliced waveforms

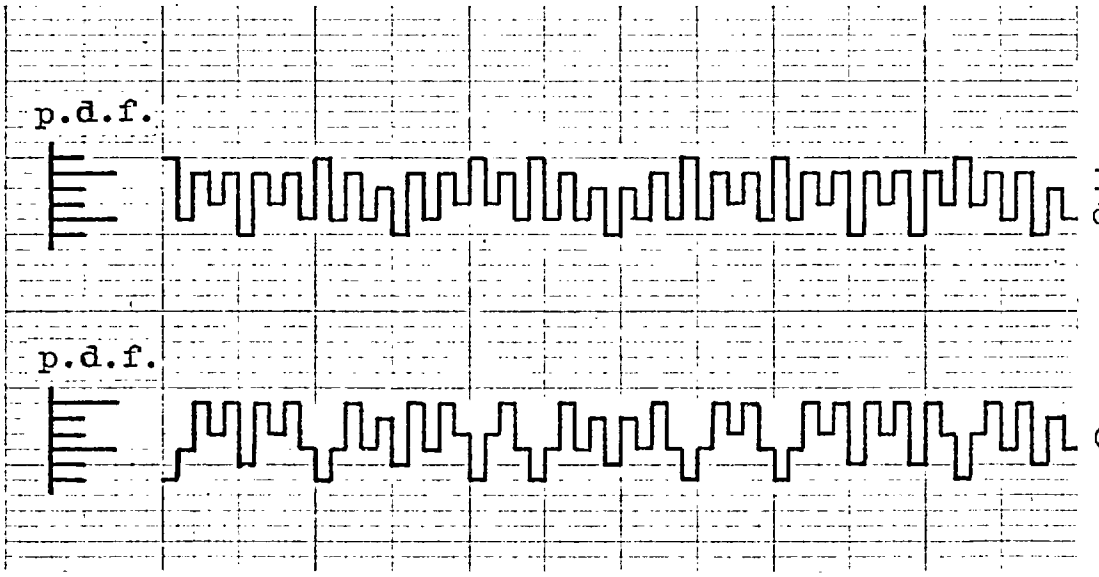

(b) Inverted dither and the quantizing noise Q_{01}

Figure 4.17. Waveforms associated with part of the six-level dither sequence showing derivation of Q_{01}.

ation by s then modulates this spectrum to a centre frequency of 3 MHz, producing a rising spectrum within the video band. The term s(y+z) thus contributes nothing to the subjectively important low frequency part of the video band. For other readout separations (and for adjacent readouts with one inverted) the term s(y+z) contributes accordingly at low frequencies. Within one field the eye is equally sensitive to the vertical spatial spectrum of the noise and, since the 3 MHz patterns inverts line by line, adjacent readouts - separated temporally by 594 elements - again produce a less objectionable noise.

In areas of constant picture intensity, much of the quantizing error is contained in the 3 MHz component, which is barely perceptible at a viewing ratio of 8. In detailed regions however, the quantizer non-linearity causes inter-modulation between the picture detail and the 3 MHz component which is therefore reduced in favour of low frequency "noise". It is of interest to record that although there was no statistically significant variation of opinion over the six test pictures, the lowest rating was given to the slide "Beeches". This is the most detailed picture and is the one for which the Q-equations would be expected to be least valid.

4.6. FURTHER DITHER CONFIGURATIONS

The development of Roberts' scheme for linearization has taken the form of an investigation of digital spectrum shaping which weights quantizing noise in favour of high frequencies ~~according~~ exploit to a subjective noise visibility characteristic. For a 6 level dither generator, it is desired to find at least three binary components which produce the optimum spectrum of quantizing noise for any slicing level. The observations of Section 4.4.2 and inspection of the Q-equations suggest that, using a S.R.G. clocked at 6 MHz, two adjacent readouts and a 3 MHz square wave may be the best binary components for a 6 level dither. A similar analysis for the 8 level dither $\frac{1}{2}q(\frac{1}{2}x + \frac{1}{4}y + \frac{1}{8}z)$ generated from the same binary components, shows its performance to be inferior to that of the 6 level dither in respect of the resultant level of low frequency quantizing noise.

Optimization on the basis of the Q-equations reduces to a search for at least three high frequency binary inputs of which the cross products also favour high frequencies, either singly or in combination. Clocking the S.R.G. at 3 MHz appears promising in view of the high frequency product of its output with a 3 MHz square wave.

One of the arrangements considered for generating a six level dither is shown in Figure 4.18, in which three

adjacent readouts were taken from a modulated half-rate m-sequence and decoded with respective weights 1/6, 1/2 and -1/6. Using the Q-equations for a 6 level dither, it can be shown that the corresponding quantizing noises become :

$$Q_{45} = q/24.(2sy'_1 + 4sy'_2 - 3sy'_1y'_2 - 3y'_1y'_2 + 3s)$$
$$Q_{34} = q/24.(-4sy'_1 - 2sy'_2 - 3sy'_1y'_2 + 3y'_1y'_2 + 3s)$$
$$Q_{23} = q/24.(-sy'_1 - 5sy'_2 - 3y'_1 + 3y'_2)$$
$$Q_{12} = q/24.(-4sy'_1 - 2sy'_2 + 3sy'_1y'_2 - 3y'_1y'_2 - 3s)$$
$$Q_{01} = q/24.(2sy'_1 + 4sy'_2 + 3sy'_1y'_2 + 3y'_1y'_2 - 3s)$$
$$Q_{50} = q/24.(5sy'_1 + sy'_2 + 3y'_1 - 3y'_2)$$

where y'_1 and y'_2 are adjacent outputs of a S.R.G. clocked at 3 MHz and s represents the 3 MHz square wave.

Inspection of these equations shows that there are again only two distinct spectra corresponding to the sets

(a) : Q_{01}, Q_{12}, Q_{34} and Q_{45} ; and (b) : Q_{50} and Q_{23}

Collecting dependent terms in the Q-equations :-

$$Q_{45} = q/24.\left[2s(y'_1 + 2y'_2) - 3sy'_1y'_2 - 3y'_1y'_2 + 3s\right]$$
$$Q_{23} = q/24.\left[-s(y'_1 + 5y'_2) - 3(y'_2 - y'_1)\right]$$

and similar expressions for the other 4 noises.

From the corresponding autocorrelation functions, it can be shown that the power spectral envelopes become :

(a) $$\left(\frac{q}{24}\right)^2.\left[\frac{8}{N}\left(\frac{\sin^2\delta w/2}{\delta w/2}\right)^2.(8\cos^2\delta w + 1) + \frac{72}{N}\left(\frac{\sin^2\delta w/2}{\delta w/2}\right)^2 + 9s^2\right]$$

(b) $$\left(\frac{q}{24}\right)^2.\left[\frac{8}{N}\left(\frac{\sin^2\delta w/2}{\delta w/2}\right)^2.(5\cos^2\delta w + 4) + \frac{72}{N}\left(\frac{\sin^2\delta w}{\delta w}\right)^2\right]$$

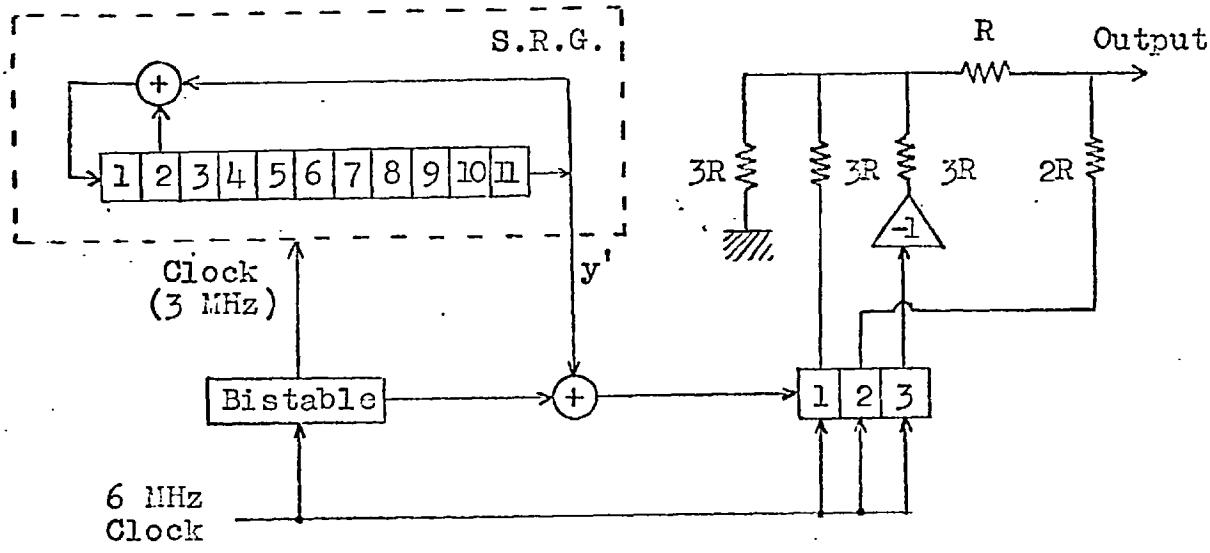

Figure 4.18. Dither generator with 3 MHz S.R.G. clock frequency

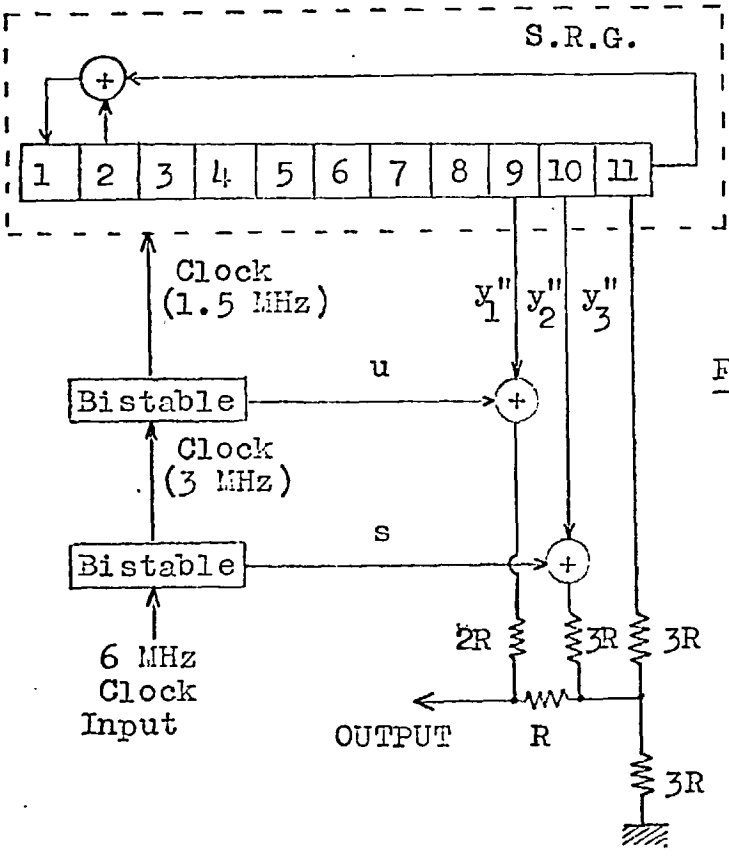

Figure 4.19. Dither generator with 1.5 MHz SRG clock frequency.

and the line spacing $1/2N\delta$ Hz.

The quantizing noise spectrum (c) for all slicing levels using an uncorrelated dither is given by :

$\left(\frac{q^2}{12}\right)\frac{2}{N}\left(\frac{\sin\delta w/2}{\delta w/2}\right)^2$ envelope of lines at harmonics of $1/N\delta$ Hz.

Rationalized to a common line spacing $1/2N\delta$, this may be written

$\left(\frac{q^2}{12}\right)\frac{1}{N}\left(\frac{\sin\delta w/2}{\delta w/2}\right)^2$ envelope of lines at harmonics of $1/2N\delta$ Hz.

The three spectral envelopes, (a), (b) and (c), are plotted in Figure 4.20 in which the amplitude scale is relative to $q^2/12N$. It can be seen that curve (b) represents a considerable subjective improvement over curve (c), but the overall objectionability is probably determined by the low frequency level of curve (a). On the test pictures of Fig. 4.9 , this system effected about 1 dB further improvement over the previous dither, but four of the spectra still contain a strong 3 MHz component which caused some Moiré interference on Test Card C. This was overcome by a third dither generator shown in Figure 4.19 , but which otherwise gave a similar performance.

By clocking the S.R.G. at only 1.5 MHz, a low bandwidth binary sequence is obtained which can be modulated to produce a rising spectrum by either a 3 MHz or a 1.5 MHz square wave. In the arrangement of Figure 4.19 therefore, two of the binary dither components have rising spectra and,

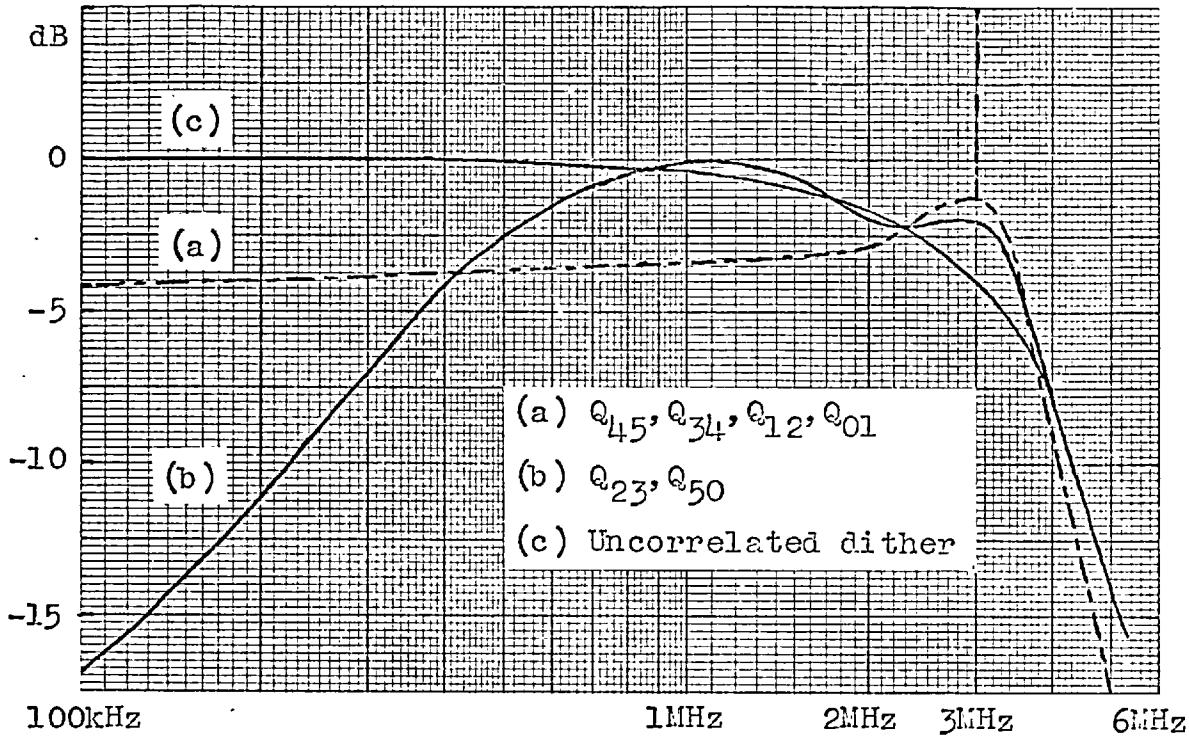

Figure 4.20. Quantizing noise spectra generated by the dither of figure 4.18.

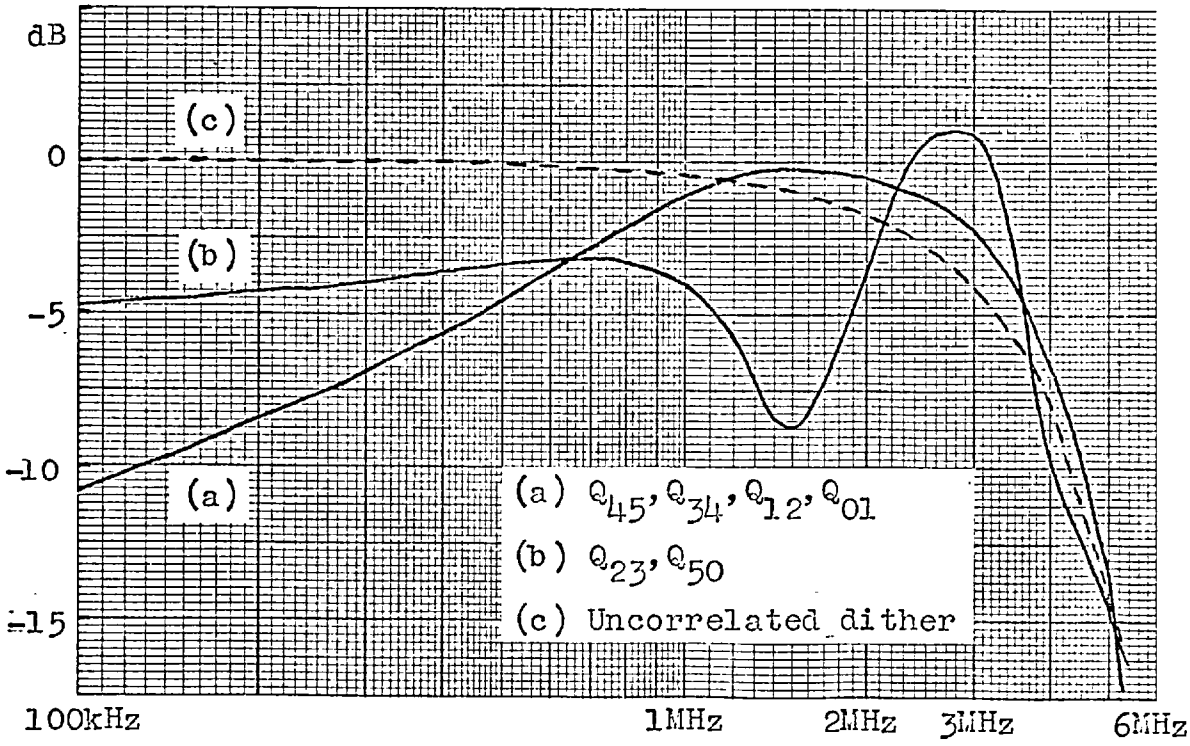

Figure 4.21. Quantizing noise spectra generated by the dither of figure 4.19.

since the product of the 3 and 1.5 MHz square waves is a further 1.5 MHz square wave (though its transitions occur between those of the prbs), most of the cross-products of these components also favour high frequencies. Substituting into the Q-equations the designations s and u for the 3 and 1.5 MHz square waves respectively, and using y''_1 , y''_2 and y''_3 to denote outputs of a S.R.G. clocked at 1.5 MHz, we obtain :-

$$Q_{45} = \frac{q}{8}(-sy''_1 + \tfrac{1}{3}uy''_2 + \tfrac{1}{3}y''_3 + suy''_1y''_2 + sy''_1y''_3 + uy''_2y''_3 + suy''_1y''_2y''_3)$$

$$Q_{34} = \frac{q}{8}(sy''_1 + \tfrac{1}{3}uy''_2 + \tfrac{1}{3}y''_3 + suy''_1y''_2 + sy''_1y''_3 - uy''_2y''_3 - suy''_1y''_2y''_3)$$

$$Q_{23} = \frac{q}{4}(sy''_1 - \tfrac{1}{3}uy''_2 - \tfrac{1}{3}y''_3)$$

$$Q_{12} = \frac{q}{8}(sy''_1 + \tfrac{1}{3}uy''_2 + \tfrac{1}{3}y''_3 - suy''_1y''_2 - sy''_1y''_3 + uy''_2y''_3 - suy''_1y''_2y''_3)$$

$$Q_{01} = \frac{q}{8}(-sy'' + \tfrac{1}{3}uy'' + \tfrac{1}{3}y'' - suy''y'' - sy''y'' - uy''y'' + suy''y''y'')$$

$$Q_{50} = \frac{q}{4}(-sy''_1 - \tfrac{1}{3}uy''_2 - \tfrac{1}{3}y''_3)$$

By Fourier integration of the respective autocorrelation functions, it can be shown that (see Appendix 8.2)

sy" has spectrum envelope		$\frac{2}{N}\cos^2\delta w.\left[\frac{\sin^2\delta w/2}{\delta w/2}\right]^2$
uy" " " "		$\frac{2}{N}\left[\frac{\sin^2\delta w}{\delta w}\right]^2$
suy" " " "		$\frac{1}{N}(1-\cos 2\delta w)\left[\frac{\sin^2\delta w/2}{\delta w/2}\right]^2$

and y" has spectrum envelope $\frac{2}{N}\left[\frac{\sin 2\delta w}{2\delta w}\right]^2$

.....of lines at harmonics of $1/4N\delta$ Hz.

Substituting these expressions into the above Q-equations, again only two distinct spectra are obtained and these are plotted as curves (a) and (b) in Figure 4.21. Curve (c) again shows the spectrum for all levels using the uncorrelated dither and has the form

$\frac{q^2}{12}\cdot\frac{1}{2N}\left[\frac{\sin\delta w/2}{\delta w/2}\right]^2$ referred to the line spacing $1/4N\delta$ Hz.

The amplitude scale of Figure 4.21 is relative to $q^2/24N$.

Whereas in Fig. 4.20 it is the (a) curve which sets the overall low frequency noise level, it is the (b) curve which does this in Fig. 4.21. This typifies the outcome of attempts to optimize the quantizing noise spectra for a 6 level dither. In spite of a systematic search, the author was unable to discover a third binary dither component of high frequency character which would cause further overall reduction of low frequency quantizing noise. However, even though the proposed systems are not optimum, their figures of improvement over Roberts' system are very close to the reduced visibility of triangular noise.

It should be possible to find dither components which produce a better fit of quantizing noise to subjective visibility, but this remains for future work. The improvement

might also be increased towards 8.5 dB by introducing vertical correlation into the dither (see p.128), which was not considered in the configurations described in this Section. There would perhaps be scope for this in a more complex dither of 16, or more, levels as is required to completely remove contours for all video situations.

The systems discussed so far have attempted to reduce the visibility of quantizing noise by a process of digital spectrum shaping which operates independently (approximately) of the video signal. In the next Chapter, the compatibility of this process with conventional pre and de-emphasis techniques is considered. For the television signal, reduction of quantizing noise power by R-C pre and de-emphasis filters around the quantizer can be increased significantly if the quantizing noise is first weighted in favour of high frequencies.

CHAPTER 5

QUANTIZATION WITH PRE & DE-EMPHASIS

5.1. PRE & DE-EMPHASIS NETWORKS

Most signals transmitted through a noisy channel have a non-uniform power density spectrum over the channel bandwidth. It is therefore possible to improve the output S/N ratio at certain frequencies by linear pre-emphasis of the signal before transmission and an inverse operation at the receiver. The pre-emphasis filter increases signal power in that part of the spectrum where this is low with a corresponding reduction in power where signal power is high in order to maintain transmitted power constant. Thus, where the original signal is of low power added noise is reduced, and vice-versa. FRANKS[33] has shown that the pre and de-emphasis filters which maximize S/N ratio at the receiver are essentially inverse for moderately high S/N ratios on the channel, and are given by :

$$\frac{1}{H_1(w)} \quad = \quad H_2(w) \quad = \quad \left[\frac{\mu F(w)}{N(w)}\right]^{\frac{1}{4}}$$

where $H_1(w)$ and $H_2(w)$ are the voltage transfer characteristics of the pre and de-emphasis networks, respectively ;

$F(w)$ is the signal power density spectrum ;

$N(w)$ is the channel noise power density spectrum ;

and μ is a constant which is adjusted to meet the maximum mean signal power constraint of the channel.

FINK et al[32] have estimated a typical video spectrum (see Figure 5.1) from measurements on a number of N.T.S.C. test slides. The monochrome signal spectrum falls monotonically by almost 60 dB over the band and would seem to be well suited to pre and de-emphasis techniques. However, the subjective noise visibility characteristic, W(w), is of opposite slope to the signal power spectrum so that emphasis tends to increase noise power where it is most visible. A more relevant criterion is that of signal/weighted-noise ratio, for which the optimum emphasis filters offer a somewhat reduced improvement. BRUCE[14] has shown these filters to be of the form :

$$\frac{1}{H_1(w)} = H_2(w) = \left[\frac{\mu F(w)}{W(w).N(w)}\right]^{\frac{1}{4}}$$

and it was estimated that for monochrome television subject to a mean power constraint, optimum pre and de-emphasis can improve S/N ratio by only 2.8 dB if the noise N(w) is white. In deriving this figure, Bruce used the W(w) characteristic of BARSTOW & CHRISTOPHER[3].

It is evident that a much greater improvement in S/N ratio can be obtained by emphasis networks if the additive noise spectrum N(w) rises with frequency. Such a situation was achieved at the end of Chapter 4, where pseudo-random

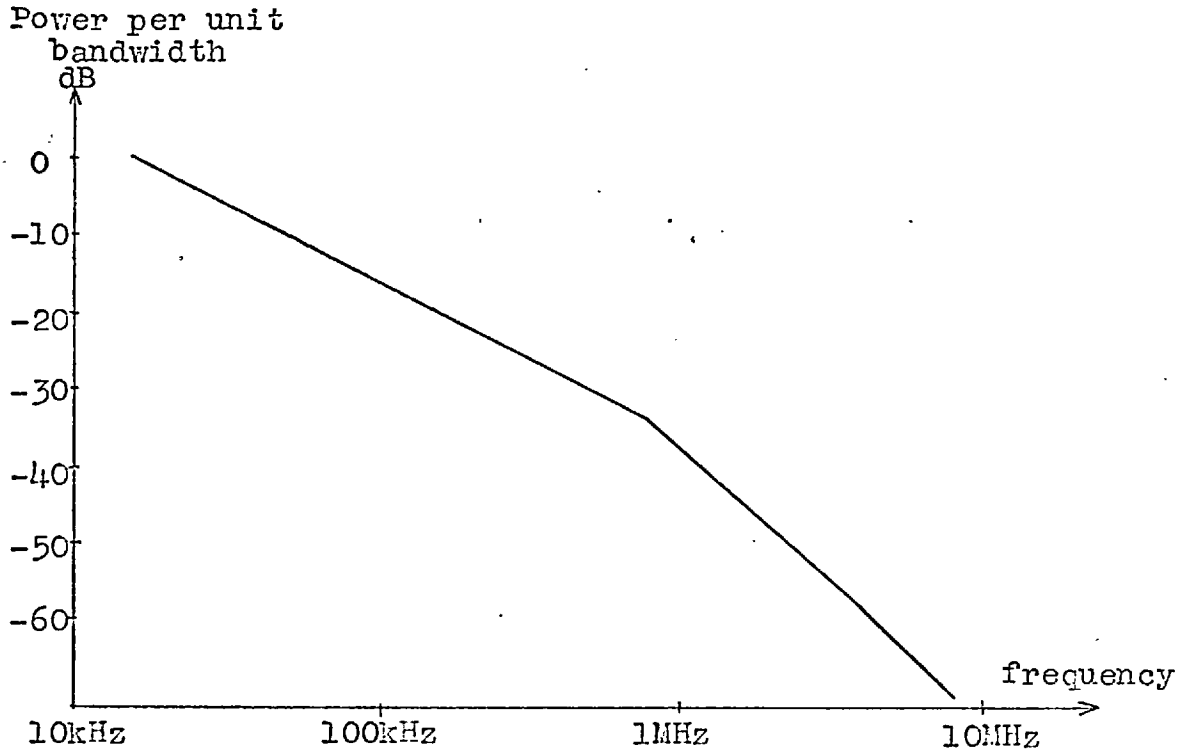

Figure 5.1. Video power spectrum estimated by FINK et al (ref. 32) from N.T.S.C. test slides.

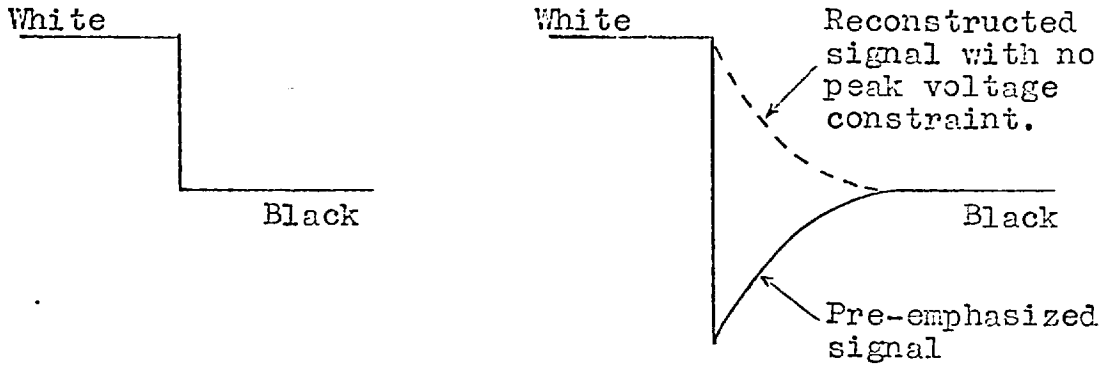

(a) Fast edge corresponding to highest video frequency

(b) 6 dB h.f. emphasis

Figure 5.2. Illustration of the deficiency of emphasis for fast edges in the television waveform.

quantizing noise was digitally weighted in favour of high frequencies with the object of reducing its visibility. It would therefore seem that pre and de-emphasis could be used around the pseudo-random quantizer to achieve a further reduction in noise visibility by reducing the quantizing noise power. The remainder of this Chapter describes an experimental investigation of the compatibility of these processes.

With the pre and de-emphasis circuits to be described, no constraint was included on the pre-emphasized signal. The mean power constraint imposed by Bruce is unrealistic because television signals have a peak voltage constraint under which emphasis can theoretically effect no linear improvement whatever. Analysis of emphasis relates only to average properties of the television signal and, although the power spectrum shows high frequency components to be 60 dB below the lows, fast black to white transitions do occur in most pictures.

Consider for example, the waveforms of Figure 5.2 which depict the effect on a fast, full amplitude transition of 6 dB emphasis of high frequencies over the lows. The overshoot of the pre-emphasized signal doubles the video amplitude so that a flat attenuation of 6 dB must be included in order that the signal may be transmitted without clipping and reconstructed faithfully at the receiver. The S/N ratio is

thus reduced by 6 dB, exactly nullifying the maximum possible advantage of the emphasis which would occur for added noise consisting only of very high frequency components.

If the signal is pre-emphasized without a flat attenuation of the lows to effect a peak constraint, the reconstruction at the receiver will be the dotted curve of Figure 5.2(b) which will appear as a streak in the image. For small amounts of emphasis, streaks will occur only on those edges near peak black or white and of duration that can be minimized by emphasizing only the very high frequency end of the video spectrum. Furthermore, in consequence of the Mach phenomenon (Sec. 1.3.1) the only degradation associated with undershoots of short duration is an apparent reduction in the contrast of the affected edges (SCHREIBER & KNAPP[105]).

Thus emphasis must be non-linear in order to accomplish an increase in the received S/N ratio. However, short undershoots are quite acceptable and for the experiments to be described it was decided to include no adjustment of low frequency gain. In fact, with the rapidly falling video spectrum of Fig. 5.1 and the moderate amount of emphasis adopted, an adjustment of gain according to a mean power constraint is quite negligible.

Pre-emphasis of the video signal alters its p.d.f. so that an equal step quantizer is no longer optimum in generating the minimum mean square error. A suitable compander

could be designed from measurements of the emphasized signal p.d.f., but the results calculated by Max for the Gaussian distribution suggest that the improvement would be much less than 3 dB. Companding was therefore not included in the experimental system.

5.2. AN EXPERIMENTAL SCHEME

5.2.1. Quantization

Bruce applied pre and de-emphasis techniques to the straight quantizing error of a conventional PCM equipment and found that only 5 dB emphasis of the high frequencies over the lows is sufficient to remove the contours in a 4 bits/sample image. In view of this result, a simple dither signal of only 4 levels was used in the experimental pseudo-random quantizer with pre and de-emphasis, since this reduced the number of dither components to two. The output of the 2 bit quantizer therefore had only 16 levels, but contours were smoothed out in the de-emphasis filter. A schematic diagram of the system is shown in Figure 5.3(a). The dither signal generator is shown in Figure 5.3(b), and is similar to the final configuration considered in Chapter 4 (Fig. 4.19) except that only the two high frequency binary components have been used.

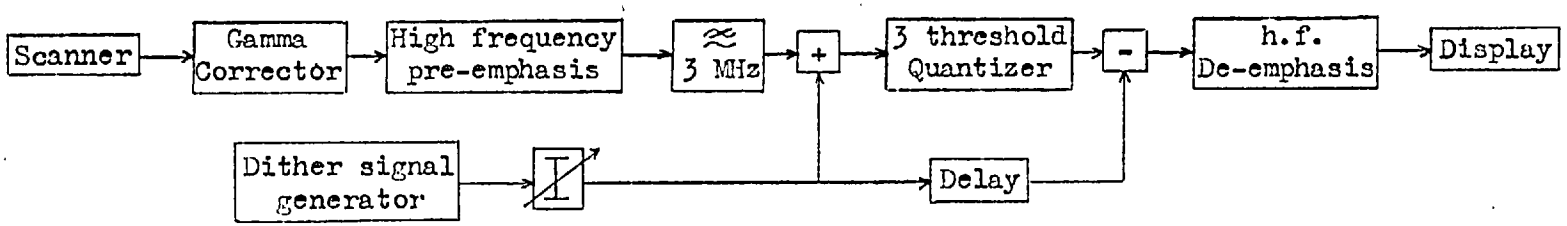

(a) System schematic diagram

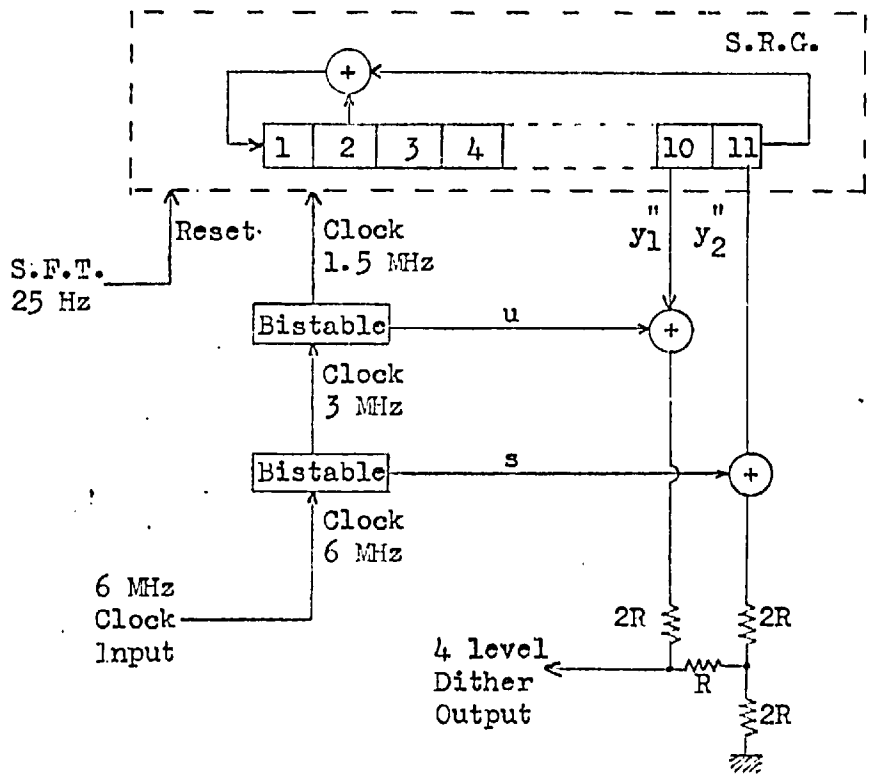

(b) The 4 level h.f. dither signal generator

Figure 5.3. 2 bit pseudo-random quantization with high frequency pre and de-emphasis.

The dither signal may be written $\frac{1}{2}q(\frac{1}{2}sy''_1 + \frac{1}{4}uy''_2)$, where s and u are 3 and 1.5 MHz square waves respectively, and y''_1 and y''_2 are outputs of the S.R.G., clocked at 1.5 MHz.

As in Section 4.5.1, the Q-equations follow from the four binary functions generated by slicing the 4 level dither :

3-0 : constant (-1)

0-1 : $sy''_1 \vee uy''_2 \equiv \frac{1}{2}(sy''_1 + uy''_2 + 1 - suy''_1y''_2)$

1-2 : sy''_1

2-3 : $sy''_1 \cdot uy''_2 \equiv \frac{1}{2}(sy''_1 + uy''_2 - 1 + suy''_1y''_2)$

Multiplying the above expressions by the scaling factor $\frac{1}{2}q$, and subtracting the dither $\frac{1}{2}q(\frac{1}{2}sy''_1 + \frac{1}{4}uy''_2)$, the Q-equations (excluding d.c. components) become :-

$$Q_{30} = \tfrac{1}{4}q(-sy''_1 - \tfrac{1}{2}uy''_2)$$
$$Q_{01} = \tfrac{1}{4}q(\tfrac{1}{2}uy''_2 - suy''_1y''_2)$$
$$Q_{12} = \tfrac{1}{4}q(sy''_1 - \tfrac{1}{2}uy''_2)$$
$$Q_{23} = \tfrac{1}{4}q(\tfrac{1}{2}uy''_2 + suy''_1y''_2)$$

The autocorrelation functions and power spectra of the terms sy", uy", suy" are derived in Appendix 8.2. Substituting these into the Q-equations, only two distinct spectra emerge - (a) : Q_{01}, Q_{23} and (b) : Q_{12}, Q_{30} - and these spectra are plotted as the broken curves in Figure 5.4(b). In comparison with curve (c), which represents the noise spectrum for all levels using an uncorrelated dither, the 4 level dither is

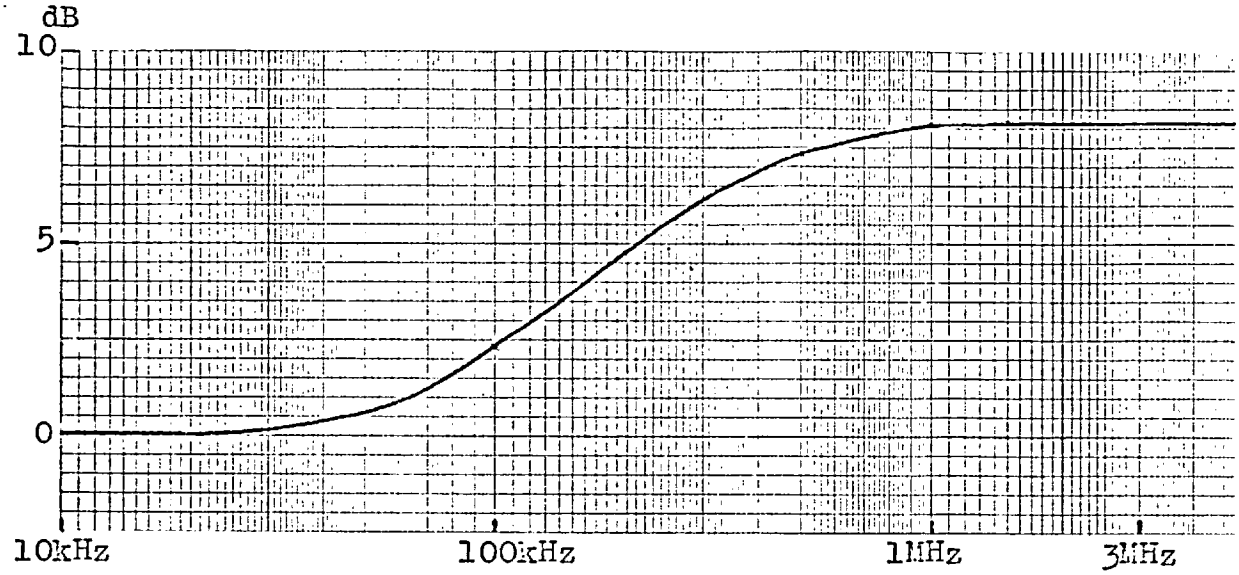

Figure 5.4(a). Pre-emphasis characteristic used in the experiments.

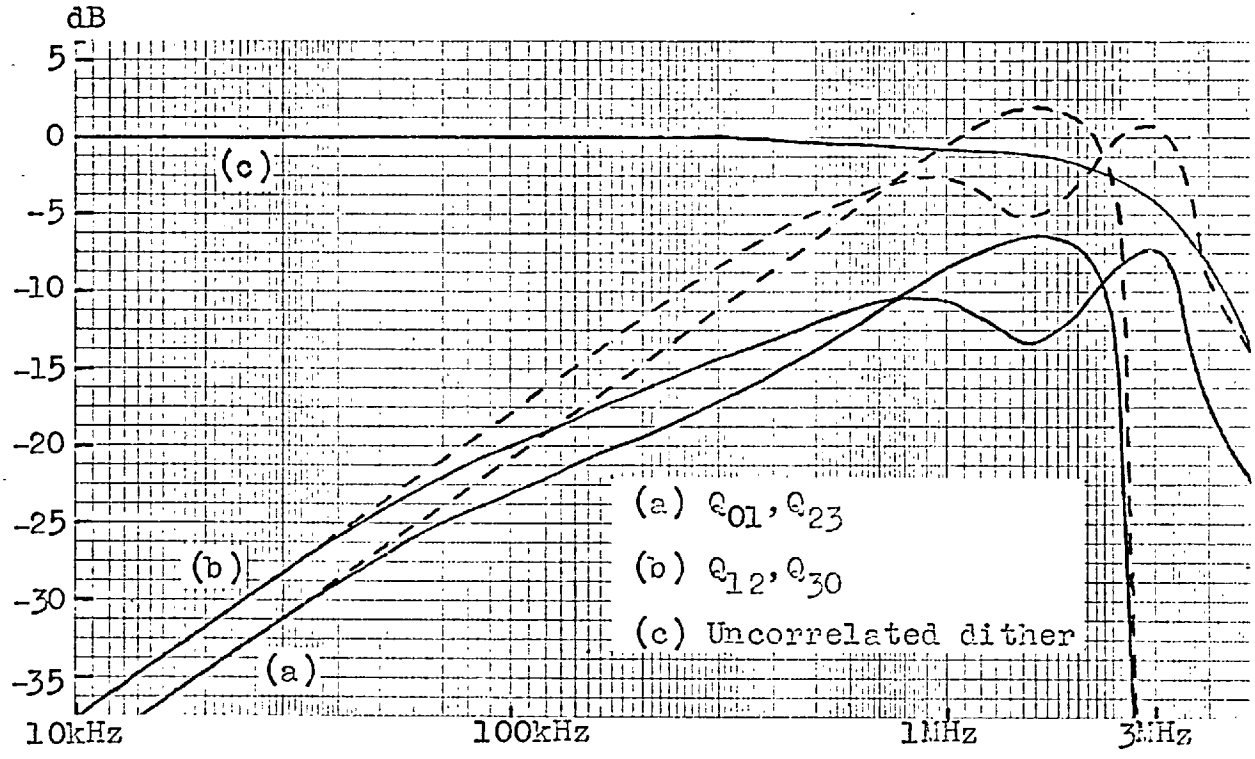

Figure 5.4(b). Quantizing noise spectra generated by the dither of figure 5.3(b),
Continuous curves (a) & (b) - with emphasis
Broken curves (a) & (b) - without emphasis.

extremely successful in transferring the noise to the high frequency end of the video band.

5.2.2. Pre and De-emphasis Filters

The amplitude and breakpoints of the pre-emphasis filter characteristic shown in Figure 5.4(a) were determined empirically by variation of these parameters in the system of Fig. 5.3, keeping the de-emphasis filter complementary over the video band. With less than 6 dB emphasis of the high frequencies, most of the test pictures were observed to have visible contours. As the amount of emphasis was increased, it was found that the quantizing noise became of a more low frequency nature until at 12 dB very low frequency noise predominated such that any improvement in signal/weighted-noise ratio due to pre and de-emphasis was lost.

The low frequency noise arises from intermodulation in the quantizer non-linearity between the high frequency dither and the emphasized video signal. The curves of Figure 5.4(b) only describe quantizing noise in areas where the picture signal varies by less than $\frac{1}{4}q$ volts. The result of pre-emphasis is to increase high frequency scanner noise and low amplitude picture detail in these areas until the Q-equations are no longer valid. This incompatibility between

pre and de-emphasis and the digital spectrum shaping of the pseudo-random quantizer thus restricts the useful degree of pre-emphasis. The 8 dB range of Fig. 5.4(a) was chosen since this caused no predominance of low frequency quantizing noise.

It is desirable to emphasize only the very high video frequencies in order to minimize the duration of streaks in the received image. On the other hand, reducing the frequencies of the break points of the emphasis characteristic, while having little effect on the amount of low frequency inter-modulation noise appearing at the output of the dither subtractor, allows the de-emphasis filter to exclude more of this noise from the display. The break points of the characteristic of Fig. 5.4(a) were chosen as an approximate compromise between these considerations.

The de-emphasis characteristic is not shown in Fig.5.4, but this complemented pre-emphasis such that the combined transfer characteristic was flat at 0 $\pm$ 0.25 dB over the video band. The characteristics were realized respectively by series R-C shunts across the collector and emitter loads of otherwise identical video amplifiers.

Using the characteristic of Figure 5.4(a), the predicted spectra of the de-emphasized quantizing noises are given by the continuous curves of Figure 5.4(b). Weighting these spectra by the function W(w) due to Gilbert and integrating over the range 0 - 3 MHz, the Q-equations predict a reduction

of quantizing noise visibility of about 20 dB over Roberts' proposal for an uncorrelated dither. This figure was confirmed in the absence of a picture signal by subjective comparison with white Gaussian noise. The following Section describes tests on a range of pictures which were carried out to determine a figure of merit for the system with the S.R.G. frame-synchronized, but square waves alternating to create the impression of migrating noise.

5.3. SUBJECTIVE EVALUATION

The testing procedure and viewing conditions described in Section 4.4.1 were again employed to assess the pseudo-random quantizer in terms of additive white Gaussian noise. Six observers were tested individually and all of the pictures of Figure 4.9 were used. Four readings were taken for each picture, subjected to a "pseudo-random" dispersion over 9 dB to prevent learning. Each observer took approximately one hour to complete a test, but a short rest period was allowed in the middle. The instruction given was to degrade the one image until the two displays were considered to be equally acceptable.

The grand mean of the 144 readings rated the 2 bit quantized image as equivalent to a signal/white-noise ratio of 32.2 dB, with a variance of personal means from the overall

mean of 0.8 dB^2. An analysis of variance on the 6 x 6 table of mean personal opinions for each picture showed the between-observer variance estimate to be insignificantly higher than that based on the residual degrees of freedom. The between-picture variance was extremely significant (the ratio of this to residual in Snecedor's test being greater than the 0.1 % level). Table 5.1 shows the mean opinions over the 24 readings for each picture. The order of rating seems to be a function of the amount of fine picture detail, the lowest rating being for the slide "Beeches". This is the picture which would be expected to produce the most low frequency noise by intermodulation.

Table 5.1. System ratings for the test pictures of Fig. 4.9.

Test picture	Flick	Fruit seller	Helicopter	Felicity	Beeches	Church
Equivalent S/N ratio	32.4	33.4	32.4	32.0	31.3	31.8

It is a little surprising that "Fruit seller" should be rated as best since this also contains large amounts of fine detail. However, it has considerable areas at constant black and it is suggested that the observers found these areas to be the most restful in which to make their comparisons. Likewise, the constant brightness areas of "Church" may have been avoided, since most of these are at highlight luminance,

and comparisons made on the more detailed regions. This could account for the low rating of this picture.

No appreciable streaking resulted from peak-clipping the pre-emphasized signal and only one of the six observers noticed this on the slide "Church". Neither was any patchiness of the noise apparent corresponding to the two distinct quantizing noise spectra.

Single frame photographs indicating image quality are given in Figure 5.5 for the slides "Flick" and "Felicity". Satisfactory performance was obtained on a number of other slides and for moving pictures, but fuzzy contours were visible on a grey scale. This represents the most stringent test of the system and for complete satisfaction a dither of 8 or 16 levels would probably be necessary.

Summary

By a suitable choice of dither combined with a moderate amount of pre and de-emphasis, the visibility of apparently migrating quantizing noise has been reduced by 10 dB over Roberts' initial proposal. The undershoots, inherent in the use of pre and de-emphasis, are not objectionable and the more important restriction on the amount of emphasis is connected with the generation of low frequency quantizing noise by intermodulation. The final noise spectrum is probably rather flat for most pictures, the high frequency noise predicted by Figure 5.4(b) being supplemented at low

(a) "Flick"

(b) "Felicity"

Figure 5.5. 2 bit pseudo-random quantization with h.f. pre and de-emphasis (single frame exposures).

frequencies by intermodulation products. The equivalent S/N ratio of the image is dependent upon the amount of fine detail in the picture, but so is the objectionability of any given level of random noise.

In terms of additive white Gaussian noise, image quality with completely synchronized quantizing noise would be somewhat better than 32 dB S/N and for many still subjects an observer might have difficulty in distinguishing the processed picture from the original. However, psychometric tests for this condition would need to be much more elaborate than those described here, involving moving pictures and carefully chosen subject material. The laboratory facilities for moving pictures were deemed to be inadequate for reliable tests of this nature.

5.4. SOME REMARKS ON NOISE-FEEDBACK QUANTIZATION

It is interesting to compare the pseudo-random quantizer with the noise-feedback coder developed at Bell Laboratories (CUTLER[21]), which has the same objective of weighting the quantizing noise spectrum independently of the video signal. The two schemes seem to be directly alternative means of efficient television coding and it is very relevant to discuss their relative merits.

A block schematic diagram of the noise-feedback coder is shown in Figure 5.6. The quantizing error made on each video sample is applied to the digital filter, D(w), of which the output is added to the next video sample prior to quantization. This feedback loop shapes the power spectrum of the quantizing noise without affecting the power spectrum of the signal, and its effect is to replace each transition between thresholds by a succession of rapid jumps back and forth.

SPANG[112] produced a mathematical specification for a filter D(w) which increased the quantizing noise power slightly, but transferred 95 % of this to the top 20 % of the signal band. It was then proposed to increase the sampling rate by 20 % above twice the maximum video frequency and to remove the additional band by a low-pass filter at the receiver. This would improve the S/N ratio by almost 13 dB.

KIMME & KUO[68] designed a noise-feedback coder for use with pre and de-emphasis filters specifically for a low resolution television system. Using a noise weighting function W(w) measured on this system (BRAINARD et al[10]), they designed optimum digital filters which maximized the r.m.s. signal/weighted-noise ratio at the output of the de-emphasis network. BRAINARD[9] carried out a subjective evaluation of the quantizer using the arrangement shown in Figure 5.7. Companding was included to match the quantizer

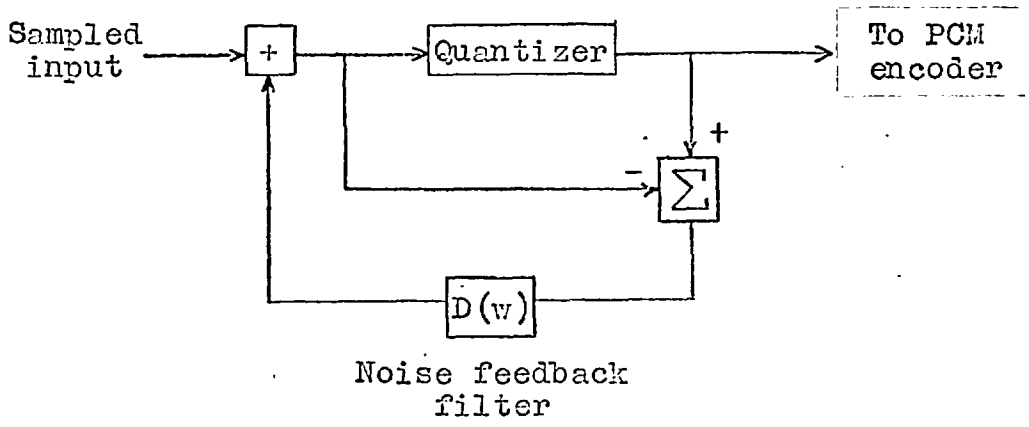

Figure 5.6. Noise feedback quantizer due to CUTLER (21).

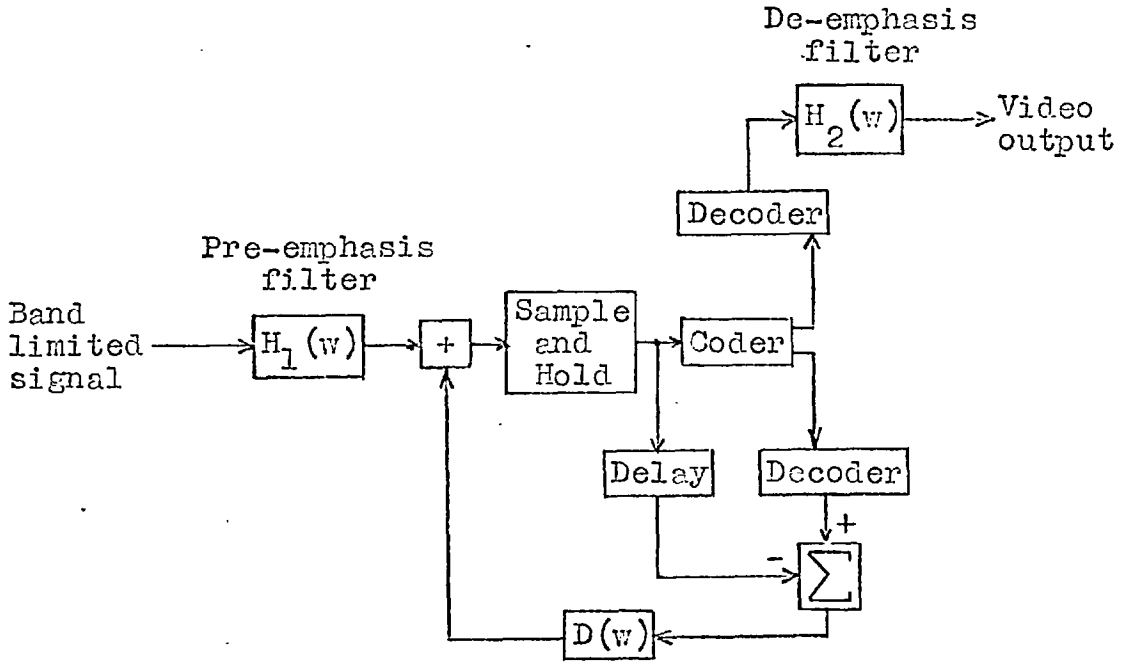

Figure 5.7. Noise feedback system with pre and de-emphasis investigated by BRAINARD (9).

threshold spacing to the p.d.f. of the pre-emphasized signal. Quantization was accomplished by a 3 bits/sample PCM coder and decoder, and regeneration of the coded signal was included to eliminate the possibility of pulse width modulation. The filter $H_1(w)$ pre-emphasized the highs by 20 dB over the lows and the filter $H_2(w)$ was the inverse of $H_1(w)$ over the video band. Observer tests were carried out on a 5" display of 225 lines with 2:1 interlace at a viewing ratio of 8. From comparisons of the 3 bits/sample image with the unprocessed signal degraded by additive noise, it was concluded that noise feedback combined with pre and de-emphasis reduced weighted quantizing noise by 11.7 dB relative to conventional PCM.

Brainard stated an equivalent r.m.s. signal/weighted-noise ratio for the frozen 3 bit quantizing error, but it is difficult to compare this directly with the equivalent peak-peak signal/r.m.s.noise ratio given in Section 5.3 for migrating 2 bit pseudo-random quantizing noise. However, it seems likely that for a specified coder capacity, pseudo-random quantization using a completely synchronized dither and possibly companding is capable of similar performance to noise feedback coding.

There is a basic difference between the systems which may be significant for coarse quantization. For constant video inputs, the noise-feedback coder will limit cycle at

a frequency determined by the video level. This is likely to produce patterning in areas of constant brightness which would be particularly objectionable if pre and de-emphasis were not used. In the pseudo-random system, errors are transformed into an apparently additive noise although patchiness may be visible on some pictures without pre and de-emphasis.

A further advantage of pseudo-random quantization is the possibility of conveniently extending spectral shaping to two dimensions. An excessive amount of storage would be necessary to incorporate this in a noise-feedback coder.

In terms of coder complexity, the two schemes appear to be very similar. Brainard's system employed 20 dB emphasis of high video frequencies over the lows and, although it is presumed that a mean power constraint was included, much more prominent streaking would be expected than was obtained with the 8 dB filters in the pseudo-random system.

5.5. SOME APPLICATIONS OF PSEUDO-RANDOM QUANTIZATION

Chapter 6 is devoted to consideration of the specific application of pseudo-random quantizing to a video telephone system. The present Chapter will be concluded with a short discussion of some more general applications and of compatibility with other schemes of television data compression.

It has been demonstrated that an apparently continuous image with added random noise equivalent to 32 dB signal/white-noise ratio can be obtained from only 2 bits/sample. On the quality grading scale of PROSSER & ALLNATT[96] this would be expected to meet with almost 95 % favourable opinions over a large observer population. Only in very demanding applications would it be necessary to use 3 bit quantization.

Pseudo-random dithering techniques are not only of relevance to continuous half-tone pictures. BYLANSKI[16] has illuminated the difficulties associated with obtaining a two level signal from typescript due to imperfections in type face and irregularties in background luminance. In severe cases near analogue transmission may be necessary for complete legibility, but it is thought that 2 bit pseudo-random coding may be sufficient. A two level transmission scheme might even be devised using a low amplitude pseudo-random perturbation of the single threshold and relying on visual integration over successive frames to improve legibility.

In many applications of coarse pseudo-random quantization, migrating pseudo-noise may be preferable to allow extraction of picture detail by visual or photographic integration over two or more frames. Facsimile transmitters only communicate single frames, but a received image could be improved by computer processing. Graham's noise stripping technique can be applied for S/N ratios down to 28 dB. HUANG et al[58] have

reported application of noise stripping at even lower S/N ratios without smearing of sharp edges by the transmission of a few extra bits indicating the location of edges so that no averaging is done in these regions.

The most attractive features of pseudo-random quantizing are effectiveness and simplicity of implementation. In a PCM terminal equipment, the saving in analogue to digital converter complexity may far outweigh the inclusion of a pseudo-noise generator and the ancillary circuitry. Even so, the process may be compatible with a number of more complex compression schemes. In dual band systems (see Sec. 1.3.1), where the low signal frequencies are quantized to 7 or more bits to avoid contouring, a small additional compression might be obtained by pseudo-random coding.

CHAPTER 6

THE VIDEO TELEPHONE

6.1. INTRODUCTION

Until such time as channel capacity is very much cheaper and more readily available, the video telephone can only become economically feasible for large scale use if some form of bandwidth compression is employed. The required compression ratio depends on the system specification, but no confident estimate of this can be made until more is known of subscriber requirements and reactions to visual communication.

Until the present, attention has been restricted to a conventional type of image with a reduced resolution which effects an economic compromise between fidelity and channel capacity. This work is reviewed in the next Section, but CHERRY[19] has recently proposed that a simple "cartoon-like" representation might be sufficient to supplement verbal communication with the necessary gestures and facial expressions. The image might be obtained by differentiating a quantized conventional video signal and would involve a very small amount of data (although the storage or contour tracing problems seem formidable), but the psychological aspects of such a representation are as yet unknown.

The latter part of this Chapter describes two experimental

video telephone systems which presented a conventional type of image, and which were constructed primarily to investigate a possible application of pseudo-random quantization.

6.2. REVIEW

In 1964, HALL[50] reported an experimental variable parameter television system at Bell Laboratories which was used to determine acceptable standards for a Picturephone. As the result of subjective tests, a 500 kHz, 275 line system was specified with 30 frames/sec. and 2:1 interlace. The aspect ratio was 4:3 with the longer dimension vertical since this was expected to minimize the amount of background to the user's head. Horizontal line scanning was employed and the design included a generous allowance of 0.5 for the Kell factor. The Picturephone had a picture height of 5.75" and was designed for a viewing distance of 36". Hall also described an experimental Picturephone service between two of the Bell Laboratories. The service was installed with a carefully equalized 500 kHz analogue channel and was expected to provide essential statistical data on usage.

In 1965, LUNN & MUMFORD[77] described a 228 line system with 555 kHz video bandwidth. The aspect ratio and scan direction were similar to those of the Picturephone, but the design provided a Kell factor of unity ; horizontal

resolution was therefore 60 % greater than that of the Picturephone. Again 2:1 line interlace was employed, but with the British frame frequency of 25 Hz. The picture height and proposed viewing distance were respectively 5" and 30". The system occupies only one sixth of the bandwidth of the conventional 405 line system, but analogue channels of this capacity are still prohibitively expensive and the useful distance between subscribers is severely limited by crosstalk.

It now appears that the video telephone will become feasible through developments in digital communications and PURTON & LUNN[98] have adapted the system of Lunn and Mumford for transmission by PCM. A data rate of 1.6 Mb/sec. was chosen since this can at present be transmitted satisfactorily through existing audio cables, provided regenerative repeaters are fitted at 2000 yard intervals. Also, it would seem that a channel capacity of this order will be preserved as a basic unit in future high speed digital systems. KELLEY[65] has described work at Bell Laboratories on a 225 Mb/sec. system which can be allocated as 144 units of 1.564 Mb/sec. by time division multiplex.

The specification of the system proposed by Purton and Lunn is summarized in Figure 6.1. A nominal 533 kHz video bandwidth was secured by sampling at 1.066 MHz, and the video signal was quantized to 8 levels (i.e., 3 bits). The associated data rate of 3.198 Mb/sec. was halved by dot-interlace,

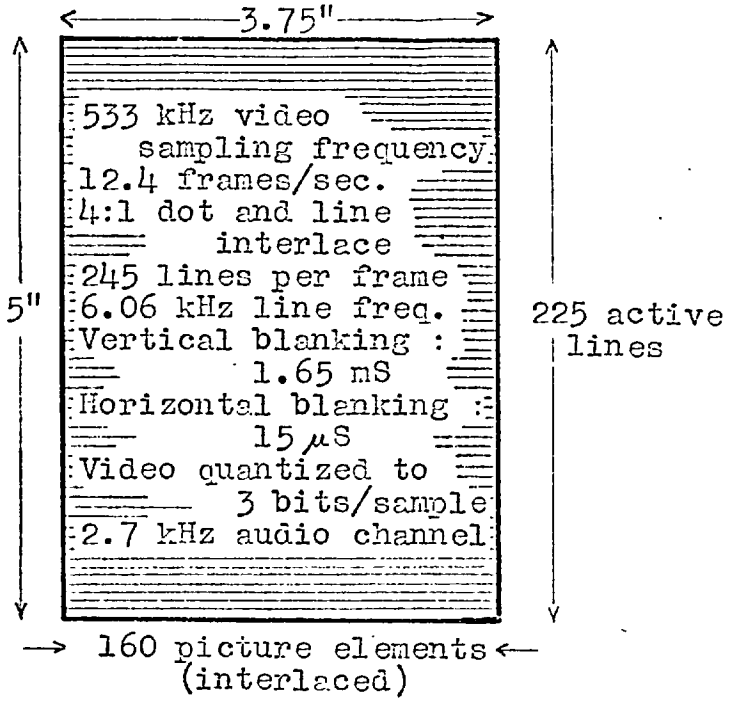

Figure 6.1. 1.6 Mb/sec. video telephone standards proposed by PURTON and LUNN (98).

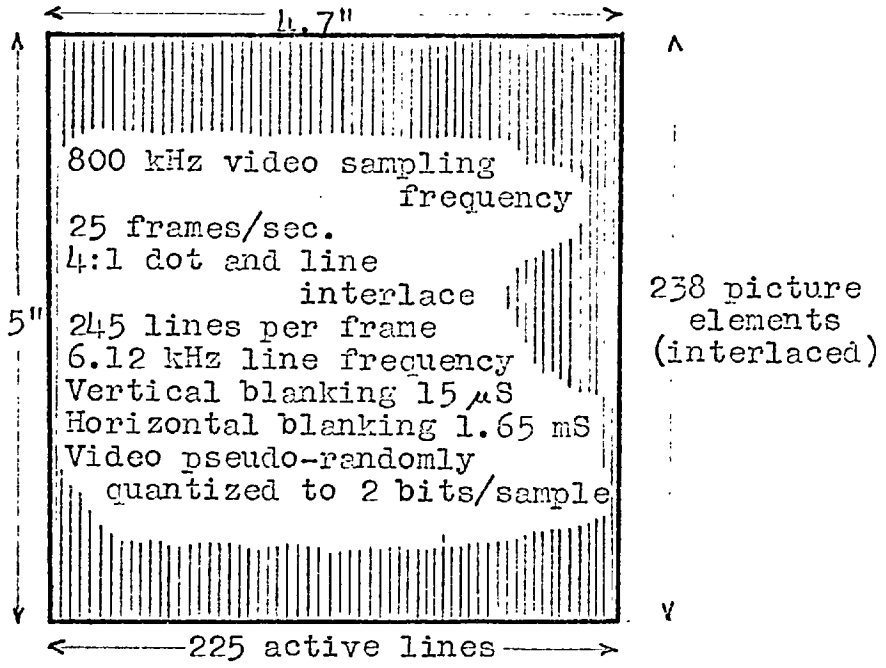

Figure 6.2. Standards of the 1.6 Mb/sec. video telephone with dot-interlace simulated in the laboratory.

giving a frame frequency of 12.4 Hz. A 2.7 kHz audio channel was time division multiplexed with the video by transmitting 6 bit speech samples during the line blanking intervals. The image had pronounced intensity contours due to the 8 level quantization and, although these enhanced the subjective sharpness of the low resolution display, they would probably be unacceptable to most observers.

In 1967, MOUNTS[85] described a low resolution digital television system designed for investigating data compression schemes. The video signal was sampled at 1.536 MHz and quantized to 8 bits/sample, so that without data reduction the signal required 8 units of 1.536 Mb/sec. The raster had 160 lines/frame with unity aspect ratio, and 60 non-interlaced frames per second. Horizontal line scanning was employed at 9.6 kHz.

DEUTSCH[29] (1966) has made various proposals for a phone-vision system using a high order of pseudo-random interlace to reduce the data rate. However, it seems that 4:1 represents the limit of interlace without motion blurring and this order can be realized equally well by regular dot and line interlace. Furthermore, pseudo-random scanning is incompatible with most schemes for reducing sample amplitude data since it "scrambles" the redundancy of typical pictures.

There is considerable disagreement between the proposed standards for a video telephone, but it is possible to draw

some very general conclusions. It would seem that a raster of at least 250,000 picture elements is necessary to provide useful resolution though the best value for the Kell factor is in some doubt. A 4:3 vertical aspect ratio is most efficient in terms of occupied screen area, but this calls for careful subject positioning and is perhaps restrictive of movement. For these reasons a square aspect ratio may be preferable. A picture height of 5" and a viewing ratio of 6 seem to be suitable for office conditions. Transmission is most likely to be by PCM so that minimization of the number of quantization levels is extremely important. In addition, a digital system can conveniently include dot-interlace.

6.3. EXPERIMENTAL VIDEO TELEPHONE SYSTEMS

Two experimental video telephone systems were constructed in the laboratory - one with dot-interlace, and one without. The objective was to assess this application of pseudo-random quantization and to estimate the most acceptable system which may be transmitted through a 1.6 Mb/sec. channel.

6.3.1. A Video Telephone System With Dot-interlace

Picture Standards

A system similar to that of Purton and Lunn (Fig. 6.1)

was considered, using 2 bit pseudo-random quantization instead of 3 bit straight coding. This reduction of sample amplitude data was exploited to increase the number of picture elements by 50 %. The system standards are summarized in Figure 6.2 , and assume a 10:1 ratio of active to blanked sweep. Hence, of the 245 lines/frame about 225 carry picture information, and the number of active picture elements per line is 238 - about 50 % more than in the system of Purton and Lunn. To give a Kell factor of unity the image aspect ratio must be nearly unity, which allows some freedom of subject movement.

The direction of scan was rotated through 90° since BURDETT[15] found that with unity Kell factor, intelligibility of typescript is slightly higher if the scan direction is vertical. Another factor which was considered in deciding the scan direction arises from the disadvantage of line interlace. Subjective line pairing and crawl occur whenever the eye moves across the scanning lines. Thus the vertical scan favours vertical picture and eye movements.

Experimental Details

The 225 x 238 element raster of Fig. 6.2 was realized by extending and delaying the field and line blanking intervals of the 405 line system as shown in Figure 6.3(a). The composite blanking signal selected a central quarter of

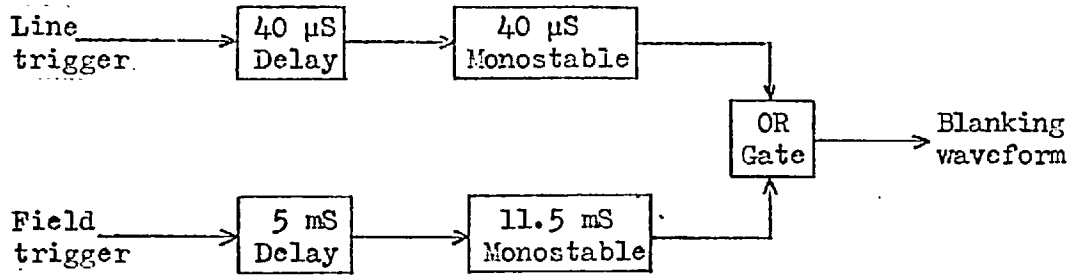

(a) Blanking waveform generator for selecting one quarter of the conventional 405 line raster.

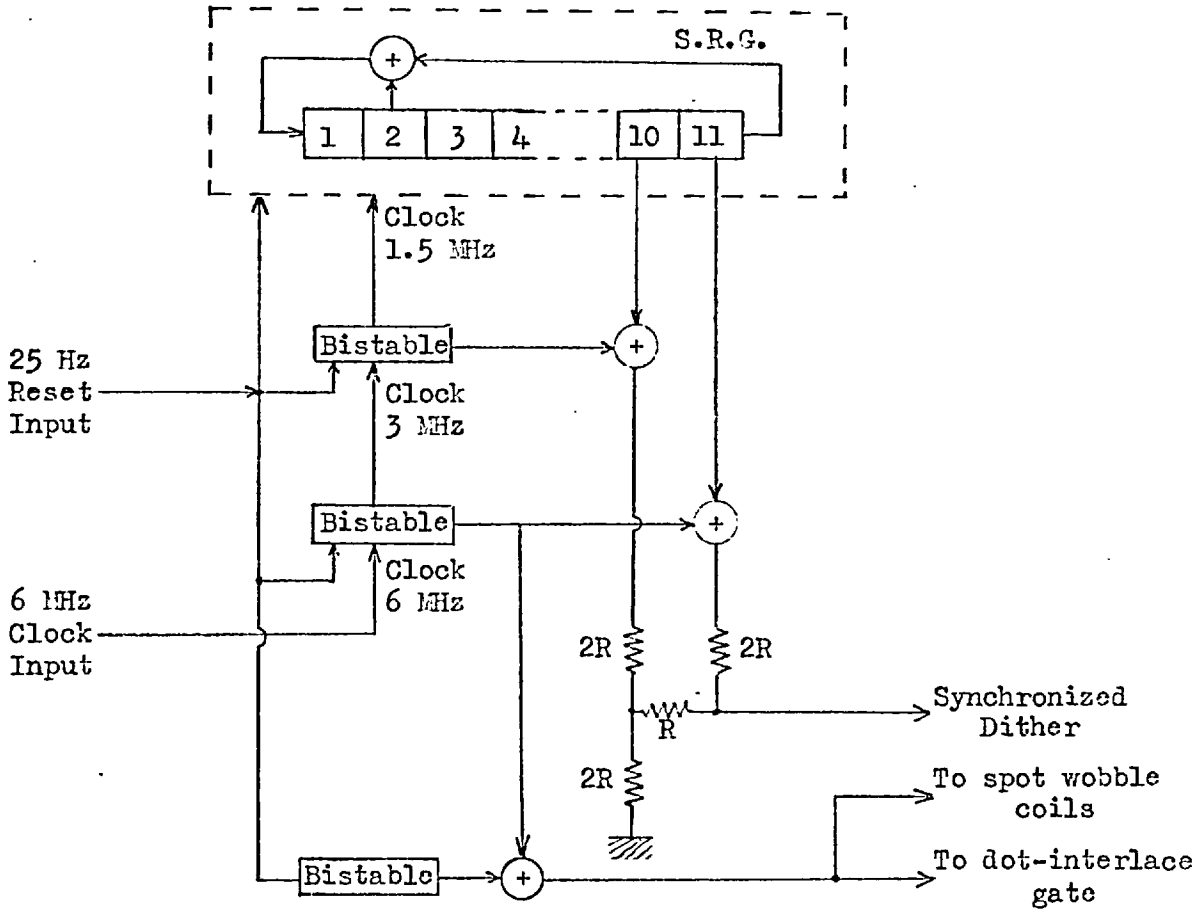

(b) Generator of frame-synchronized 4 level dither and alternating dot-interlace and spot wobble signals.

Figure 6.3. Blanking and dither generators of the experimental 1.6 Mb/sec. video telephone system employing dot-interlace.

the full sized raster. Vertical scanning was achieved by turning the monitor on to its side and by rotating the slide in the flying spot scanner. Picture size was then reduced to fit the smaller image raster by expanding the raster on the face of the scanner tube. The 3 MHz low-pass filter at the output of the scanner reduced video bandwidth to the equivalent of an 800 kHz video telephone. Finally, the monitor width and height controls were adjusted to give an image size 5" high x 4.7" wide, and a viewing ratio of 6 was used.

Two bit quantization with pre and de-emphasis was performed using the 4 level dither and filters described in Chapter 5. The dither was frame-synchronized by applying the frame reset signal to the 3 MHz and 1.5 MHz bistables as well as to the S.R.G., as shown in Figure 6.3(b).

Dot-interlace

A dot-interlace signal which covered the entire raster in 4 fields was generated by adding modulo-2 a square wave of frame frequency (12.5 Hz) to the synchronized 3 MHz square wave. The signal operated a high speed video blanking circuit inserted between the dither subtractor and the de-emphasis filter (Fig. 5.3(a)).

The importance of the choice of dot pattern in minimizing dot crawl effects in the image has been discussed by TEER[116].

These effects are exhibited by the dot pattern of Figure 4.12(b) (p.162), which was considered in Chapter 4 as a dither component. The pattern gives the field sequence illustrated in Figure 6.4(a) in which the inherent linear progressions are seen as dot crawl in the directions indicated by the arrows. The dot-interlace generator of Fig. 6.3(b) produces the field sequence of Figure 6.4(b) for which there is no apparent crawl on still pictures, although vertical dot jitter is visible on close inspection. This was the pattern used in the present experimental system. The major problem in the design of this system was found to arise from the flicker associated with dot-interlace.

To transmit a picture as 4 dot fields, the 3 MHz band-limited video signal is sampled at only half the corresponding Nyquist rate which therefore causes an "inverted" video spectrum to be aliased into the nominal video band. Figure 6.5 shows the form of the resulting spectrum and, since the interlace pattern alternates at 12.5 Hz, the aliased interference also alternates in phase at this frequency. For the predominantly low frequency television signal, most of the interference is at high frequencies and appears as flicker in detailed regions of the picture.

Aliasing is rather more pronounced for the pseudo-random quantized signal which has high frequency noise distributed over regions of low picture detail. In addition

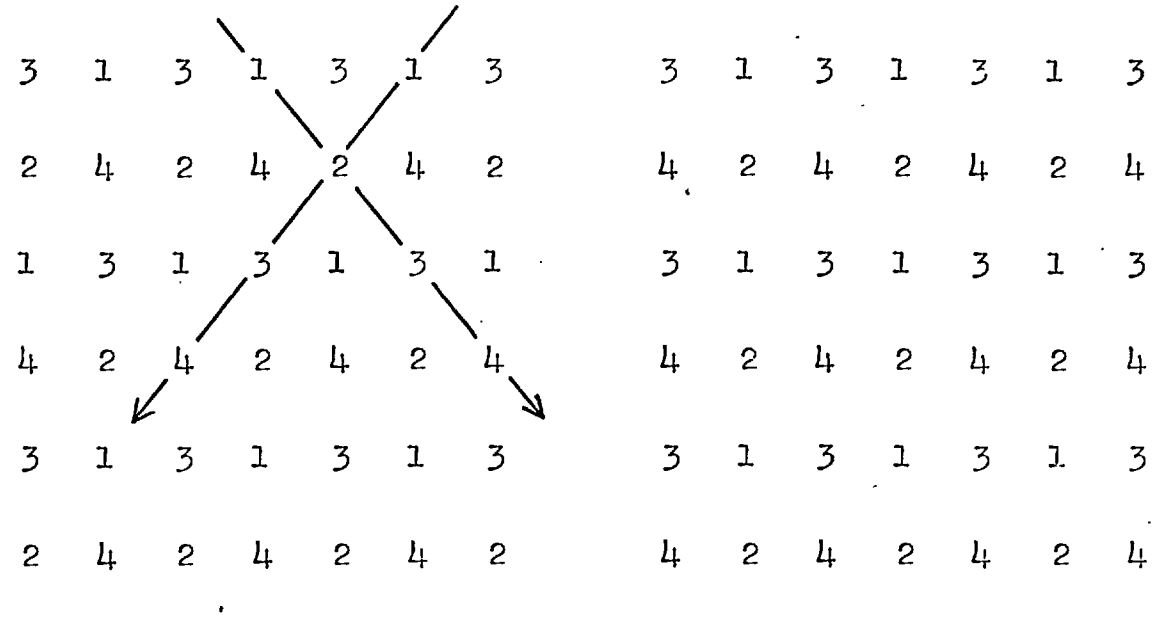

Figure 6.4. Field sequences for 4:1 dot-interlace generated by

(a) 3 MHz square wave ⊕ ½(line freq.) square wave ;

(b) 3 MHz square wave ⊕ 12.5 Hz square wave.

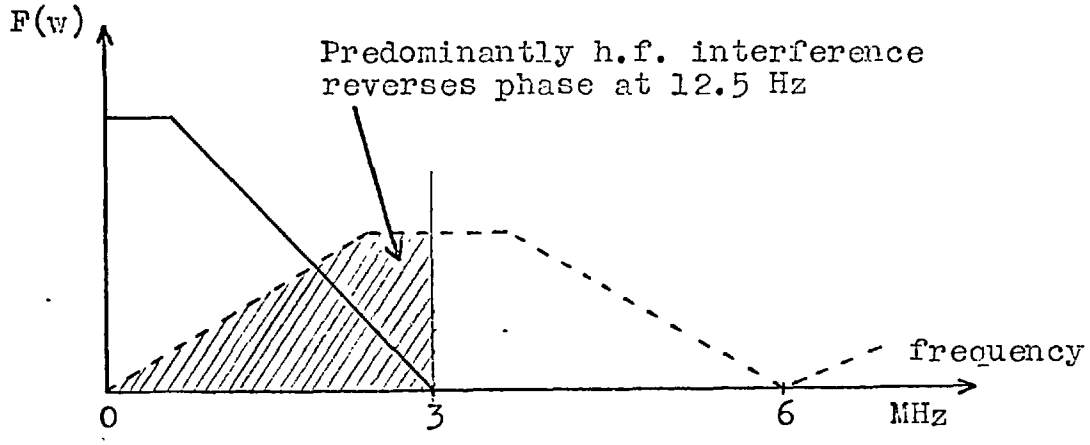

Figure 6.5. Aliasing caused by dot-interlace.

to causing flicker in detailed areas of the image, dot-interlace aliases quantizing noise into the low frequency end of the video band and (if the dither is frame-synchronized) causes it to flicker at 12.5 Hz. The photograph of Figure 6.6 shows a full size, 4 field exposure of the 1.6 Mb/sec. image, but this has integrated out the aliased interference. The indicated picture quality was marred by relatively large area flicker located mainly in the simply organized regions of the picture. With the dither asynchronized, the subjectively equivalent S/N ratio was several dB lower than for the corresponding situation without dot-interlace.

The specifications of the optimum dither are clearly different in dot-interlaced and non-dot-interlaced systems. With dot-interlace it is desirable to confine quantizing noise to a narrow band around 1.5 MHz since this causes the least objectionable aliasing, but is unlikely that dot-interlace and pseudo-random quantization could be made entirely compatible even with more suitable pre and de-emphasis networks. It is felt that it might be possible to reduce the degradation of dot-interlace to about 3 dB for the asynchronous dither, but the preferred frozen noise cannot be achieved since the 12.5 Hz flicker is as objectionable as migrating noise. However, the flicker might be reduced somewhat by means of a longer persistence phosphor. Purton and Lunn reported a considerable reduction of 12.5 Hz dot jitter

Figure 6.6. 225 line image of the simulated 1.6 Mb/sec. system employing pseudo-random quantization and dot-interlace. (Full size, 4 field exposure).

without objectionable movement blur using a phosphor decay time of 75 mS. Also, the results of HAANTJES & DeVIJER[47] suggest that the C.F.F. might be reduced by about 10 Hz without movement blur, but it is difficult to predict the corresponding reduction in noise-like flicker at 12.5 Hz, particularly as this is known (BARTLEY[5]) to be close to a resonance frequency of the visual system.

Spot Wobble

At a viewing ratio of 6, the dot structure of the 1.6 Mb/s image was clearly visible. It is possible to soften this and to create a more continuous picture with reduced Moiré interference with fine detail, but extensive tests are required to determine whether this is desirable. JESTY[62] found that in terms of preferred viewing distance spot wobble produced a significant improvement in picture quality, but tests carried out in the present experiment showed that some observers preferred the impression of sharpness created by a prominent dot structure.

The dot structure, which is just visible in the 4 field exposure of Fig. 6.6 , was removed by means of a high Q series tuned circuit shunted across the de-emphasis network and tuned to 3 MHz. The image then appeared continuous in the vertical direction (but the flickering aliased noise was unaffected).

The vertical line structure was softened by a horizontal spot wobble signal applied synchronously to the scanner and monitor deflection systems. For this purpose a sinusoidal signal was obtained from the 3 MHz square wave which operated the dot-interlace gate, but owing to the very low bandwidth of the deflection circuits it was necessary to construct separate spot wobble coils. These were taped to the necks of the scanner and display tubes and sufficient capacitance was shunted across each coil to tune it to 3 MHz. The coils were excited by common base transistor amplifiers driven by the 3 MHz square wave and spot wobble amplitude was adjusted to just close the gaps between interlaced lines without overlap. Figure 6.7 shows a 4 field exposure of the softened picture, but this somewhat underestimates the visibility of the wobble signal at close range and again the aliased interference has been integrated out.

Although MOUNTS[85] has remarked that spot wobble lowers the spatial frequencies of noise added to the video signal, no significant increase was noticed in quantizing noise visibility.

MONTEATH[82] has pointed out that in a system employing synchronous spot wobble, the video bandwidth should be increased to accommodate signal components around the wobble frequency. This was not done for the picture shown in Fig.6.7 which therefore appears defocussed and is little better than

Figure 6.7. 225 line image of the simulated 1.6 Mb/sec. system employing pseudo-random quantization and dot-interlace, with synchronous spot wobble.

the result of receiver spot wobble only.

Lighting Conditions

One of the major difficulties associated with designing a video telephone lies in its likely use under high office lighting conditions. This calls for high peak picture luminance in order to obtain good contrast and presents stringent requirements for satisfactory flicker fusion. The situation can be improved by fitting the display with a neutral density filter and perhaps a short viewing hood. Contrast is increased since light from the phosphor is only attenuated once by the filter whereas ambient illumination reflected from the screen is attenuated twice. The simulated display in the laboratory was fitted with a curved polaroid filter in a matt black hood. With less than 10 ftL highlight luminance and two 250 W photo-flood lamps directed from a distance of two feet on to the screen, contrast was still good.

6.3.2. A Video Telephone System Without Dot-interlace

In view of the importance of flicker fusion, an alternative system was investigated which again used 2 bit pseudo-random quantization, but which did not include dot-interlace. Instead, only half the number of picture elements of the previous system was specified to maintain the 1.6 Mb/sec. data rate. Figure 6.8 summarizes the new standards which were

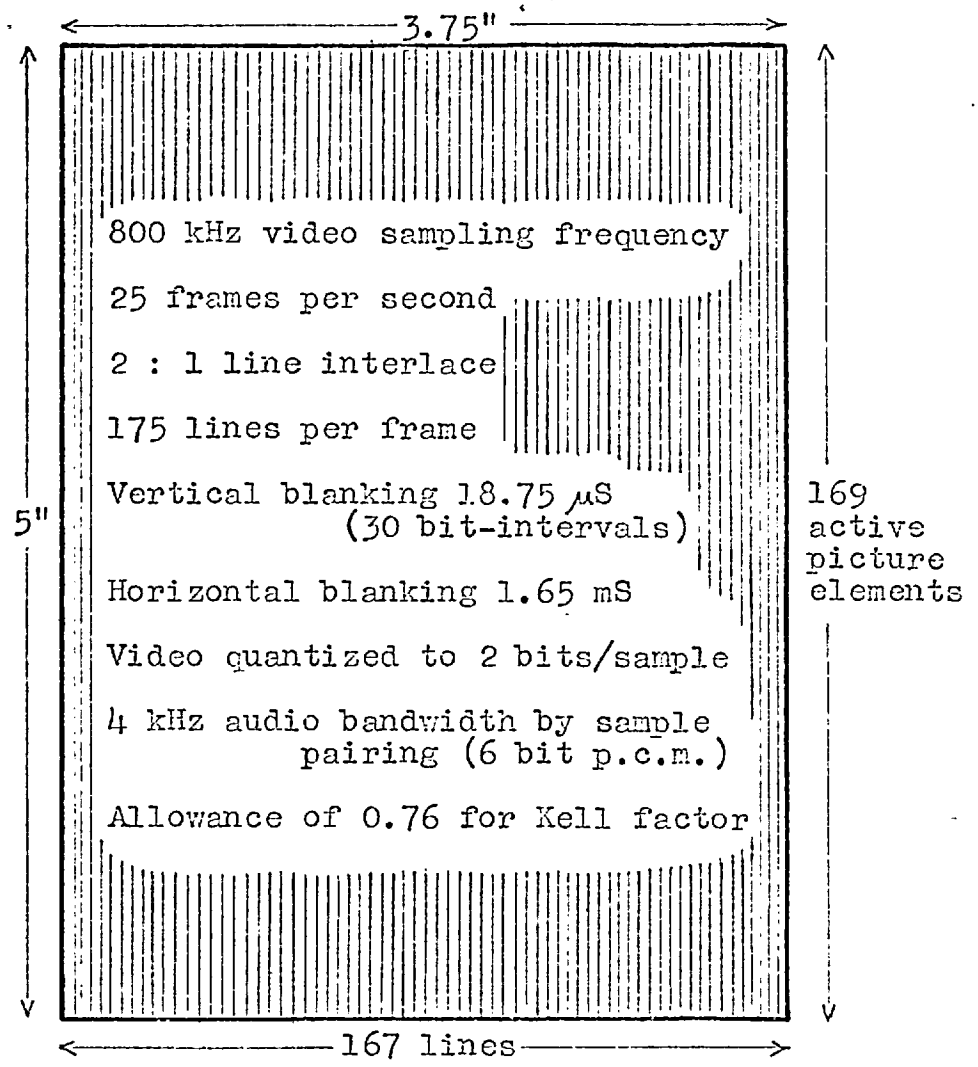

Figure 6.8. Summary of standards of the experimental system without dot-interlace.

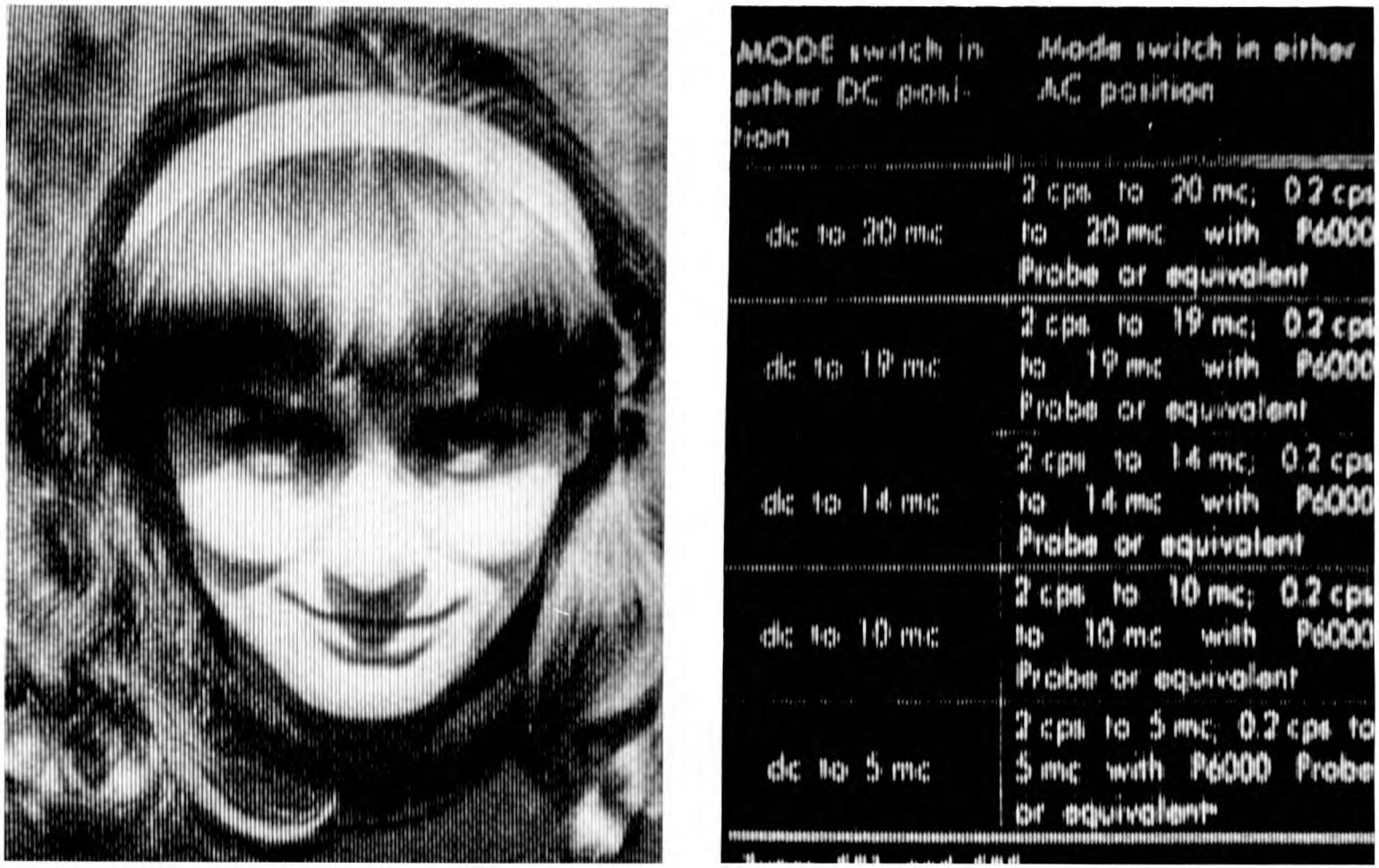

(a) (b)

Figure 6.9. 167 line images of the simulated 1.6 Mb/sec. system which used pseudo-random quantization without dot-interlace (Full size, 2 field exposures).

simulated by reducing the field and line unblanking intervals (see Fig.6.3(a)) to 8.25 mS and 28.2 μS respectively. The numbers of horizontal and vertical picture elements were reduced equally from those of the previous system by a factor of $\sqrt{2}$, and the picture width was compressed to give an aspect ratio of 4:3, allowing for a Kell factor of 0.76. This was done to avoid increasing the visibility of the line structure at the proposed viewing ratio. The system has a similar number of active picture elements to the Bell Picturephone, but with fewer lines so that horizontal and vertical resolutions are more nearly equal.

The line scanning frequency of 4.4 kHz is too low for adequate speech sampling, therefore the line retrace interval has been extended over that proposed by Purton and Lunn to accommodate two 6 bit speech samples per interval. By sampling the speech at 8.8 kHz and pairing samples, a speech bandwidth of 4 kHz may be obtained, but with the introduction of 230 μS delay into the speech path. This would not be subjectively detectable and pairing can be accomplished with only a small increase in coder complexity.

Figure 6.9 illustrates the image quality and resolution of the new 175 line system. The photographs show single frame (40 mS) exposures and completely represent the appearance of the image since the synchronized dither gave no visible flicker or migrating noise. The apparent S/N ratio

of Figure 6.9(a) is lower than for the corresponding 405 line image shown in Figure 5.5(a) since the viewing distance for the noise has been reduced relative to that of the picture. Also, in relation to system resolution the picture is less redundant and the runs of uniform intensity in the video signal are reduced in length. The dither is therefore less successful in generating high frequency quantizing noise.

6.4. CONCLUSION

Pseudo-random quantization certainly improves the prospects of transmitting an image of low but useful resolution through an economic channel, but a much deeper assessment of subjective reactions to frozen noise is called for than was attempted in Section 4.4.1. Synchronized noise can be tolerated at a lower S/N ratio than migrating noise, but it is clear from the quality of Figure 6.9 that at least 3 bit quantization is necessary in a low resolution system where the signal redundancy is much reduced. Frozen noise rapidly becomes more objectionable as picture highlight luminance is increased so that this will be another deciding factor in quantizing fineness.

The decision as to which of the systems considered should be studied further rests mainly on the extent to which increased phosphor persistence can reduce the large area

flicker of the aliased quantizing noise. The reduced picture redundancy in the second system caused a noticeable increase in quantizing noise visibility which may slightly offset the flicker disadvantage of the first system.

The author's colleagues who saw the systems in the laboratory gave quite favourable opinions of both systems (it was not possible to make a reliable comparison owing to the time taken to set up each system), but their opinions were not influenced by any cost criterion. Both systems were probably too noisy to be acceptable for commercial exploitation for which at least 3 bit quantization would be necessary. Without dot-interlace, a 1.6 Mb/sec. system employing 3 bit coding would not have sufficient spatial resolution. If a longer persistence phosphor can reduce the flicker of dot-interlace and 3 bit quantization to an acceptable level, then a 1.6 Mb/s system could be obtained with only $\frac{2}{3}$ of the resolution of the first system considered. This in fact would be identical to the system proposed by Purton and Lunn except for the direction of scan.

It seems likely that unless some other form of bandwidth compression can be included it will be necessary to occupy two units of 1.6 Mb/sec. in order to obtain sufficient resolution with an acceptable noise level. A system similar to the second one investigated, but with 3 bit quantization and 50 % more picture elements (giving a square raster) would give a comparatively good picture from 3.2 Mb/sec.

CHAPTER 7

CONCLUSION

7.1. SUMMARY OF THE RESULTS OBTAINED

The pseudo-random quantizing scheme which was proposed and computer simulated by L.G. Roberts has been implemented using a shift register generator as the pseudo-random noise source. Some qualitative observations were made on image quality with both synchronized and migrating noise from which it appears that the "dirty window" effect of synchronized noise is to be preferred if it is not of sufficient intensity to mask picture detail. With an asynchronized dither, the 2 bit quantizer produces an image similar to the original degraded with additive white Gaussian noise at 22 dB S/N ratio.

Roberts' work was shown to be a particular application of quantizer linearization by dithering, for which the optimum noise-like dither has independent samples with amplitudes distributed uniformly over one quantum. However, this is not the optimum dither condition which minimizes the objectionability of television quantizing noise. It has been proposed in this thesis to introduce correlation between dither samples in order to shape the quantizing noise power spectrum to ~~match~~ exploit the subjective function of

noise visibility. To this end, the properties of the shift register generator were described and various noise spectra generated to demonstrate the advantages of spectrum shaping in both the horizontal and vertical image directions. A set of Q-equations was devised which partially specifies the operation of the quantizer by relating quantizing noise spectra to the weighting function, which generates the multilevel dither, and its binary inputs. The Q-equations are only valid in areas of the image where the picture signal amplitude is constant, but these are precisely the areas where the viewer is most aware of noise.

Simple six level dithers were considered which very nearly realized ~~the~~ ~~expected~~ 6 dB reduction in noise visibility by shaping the power spectrum of the quantizing noise and which illustrated the useful validity of the Q-equations. It was then proposed to use a dither which ~~over~~emphasized the high frequency end of the quantizing noise spectrum and to employ pre and de-emphasis filters to gain an overall reduction of noise power. However, it was discovered that high frequency pre-emphasis reduces the areas of constant intensity in the picture signal and restricts the effectiveness of the dither in confining quantizing noise to high frequencies. Observer tests were carried out to determine the additional advantage of pre and de-emphasis around a 2 bit quantizer. A simple four level dither was

found to be sufficient for most pictures since the pre and de-emphasis filters were capable of removing the remanent contours. With a frame-alternating dither creating the impression of migrating noise, image quality was judged to be equivalent to the original degraded with additive white noise at 32 dB S/N ratio. This performance is comparable to that reported of a noise-feedback quantizer invented by Cutler and some comparisons were made between the two schemes.

A particular application of pseudo-random quantization was considered in relation to the video telephone. Two 1.6 Mb/sec. systems were simulated using the 2 bit pseudo-random quantizer with pre and de-emphasis, and photographic results have been presented. It appears that the equivalent S/N ratio of the quantized image is diminished in low resolution systems where signal redundancy is generally lower and the Q-equations are less valid. It was also realized that pseudo-random quantization is not entirely compatible with dot-interlace owing to increased 12.5 Hz flicker, but this could be minimized by a more suitable dither and pre and de-emphasis networks, and by increasing the phosphor persistence.

7.2. PROPOSALS FOR FURTHER WORK

This thesis has described a method of significantly reducing the necessary codelength for digital transmission of a satisfactory television image, and subjective experiments have been carried out to investigate the possible magnitude of this reduction. A great deal of work remains in developing an optimum dither signal along the lines indicated.

The 4 and 6 level dithers considered still leave visible contours on certain critical pictures such as a grey scale, although these are considerably reduced by pre and de-emphasis. To cope with all situations, a 16 level dither is probably necessary for which the Q-equations become more complicated. Only binary inputs to the dither weighting network have been considered so far, comprising S.R.G. outputs or products of these with appropriate square waves. It is possible that other components - not necessarily binary - might be used to facilitate further reduction of quantizing noise visibility, with or without additional pre and de-emphasis of the video signal. However, even the simple dither configurations presented here represent the outcome of an intensive search and optimization may be difficult. The aid of a computer could be essential in conducting an exhaustive search of dither components and in analysing the performance of complex dithers.

No use was made of line-to-line correlation in the dither to shape the vertical spatial spectrum of the quantizing noise, but it appears that a further improvement of at least 2.5 dB in equivalent S/N ratio might be obtained by this means. Also, the subjective evaluations were conducted for migrating noise on still pictures whereas in general a frame-synchronized dither would be more acceptable. There is some doubt as to the shape of the two-dimensional subjective weighting function, $W(w_x, w_y)$, for frozen noise. It would be of great value to conduct tests of the visibility of additive pseudo-noise, exploiting the flexibility of the S.R.G. for generating a range of two-dimensional spatial spectra, in order to determine $W(w_x, w_y)$. Of particular interest is the behaviour of a peak in $W(w_x, w_y)$ which might permit the optimum dither to confine some quantizing noise to very low spatial frequencies. This could also have some bearing on the visibility of the low frequency intermodulation products resulting from the additional use of pre and de-emphasis networks. Having found an optimum two-dimensional frame-synchronized dither, further tests will then be required to determine the minimum acceptable quantizing fineness for a wide range of moving pictures.

Further experimental work should preferably include time sampling in order to ensure that observed improvements

are due entirely to amplitude dithering and that similar performance will be obtained in a complete PCM system. In the laboratory system, the video signal presented to the quantizer was sharply bandlimited and most quantizer transitions were due to steps in the pseudo-random dither. However, owing to the finite risetimes of these steps and of the quantizer threshold detectors, signal dependent time-warping of the threshold crossings (pulse width modulation) did occur, causing transients to remain after subsequent subtraction of the dither. On the basis of reasonable agreement with estimates from Q-equation theory, it was concluded that these transients did not significantly reduce noise visibility. Nevertheless, this source of error requires evaluation.

Pseudo-random coding was considered in application to a digital video telephone system which itself presents an extensive programme of testing, preferably in conjunction with verbal communication, to determine acceptable standards of resolution, size and shape, line structure, etc. In particular, an investigation is needed of the extent to which an increase in phosphor persistence can reduce flicker in a system employing pseudo-random quantization and dot-interlace. More generally, subjective tests are required to determine the efficiency of pseudo-random quantization in low resolution television systems.

8. APPENDICES

8.1. MEAN SQUARE ERROR FOR THE EQUAL STEP QUANTIZER

Consider a sample, amplitude v, of a signal with p.d.f. p(v) applied to an equal step quantizer for which q is the step size and h the number of steps. The signal is confined to the amplitude range $0 \leq v \leq hq$. The quantizer thresholds are located at v_j volts ($v_j = rq$, where $r = 1, 2, .. j, ... (h-1)$) as shown in Figure 8.1 :

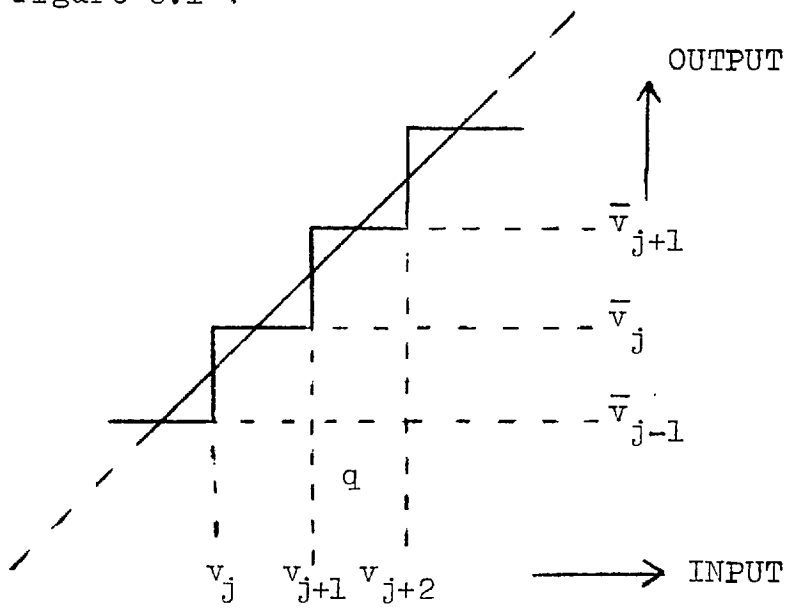

Figure 8.1. Equal step quantizer characteristic.

For signal inputs between v_j and v_{j+1} the chosen output is $\bar{v}_j$, where

$$\bar{v}_j = \tfrac{1}{2}(v_j + v_{j+1})$$

The error, e , made on sample v within the range v_j to v_{j+1} is

$$e_j = v - \bar{v}_j$$

The mean square error over the interval v_j to v_{j+1} is

$$\overline{e_j^2} = \int_{v_j}^{v_{j+1}} (v - \bar{v}_j)^2 . p(v)\, dv$$

Summing over all values of j :

$$E = \overline{e^2} = \sum_j \int_{v_j}^{v_{j+1}} (v - \bar{v}_j)^2 . p(v)\, dv$$

For small quantizing steps (or for a uniform p.d.f., p(v)), p(v) can be assumed constant over one step, so that :

$$p(v) = p(v_j)$$

$$\text{Hence,} \quad E = \frac{1}{3} \sum_j \left[(v - \bar{v}_j)^3 \right]_{v_j}^{v_{j+1}} . p(v_j)$$

$$= \frac{1}{12} \sum_j (v_{j+1} - v_j)^3 p(v_j)$$

Putting $p(v_j).(v_{j+1} - v_j) = p_j$, the probability that the input is between the j^{th} and $(j+1)^{st}$ levels, and substituting $(v_{j+1} - v_j) = q$, the mean square error becomes :

$$E = \frac{q^2}{12} \sum_j p_j = \frac{q^2}{12}$$

8.2. AUTOCORRELATION AND POWER SPECTRA OF SOME MODULATED M-SEQUENCES (used in Section 4.6)

A It was shown in Chapter 2 that with S.R.G. clock frequency $1/\delta$ Hz, the binary m-sequence has power spectrum envelope

$$\frac{2}{N}\left(\frac{\sin \delta w/2}{\delta w/2}\right)^2 \quad \text{of lines at harmonics of } 1/N\delta \text{ Hz.}$$

Where $1/\delta = 6$ MHz, the envelope has its first zero at 6 MHz.

Substituting 4δ for δ it follows that the m-sequence, y", generated by clocking the same S.R.G. at only 1.5 MHz has the power spectrum envelope

$$\frac{2}{N}\left(\frac{\sin 2\delta w}{2\delta w}\right)^2 \quad \text{of lines at harmonics of } 1/4N\delta \text{ Hz.}$$

B It was also shown in Chapter 2 (p.70) that with S.R.G. clock frequency $1/2\delta$, the product of the m-sequence and a square wave of period 2δ has the power spectrum envelope

$$\frac{2}{N}\left(\frac{\sin^2 \delta w/2}{\delta w/2}\right)^2 \quad \text{of lines at harmonics of } 1/2N\delta \text{ Hz.}$$

Hence, substituting 2δ for δ it follows that the product uy" has the power spectrum envelope

$$\frac{2}{N}\left(\frac{\sin^2 \delta w}{\delta w}\right)^2 \quad \text{of lines at harmonics of } 1/4N\delta \text{ Hz.}$$

C The autocorrelation function of the product, sy", of the quarter-rate m-sequence and a square wave of period 2δ is shown in Figure 8.2. This is given at integral shifts of δ by the product of the respective autocorrelation coefficients.

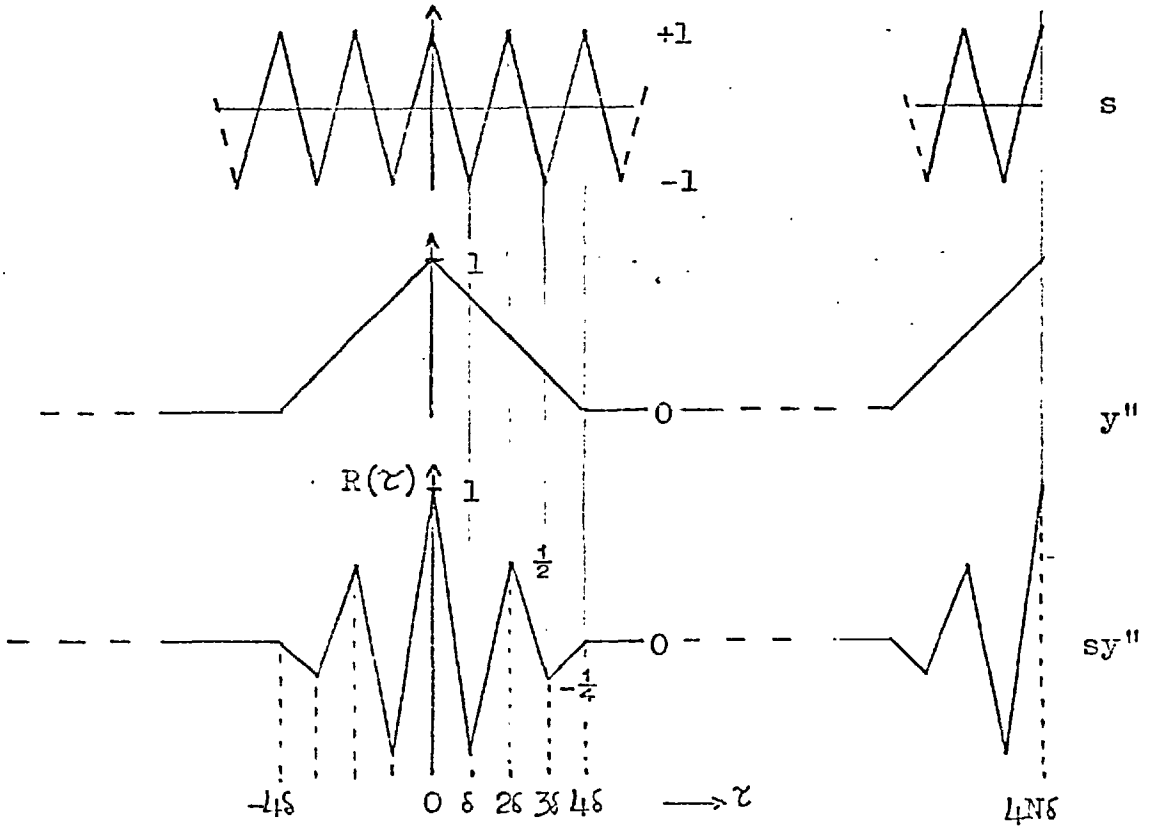

Figure 8.2. Determination of the autocorrelation function of the product sy" of a quarter-rate m-sequence and a square wave of period 2δ.

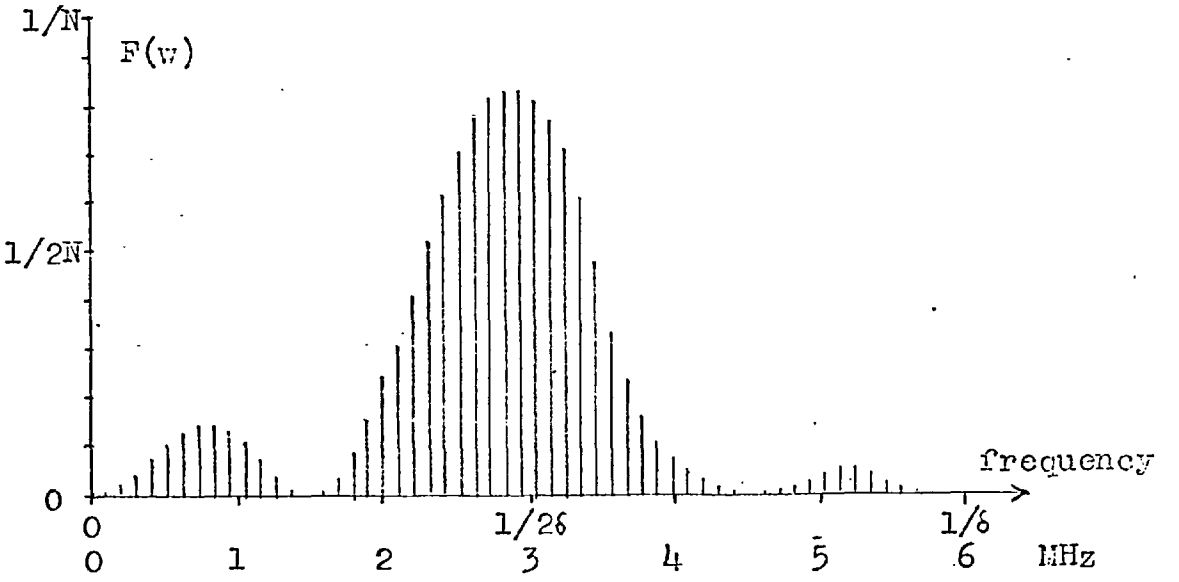

Figure 8.3. Power spectrum of the product sy" - lines are at harmonics of 1/4Nδ.

For large N, the out-of-phase correlation of the m-sequence can be neglected together with the associated attenuation of lines at harmonics of $1/2\delta$ in the power spectrum.

The sequence sy" has period $4N\delta$ and therefore has a spectrum of lines at harmonics of $1/4N\delta$ Hz. The envelope is given by :

$$F(w) = \frac{4}{4N\delta}\int_0^{2N\delta} R(\tau).\cos w\tau\, d\tau$$

which, from Fig.8.2 is given by :

$$F(w) = \frac{1}{N\delta}\left\{\int_0^{\delta}(1 - \frac{7\tau}{4\delta}).\cos w\tau d\tau + \int_{\delta}^{2\delta}(\frac{5\tau}{4\delta} - 2).\cos w\tau d\tau \right.$$

$$\left. + \int_{2\delta}^{3\delta}(2 - \frac{3\tau}{4\delta}).\cos w\tau d\tau + \int_{3\delta}^{4\delta}(\frac{\tau}{4\delta} - 1).\cos w\tau d\tau \right\}$$

On evaluation, this reduces to :

$$F(w) = \frac{2}{N}.\cos^2\delta w\left(\frac{\sin^2\delta w/2}{\delta w/2}\right)^2$$

and the form of this function is shown in Figure 8.3.

D The product su gives a further 1.5 MHz square wave which is time-shifted by δ secs from u. The transitions of su occur midway between those of u. As the result of this phase shift, the sequence suy" is not identical to the sequence uy". The autocorrelation function of suy" is derived in

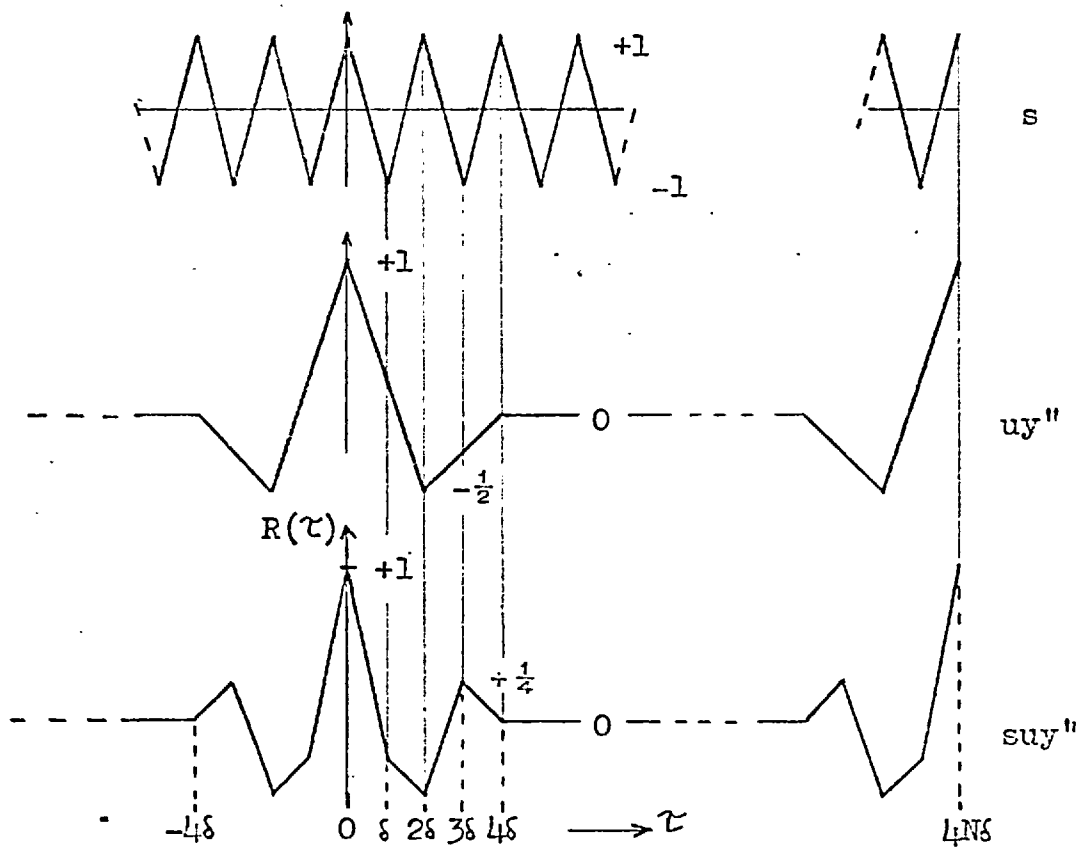

Figure 8.4. Determination of the autocorrelation function of the product suy" of 3 and 1.5 MHz square waves and a quarter-rate m-sequence.

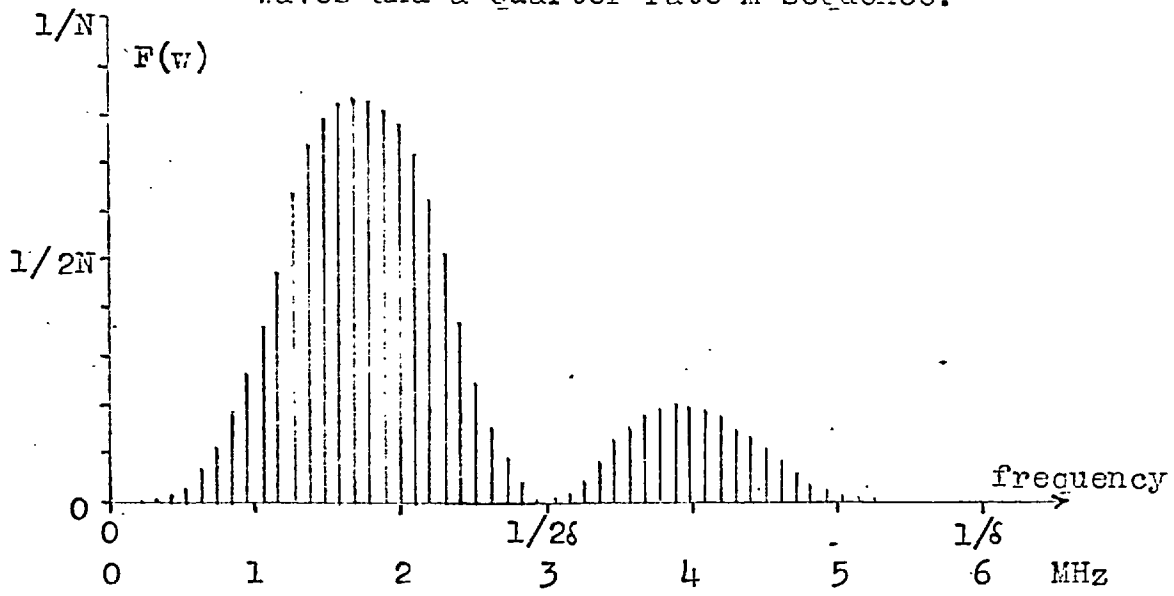

Figure 8.5. Power spectrum of the product suy" - lines are at harmonics of 1/4Nδ.

Figure 8.4 from the products of the coefficients of the sequences uy" and s. Again the out-of-phase correlation of the m-sequence has been neglected.

The sequence suy" has period $4N\delta$ and therefore has a spectrum of lines at harmonics of $1/4N\delta$ Hz. Referring to Fig. 8.4, the envelope is given by :

$$F(w) = \frac{4}{4N\delta}\left\{\int_0^{\delta}(1 - \frac{5\tau}{4\delta}).\cos w\tau d\tau - \int_{\delta}^{2\delta}\frac{\tau}{4\delta}.\cos w\tau d\tau + \int_{2\delta}^{3\delta}(\frac{3\tau}{4\delta} - 2).\cos w\tau d\tau + \int_{3\delta}^{4\delta}(1 - \frac{\tau}{4\delta}).\cos w\tau d\tau\right\}$$

On evaluation, this reduces to :

$$F(w) = \frac{1}{N}(1 - \cos 2\delta w)\left(\frac{\sin^2 \delta w/2}{\delta w/2}\right)^2$$

and the form of this function is shown in Figure 8.5.

8.3. CIRCUIT DIAGRAMS AND DESCRIPTION OF THE APPARATUS

Figure 8.6(a) shows a rear view of the equipment rack and power supplies. Panel 1 (immediately above the power supplies) contained a composite line and field blanking generator, 6 MHz clock pulse amplifier and a number of video amplifiers. The circuit diagram of a blanked video amplifier for adding or subtracting noise is given in Figure 8.7.

Panel 2, also shown in Figure 8.6(c), contained the S.R.G. and its reset circuitry. Figure 8.8 shows the circuit diagram of a bistable and Figure 8.9 the modulo-2 adder. Multilevel noise was generated in a blanked amplifier connected by a resistive weighting network to the desired points on the patch panel. Figure 8.10 shows the logic circuitry and Figure 8.11 the associated timing diagrams of the S.R.G. clock and reset pulse generators. Each pulse train was amplified by the circuit of Figure 8.12 in order to drive the 18 bistables.

Panel 3 contained the six-input modulo-2 adder which comprised a sequence of 5 two-input adders in a design due to ROBINSON [101] (the operation of this circuit is also that of a Gray-to-binary code converter). Additional delay toggles and the 3 and 1.5 MHz square wave generators were identical to the S.R.G. bistables. This panel also included two

further two-input modulo-2 adders and a video dot-interlace gate.

Panel 4 contained the quantizer, designed to take up to eight threshold detectors on separate plug-in cards. Figure 8.13 shows the circuit diagram of one detector together with the input and output video amplifiers.

Finally, panel 5 contained the 3 MHz notch filter, video pre and de-emphasis networks and some low-frequency sampling equipment which was used to investigate pseudo-random quantization of speech signals.

Figure 8.6(b) shows a front view of the rack and part of the set-up for subjective measurements.

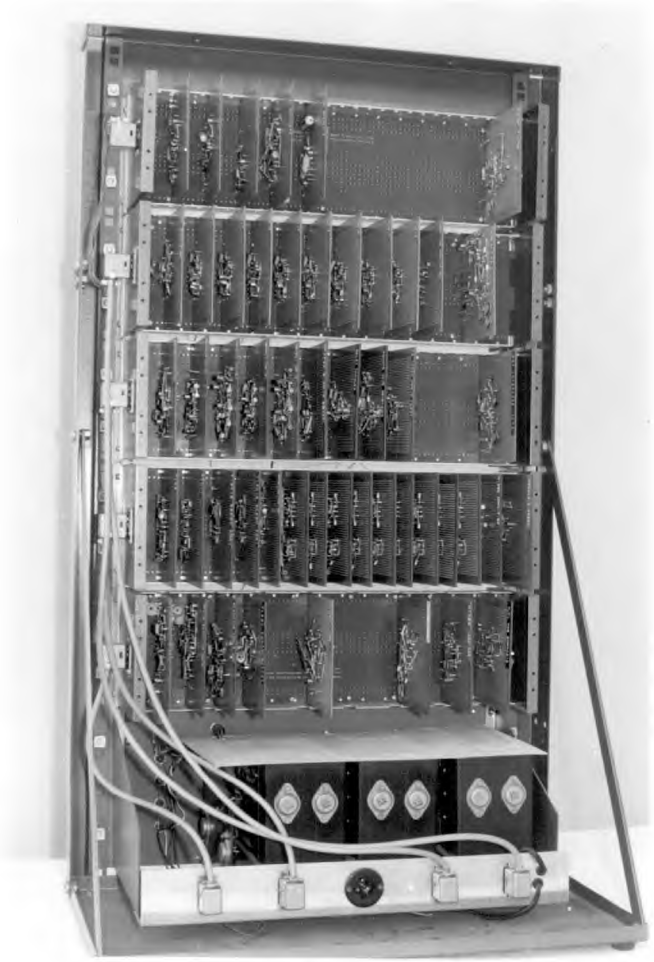

(a) The equipment rack - rear view.

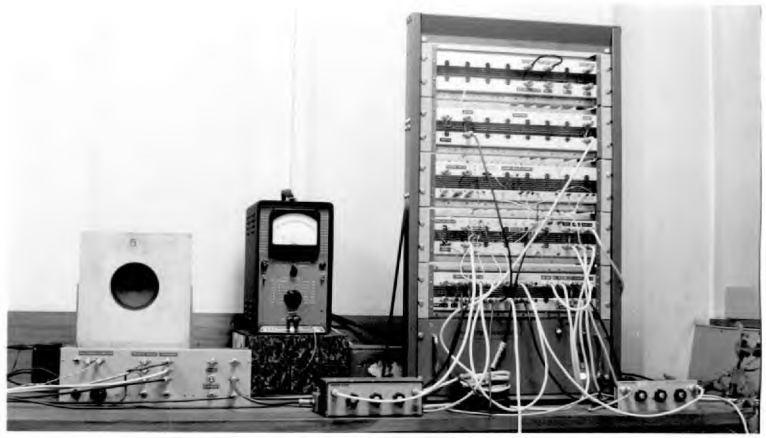

(b) Part of the experimental set-up.

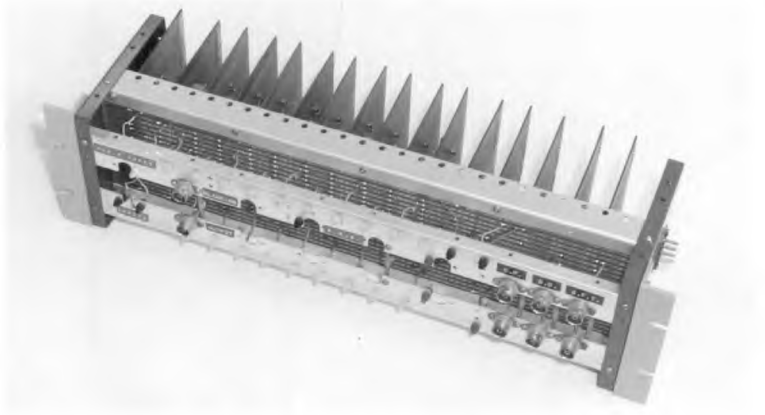

(c) The S.R.G. unit.

Figure 8.6. Views of the apparatus.

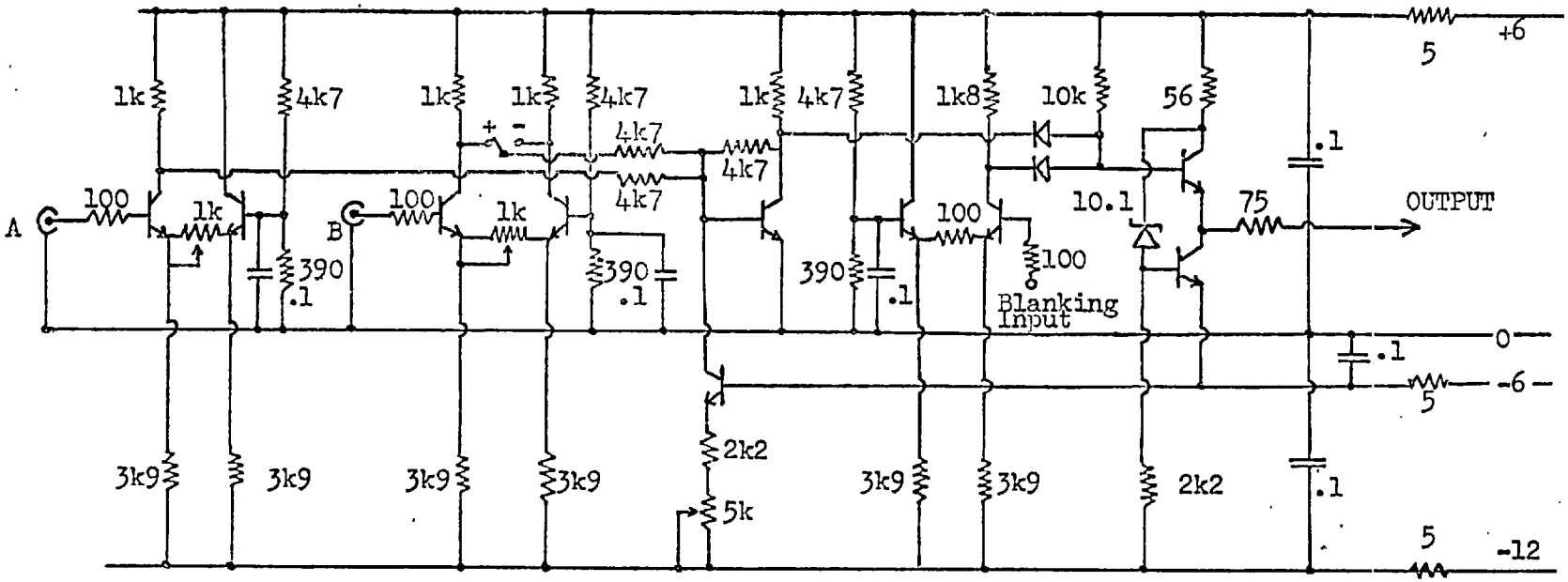

Transistors P346A
Diodes AAZ13

Resistances in Ω
Capacitances in μF

Inputs and output : 0 to 1 volt at 75 Ω

Figure 8.7. Video Adder/Subtractor with blanking.

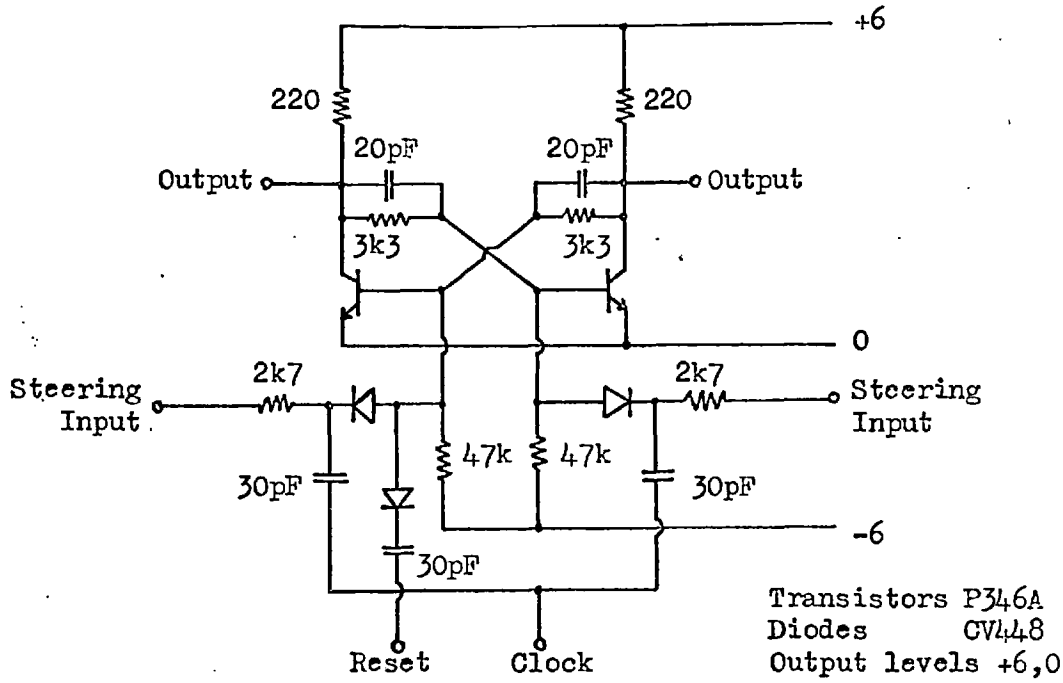

Figure 8.8. Bistable and steering circuit.

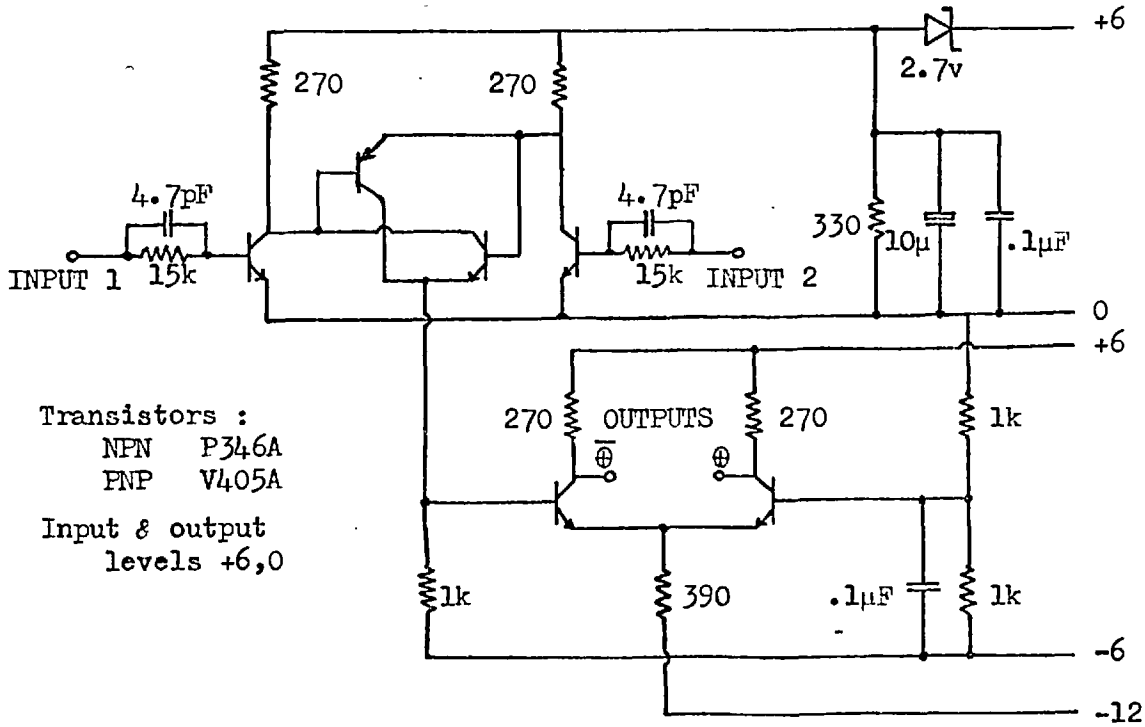

Figure 8.9. Two input modulo-2 adder

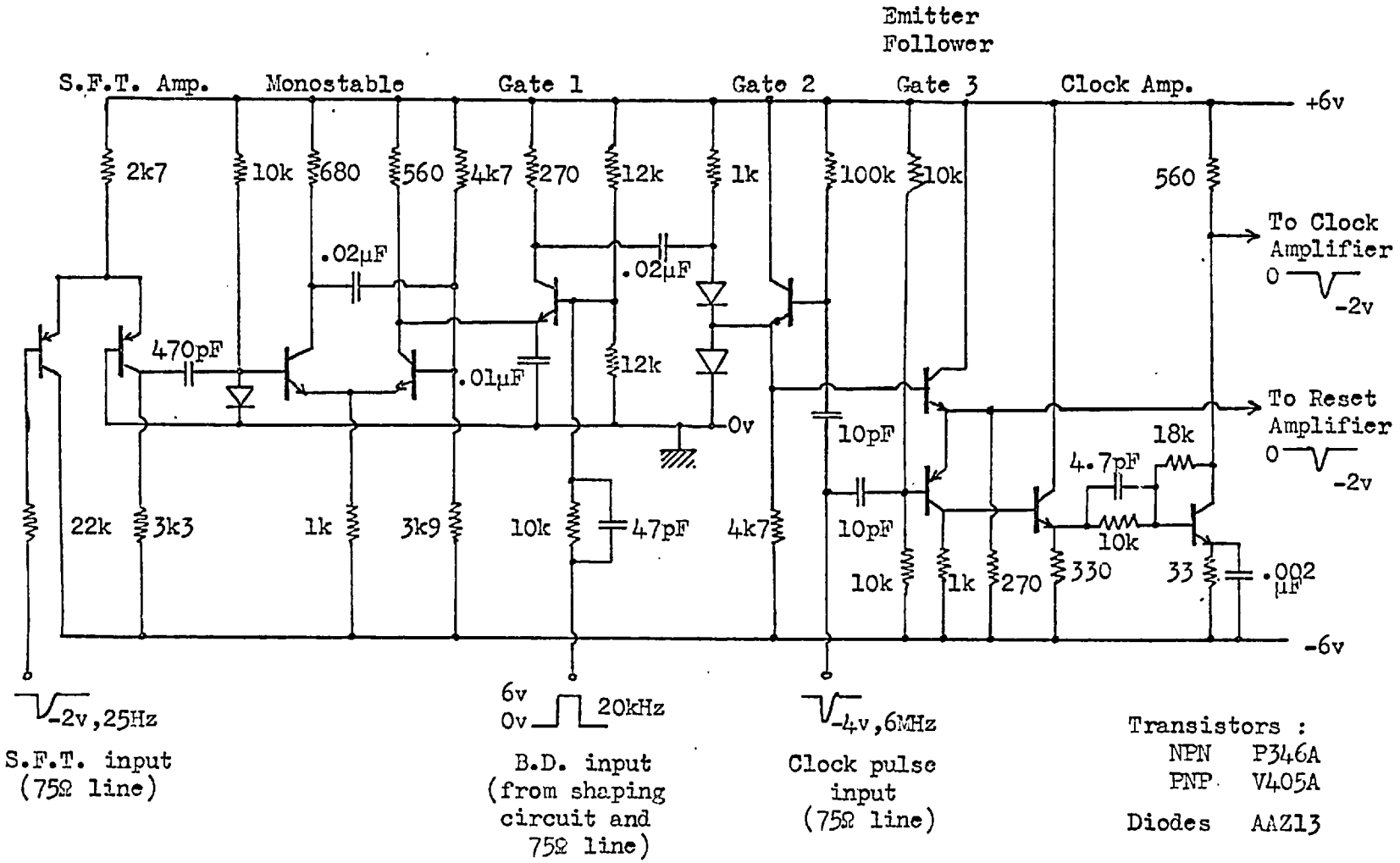

Figure 8.10. Gating circuitry for S.R.G. frame-synchronization.

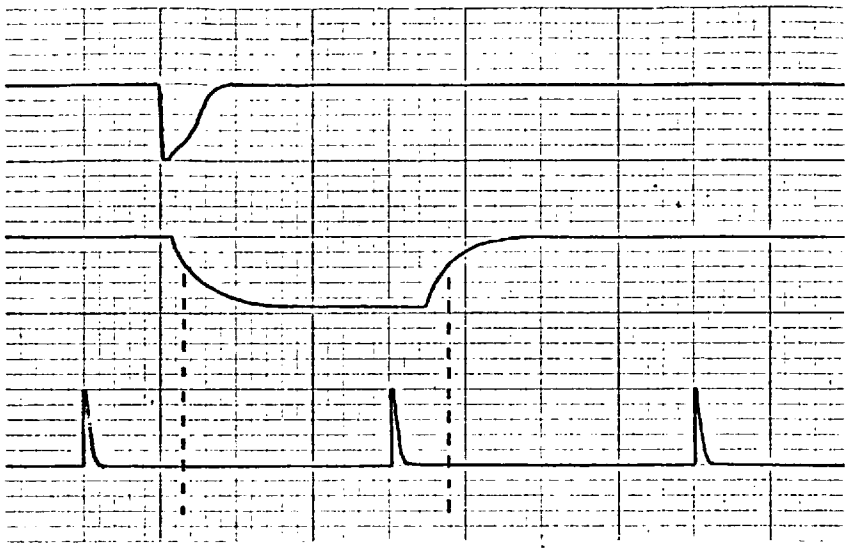

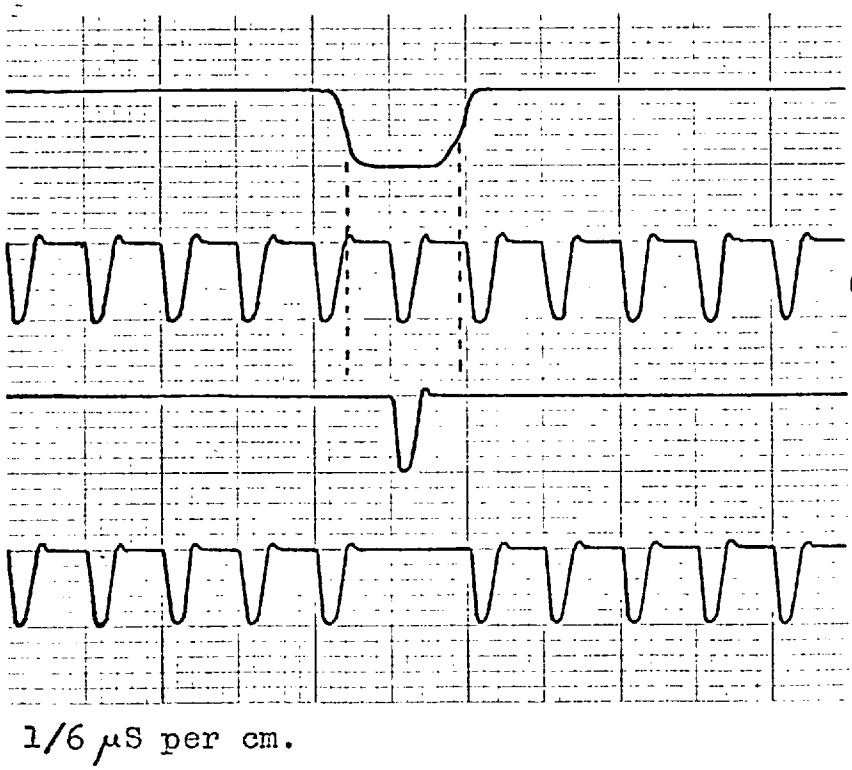

Figure 8.11. Timing diagrams for S.R.G. frame-synchronization.

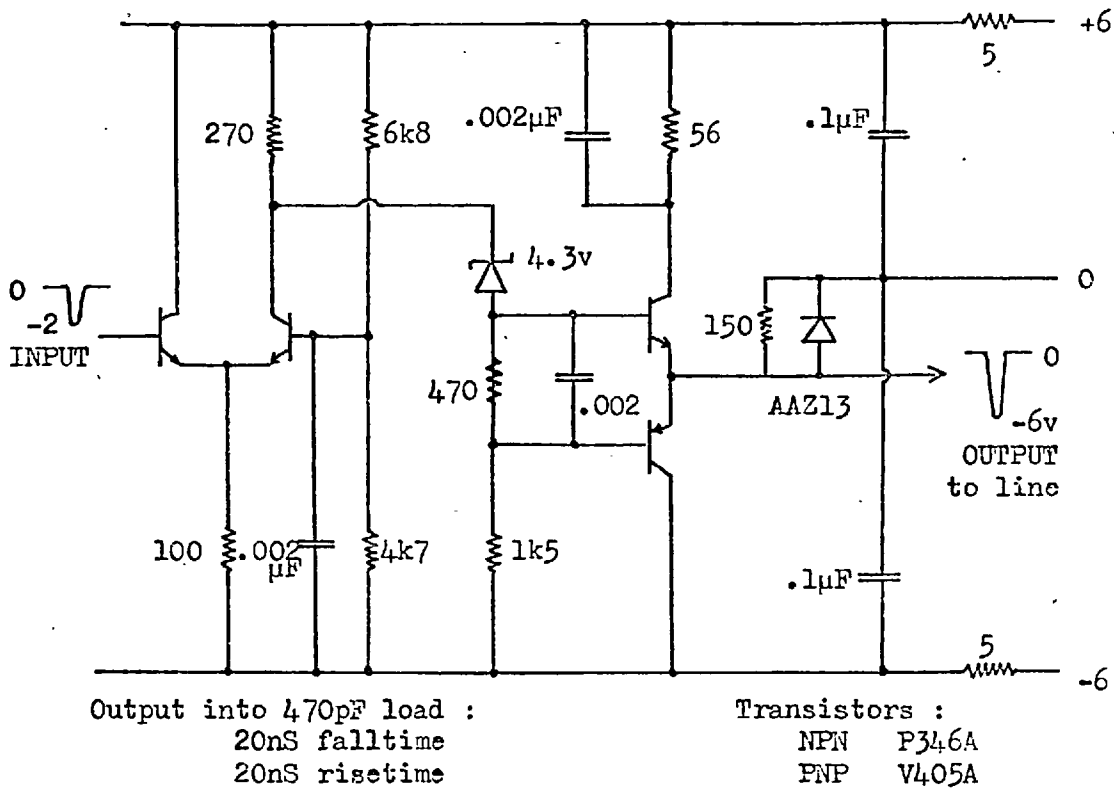

Figure 8.12. Clock or reset pulse amplifier.

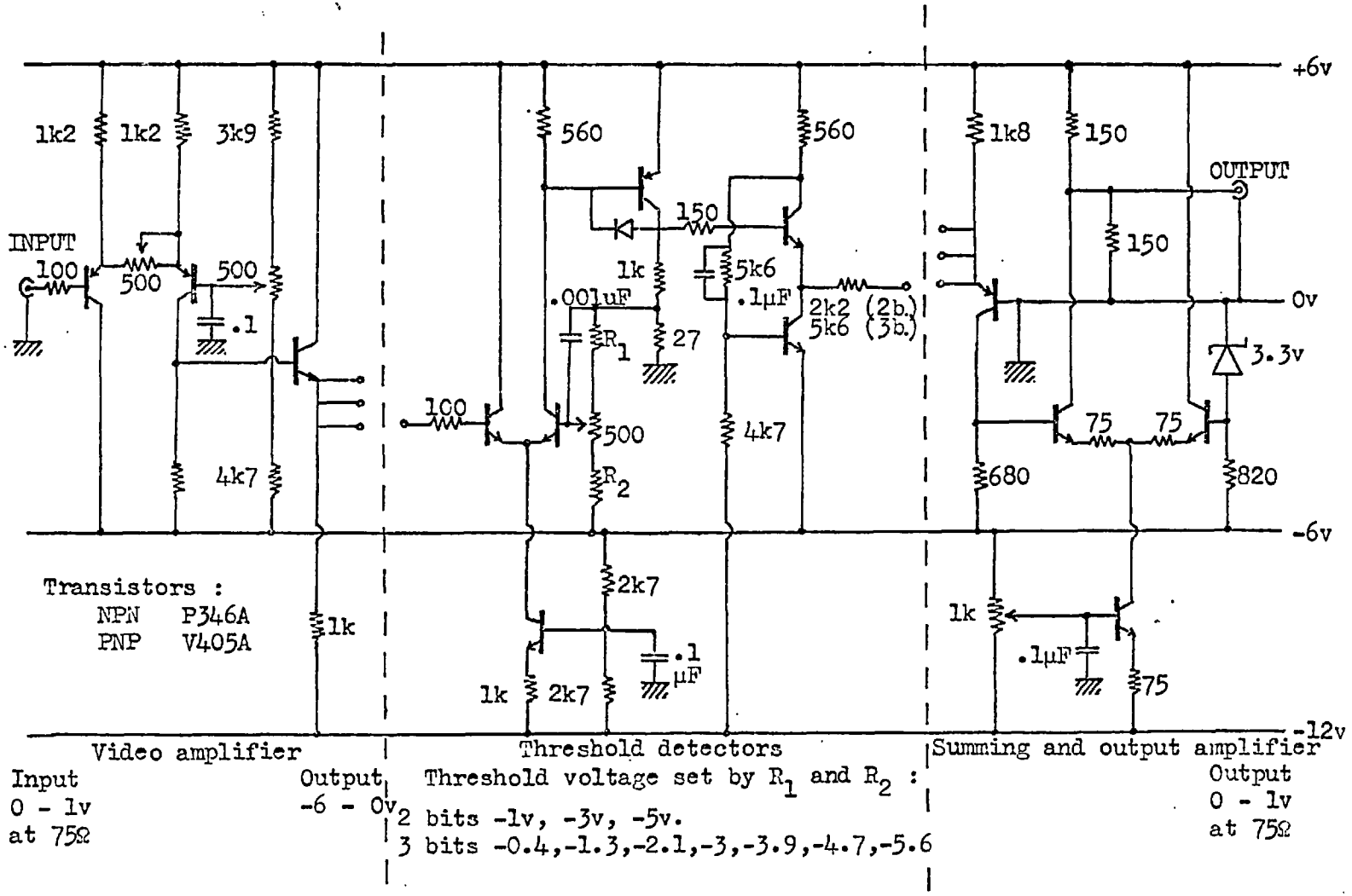

Figure 8.13. The Quantizer.

BIBLIOGRAPHY

1 AKHTAR, S.A-u-D. - "Video Bandwidth Compression Using Hologram Technique", M.Sc. Thesis, University of British Columbia, August, 1965.

2 BALDWIN, M.W. - "The Subjective Sharpness of Simulated Television Images", Proc. I.R.E., 28, 10, 1940, pp 458 - 468.

3 BARSTOW, J.M. & CHRISTOPHER, W.N. - "The Measurement of Random Video Interference to Monochrome and Color Television Pictures", Trans. A.I.E.E., 81 Part 1, pp 313 - 320, November, 1962.

4 BARSTOW, J.M. & CHRISTOPHER, W.N. - "The Measurement of Random Monochrome Video Interference", Trans. A.I.E.E. 73, Part 1, p 735, January 1954.

5 BARTLEY, S.H. - "The Psychophysiology of Vision" in Handbook of Experimental Psychology, S.S.STEVENS Ed., Wiley & Sons, N.Y., 1951.

6 BEDFORD, A.V. - "Mixed Highs in Colour Television", Proc. I.R.E., 38, pp 1003 - 1009, Sept. 1950.

7 BENNETT, W.R. - "Spectra of Quantized Signals", B.S.T.J. 27, pp 446 - 472, July 1948.

8 BRAINARD, R.C. - "Low Resolution TV : Subjective Effects of Noise Added to a Signal", B.S.T.J., 46, 1, pp 233 - 260, January 1967.

9 BRAINARD, R.C. - "Subjective Evaluation of PCM Noise-Feedback Coder for Television", Proc. I.E.E.E., 55, 3, pp 346 - 355, March 1967.

10 BRAINARD, R.C., KAMERER, F.W., & KINNE, E.G. - "Estimation of the Subjective Effects of Noise in Low Resolution Television Systems", I.R.E. Trans. IT-8, pp 99 - 106, February 1962.

11 BRAINARD, R.C., MOUNTS, F.W., & PRASADA, B. - "Low Resolution TV - Subjective Effects of Frame Repetition and Picture Replenishment", B.S.T.J., 46, 1, pp 233 - 260, January 1967.

12 BROWN, E.F. - "A New Crispener Circuit for Television Images", J.S.M.P.T.E., 72, pp 849 - 853, Nov. 1963

13 BROWN, E.F. - "Low Resolution TV - Subjective Comparison of Interlaced and Non-Interlaced Pictures", B.S.T.J., 46, 1, pp 199 - 232, January 1967.

14 BRUCE, R.A. - "Optimum Pre-Emphasis and De-Emphasis Networks for Transmission of Television by PCM", I.E.E.E. Trans. COM-12, pp 91 - 96, Sept. 1964.

15 BURDETT, F.A. "The Effect of Scan Direction on the Intelligibility of a Picture", I.E.E. Report of International TV Conference, May-June 1962, pp 27 - 34.

16 BYLANSKI, P.W.J. - "Coding and Modulation for Bandwidth Compression of Television and Facsimile Signals", Ph.D. Thesis, Univ. of London (Imperial Col.) 1966.

17 CARBREY, R.L. - "Video Transmission Over Telephone Cable Pairs by PCM", Proc. I.R.E., 48, pp 1546 - 1561, September 1960.

18 CHERRY, E.C. - "On Human Communication", Science Editions Inc., N.Y., 1961.

19 CHERRY, E.C. - Imperial College internal communication, 1967.

20 CHERRY, E.C., KUBBA, M.H., PEARSON, D.E. & BARTON, M.P. - "An Experimental Study of the Possible Bandwidth Compression of Visual Image Signals", Proc. I.E.E.E., 51, 11, pp 1507 - 1517, November 1963.

21 CUTLER, C.C. - "Transmission Systems Employing Quantization", U.S. Patent 2 927 962, March 8th, 1960.

22 DAVID, E.E. - "Digital Simulation in Research on Human Communication", Proc. I.R.E., 49, 1, pp 319 - 329, January 1961.

23 DELORAINE, E.M. & REEVES, A.H. - "The 25th Anniversary of Pulse Code Modulation", I.E.E.E. Spectrum, 2, pp 56 - 63, May 1965.

24 DERIUGIN, N.G. - "The Power Spectrum and the Correlation Function of the Television Signal", Telecommunications, 7, pp 1 - 12, 1957.

25 DEUTSCH, S. - "The Possibilities of Reduced Television Bandwidth", I.R.E. Trans. BTR-2, pp 69 - 82, October 1956.

26 DEUTSCH, S. - "Narrow-Band TV Uses Pseudo-Random Scan", Electronics, 35, April 27th 1962, pp 49 - 51.

27 DEUTSCH, S. - "Pseudo-Random Dot Scan Television Systems", I.E.E.E. Trans. BC-11, 1, pp 11 - 21, July 1965.

28 DEUTSCH, S., BALABAN, P. & ATZMON, A. - "Experimental Results of Pseudo-Random Dot Scan", O.A.R. U.S.A.F. Contract AF-19(628)3815, Polytechnic of Brooklin, January 1966.

29 DEUTSCH, S. - "A 210 Kc/sec Phonevision System", Proc. Society for Information Display Symposium, Boston, October 20th, 1966.

30 EASTON, R.A., MARKIN, J. & SOBEL, A. - "Subjective Brightness of a Very Short Persistence Television Display Compared to One with Standard Persistence", J. Opt. Soc. 57, 7, pp 957 - 962, 1967.

31 FATCHAND, R. - "Visibility of Noise on Television Pictures", Nature 181, 4626, pp 1797, 1958.

32 FINK, D.G. - (Ed.) "Television Engineering Handbook", McGraw-Hill Co. Inc., 1957.

33 FRANKS, L.E. - "A Model for the Random Video Process", B.S.T.J., 45, 4, pp 609 - 630, April 1966.

34 FURMAN, G.G. - "Removing the Noise from the Quantizing Process by Dithering:Linearization", U.S. Govt Research Report AD 296598, February 1963.

35 FURMAN, G.G. - "Improving the Quantization of Random Signals by Dithering", RAND Corp. Memo. RM-3504-PR, May 1963.

36 GABOR, D. & HILL, P.C.J. - "Television Bandwidth Compression by Contour Interpolation", Proc. I.E.E. 108, Part B, No. 39, p 303, 1961.

37 GARRATT, G.R.M. & MUMFORD, A.H. - "The History of Television", Proc. I.E.E. 99, 111 A, p 25, 1952.

38 GILBERT, M. - "The Visibility of Noise as a Function of Frequency", B.B.C. Eng. Div. Monograph No. 3, Part 2, pp 13 - 16, October 1955.

39 GOLDMARK, P.C. & HOLLYWOOD, J.M. - "A New Technique for Improving the Sharpness of Pictures", Proc. I.R.E. 39, pp 1314 - 1322, October 1951.

40 GOODALL, W.M. - "Television by PCM", B.S.T.J. 30, pp 33 - 49, January 1951.

41 GRAHAM, D.N. - "Image Transmission by Two-Dimensional Contour Coding", Proc. I.E.E.E., 55, 3, pp 336 - 346, March 1967.

42 GRAHAM, R.E. - "Predictive Quantizing of Television Signals", Bell Telephone System Mono. 3272, 1958.

43 GRAHAM, R.E. - "Subjective Experiments in Visual Communication", I.R.E. National Convention Record 1958, 6, part 4, pp 100 - 106.

44 GRAHAM, R.E. - "Snow Removal - A Noise Stripping Process for Picture Signals", I.R.E. Trans. IT-8, pp 129 - 144, February 1962.

45 GRAHAM, R.E. & KELLY, J.L.Jr - "Computer Simulation Chain for Research on Picture Coding", I.R.E. Wescon Convention Record 1958, part 4, pp 41 - 46.

46 GREGORY, R.L. - "Eye and Brain", World Univ. Lib., 1966.

47 HAANTJES, J. & deVRIJER, F.W. - "Flicker in Television Pictures", Wireless Engineer, 28, 329, pp 40 - 42, February 1951.

48 HAANTJES, J. & TEER, K. - "Multiplex Television Transmission Sub-Carrier and Dot-Interlace Systems", Wireless Engineer, 31, pp 225 - 233, 266 - 273, September, October, 1954.

49 HACKING, K. - "The Relative Visibility of Random Noise over the Grey Scale", J. Brit. I.R.E., 23, 4, pp 307 - 310, April 1962.

50 HALL, A.D. - "Experiments with Picturephone Service", Bell Labs Record 42, 4, pp 114 - 120, April 1964.

51 HARRISON, C.W. - "Experiments with Linear Prediction in Television", B.S.T.J., 31, pp 764 - 783, July 1952.

52 HOWSON, E.A. & BELL, D.A. - "Reduction of Television Bandwidth by Frequency-Interlace", J. Brit. I.R.E 20, 2, pp 127 - 136, February 1960.

53 HUANG, T.S. - "A Method of Picture Coding", M.I.T. Research Lab. of Electronics Q.P.R., No. 57, pp 109 - 115, April 15th, 1960.

54 HUANG, T.S. - "Pseudo-Random Scanning", I.E.E.E. Trans. COM-12, 3, p 105, September 1964.

55 HUANG, T.S. - "Subjective Effect of Two-Dimensional Pictorial Noise", I.E.E.E. Trans. IT-11, 1, pp 43 - 53, January 1965.

56 HUANG, T.S. - "Optimum Scanning Direction in Television Transmission", M.I.T. Res. Lab. of Electronics Q.P.R. No. 77, pp 325 - 331, April 15th 1965.

57 HUANG, T.S. & HARTMANN, H.P. - "Subjective Effect of Additive White Pictorial Noise with Various Probability Distributions", M.I.T. Res. Lab. Elect. Q.P.R. No. 85, pp 317 - 319, April 15th 1967.

58 HUANG, T.S., TRETIAK, O.J., PRASADA, B. & YAMAGUCHI, Y. - "Design Considerations in PCM Transmission of Low Resolution Monochrome Still Pictures", Proc. I.E.E.E., 55, 3, pp 331 - 335, March 1967.

59 ISHIKAWA, T. - "Linearization of Contactor Control Systems by External Dither Signals", Stanford Electronics Labs (California) Tech. Report No. 2103 - 2, October 1st, 1960.

60 JAFFE, R.C. - "Causal and Statistical Analysis of Dithered Systems Containing 3 Level Quantizer", M.S. Thesis, M.I.T., 1959.

61 JESTY, L.C. - "Television as a Communication Problem", Proc. I.E.E., 99, 111 A, pp 761 - 769, 1952.

62 JESTY, L.C. - "The Relation Between Picture Size, Viewing Distance and Picture Quality", Proc. I.E.E., 105 B, pp 425 - 439, 1958. Discussion includes a contribution by R.D.A. MAURICE.

63 JULESZ, B. - "A Method of Coding Signals Based on Edge Detection", B.S.T.J., 38, 4, pp 1001 - 1020, 1959.

64 JULESZ, B. - "Visual Pattern Discrimination", I.R.E. Trans. IT-8, 2, pp 84 - 92, February 1962.

65 KELLEY, R.A. -"An Experimental High Speed Digital Transmission System", Bell Labs Record 45, 2, pp 44 - 48, February 1967.

66 KELLY, D.H. - "Information Capacity of a Single Retinal Channel", I.R.E. Trans. IT-8, 4, pp 221 - 226, 1962.

67 KILVINGTON, T., JUDD, D.L. & MEATYARD, L.R. - "An Investigation of the Visibility of Noise in Television Pictures", P.O. Radio Report No 2289, 1954.

68 KIMME, E.G. & KUO, F.F. - "Synthesis of Optimal Filters for a Feedback Quantizing System", I.E.E.E. Trans. CT-10, pp 405 - 413, September 1963.

69 KITSOPOULOS, S.C. & KRETZMER, E.R. - "Computer Simulation of a Television Coding Scheme", Proc. I.R.E., 49, p 1076, June 1961.

70 KORDONSKIY, E.V. - "Improving the Characteristics of a Quantizing Device by Adding Low-Frequency Noise to the Signal", Telecom. & Radio Eng. (from the Russian) Pt 1, No 10, pp 26 - 31, 1964.

71 KORTMAN, C.M. - "Data Compression by Redundancy Reduction" I.E.E.E. Spectrum, 4, 3, pp 133 - 139, March 1967.

72 KOVASZNAY, L.S.G. & JOSEPH, H.M. - "Image Processing", Proc. I.R.E. May 1955, pp 560 - 570.

73 KRETZMER, E.R. - "Reduced Alphabet Representation of Television Signals", I.R.E. Convention Record, 1956, Part 4, pp 140 - 147.

74 LEWIS, N.W. - "Television Bandwidth and the Kell Factor" Electronic Technology, 39, 2, pp 44 - 47, 1962.

75 LIMB, J.O. - "Source-Receiver Encoding of Television Signals", Proc. I.E.E.E., 55, 3, pp 364 - 379, March 1967.

76 LOWRY, E.M. & DePALMA, J J. - "Sine-Wave Response of the Visual System, 1 . The Mach Phenomenon", J. Opt. Soc. Am., 51, 7, pp 740 - 746, July 1961.

77 LUNN, G.J. & MUNFORD, H. - "Television and the Telephone" A.T.E. Journal, 21, 2, pp 54 - 60, April 1965.

78 MARSH, A.H. - "Perception of Visual Forms in Intensely Noisy Television Images", Ph.D. Thesis, Univ. of London (Imperial College), 1967.

79 MAURICE, R.D.A. - "The Visibility of Noise over the Grey Scale", B.B.C. Eng. Div. Monograph No 3, Part 1, pp 5 - 12, October 1955.

80 MAX, J. - "Quantizing for Minimum Distortion", I.R.E. Trans. IT-6, 1, pp 7 - 12, March 1960.

81 MERTZ, P. - "Perception of Television Noise", J.S.M.P.T.E., 54, pp 8 - 34, January 1950.

82 MONTEATH, G.D. - "Vertical Resolution and Line Broadening", B.B.C. Eng. Div. Mono. 45, Dec. 1962.

83 MOON, P. & SPENCER, D.E. - "The Visual Effect of Non-Uniform Surrounds", J. Opt. Soc. Am. 35, p 233, March 1945.

84 MORONEY, M.J. - "Facts from Figures", Penguin Books, 1951.

85 MOUNTS, F.W. - "Low Resolution TV : An Experimental Digital System for Evaluating Bandwidth Reduction Techniques", B.S.T.J., 46, 1, pp 167 - 198, January 1967.

86 NEWELL, G.F. & GEDDES, W.K.E. - "Tests of Three Systems of Bandwidth Compression of Television Signals", Proc. I.E.E., 109 B, 46, pp 311 - 324, July 1962.

87 NEWELL, G.F. & GEDDES, W.K.E. - "Visibility of Small Luminance Perturbations in Television Displays", Proc. I.E.E., 110, 11, pp 1979 - 1984, 1963.

88 NISHIKAWA, S., MASSA, R.J. & MOTT-SMITH, J.C. - "Area Properties of Television Pictures", Phys. Sci. Res. Paper No 23 (U.S.A.F. Project), 1964.

89 OLIVER, B.M. - "Efficient Coding", B.S.T.J., 31, 4, pp 724 - 750, July 1952.

90 OLIVER, B.M., PIERCE, J.R. & SHANNON, C.E. - "The Philosophy of PCM", Proc. I R.E., 36, pp 1324 - 1331, November 1948.

91 O'NEAL, J.B. Jr - "Delta Modulation Quantizing Noise : Analytical & Computer Simulation Results for Gaussian and Television Input Signals", B.S.T.J., 45, 1, pp 117 - 141, January 1966.

92 PEARSON, D.E. - "Fidelity Criteria for Visual Image Transmission over Noisy Communication Channels", Ph.D. Thesis, Univ. of London (Imperial Col.) 1965.

93 PIERCE, J.R. & KARLIN, J.E. - "Reading Rates and the Information Rate of a Human Channel", B.S.T.J., 36, March 1957.

94 POWELL, P.G. - "A Study of Visual Perception", D.I.C. Thesis, October 1966.

95 PRATT, W.K. - "A Bibliography on Television Bandwidth Reduction Studies", I.E.E.E. Trans. IT-13, 1, pp 114 - 115, January 1967.

96 PROSSER, R.D. & ALLNATT, J.W. - "Subjective Quality of Television Pictures Impaired by Random Noise", Proc. I.E.E., 112, 6, pp 1099 - 1102, June 1965.

97 PROSSER, R.D., ALLNATT, J.W. & LEWIS, N.W. - "Quality Grading of Impaired Television Pictures", Proc. I.E.E., 111, 3, pp 491 - 502, March 1964.

98 PURTON, R.F. & LUNN, G.J. - "An Experimental 1.6 Mb/s PCM Video Telephone System for Use on Audio Cables", I.E.E. Conf. 'Transmission Aspects of Communications Networks', 24th February 1964.

99 ROBERTS, L.G. - "PGM Television Bandwidth Reduction Using Pseudo-Random Noise", S.M. Thesis, M.I.T., 1961.

100 ROBERTS, L.G. - "Picture Coding Using Pseudo-Random Noise", Trans. I.R.E. IT-8, 2, pp 145 - 154, February 1962.

101 ROBINSON, A.H. - "Automatic Digital Encoding for Bandwidth Reduction in Visual Image Transmission Systems", Ph.D. Thesis to be submitted, University of London (Imperial College).

102 ROSS, D T. - "Sampling and Quantizing", in 'Notes on Analog-Digital Conversion Techniques', Ed. SUSSKIND, M.I.T. Press 1957, pp 2.1 - 2.77.

103 SCHLESINGER, K. - "Dot Arresting Improves TV Picture Quality", Electronics, 24, p 96, September 1951.

104 SCHREIBER, W.F. - "Picture Coding", Proc. I.E.E.E., 55, 3, pp 320 - 330, March 1967.

105 SCHREIBER, W.F. & KNAPP, C.F. - "Television Bandwidth Reduction by Digital Coding", I.R.E. Nat. Conv. Record 6, Part 4, pp 88 - 99, 1958.

106 SCHREIBER, W.F., KNAPP, C.F. & KAY, N.D. - "Synthetic Highs - An Experimental Television Bandwidth Reduction System", 84th S.M.P.T.E. Convention, Detroit, October 23rd 1958.

107 SEYLER, A.J. - "Frame-Run Coding of Television Signals, A New Method for Bandwidth Reduction", Comm. of Australia P.M.G.'s Dept, Res. Lab. Report 5064, September 1959.

108 SEYLER, A.J. - "An Integrated System Design for the Coding of Visual Messages", Comm. of Australia P.M.G.'s Dept, Res. Lab. Report 5488, August 1961.

109 SEYLER, A.J. & BUDRIKIS, Z.L. - "Detail Perception after Scene Changes in Television Image Presentations", I.E.E.E. Trans. IT-11, 1, pp 31 - 43, Jan. 1965.

110 SHANNON, C.E. - "Coding Theorems for a Discrete Source with a Fidelity Criterion", in 'Information and Decision Processes', Ed. R.E. MACHOL, McGraw-Hill Co. Inc., 1960.

111 SHANNON, C.E. - "The Mathematical Theory of Communication" University of Illinois Press, September 1949.

112 SPANG, H.A. III - "Quantizing Noise Reduction", G.E. Res. Lab. Report No 62-RL-(2999E), April 1962.

113 STEVENS, S.S. (Ed.) - "Handbook of Experimental Psychology", J. Wiley & Sons, N.Y., 1951.

114 STUCKI, P. - D.I.C. Thesis to be submitted.

115 SZIKLAI, G.C. - "Some Studies in the Speed of Visual Perception", I.R.E. Trans IT-2, p 125, Sept. 1956.

116 TEER, K. - "Investigations into Redundancy and Possible Bandwidth Compression in Television Transmission", Philips Res. Reports 14, pp 501 - 556, 1959 (I & II) and 15, pp 30 - 96, 1960 (Part III).

117 THOMPSON, J.E. - "Improvements in or Relating to Pseudo-Random Quantizers", U.K. Patent 11750/67, March 1967.

118 THOMPSON, J.E. & SPARKES, J.J. - "A Pseudo-Random Quantizer for Television Signals", Proc. I.E.E.E., 55, 3, pp 353 - 355, March 1967.

119 TRETIAK, O.J. - "Scanner Display (S C A D)", M.I.T. Res. Lab. Elect. Q.P.R. No 83, pp 129 - 142, October 15th 1966.

120 WATTS, D.G. - "A General Theory of Amplitude Quantization with Applications to Correlation Determination", Proc. I.E.E., 109 C, pp 209 - 218, 1962.

121 WATTS, D.G. - "A Study of Amplitude Quantization with Applications to Correlation Determination", Ph.D. Thesis, Univ. of London (Imperial College), 1962.

122 WEAVER, L.E. - "Subjective Impairment of Television Pictures", Electronic & Radio Engineer, 36, 5, pp 170 - 179, May 1959.

123 WIDROW, B. - "A Study of Rough Amplitude Quantization by Means of Nyquist Sampling Theory", Trans. I.R.E. CT-3, pp 266 - 276, 1956.

124 WIDROW, B. - "Statistical Analysis of Amplitude Quantized Sample Data Systems", Trans. A.I.E.E. (Applications and Industry), 79, pp 555 - 568, January 1961.

125 WILLMER, E.N. & WRIGHT, W.D. - "Colour Sensitivity of the Fovea Centralis", Nature 156, pp 119 - 121, July 28th, 1945.